Epigenetic modification of the frataxin gene for the treatment of Friedreich's ataxia



María Gabriela Vilema Enríquez

Pembroke College

Department of Physiology, Anatomy and Genetics

University of Oxford

Trinity 2018

A thesis submitted towards the degree of Doctor of Philosophy

ABSTRACT

Friedreich's Ataxia (FRDA) is a recessive neurodegenerative disease caused by the partial silencing of the frataxin gene (*FXN*). Long GAA triplet repeat expansions in the first intron of *FXN* are responsible for the reduced levels of frataxin, an essential mitochondrial protein involved in iron-sulphur cluster biosynthesis. The precise mechanisms of *FXN* silencing remain unclear, but in the last few years, epigenetic silencing of *FXN* was reported to have a major role in the development of FRDA. The presence of expanded GAA repeats has been shown to induce a repressive heterochromatin environment at the *FXN* locus, with increased levels of methylated histones H3K9me2/3, H3K27me3 and H4K20me3, as well as reduced acetylation of histones H3 and H4, demonstrating epigenetic repression of *FXN*.

In this thesis, first HDAC3 and G9a were targeted by siRNA-mediated knockdown to increase overall acetylation and reduce methylation and promote transcription of *FXN.* Using a human *FXN*-GAA-Luciferase (*FXN*-GAA-Luc) repeat expansion reporter model of FRDA, HDAC3 knock-down was shown to increase FXN mRNA levels with no effect on protein, while G9a knock-down did not show an effect on either FXN mRNA or protein levels.

Next, the Structural Genomics Consortium epigenetic compound library set was screened in the *FXN*-GAA-Luc reporter model of FRDA to identify compounds that can restore *FXN* expression. Amongst the hits was a group of compounds targeting methyltransferases which increased frataxin protein expression, assessed by the FXN-GAA-Luciferase assay. Concentration-response curves and direct siRNA-mediated knock-down of the targets showed that the methyltransferases SUV4-20 play an important role in the silencing of *FXN.* The specific inhibitor of SUV4-20, the probe A-196, was then tested in FRDA patient-derived fibroblasts and was able to

increase the expression of mature FXN protein by 1.5-fold in the FRDA line GM04078. When A-196 was tested for its ability to modify a wide range of cellular phenotypes in FRDA patient cells, such as altered mitochondrial membrane potential and mitochondrial ROS generation, it showed only modest effects that did not reach statistical significance. Therefore, in collaboration with Oxford SGC, more stable and potent A-196 analogues were synthesized and tested in the FXN-GAA-Luciferase reporter cell line, and two new variants were found to increase FXN protein expression.

In summary, the work has defined SUV4-20 as a novel therapeutic target for FRDA and identified compound A-196 as a potential small molecule candidate for hit-to-lead development as a new drug for this fatal disease.

DECLARATION

The work presented in this thesis was performed at the University of Oxford by the author, except where acknowledgment is made. This work has not been submitted for any other degree in this or any other university or learning institute.

This work is dedicated with immense love to my grandfather

Victor Raúl Enríquez Borja

who was always proud of my achievements

Sadly, life did not allow him to share this new one with me and all my family

This work is in your loving memory grandpa

ACKNOWLEDGMENTS

The path that took me to the place where I am currently was steep and full of obstacles. Nevertheless, the things I have learnt and the people I have met, made my journey a great experience. This adventure would have not been possible to complete without the support of my loved ones. My immense gratitude to my family in special to my mother Mery, my father Luis, my sister Cristina and my number one fan, my sweet grandmother, María. I would not be the person that I am today if it were not for you all.

A heartfelt thank you to my husband Kuba for bringing joy to my life, for being my every day support, for comforting me when needed and specially for holding my hand to walk beside with me in the last years.

I am extremely grateful to Prof Richard Wade-Martins for his support throughout my degree. Thank you very much for opening the doors of your laboratory and the University of Oxford to me; as well as for the trust, patience, guidance and time.

I could not leave aside the gratitude to the Ecuadorian government and the national scholarships program for funding my studies. Thank you very much "Secretaría de Educación Superior, Ciencia, Tecnología e Innovación – SENESCYT".

A special thank you to Dr Gabriele Corda for his guidance and for his careful review of my thesis. Thank you as well Dr Charmaine Lang for the valuable comments on this work, Mindaugas Jonikas for the advice on imaging and many thanks to Drs Saba Saqlain, Irene del Molino del Barrio, Marta Cherubini and Dayne Beccano-Kelly for helping with some of the phenotypic assays.

I am also grateful to Prof Paul Brennan, Robert Quinlan and Roberta Mazzone for the support with the medicinal chemistry and to Dr Suzanne Ackloo for providing the negative probes that were used in this thesis.

Constant support was also provided by Drs Phillippa Carling and Brent Ryan. Thank you both for the guidance.

A big thank you to Dr Javier Camacho for always being available to discuss my research with me, as well as for, at the distance, having supported and motivated me in my first years in Oxford.

A special gratitude to Nora, Natalie, Tara, Siv, Peter, Mel, Milena, Bryan, Matt, Deepak, Uroosa and Janine for making the laboratory a nice place to work in. With special mention to Becky and Sarah for their friendship, support and the numerous shared experiences.

I would also like to thank my fellow Pembroke College friend Christiane Lorenz for being one of the first friendly faces here in Oxford.

My sincere gratitude to Sarah Noujaim for the friendship and all the support offered during my three years at the department.

Finally, last but by no means least, to the previous member of the Richard Wade-Martins laboratory Drs Michele Lufino, Ana Silva and Rachel Pinacho for the continuous support in my first years in Oxford. I am also grateful to Dr Mang Ching Lai for his friendship.

PUBLICATIONS AND PRESENTATIONS ARISING FROM THIS WORK

Vilema-Enríquez G, Quinlan R, Corda G, Lufino M, Brennan P & Wade-Martins R. Dissection of epigenetic mechanisms underlying the GAA-mediated FXN silencing in Friedreich's ataxia to identify FXN up-regulating compounds. Short talk. Department of Physiology, Anatomy and Genetics, Sherrington talks – Oxford, United Kingdom 2018.

Vilema-Enríquez G, Carling P J, Corda G, Lufino M & Wade-Martins R. Dissection of epigenetic mechanisms underlying the GAA-mediated FXN silencing in Friedreich's ataxia to identify FXN up-regulating compounds. Poster presentation. Second International Ataxia Research Conference – Pisa, Italy 2017.

Vilema-Enríquez G, Silva A. M , Lufino M & Wade-Martins R. Dissection of epigenetic mechanisms underlying the GAA-mediated FXN silencing in Friedreich's ataxia to identify FXN up-regulating compounds. Poster presentation. Department of Physiology, Anatomy and Genetics, Poster day – Oxford, United Kingdom 2016.

TABLE OF CONTENTS

Abstract 2

Declaration 4

Acknowledgments 6

Publications and presentations arising from this work 8

Table of contents 9

List of figures 12

List of tables 16

List of abbreviations 17

Chapter 1 20

Introduction 20

1.1. Friedreich's ataxia 20
1.2. Frataxin gene 30
1.3. Frataxin protein 32
1.4. Epigenetic mechanisms of gene silencing 36
1.5. Epigenetic therapeutic approaches for FRDA 53
1.6. Other therapeutic interventions 56
1.7. Thesis hypothesis 61
1.8. Thesis aims 61

Chapter 2 63

Materials and Methods 63

2.1. Materials 63
2.2. Methods 69

Chapter 3 86

Exploring the role of histone deacetylase 3 and Euchromatic histone lysine N-methyltransferase 2 in the expression of FXN 86

3.1. Introduction 86
3.2. Results 88
3.3. Discussion 102

Chapter 4 105

Identification of novel therapeutic targets for FRDA using the SGC epigenetic probes collection 105

4.1. Introduction 105
4.2. Results 108
4.3. Discussion 126

Chapter 5 131

Validation of A-196 in FRDA patient-derived cell lines 131

5.1. Introduction 131
5.2. Results 134
5.3. Discussion 155

Chapter 6 162

Improving the potency and stability of A-196 as a potential therapeutic molecule 162

6.1. Introduction 162
6.2. Results 164
6.3. Discussion 177

Chapter 7 182

Final discussion and future directions 182

7.1. Exploring the role of HDAC3 and G9a in the expression of FXN 182
7.2. Identification of novel therapeutic targets for FRDA using the SGC epigenetic probes collection 186
7.3. Validation of A-196 in FRDA patient-derived cell lines 189

7.4. Improving the potency and stability of A-196 as a potential therapeutic molecule 193
7.5. Future directions 195
References 197
Appendices 216
SGC epigenetics probes collection 216

LIST OF FIGURES

Figure 1. Schematic representation of the human frataxin gene and its regulatory components 31

Figure 2. Schematic representation of the FXN protein processing 34

Figure 3. Schematic representation of the histone tails of H3 and H4 and the most relevant lysine residues for this work 49

Figure 4. Friedreich's ataxia treatment pipeline 58

Figure 5. Schematic representation of the pBAC-FXN-MS2-Luc and pBAC-FXN-GAA-MS2-Luc vectors 64

Figure 6. Adenylate kinase reaction for bioluminescent assay 73

Figure 7. Different concentrations of HDAC3 siRNA down-regulate the protein to a similar extent 89

Figure 8. HDAC3 knock-down up-regulates FXN mRNA levels in both cell lines 91

Figure 9. HDAC3 knock-down has no effect on FXN protein levels 92

Figure 10. Luciferase assay shows no difference between the control and HDAC3 siRNA transfected cells 93

Figure 11. Different concentrations of G9a siRNA efficiently down-regulate G9a protein in Luc-reporter cell lines 94

Figure 12. G9a siRNA has no effect on frataxin mRNA levels in both cell lines 95

Figure 13. G9a siRNA at three different concentrations does not change FXN protein levels 96

Figure 14. Luciferase expression associated with *FXN*-luciferase fusion protein is unaltered upon G9a siRNA knock-down 97

Figure 15. Pulsed-field gel confirms that both fosmids correspond to *FXN* locus sequences 98
Figure 16. DNA gel electrophoresis of fosmid clones 100
Figure 17. Optimization of the probes labelling 101
Figure 18. Optimization of 3D DNA FISH 102
Figure 19. Pipeline used for the SGC epigenetic chemical probes screen 110
Figure 20. A group of chemical inhibitors of several methyltransferases increase FXN-Luc protein expression in the *FXN*-GAA-Luc cell line 111
Figure 21. Hit probes show not to be toxic for the *FXN*-GAA-Luc cell line 112
Figure 22. Concentration-response curves of the hit molecules 115
Figure 23. siRNA-mediated knock-down of SUV4-20H1 and SUV4-20H1 + SUV4-20H2 up-regulate FXN-Luc protein expression 117
Figure 24. siRNA targeting of G9a+GLP shows a trend in increase of FXN-Luc protein expression assessed by the luciferase assay 118
Figure 25. Down-regulation of EZH1 and EZH2 have little effect on the expression of FXN-Luc protein assessed by the luciferase assay 120
Figure 26. Knock-down of DOT1L in the *FXN*-GAA-Luc cell line 121
Figure 27. Chemical structures of the lead compound and its related inactive probes 122
Figure 28. A-196 decreases H4K20me2 and H4K20me3 while increasing H4K20me1 by inhibiting the SUV4-20 family of proteins 124
Figure 29. A-196 increases FXN-Luc protein expression in a significant manner at 10 μM 125
Figure 30. A-196 increases mature frataxin protein expression in the GM04078 cell line 136

Figure 31. The lymphoblastoid cell line GM16220 has a modest increase in FXN protein after A-196 treatment 138
Figure 32. Mitochondrial mass is decreased in patient-derived fibroblasts 141
Figure 33. Mitochondrial membrane potential is reduced in FRDA patient-derived fibroblasts 143
Figure 34. FRDA patient-derived fibroblasts have more mitochondrial ROS than control fibroblasts 144
Figure 35. Nrf2 is reduced in the nucleus of FRDA patient-derived fibroblasts 146
Figure 36. Calcium release is altered in the FRDA patient-derived cell line GM03816 148
Figure 37. A-196 increases slightly the number of mitochondria in FRDA patient-derived fibroblasts 150
Figure 38. Mitochondrial membrane potential is slightly increased in FRDA patient-derived fibroblasts after A-196 treatment 151
Figure 39. FRDA patient-derived fibroblasts show a modest decrease in mitochondrial ROS production after A-196 treatment 152
Figure 40. A-196 treatment of FRDA patient-derived lines has no effect on the cellular localization of Nrf2 153
Figure 41. Calcium release shows a differential response to A-196 treatment in FRDA patient-derived fibroblasts 154
Figure 42. A-196 and GSK343 show synergistic effects at several concentrations of both drugs 166
Figure 43. Chemical inhibition of the methyltransferases of H3K9 and H3K27 in conjunction, show to increase FXN-Luc protein expression more efficiently that the inhibition of each lysine residue alone 170

Figure 44. Synthesized A-196 analogues 174

Figure 45. Screen of A-196 derivatives using the *FXN*-GAA-Luc cell line finds new compounds capable of increasing FXN-Luc protein 175

Figure 46. RQ3-014 increases FXN-Luc protein in a concentration-dependent manner 176

Figure 47. RM-002 increases FXN-Luc protein expression significantly at concentrations between 0.1 μM to 10 μM 177

LIST OF TABLES

Table 1. Observed FRDA prevalence in Europe and predicted carrier rate. 21

Table 2. Summary of mutations published for the *FXN* gene 23

Table 3. DNA methylation changes in FRDA models 42

Table 4. Histone acetylation changes at the *FXN* locus 45

Table 5. Histone methylation marks on the *FXN* gene 50

Table 6. List of the cell lines used in this study 63

Table 7. List of the media and buffers formulations 64

Table 8. List of primers and their sequences 65

Table 9. List of antibodies used for western blotting, fluorescence cytochemistry, immunocytochemistry and 3D DNA FISH 66

Table 10. List of the siRNA sequences 67

Table 11. List of chemical probes used for the validation of targets 69

Table 12. List of probes divided by groups based on the SGC recommendations .. 108

Table 13. Combination index corresponding to the combination of A-196 and GSK343 168

Table 14. Combination index corresponding to the combination of A-366 and GSK343 171

Table 15. Metabolic stability of A-196 in human liver microsomes 173

Table 16. Metabolic stability of A-196 in mouse liver microsomes 173

Table 17. SGC chemical probes used in the screen. Information taken from SGC and uniprot 216

LIST OF ABBREVIATIONS

5-aza-CdR: 5-aza-2'-deoxycytidine

5hmC: 5-hydroxymethylcytosine

5mC: 5-methylcytosine

aa: amino acid

ADME: absorption, distribution, metabolism and excretion

AK: adenylate kinase

BCA: bicinchoninic acid

BSA: bovin serum albumin

CCCP: carbonyl cyanide m-chloro phenyl hydrazone

ChIP: chromatin immunoprecipitation

CI: combination index

CNS: central nervous system

CpG islands: cytosine–phosphoguanine islands

DNMT: DNA methyl- transferase

DOT1L: Disrupter of telomeric silencing 1-like

DRG: dorsal root ganglia

EHMT1: Euchromatic histone-lysine N-methyltransferase 1

EHMT2: Euchromatic histone-lysine N-methyltransferase 2

EPO: Erythropoietin

ER: endoplasmic reticulum

EZH: Enhancer of Zeste Homolog

FARR: Friedreich's ataxia with retained reflexes

FBS: Fetal Bovine Serum

FDA: Food and Drug Administration

FECH: Ferrochelatase

FRDA: Friedreich's ataxia

FXN: frataxin gene

FXN: frataxin protein

FXN-Luc: Frataxin-luciferase

H3: histone 3

H3K9me3: H3K9 trimethylation

H4: histone 4

HATs: histone acetyl- transferases

HDACi: histone deacetylase inhibitors

HDACs: histone deacetylases

HMTs: histone methyltransferases

hPDL: human periodontal ligament cells

HSV: herpes simplex virus

ISC: iron-sulphur clusters

ISCU: iron–sulphur cluster assembly enzyme

K: lysine

K_i: inhibition constant

KMT5B: Lysine methyltransferase 5B

KMT5C: Lysine methyltransferase 5C

LB: Luria-Bertani

LN alleles: large normal alleles

LOFA: Late-onset Friedreich's ataxia

LSD: lysine-specific histone demethylase

MoA: mode of action

MPP: mitochondrial processing peptidase

Nrf2: Nuclear factor erythroid-derived 2-related factor 2

Pen-Strep: Penicillin-Streptomycin

PEV: position effect variegation

PFG: Pulsed-field gel

PKMTs: protein lysine methyltransferases

PRMTs: protein arginine methyltransferases

rhuEPO: recombinant human erythropoietin

RIPA: Radioimmunoprecipitation assay

RNAPII: RNA polymerase II

ROS: Reactive oxygen species

RPMI: Roswell Park Memorial Institute

SAM: S-adenosylmethionine

SDS: Sodium dodecyl sulfate

SGC : Structural Genomics Consortium

SN alleles: small normal alleles

SSC: Saline-sodium citrate

SUV4-20H1: Suppressor of variegation 4-20 homolog 1

SUV4-20H2: Suppressor of variegation 4-20 homolog 2

TAD: transcription activation domain

TALE: transcription activator-like effectors

TET: ten-eleven translocation

TSS: transcription start sites

UTR: untranslated region

VLOFA: very late-onset Friedreich's ataxia

$\Delta\Psi_m$: mitochondrial membrane potential

CHAPTER 1

Introduction

1.1. Friedreich's ataxia

1.1.1. Friedreich's ataxia

Friedreich's ataxia (FRDA) is a neurodegenerative disease that was first described by the German pathologist and neurologist Nikolaus Friedreich in a series of publications between 1863 and 1877 (Friedreich, 1863a, 1863b, 1863c, 1876, 1877). He presented the clinical findings of six patients with a severe disorder of the nervous system, as well as the observations that he made on the autopsies of four of them. Friedreich was particularly fascinated by the spinal cord lesions and the destruction of the dorsal columns (Koeppen, 2013). Even though he acknowledged the hereditary nature of the pathology, only after several years of the first description of the disease he reported many of the main features including ataxia, cardiomyopathy, an onset which mainly occurs in adolescence, sensory neuropathy, scoliosis and foot deformity (Delatycki and Corben, 2012). Given the contributions of Nikolaus Friedreich to the description of a "new" disorder in the late 19th century, the disease was named after him.

1.1.2. Prevalence

FRDA is the most frequently inherited autosomal recessive ataxia in Europe, the Middle East, North Africa, and South Asia (Indian subcontinent). A lower-than-average prevalence has been reported in Mexico and FRDA has not been

documented in Southeast Asians, in sub-Saharan Africans, or among Native Americans (Bidichandani and Delatycki, 1993). The estimated prevalence of FRDA is 1 in 50,000 in the Caucasian population, with a carrier frequency of 1 in 60 to 1 in 100 (Bidichandani and Delatycki, 1993; Campuzano *et al.*, 1996).

Table 1 shows the observed FRDA prevalence in Europe organized by country, and the predicted FRDA carrier rate (Vankan, 2013).

Table 1. Observed FRDA prevalence in Europe and predicted carrier rate.

Country	Observed FRDA prevalence	Predicted FRDA carrier rate
North Spain	1 in 20,000	1 in 55
Portugal	1 in 100,000	1 in 95
Ireland	1 in 23,000	1 in 58
France	1 in 43,000	1 in 85
South-west Germany	1 in 53,000	1 in 99
North-east Germany	1 in 149,000	1 in 124
Italy	1 in 80,000	1 in 110
United Kingdom	1 in 54,000	1 in 76
Switzerland	1 in 45,000	NA*
Austria	1 in 54,000	1 in 198
Netherlands	1 in 60,000	1 in 92
Norway	1 in 100,000	1 in 177
Sweden	1 in 420,000	1 in 248
Finland	1 in 750,000	NA*
Denmark	1 in 140,000	1 in 141
Czech Republic	1 in 250,000	1 in 248
Poland	1 in 250,000	NA*
Russia	1 in 300,000	1 in 336

*NA not available

1.1.3. Genetics

In 96% of cases FRDA is caused by a biallelic expansion of an unstable GAA sequence in the first intron of the frataxin gene (*FXN*), a gene which is mapped to chromosome 9 (9q13-21) (Chamberlain *et al.*, 1988; Campuzano *et al.*, 1996). The GAA insertion in the first intron is localized within an Alu sequence. Evolutionarily, the GAA repeats are present in nonhuman primates such as chimpanzees, orangutans, gorillas and rhesus macaques. The GAA repeat was also found in a more distant relative, the tamarin, suggesting that it arose at least 40 million years ago and throughout the majority of the primate evolution, it remained relatively small, with a punctuated expansion in the human genome (Justice *et al.*, 2001). In Western Europe, the age of the founding mutation was estimated at least 682 ± 203 generations ago. This suggests a Palaeolithic origin. However, it is difficult to state if that is the age of the mutation *per se*; or the age of the population bottleneck (Vankan, 2013).

Even though in the majority of cases the two *FXN* alleles are expanded, a small percentage (4%) of patients are compound heterozygous for the GAA expansion and a different mutation. Table 2 summarizes the published mutations found in the *FXN* gene.

The length of the expanded GAA tract, particularly that of the smaller allele in homozygous for the GAA expansion individuals, correlates with earlier age at onset and severity of disease (Dürr *et al.*, 1996). FRDA typically presents before the age of 25, with an average age of symptom onset occurring in the mid-teen years. Patients are bound to a wheelchair on average ten years after diagnosis, in this way depending for mobility (Dürr *et al.*, 1996; Delatycki, Paris, *et al.*, 1999).

Table 2. Summary of mutations published for the *FXN* gene

Gene region	Mutation	Type of mutation	Effect	Reference
Exon 1	c.1 A>C	Missense	p.M1L (incorrect initiation)	(Cossée *et al.*, 1999)
	c.2 T>C	Missense	p.M1T (incorrect initiation)	(Cossée *et al.*, 1999)
	c.2 del T	Missense	p.M1S (incorrect initiation)	(Zhu *et al.*, 2002)
	c.3 G>T	Missense	p.M1I (incorrect initiation)	(Zühlke *et al.*, 1998)
	c.3 G>A	Missense	p.M1I (incorrect initiation)	(Potter, Miller and Anderson, 2000)
	c.11-12 del TC	Frameshift	p.L4RfsX90	(Spacey *et al.*, 2004)
	c.100 del G	Frameshift	p.A34PfsX75	(Gellera *et al.*, 2007)
	c.104 del C	Frameshift	p.P35HfsX75	(Gellera *et al.*, 2007)
	c.118 C>T	Missense	p.R40C	(Van Driest *et al.*, 2005)
	c.118 delC	Frameshift	p.R40VfsX75	(De Castro *et al.*, 2000)
	c.157 delC	Frameshift	p.R53AfsX75	(Cossée *et al.*, 1999; Gellera *et al.*, 2007)
	c.157 insC	Frameshift	p.R53PfsX92	(Cossée *et al.*, 1999)
Intron 1	g.IVS1+5 G>C	Splice donor site mutation	Aberrant splicing predicted	(McCormack *et al.*, 2000)
Exon 2	c.202_205 delGTCAinsTTG	Frameshift	p.V68LfsX75	(Pook *et al.*, 2000)
Exon 3	c.296_297 insT	Frameshift	p.A99VfsX111	(De Castro *et al.*, 2000)
	c.317 T>G	Nonsense	p.L106X	(Campuzano *et al.*, 1996)
	c.317 T>C	Missense	p.L106S	(Bartolo, Mendell and Prior, 1998)
	c.317 delT	Nonsense	p.L106X	(Pook *et al.*, 2000)
	c.340_352 del13	Frameshift	p.A114TfsX128	(Pook *et al.*, 2000)
	c.354 C>G	Nonsense	p.Y118X	(Gellera *et al.*, 2007)
	c.364 G>T	Missense	p.D122Y	(Cossée *et al.*, 1999)

Exon 3/ Intron3	c.381_384 delTGGG + IVS3+1_+9 delGTACCTCTT	Splice donor site mutation	Aberrant splicing predicted	(Gellera *et al.*, 2007)
Intron 3	g.IVS3+1 G>A	Splice donor site mutation	Aberrant splicing predicted	(Doudney *et al.*, 1998)
	g.IVS3-2 A>G	Splice donor site mutation	Aberrant splicing predicted	(Campuzano *et al.*, 1996)
Exon 4	c.389 G>T	Missense	p.G130V	(Bidichandani, Ashizawa and Patel, 1997; Forrest *et al.*, 1998; Cossée *et al.*, 1999; McCabe *et al.*, 2002)
	c.438 C>G	Missense	p.N146K	(Zühlke *et al.*, 2004)
	c.460 A>T	Missense	p.I154F	(Campuzano *et al.*, 1996; Filla *et al.*, 1996; Gellera *et al.*, 2007)
	c.464 T>C	Missense	p.W155R	(Labuda, Poirier and Pandolfo, 1999)
	c.465 G>A	Nonsense	p.W155X	(De Castro *et al.*, 2000)
	c.467 T>C	Missense	p.L156P	(Campuzano *et al.*, 1996)
Intron 4	g.IVS4+2 T>G	Splice donor site mutation	Aberrant splicing predicted	(Forrest *et al.*, 1998)
	g.IVS4+3 delA	Splice donor site mutation	Aberrant splicing predicted	(Cossée *et al.*, 1999)
Exon 5A	c.493 C>T	Missense	p.R165C	(Forrest *et al.*, 1998; McCormack *et al.*, 2000)
	c.494 G>C	Missense	p.R165P	(De Michele *et al.*, 2000)
	c.517 T>G	Missense	p.W173G	(Cossée *et al.*, 1999; Gellera *et al.*, 2007)

	c.544 C>T	Missense	p.L182F	(Forrest *et al.*, 1998)
	c.545 T>A	Missense	p.L182H	(Cossée *et al.*, 1999)
	c.548 A>G	Missense	p.H183R	(Cossée *et al.*, 1999)
	c.557 T>G	Missense	p.L186R	(Zühlke *et al.*, 2004)
	c.593 T>G	Missense	p.L198R	(Al-Mahdawi, Pook and Chamberlain, 2000)
	g.120032_122808 del	Deletion of exon 5A	Premature termination predicted	(Zühlke *et al.*, 2004)

*c. Coding DNA, g. Genomic DNA, p. Protein, > substitution, - range, del deletion, ins insertion, X stop codon, fsX frame shift.

1.1.4. Diagnosis

FRDA is diagnosed by detecting the pathogenic variants in both alleles of the frataxin gene. The most common variant (96%) is the biallelic expansion of the GAA repeat in the first intron of *FXN,* while the remaining variants (4%) present one expanded allele and another intragenic pathogenic mutation on the other allele. Direct molecular diagnosis through determination of the size of the repeat expansion is required. Single-gene testing is targeted to intron 1 of the *FXN* gene. PCR amplification of the region surrounding the GAA repeat in intron 1 of *FXN* is used to assess the length of the GAA expansion. If only one abnormal allele is present, sequence analysis of *FXN* is performed; and if no pathogenic inactivating variant is found, deletion/duplication analysis is conducted. A multi-gene panel that includes other genes of interest in addition to *FXN* may also be considered and used at each clinician's consideration (Bidichandani and Delatycki, 1993).

1.1.5. Clinical features

Typical FRDA is observed in about 75% of affected individuals, while atypical FRDA refers to Friedreich's ataxia with retained reflexes (12%), late-onset FRDA and very late-onset FRDA (15%). In FRDA with retained reflexes (FARR) individuals show brisk tendon reflexes, particularly knee jerks. Reflexes may be retained for more than ten years post onset of disease. Late-onset FRDA (LOFA) is characterized by symptoms onset after the age of 25 years and very late-onset FRDA (VLOFA) after 40 years (Bidichandani and Delatycki, 1993; Delatycki and Corben, 2012).

Neurologic and neuromuscular manifestations

FRDA is characterized clinically by progressive gait and limb ataxia, sensory loss and muscle weakness (Patel and Isaya, 2001). Gait ataxia is caused by the combination of spinocerebellar degeneration and loss of proprioception (joint-position sense). This feature is the earliest symptom in the vast majority of cases. Most patients within five years of symptom onset exhibit dysarthria, diminished or absent joint-position and vibration sense distally, as well as lower-extremity weakness. These neurologic manifestations result from the progressive degeneration of the posterior columns, corticospinal tracts, dorsal root ganglia (DRG), dorsal spinocerebellar tracts of the spinal cord, and cerebellum. In addition, individuals exhibit a mixed axonal peripheral neuropathy, due to the involvement of peripheral sensory and motor neurons (Bidichandani and Delatycki, 1993).

Gait becomes ataxic and unsteady with increasing falls. Walking becomes problematic on uneven terrain or in poor light. Many patients describe a long history of trips, clumsiness or inability to do sports. With time, patients'

dependence on aids to walk increases, starting with walls, furniture, other people, to ultimately sticks, crutches, wheeled walkers and wheelchairs. Limb ataxia causes difficulty with daily activities such as handwriting, dressing, washing, the use of cutlery and carrying food or drinks (Parkinson *et al.*, 2013).

Pyramidal weakness is much more prominent in the lower limbs when compared to the upper limbs and it is a relatively late sign. Moreover, in a significant proportion of cases, wasting is present (Harding, 1981; Filla *et al.*, 1990; Dürr *et al.*, 1996).

Abnormalities of eye movements are a frequent early sign in FRDA. The most common are square wave jerks, but abnormalities of saccades, pursuit, fixation, and vestibular-ocular reflex are also present (Fahey *et al.*, 2008; Fortuna *et al.*, 2009). All FRDA patients show reduced retinal nerve fibre layer thickness all through the four quadrants on optical coherence tomography (Parkinson *et al.*, 2013).

Speech becomes slurred and slow. More than 90% of individuals present dysarthria as a common and early sign of FRDA, which progresses with disease duration. In fact, its severity was found to correlate with disease duration. Dysarthria is generally of three types: mild dysarthria, characterized by consonant imprecision and decreased pitch variation, increased velopharyngeal involvement evident as hypernasality, and increased laryngeal dysfunction evident as increased strained-strangled vocal quality (Folker *et al.*, 2010).

Dysphagia is a common symptom that can become problematic in the latter stages of the disease. It is characterized by oral and pharyngeal stage impairment relating to the lack of coordination, weakness and spasticity. Patients can cough or choke on

solids or liquids including saliva. Aspiration pneumonia secondary to dysphagia is a recognized cause of death (Delatycki and Corben, 2012; Vogel *et al.*, 2014).

Sensorineural hearing loss occurs in 13% of FRDA patients (Dürr *et al.*, 1996). Auditory neuropathy affects a minority of individuals and difficulty hearing in background noise is common. Furthermore, a significant correlation between disease duration and functional hearing has been reported (Rance *et al.*, 2010).

Bladder symptoms including urinary frequency and urgency have been reported in 41% of individuals (Delatycki, Paris, *et al.*, 1999). Urodynamic studies show uninhibited contractions and altered bladder capacity as well as urgency incontinence (Vezina, Bouchard and Bouchard, 1982; Nardulli *et al.*, 1992).

Even though cognition was initially thought not to be impaired in FRDA patients, recent studies have shown that in many patients, specific aspects of cognitive function may be affected. Motor, mental reaction times and motor planning are impaired (Wollmann *et al.*, 2002; Corben *et al.*, 2006, 2010, 2011). Individuals with FRDA show an intelligence profile characterized by concrete thinking and poor capacity in concept formation as well as visuospatial reasoning, accompanied by reduced speed of information processing (Mantovan *et al.*, 2006). Motor overflow (unintentional movement that accompanies voluntary task execution) is also more prevalent in individuals with FRDA, in addition to problems with attention and working memory (Klopper *et al.*, 2011; Low *et al.*, 2013). Furthermore, cognitive difficulties seem to be more severe in patients with earlier onset and larger GAA repeat expansions than in patients with later onset and smaller GAA repeats (Nachbauer *et al.*, 2014). More recently, the Hayling Sentence Completion Task, which is a robust and well-documented measurement of inhibitory control, showed

that FRDA individuals have impaired inhibition and cognitive flexibility (Corben *et al.*, 2017).

Scoliosis is present in most FRDA patients, with a high prevalence of double thoracic and lumbar curves. In some cases, patients need the prescription of a brace and in others, spinal surgery is needed (Labelle *et al.*, 1986; Shapiro and Specht, 1993; Milbrandt, Kunes and Karol, 2008).

Non-neurologic features

Cardiac complications are found in the majority of FRDA cases even though patients are often asymptomatic. In two thirds of patients, hypertrophic cardiomyopathy, which is defined as increased thickness of the interventricular septum is present (Delatycki, Knight, *et al.*, 1999). Dilated cardiomyopathy or asymmetric septal hypertrophy, although less common, have also been described in FRDA patients. These may be caused by a progression from hypertrophic cardiomyopathy (Casazza and Morpurgo, 1996). No correlation between the presence of cardiac complications and the severity of neurological involvement has been described (Weidemann *et al.*, 2012). In the later stages of disease, arrhythmias, especially atrial fibrillation, and congestive heart failure occur frequently and are the most common cause of mortality reaching 59% (Tsou *et al.*, 2011).

Diabetes mellitus is present in up to 30% of individuals with FRDA and a further 49% have impaired glucose tolerance (Dürr *et al.*, 1996; Cnop, Mulder and Igoillo-Esteve, 2013). Even though the mechanism of the association between FRDA and diabetes is unclear, it has been reported that pancreatic β-cell dysfunction plays a central role in the development of diabetes. This phenomenon is likely to result

from the mitochondrial dysfunction and higher sensitivity to metabolic and endoplasmic reticulum stress-induced β-cell death (Cnop *et al.*, 2012). Diabetes typically presents as a later feature in patients with FRDA, who sometimes require insulin treatment.

1.2. Frataxin gene

1.2.1. Chromosomal localization and components

The *FXN* gene resides on the long arm of chromosome 9 (Figure 1 A) and encodes the mitochondrial protein frataxin. The gene was initially called X25 and is also known as FRDA and FXN. The frataxin gene contains five exons and four introns, and three putative cytosine–phosphoguanine (CpG) islands (Figure 1 B) (Yandim, Natisvili and Festenstein, 2013). The gene contains within its first intron a polymorphic $(GAA)_n$ repeat in the centre of an Alu element. It is thought that the GAA repeats arise from a tract of adenine residues of this abundant transposable element (Campuzano *et al.*, 1996; Chauhan *et al.*, 2002).

In the *FXN* gene, the normal sequence corresponds to a moderately polymorphic trinucleotide repeat. Normal alleles can be distributed into two main groups, small normal (SN) alleles containing less than ten repeats, and large normal (LN) alleles with more than 9 repeats and up to 36 repeats. All LN alleles are interrupted by a GAGGAA hexanucleotide repeat. No normal stable allele contains more than 27 uninterrupted GAA repeats (Montermini *et al.*, 1997). The analysis of five polymorphic markers within or close to the *FXN* gene, in normal and expanded repeats, shows that most if not all LN alleles derive from a single founder chromosome. These alleles represent a reservoir for large expansion events,

probably through premutation intermediates. The disease-causing expanded alleles have more than 70 repeats and are thought to be originated from alleles at risk, ranging from 42 to 60 GAA repeats (Cossée *et al.*, 1997; Montermini *et al.*, 1997). Non-pathological *FXN* contains up to 40 GAA repeats, whereas disease-associated alleles contain 70 to 1500 and most commonly between 600 to 900 repeats (Schmucker and Puccio, 2010).

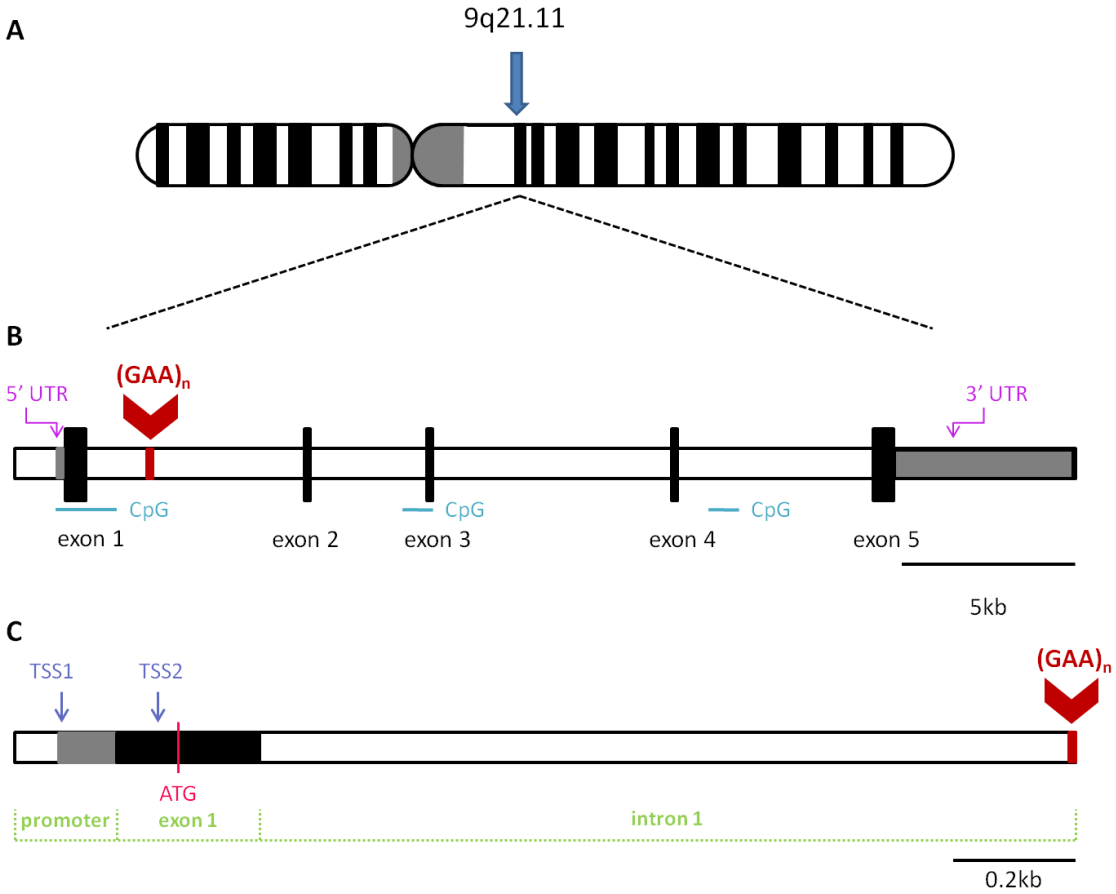


Figure 1. Schematic representation of the human frataxin gene and its regulatory components

(**A**) Idiogram of human chromosome 9 depicting the localization of the *FXN* gene (**B**) The full genomic locus of the *FXN* forward strand, which consists of five exons and four introns. The first intron of *FXN* contains a variable number of $(GAA)_n$ triplet repeats. Normal ranges are between 5 and 60, higher numbers (70-1500) are associated with Friedreich's ataxia (**C**) Regulatory elements located at the 5' end of *FXN*. The gene is known to be transcribed from two transcription start sites (TSS). The first one (TSS1) is located 221 bp upstream of the ATG translation start site, whereas the second one (TSS2) is only 62 bp upstream. Adapted from Yandim, Natisvili and Festenstein, 2013.

Two major transcription start sites (TSS) have been identified in the *FXN* gene (Figure 1 C). TSS1 is found 221 bp upstream of the ATG translation start site (Campuzano *et al.*, 1996), while TSS 2 is located 62 bp upstream (Kumari, Biacsi and Usdin, 2011). Even though several other TSSs were also reported (Puspasari *et al.*, 2011), only TSS1 and TSS2 have been widely accepted by the scientific community. Amongst both, TSS2 has been suggested to be the primary transcription start site in lymphoblastoid cell lines (Kumari, Biacsi and Usdin, 2011).

1.3. Frataxin protein

Frataxin (FXN) is a nuclear encoded mitochondrial protein of which its reduced expression is the cause of Friedreich's ataxia. In FRDA, the GAA expansion leads to partial transcriptional silencing of *FXN,* resulting in the expression of structurally and functionally normal frataxin, but at lower levels compared to normal. These levels are estimated to be between 5-30% compared to healthy individuals (Martelli, Napierala and Puccio, 2012).

1.3.1. Frataxin sequence

FXN encodes frataxin, a protein highly conserved in most organisms (Pastore and Puccio, 2013). Frataxin family sequence alignment, which includes frataxin homologues on different species, shows two distinct regions. First, a N-terminal composed of 70 to 90 residues, which is completely absent in prokaryotes, and in eukaryotes is poorly conserved (Huynen *et al.*, 2001). Second, the C-terminus of the protein comprises a highly conserved region of 100 to 120 amino acids that is conserved in most organisms. Three tryptophans, which are residues with a relatively low occurrence in proteins, are amongst the most conserved residues.

This finding suggests that their conservation could have an important functional and/or structural role.

1.3.2. Cellular localization

The first evidence that frataxin is a mitochondrial protein came from tagging the human frataxin sequence at the 3' end with β-galactosidase in a eukaryotic expression vector. This experiment showed that frataxin co-localized with cytochrome-c oxidase, a mitochondrial protein (Koutnikova *et al.*, 1997). Additionally, immunocytofluorescence and immunocytoelectron microscopy experiments further identified that frataxin is associated with mitochondrial membranes and crests (Campuzano *et al.*, 1997). It is currently well accepted that frataxin is encoded in the nucleus, expressed in the cytoplasm and imported into the mitochondria through a signal peptide contained in the N-terminus (Campuzano *et al.*, 1997).

1.3.3. Frataxin maturation

The frataxin protein is synthesized as a precursor of 210 amino acids (23 kDa) and imported to the mitochondria where it undergoes maturation by the mitochondrial processing peptidase (MPP) (Figure 2). This two-step process, leads to the production of an intermediate 19 kDa form, which is then cleaved between residues 42-210 to form a mature product of 14 kDa (residues 81-210) (Koutnikova, Campuzano and Koenig, 1998; Condò *et al.*, 2007; Schmucker *et al.*, 2008).

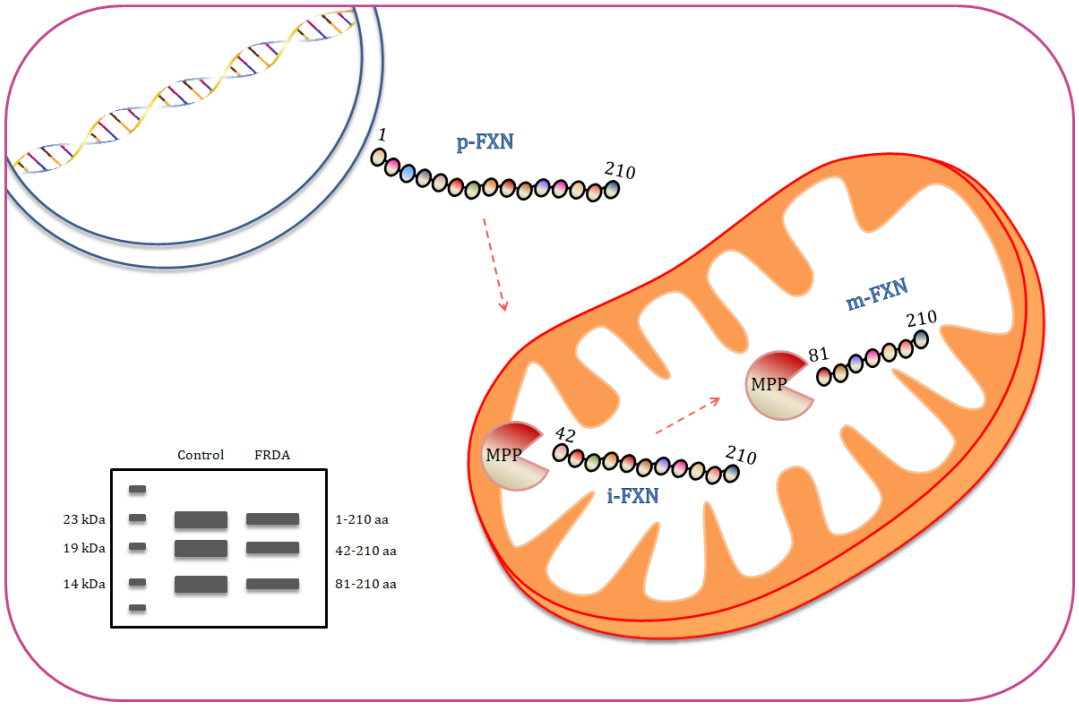


Figure 2. Schematic representation of the FXN protein processing

The nuclear-encoded FXN protein is synthesized as a 210 amino acid (aa) precursor (p-FXN). The FXN protein has a N-terminal mitochondrial-targeting sequence that directs the protein for processing. This two-step maturation process is carried out by the mitochondrial processing peptidase (MPP), where an initial cleavage generates the intermediate form (i-FXN) that will be then further cleaved to form the mature and functional FXN protein (m-FXN). A representation of a western blot illustrating all forms of frataxin protein from a control and a FRDA patient is shown in the bottom left-hand corner.

1.3.4. Frataxin expression

The expression of FXN protein is in the range of pg of frataxin per µg of total protein even in healthy individuals, which shows that frataxin is expressed at a relatively low level (Boehm *et al.*, 2011). Its expression is somewhat higher in the cortical region of the DRG and the granular layer of the cerebellum, in addition to tissues with high metabolic rate, which are rich in mitochondria such as the heart, pancreas, brown fat, liver, muscle and kidney (Campuzano *et al.*, 1996, 1997; Koutnikova *et al.*, 1997).

1.3.5. Frataxin function

The impact of the cellular function of frataxin is clearly reflected by the early embryonic lethality in *Fxn* knock-out mice (Cossée *et al.*, 2000). Several studies have shown that frataxin is an iron-binding protein (Adamec *et al.*, 2000; Adinolfi *et al.*, 2002) with an important role in iron metabolism. Other groups showed its involvement in regulating iron utilization by the mitochondria for the biogenesis of iron-sulphur clusters (ISC) and heme, as well as for iron storage (Pastore and Puccio, 2013).

ISC are highly adaptable and essential enzyme co-factors that are known to participate in a wide range of cellular reactions and processes such as electron transfer, iron/sulphur storage, substrate binding/activation, regulation of gene expression, and enzyme activity (Johnson *et al.*, 2005). One of the main functions of frataxin is that it activates mitochondrial iron-sulphur cluster protein assembly as part of a multiprotein complex. In frataxin-deficient cells, there is general ISC protein depletion in all cellular compartments. These cells are particularly deficient in mitochondrial ISC-containing subunits of the respiratory chain complexes I, II and III and aconitase activity (Rötig *et al.*, 1997; Bürk, 2017). Frataxin-deficient cells also have iron homeostasis impairment. Li and colleagues have shown that lymphoblastoid cells and fibroblasts derived from patients with FRDA present signs of cytosolic iron depletion. Furthermore, the mitochondria of frataxin-deficient cells were overloaded with iron. This is a downstream regulatory effect that has been previously described when mitochondrial iron–sulphur cluster assembly is disrupted (Li *et al.*, 2008; Lee *et al.*, 2016).

Another function attributed to frataxin is as an iron chaperone, partly because it facilitates the formation of ISCs. In mammals, synthesis of ISCs in the mitochondrial matrix is initiated by the scaffold protein, iron–sulphur cluster assembly enzyme (ISCU). It requires the cysteine desulfurase NFS1, which needs to be stabilized by a small binding partner ISD11, that serves as the sulphur donor. Frataxin participates to the ISC assembly by providing iron to the complex, followed by the electron donor chain formation directed by ferredoxin and ferredoxin reductase (FDX2-FDXR) (Vaubel and Isaya, 2013). Frataxin has not only been proposed as the iron donor that presents iron to the ISCU/NFS1/ISD11 complex, but also has been suggested to present its iron for heme synthesis once bound to ferrochelatase (FECH) (Yoon and Cowan, 2004; Schmucker *et al.*, 2011).

The hypothesis that frataxin functions as an iron storage protein was initially suggested by observation in yeast, where frataxin can form oligomers that have ferroxidase activity. The iron-binding capacity of the yeast frataxin homolog is high in aggregates. These aggregates are able to maintain iron in a redox inactive state, at the same time as retaining the ability to release iron for biosynthetic pathways (Park *et al.*, 2003). However, this function still remains controversial in humans since human frataxin has a lower iron-binding capacity, even under conditions of iron accumulation in the mitochondria (Cavadini *et al.*, 2002).

1.4. Epigenetic mechanisms of gene silencing

The understanding of the molecular mechanisms that govern *FXN* silencing is still limited. Several mechanisms have been described, amongst those, epigenetic mechanism of gene repression, that will be discussed in this section.

1.4.1. Overview of epigenetics

Epigenetics is defined as changes in phenotype or gene expression as a result of a mechanism other than the alteration in the underlying DNA sequence (Berger *et al.*, 2009). These changes may remain throughout the cell's life, persist in the course of cell division, and be transmitted for multiple generations in a specific cell lineage. Epigenetics plays an important role as an adaptive control layer in the regulation of gene expression. It enables the organism to adjust to a changing environment, and it is influenced by the developmental stage, type of tissue, environmental conditions, and disease status of an individual (Keshet *et al.*, 2006; Mikkelsen *et al.*, 2007; De Bustos *et al.*, 2009; Van Soom *et al.*, 2014). Epigenetic mechanisms were shown to alter chromatin structure, transcript stability and nuclear organization. These changes either alone or in combination, have a great impact on gene expression and cause long-term molecular and functional outcomes (Stephens *et al.*, 2013).

In the cell nucleus, DNA is hierarchically packaged into chromosomes, where DNA is wrapped around histone proteins forming the nucleosome, the basic subunit of chromatin. The nucleosome is composed of an octamer of the four core histones (H2A, H2B, H3, H4) around which 147 base pairs of DNA are wrapped. Depending on the interaction of DNA with histone proteins, chromatin could be less condensed and easily accessible to RNA polymerase II (RNAPII) or tightly packed and inaccessible, meaning that chromatin can be characterized as euchromatin or heterochromatin (Kouzarides, 2007). The insight on how these interactions can affect chromatin remodelling come from the structure of the nucleosome. Histones are predominantly globular except for their N-terminal tails that can protrude from their own nucleosome and contact adjacent nucleosomes. Additionally, histone tails

possess a large number and type of modified residues. The most studied are the small covalent modifications namely, acetylation, methylation, and phosphorylation. These modifications not only regulate the structure of chromatin by solely being present, but they also recruit remodelling enzymes that make use of the energy derived from ATP hydrolysis to reposition nucleosomes (Kouzarides, 2007; Bannister and Kouzarides, 2011).

It has been shown that the dynamic state of gene expression is regulated in cells in part through a number of epigenetic mechanisms, namely the formation of complex DNA structures, such as RNA loops, DNA–RNA hybrids, and DNA triplexes, DNA methylation, heterochromatin formation and associated histone modifications (Allis, Jenuwein and Reinberg, 2007). These mechanisms have all been implicated in a variety of disease states, including FRDA.

1.4.2. Aberrant locus spatial configuration

Even though it is clear that FRDA is caused by low levels of frataxin expression, the precise mechanism by which gene repression happens remains to be defined. In principle, the pathological silencing could be due to reduced transcription or to abnormal post-transcriptional processing. It has been shown that the abnormal expansion of intron 1 does not significantly interfere with mRNA processing (Bidichandani, Ashizawa and Patel, 1998; Ohshima *et al.*, 1998). It is generally accepted that the events that result in reduced frataxin levels occur during transcription *per se* and that they are unlikely to occur at the post-transcriptional level. In accordance, the half-life of frataxin mRNA, which is approximately 11 hours, was not found to differ between FRDA patients and healthy individuals

(Punga and Bühler, 2010). Thus, this suggests that reduced transcription is the main molecular mechanism that causes the disease.

One way of explaining the reduced transcription of *FXN* in FRDA could be the presence of a physical-blockage that interferes with the transcription machinery. This blockage may be due to the expanded $(GAA)_n$ repeats and could have a direct impact on the RNAPII. In this regard, several groups have reported that GAA.TTC repeats adopt unusual DNA structures that impede the progress of the RNA polymerase and disturb transcription in a length dependent manner. These structures might be present either as sticky DNA, which is formed by the association of two purine.purine.pyrimidine triplexes (Bidichandani, Ashizawa and Patel, 1998; Ohshima *et al.*, 1998; Sakamoto *et al.*, 1999, 2001; Grabczyk and Usdin, 2000), or as persistent DNA-RNA hybrids known as R-loops (Grabczyk, Mancuso and Sammarco, 2007; Reddy *et al.*, 2011; Groh *et al.*, 2014).

Although these unusual spatial conformations caused by the expanded $(GAA)_n$ repeats provide a logical explanation for reduced frataxin mRNA levels, the presence of such structures has been mainly described in vitro or in *Escherichia coli*. However, one group has described so far the presence of such structures in both human FRDA cells and model cell lines (Groh *et al.*, 2014). For this reason, more evidence is needed to understand whether these DNA conformations occurs in patients and what is their contribution to FRDA pathology.

1.4.3. DNA methylation

DNA methylation is an epigenetic mechanism carried out by DNA methyl-transferase (DNMT) enzymes. It involves the transfer of a methyl group that binds

covalently onto the C5 position of the cytosine to form 5-methylcytosine (5mC). This direct chemical modification of the DNA is involved in gene regulation and cell differentiation (Holliday and Pugh, 1975; Compere and Palmiter, 1981). Currently, it is well recognized that DNA methylation, together with other regulators, is a major epigenetic feature influencing gene expression.

Amongst all human tissues, the brain has one of the highest levels of DNA methylation. Despite this fact, 5mC only accounts for roughly 1% of nucleic acids in the human genome (Ehrlich *et al.*, 1982). The majority of DNA methylation takes place on cytosines that precede a guanine, which are frequently referred as CpG sites. In general, mammalian genomes are depleted of CpG sites, but the existing ones are widely spread across the genome where they are heavily methylated (Moore, Le and Fan, 2012). Methylation of these sites occurs, with the exception of CpG islands, which have been proposed to be methylation-free zones (Bird *et al.*, 1985). The majority of gene promoters, approximately 70%, reside within CpG islands (Saxonov, Berg and Brutlag, 2006). Given that many transcription factor binding sites are rich in GCs, it is likely that CpG islands enhance binding to transcriptional start sites. Despite CpG islands' lack of common promoter elements, they enhance the accessibility of DNA and promote transcription factor binding (Moore, Le and Fan, 2012).

When CpG islands get methylated, stable silencing of gene expression takes place (Mohn *et al.*, 2008). It is commonly accepted that CpG methylation reduces the probability of transcription factor binding or that it creates additional binding sites for proteins such as MeCP2, that recognise methylated DNA and concomitantly recruit chromatin modifying enzymes like HDACs (Bird and Wolffe, 1999;

Dhasarathy and Wade, 2008). Therefore, this suggests that methylation of CpG islands leads to gene inactivation.

In FRDA, it has been shown that the region adjacent to the $(GAA)_n$ repeats is methylated in both unaffected and affected individuals, with DNA methylation being more extensive in FRDA patients (Greene *et al.*, 2007). Additionally, in autopsy samples of FRDA patients including brain, cerebellum and heart, the regions flanking the $(GAA)_n$ repeats have shown a shift in their DNA methylation profile. This profile shows hypermethylated CpG sites upstream of the repeats and downstream CpG sites becoming consistently hypomethylated (Al-Mahdawi *et al.*, 2008). Furthermore, studies on peripheral blood mononuclear cells (PBMCs) also reported considerably higher levels of DNA methylation, particularly upstream of the expanded repeats (Castaldo *et al.*, 2008; Evans-Galea *et al.*, 2012). Castaldo and colleagues reported that the extent of methylation is proportional to the size of the expansion, meanwhile Evans-Galea and colleagues presented a positive correlation between level of DNA methylation, *FXN* gene silencing, and disease severity. Interestingly, the 5′ untranslated region (UTR) of the *FXN* gene did not exhibit any difference in terms of DNA methylation when comparing healthy and FRDA-patient fibroblasts (De Biase *et al.*, 2009).

In the last few years, an alternative DNA modification, 5-hydroxymethylcytosine (5hmC) was described. It is formed by oxidation of 5mC via ten-eleven translocation (TET) enzymes (Kriaucionis and Heintz, 2009; Tahiliani *et al.*, 2009). This alternative modification has been proposed to reduce the affinity of 5mC–specific binding proteins such as histone deacetylase– associated repressive complexes, therefore modifying chromatin states (Szulwach *et al.*, 2011). Al-Mahdawi and

colleagues have recently shown that in the upstream region of the GAA repeats, DNA methylation mainly consists of 5hmC rather than 5mC. A phenomenon that was observed in at least one CpG site (Al-Mahdawi *et al.*, 2013). These new findings suggest that 5hmC may be an important epigenetic mark that contributes to FRDA pathogenesis. A summary of the methylation changes in the *FXN* gene is described in Table 3.

Table 3. DNA methylation changes in FRDA models

Chromatin modification	Localization	FRDA model	References
5mC ↑	$(GAA)_n$ upstream	Lymphoblasts	(Greene *et al.*, 2007)
5mC ↑	$(GAA)_n$ upstream	PBMCs PBMC's and buccal cells	(Castaldo *et al.*, 2008) (Evans-Galea *et al.*, 2012)
5mC ↓	$(GAA)_n$ downstream	PBMC's and buccal cells	(Evans-Galea *et al.*, 2012)
5mC ↑	$(GAA)_n$ upstream	Human brain and heart	(Al-Mahdawi *et al.*, 2008)
5mC ↓	$(GAA)_n$ downstream	Human brain and heart	(Al-Mahdawi *et al.*, 2008)
5hmC ↑	$(GAA)_n$ upstream	Human cerebellum and heart	(Al-Mahdawi *et al.*, 2013)

Increased ↑, decreased ↓

1.4.4. Heterochromatinization of the FXN gene

Molecular mechanisms of pathology develop beyond the formation of unusual DNA structures. In the last few years, heterochromatin formation, histone modifications and DNA methylation of the *FXN* gene have emerged as key mechanisms.

The human genome is thought to be comprised of over two-thirds of repetitive elements (de Koning *et al.*, 2011) and heterochromatin is in fact thought to have evolved as a protective response to restrict the spread of these elements over the genome (Bashkirov, 2002). Heterochromatinization of repetitive DNA is considered to be important for the maintenance of the nuclear architecture needed for the spatial configuration of centromeres and sister chromatid segregation during cell division (Fisher and Merkenschlager, 2002). Heterochromatin is invasive and it tends to affect the expression of nearby genes. This phenomenon was first described in *Drosophila melanogaster* where the gene responsible for red eye colour, which is considered euchromatic, was translocated to the vicinity of pericentromeric heterochromatin as a consequence of exposure to radiation. The resulting phenotype was a mosaic eye colour caused by the stochastic expression of the gene in some cells but not in others. This phenomenon is known as position effect variegation (PEV) and it refers to a gene being silenced just in a proportion of cells of the same lineage (Muller, 1930).

Festenstein and colleagues have shown that expanded $(GAA)_n$ repeats are capable of silencing a nearby gene. They showed that the expression of a human hCD2 transgene with a truncated locus control region, exhibits a variegating pattern when it is placed close to pericentromeric heterochromatin (Festenstein *et al.*, 1996). Additionally, when long microsatellite $(GAA)_n$ tracts were fused with the hCD2 gene, in a transgenic mouse model, they also induced heterochromatic silencing, even when the construct was integrated into a euchromatic location (Saveliev *et al.*, 2003). Furthermore, in FRDA the spreading of heterochromatin from the expanded $(GAA)_n$ repeats is even more obvious as seen by Chan and colleagues (Chan *et al.*,

2013). All these findings suggest that the abnormal heterochromatinization of the *FXN* gene and the deriving transcriptional repression are indeed caused by expanded intronic $(GAA)_n$ elements.

1.4.5. Histone modifications

As previously mentioned, biochemical modifications of histones alter the degree of their affinity towards DNA. This is possible either by changing the histone's electrostatic charge or by creating conformational alterations (Kouzarides, 2007; Bannister and Kouzarides, 2011). Chromatin compaction is thought to be regulated by the intermolecular interactions of histones with DNA as well as by interactions between other histones from neighbouring nucleosomes. Moreover, histones could also interact with other proteins, for example HP1, to confer a higher order compactness to DNA (Bannister *et al.*, 2001). Amongst the many covalent histone modifications, the most prevalent and well studied are the acetylation and methylation of lysine (K) residues.

Histone acetylation

Acetylation of lysine residues is a highly dynamic and regulated process carried forward by two families of enzymes with opposing actions, namely histone acetyl-transferases (HATs) and histone deacetylases (HDACs). HATs utilize the cofactor acetyl CoA to catalyse the transfer of an acetyl group to lysine side chains at the ε-amino group. By doing so, they potentially neutralize the lysine's positive charge with a direct impact on the interactions between histones and DNA; more precisely, making it weaker. On the contrary, HDACs reverse lysine acetylation, restoring the positive charge of the K residues, therefore stabilizing the local chromatin

architecture (Bannister and Kouzarides, 2011). In mammals, eighteen different HDACs have been identified. They are divided into four classes. Class I consists of HDACs 1, 2, 3, and 8. Class II consists of HDACs 4, 5, 6, 7, 9 and 10. Class III HDACs, known as sirtuins comprise SIRT1, SIRT2, SIRT3, SIRT4, SIRT5, SIRT6 and SIRT7. Lastly, class IV HDACs consists of HDAC 11 (Kouzarides, 2007).

The acetylation of multiple lysine residues is considered to generate a cumulative effect of loosening up the chromatin structure. Amongst the aforementioned residues, the acetylation of histone 3 (H3) in lysines 9 and 14, and of histone 4 (H4) in lysine 16 (H3K9, H3K14 and H4K16), are known to be strong marks for transcriptionally active euchromatin and to be the hallmark of gene activation (Workman and Kingston, 1998; Shogren-Knaak *et al.*, 2006; Karmodiya *et al.*, 2012).

In all eukaryotes, heterochromatin is characterized by histone hypoacetylation of certain residues on histones H3 and H4 (Elgin *et al.*, 2003; Kourmouli *et al.*, 2004). In FRDA, the first report of histone modifications at the *FXN* locus, showed that the coding region of *FXN* alleles in lymphoblastoid cell lines, was severely depleted in histones acetylated at the following lysine residues: H3K9, H3K14, H4K5, H4K8, H4K12 and H4K16 (Herman *et al.*, 2006). Since then, several other reports have supported this finding. A summary is presented in Table 4.

Table 4. Histone acetylation changes at the *FXN* locus

Chromatin modification	Localization	FRDA model	References
H3K9 ↓	*FXN* promoter	Lymphoblasts	(Herman *et al.*, 2006) (Kumari, Biacsi and Usdin, 2011)
		Human brain	(Al-Mahdawi *et al.*, 2008)
		HEK reporter cell line	(Lufino *et al.*, 2013)

H3K9 ↓	$(GAA)_n$ upstream	Lymphoblasts	(Herman *et al.*, 2006) (Kumari, Biacsi and Usdin, 2011) (Kim, Napierala and Dent, 2011)
		Human brain	(Al-Mahdawi *et al.*, 2008)
		HEK reporter cell line	(Soragni *et al.*, 2008) (Lufino *et al.*, 2013)
H3K9 ↓	$(GAA)_n$ downstream	Lymphoblasts	(Herman *et al.*, 2006) (Kumari, Biacsi and Usdin, 2011)
		Human brain	(Al-Mahdawi *et al.*, 2008)
		HEK reporter cell line	(Soragni *et al.*, 2008) (Lufino *et al.*, 2013)
H3K14 ↓	$(GAA)_n$ upstream	Lymphoblasts	(Herman *et al.*, 2006) (Kumari, Biacsi and Usdin, 2011) (Kim, Napierala and Dent, 2011)
		HEK reporter cell line	(Soragni *et al.*, 2008)
H3K14 ↓	$(GAA)_n$ downstream	Human brain	(Al-Mahdawi *et al.*, 2008)
		Lymphoblasts	(Kumari, Biacsi and Usdin, 2011)
		HEK reporter cell line	(Soragni *et al.*, 2008)
H4K5 ↓	*FXN* promoter	Lymphoblasts	(Kumari, Biacsi and Usdin, 2011)
H4K5 ↓	$(GAA)_n$ upstream	Lymphoblasts	(Herman *et al.*, 2006) (Kumari, Biacsi and Usdin, 2011)
		HEK reporter cell line	(Soragni *et al.*, 2008)
H4K5 ↓	$(GAA)_n$ downstream	Lymphoblasts	(Herman *et al.*, 2006) (Kumari, Biacsi and Usdin, 2011)
		Human brain	(Al-Mahdawi *et al.*, 2008)
		HEK reporter cell line	(Soragni *et al.*, 2008)
H4K8 ↓	*FXN* promoter	Human brain	(Al-Mahdawi *et al.*, 2008)
		HEK reporter cell line	(Lufino *et al.*, 2013)
H4K8 ↓	$(GAA)_n$ upstream	Lymphoblasts	(Herman *et al.*, 2006)
		HEK reporter cell line	(Soragni *et al.*, 2008) (Lufino *et al.*, 2013)
H4K8 ↓	$(GAA)_n$ downstream	Lymphoblasts	(Herman *et al.*, 2006)
		Human brain	(Al-Mahdawi *et al.*, 2008)
		HEK reporter cell line	(Soragni *et al.*, 2008) (Lufino *et al.*, 2013)

H4K12 ↓	$(GAA)_n$ upstream	Lymphoblasts	(Herman *et al.*, 2006)
H4K12 ↓	$(GAA)_n$ downstream	Lymphoblasts Human brain	(Herman *et al.*, 2006) (Al-Mahdawi *et al.*, 2008)
H4K16 ↓	*FXN* promoter	Lymphoblasts	(Kumari, Biacsi and Usdin, 2011)
H4K16 ↓	$(GAA)_n$ upstream	Lymphoblasts	(Herman *et al.*, 2006) (Kumari, Biacsi and Usdin, 2011)
H4K16 ↓	$(GAA)_n$ downstream	Lymphoblasts Human brain	(Herman *et al.*, 2006) (Kumari, Biacsi and Usdin, 2011) (Al-Mahdawi *et al.*, 2008)

Decreased ↓

Histone methylation

Histone methylation primarily occurs on the side chains of lysines and arginines. As opposed to histone acetylation, methylation does not alter the charge of the histone. Instead it introduces conformational changes in response to hydrophobic alterations. This could be explained given that lysine methylation progressively increases hydrophobicity and could interfere with the intra- or intermolecular hydrogen-bond interactions of the ε-amino group (Lee *et al.*, 2005; Kouzarides, 2007). Additionally, it is thought that histone methylation functions as a nucleation site for effector proteins, proteins that interact preferentially with methylated substrates, and often elicit their function by recruiting factors that directly impact chromatin (Ng *et al.*, 2009). Hence, the outcome of histone methylation on transcription could be either repression or activation, depending on the specific location of the methylated residue (Lee *et al.*, 2005; Kouzarides, 2007). Another difference between acetylation and methylation of histones is that there is an added level of complexity in histone methylation. Lysines can be mono-, di- or tri-

methylated by protein lysine methyltransferases (PKMTs), while arginines can be mono-, symmetrically or asymmetrically di-methylated by protein arginine methyltransferases (PRMTs) (Bannister and Kouzarides, 2011).

Histone methylation is carried out by a variety of histone methyltransferases (HMTs) (Figure 3) and it is reversed by histone demethylases. HMTs exhibit exquisite substrate specificity, not only for particular histones and their lysine residues, but also for free histones vs. nucleosomes. Dot1, Set2, and SET8, are able to methylate exclusively histone tails presented in the context of nucleosomes. On the contrary, other HMTs, such as Set9, Smyd2, LSD1 and Smyd3, prefer free histones or are capable of methylating tails from both free histones and nucleosomes (Fang *et al.*, 2002; Nishioka *et al.*, 2002; Strahl *et al.*, 2002; van Leeuwen, Gafken and Gottschling, 2002; Huang and Berger, 2008).

Amongst the various different types of histone methylation, modification of H3K4, H3K36, and H3K79 have been correlated with transcriptional activation, while methylation of H3K9, H3K27, and H4K20 are marks of repressive chromatin states (Lachner, O'Sullivan and Jenuwein, 2003; Schotta *et al.*, 2004). H3K9 di- and tri-methylation (H3K9me2, H3K9me3) are associated with silent genes in a region of 10 kb surrounding the TSS. H3K9 methylation is particularly enriched in constitutive heterochromatin regions such as satellite or telomeric repeats (Peters *et al.*, 2001; Mikkelsen *et al.*, 2007). Levels of H3K27me2 and H3K27me3 are higher at silent promoters, whereas H3K27me1 signals are higher downstream of the TSS of active promoters compared to silent ones (Barski *et al.*, 2007). Finally, H4K20 methylation has also been associated with repressive chromatin. H4K20me3 is a

heterochromatic histone mark that is enriched at pericentromeric heterochromatin regions (Schotta *et al.*, 2004).

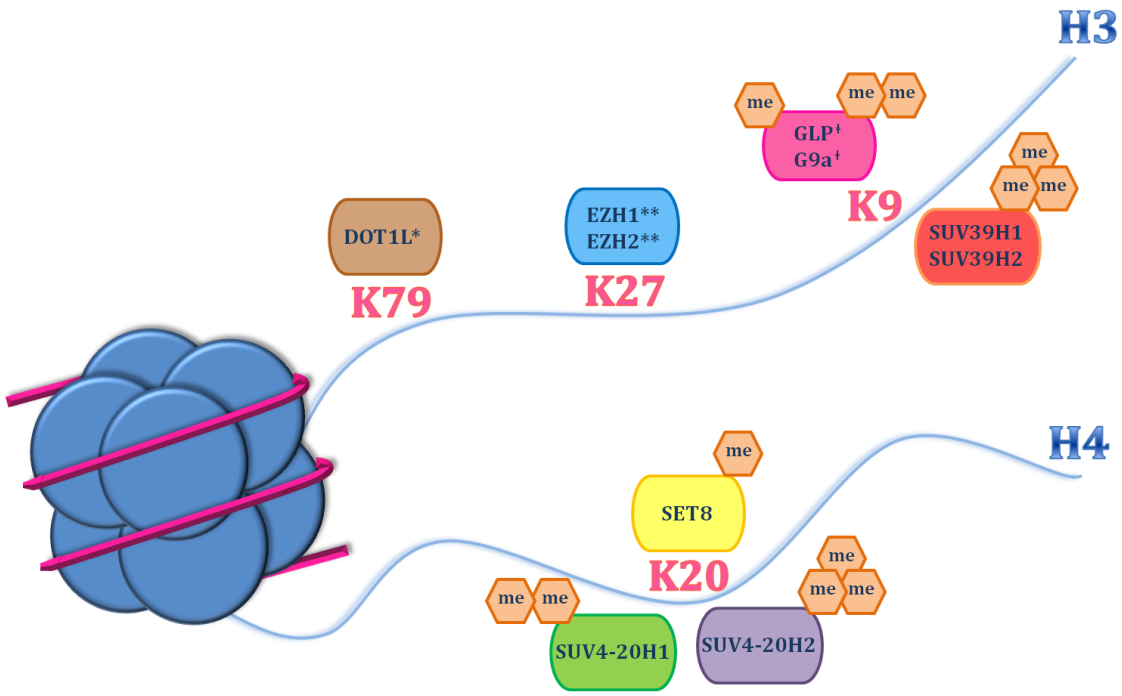


Figure 3. Schematic representation of the histone tails of H3 and H4 and the most relevant lysine residues for this work

*Disrupter of telomeric silencing 1-like (DOT1L) is currently the only enzyme found in mammals to catalyze me1, me2 and me3 of H3K79 (Feng *et al.*, 2002; Pan *et al.*, 2018) **Enhancer of Zeste Homolog 1-2 (EZH1, EZH2) are two homologs identified in mammalian cells to be responsible for all types of methylation in H3K27 (Pan *et al.*, 2018) ‡G9a and GLP are the primary enzymes responsible for H3K9me1 and H3K9me2 (Tachibana *et al.*, 2005; Shinkai and Tachibana, 2011). G9a is also known as Euchromatic histone-lysine N-methyltransferase 2 (EHMT2). GLP is also known as Euchromatic histone-lysine N-methyltransferase 1 (EHMT1). SUV4-20H1 (Suppressor of variegation 4-20 homolog 1), SUV4-20H2 (Suppressor of variegation 4-20 homolog 2).

In FRDA, chromatin immunoprecipitation (ChIP) data describing the histone modification changes on the silenced *FXN* locus have been collected. Generally, these studies report high levels of heterochromatin marks in the first intron of the $(GAA)_n$ expanded, pathologically silenced *FXN,* in a similar manner as with DNA methylation. But the silencing of a gene is a concert of various negative effects of certain epigenetic marks. It is orchestrated by DNA methylation, hypoacetylation of

certain histone residues (e.g. H3K9), together with increased methylation of histones H3 and H4, such as H3K9me2, H3K9me3, H3K27me3, and H4K20me3. The relationship between all these marks is still under study, but it is clear that more than one is necessary for gene silencing. Table 5 shows a summary of the histone methylation marks on the *FXN* locus.

Table 5. Histone methylation marks on the *FXN* gene

Chromatin modification	Localization	FRDA model	References
H3K4me2 ↓	*FXN* promoter	Lymphoblasts	(Kumari, Biacsi and Usdin, 2011)
H3K4me2/3 ↓	$(GAA)_n$ upstream	Lymphoblasts	(Punga and Bühler, 2010; Kim, Napierala and Dent, 2011; Kumari, Biacsi and Usdin, 2011)
H3K4me2/3 ↓	$(GAA)_n$ downstream	Lymphoblasts	(Punga and Bühler, 2010; Kumari, Biacsi and Usdin, 2011)
H3K9me2/3 ↑	*FXN* 5'UTR/promoter	Human brain	(Al-Mahdawi *et al.*, 2008)
		Fibroblasts	(De Biase *et al.*, 2009)
		HEK reporter cell line	(Lufino *et al.*, 2013)
H3K9me2/3 ↑	$(GAA)_n$ upstream	Lymphoblasts	(Herman *et al.*, 2006; Greene *et al.*, 2007; Punga and Bühler, 2010; Kim, Napierala and Dent, 2011; Chan *et al.*, 2013)
		Human brain	(Al-Mahdawi *et al.*, 2008)
		HEK reporter cell line	(Soragni *et al.*, 2008; Kim, Napierala and Dent, 2011; Lufino *et al.*, 2013)
H3K9me2/3 ↑	$(GAA)_n$ downstream	Lymphoblasts	(Punga and Bühler, 2010; Chan *et al.*, 2013)

H3K9me2/3 ↑	$(GAA)_n$ downstream	Human brain HEK reporter cell line	(Al-Mahdawi *et al.*, 2008) (Soragni *et al.*, 2008; Kim, Napierala and Dent, 2011; Lufino *et al.*, 2013)
H3K27me3 ↑	*FXN* 5'UTR	Fibroblasts	(De Biase *et al.*, 2009)
H3K27me3 ↑	$(GAA)_n$ upstream	Lymphoblasts	(Kim, Napierala and Dent, 2011; Chan *et al.*, 2013)
H3K27me3 ↑	$(GAA)_n$ downstream	Lymphoblasts	(Chan *et al.*, 2013)
H3K36me3 ↓	$(GAA)_n$ upstream	Lymphoblasts	(Punga and Bühler, 2010)
H3K36me3 ↓	$(GAA)_n$ downstream	Lymphoblasts	(Punga and Bühler, 2010; Kumari, Biacsi and Usdin, 2011)
H3K79me2 ↓	$(GAA)_n$ upstream	Lymphoblasts / HEK reporter cell line	(Kim, Napierala and Dent, 2011)
H3K79me2 ↓	$(GAA)_n$ downstream	Lymphoblasts / HEK reporter cell line	(Kim, Napierala and Dent, 2011)
H4K20me3 ↑	$(GAA)_n$ upstream	Lymphoblasts	(Kim, Napierala and Dent, 2011)
H4K20me1 ↓	$(GAA)_n$ downstream	Fibroblasts	(Li *et al.*, 2015)

Increased ↑, decreased ↓

1.4.6. Nuclear localization of the FXN locus

Within the nucleus, chromatin is not randomly organized and its spatial localization takes part in the regulation of several gene functions. In addition to the compaction state of chromatin, another level of regulation of gene function is the localization of different loci in the nucleus (Lemaître and Bickmore, 2015). Generally, transcriptionally repressed chromatin is sequestered either by the nucleolus or the nuclear periphery; whereas active chromatin tends to be internal (Akhtar and Gasser, 2007; Bickmore and Van Steensel, 2013). During development, the

repositioning of thousands of genes towards and away from the nuclear envelope has been associated with changes in transcription and replication timing. It has been shown that nuclear reorganization is driven by chromatin remodelling and gene relocalization is induced by chromatin decondensation without affecting transcription (Therizols *et al.*, 2014).

The nuclear envelope is a membrane bilayer whose inner side is coated with lamins and many other proteins that together form the nuclear lamina (NL). It is thought that being a large surface that establishes contacts with chromatin while remaining spatially constrained by its localization on the inner wall of the nuclear envelope, the nuclear lamina has a role in the spatial organization of chromosomes (Pombo and Dillon, 2015). This filamentous protein network has been shown to accumulate heterochromatin. It is associated with marks of gene repression (enrichment in H3K9me2 and H3K27me3) and induces H4 deacetylation (Somech *et al.*, 2005; Kind and van Steensel, 2010).

Recently, using a variety of cell models, our laboratory has found a marked increased positioning at the NL of the expanded GAA repeat *FXN* allele with a concomitant reduction in the number of transcriptionally active *FXN* alleles. Although the number of normal and expanded alleles located in the NL are significantly different, the study also found that the NL reduces the expression of both normal and expanded alleles to a similar extent (Silva *et al.*, 2015). This demonstrates that the NL's repressive action is irrespective of the GAA expansion. Furthermore, the inhibition of histone deacetylases up-regulates *FXN* transcription from both alleles, but only repositions the expanded alleles away from the NL. This might be due to the heterochromatic state of the FXN gene as a result of the GAA

expansion. In this case, it is tempting to speculate that enforced acetylation might be playing a role in the decondensation of chromatin brining, in this case, just the expanded allele to the centre of the nucleus. This pioneering work is the first one to show that the sub-cellular localization of the *FXN* locus might be playing a key role in *FXN* transcriptional state and epigenetic status.

1.5. Epigenetic therapeutic approaches for FRDA

1.5.1. DNA demethylating agents

Taking into account the pivotal role of epigenetics in FRDA, proteins that control chromatin remodelling are promising targets in the pursue of a therapy. For instance, DNA demethylating agents were shown to rescue frataxin expression in FRDA models. The first report of a demethylating agent used to study *FXN* restoration was made by Sandi and colleagues (Sandi, Al-Mahdawi and Pook, 2013). They briefly described some observations where they used nucleoside analogue DNMT inhibitors, 5-aza-2'-deoxycytidine (5-aza-CdR) and Zebularine. They discuss a one- to two-fold increase of frataxin expression in cells of a transgenic mouse model, but a decrease in frataxin expression in human FRDA cells cultured *in vitro* (Sandi, Al-Mahdawi and Pook, 2013). Later on the same year, another study was published with the same drug (5-aza-CdR), but now in combination with transcription activator-like effectors (TALE) proteins (Chapdelaine *et al.*, 2013). TALE proteins can be produced to target any nucleotide sequence starting with a thymidine and they can be fused with a transcription activation domain (TAD) for induction of expression of a gene located near the DNA attachment site (Cermak *et al.*, 2011). The work by Chapdelaine and colleagues, showed that TALE proteins

targeted to the *FXN* promoter can increase mRNA and protein levels by two-fold in FRDA patient-derived fibroblasts, but that the combination of these proteins with 5-aza-CdR produces little or no effect.

In a more recent study, human periodontal ligament cells (hPDL) of FRDA patients were treated with 5-aza-CdR. In accordance with the report by Chapdelaine and colleagues, 5-aza-CdR showed not to change the methylation pattern in the region upstream of the repeats or to change frataxin expression (Quesada *et al.*, 2015).

Even though DNA methylation is one of the most studied epigenetic changes in FRDA, to date, the evidence available supporting a potential therapeutic use of DNMT inhibitors, is still contradictory. Further studies are needed to elucidate whether this therapeutic avenue can be exploited to reverse the silencing of *FXN* gene.

1.5.2. Histone acetylation modifiers

Another promising therapeutic strategy under scrutiny is the use of HDAC inhibitors (HDACi). This class of molecules can have an effect on transcription by inducing general hyperacetylation of histones, therefore allowing the transcriptional activation of certain genes through relaxation of chromatin conformation (Butler and Bates, 2006).

Preliminary evidence on the potential efficacy of HDACi in FRDA came from Sarsero and colleagues. Using a EGFP reporter cell line, they observed that sodium butyrate, a compound with HDAC inhibition activity, induces a small increase of *FXN* expression (Sarsero *et al.*, 2003). A few years later, BML-210 a commercially available HDAC inhibitor, was shown to significantly increase (approximately 2-

fold) frataxin mRNA expression in FRDA lymphoblastoid cells (Herman *et al.*, 2006). These results led to a further development of HDAC inhibitors and the generation of three 2-aminobenzamide compounds, named 106, 136, and 109. These compounds were shown to significantly increase frataxin mRNA and protein levels in various models of FRDA (Chou, Herman and Gottesfeld, 2008; Rai *et al.*, 2010; Sandi *et al.*, 2011). Amongst all of those compounds, compound 109 was the most promising for FRDA treatment (Soragni *et al.*, 2012). In 2014 a phase I clinical trial using 109, known as well as RG2833 was completed. Even though it increased frataxin mRNA levels in patients, the trial did not meet the safety end-points as the metabolites formed in the body were potentially deleterious (Soragni *et al.*, 2014). Currently, a new generation of HDAC inhibitors is under development (Soragni *et al.*, 2015).

Finally, our laboratory has also made a contribution towards the discovery of novel HDAC inhibitors. In an *in silico* library screen of 25,000 compounds, C5 was identified. It was shown to up-regulate *FXN* gene expression in patient lymphoblastoid cells, while increasing the acetylation of H3K9 and H4K8 (Lufino *et al.*, 2013).

1.5.3. Histone methylation modifiers

Given the fact that hypermethylation of histones at the *FXN* locus has been associated with transcription repression, HMT inhibitors have also been evaluated as potential therapy for FRDA, considering that they may induce a more open chromatin structure of the pathogenic *FXN* gene.

Punga and Bühler, using the HMT inhibitor - BIX-01294, which inhibits the methyltransferase G9a, identified a significant reduction in di- and tri-methylation

of H3K9 in FRDA lymphoblastoid cells, but without an increase in frataxin mRNA levels (Punga and Bühler, 2010). Furthermore, nicotinamide, which is classified as a class III HDAC inhibitor, has been shown to also decrease the methylation marks H3K9me3 and H3K27me3, and to increase frataxin expression in FRDA cells and mouse models (Chan *et al.*, 2013). An open-label dose-escalation study established that nicotinamide has the ability to mildly increase frataxin mRNA and protein levels in PBMCs when administered at doses up to 200 times the recommended daily allowance. Unfortunately, these doses produce side effects and more importantly, this study did not demonstrate significant neurologic improvement of FRDA patients (Libri *et al.*, 2014).

Even though several new HMT inhibitors have been identified, it still remains unclear whether this class of compounds can provide an effective tool to rescue frataxin levels in FRDA patients.

1.6. Other therapeutic interventions

Several therapeutic strategies have been developed recently to treat FRDA patients. The main approaches aim to modulate mitochondrial function and mitochondrial protective pathways, to increase frataxin expression and gene therapy. In this section, some of these strategies will be described.

1.6.1. Mitochondrial function-related drugs and protective pathways

To improve mitochondrial function, molecules that are known to be antioxidants have been used in FRDA patients. The rationale of using these molecules is that a reduction of oxidative stress in key tissues should reduce the neurodegeneration and cell death seen in FRDA. EPI-743 is an enhanced version of vitamin E and it

shares features with coenzyme Q. It was used in an 18 month open-label study in three patients with G130V point mutations and showed that after 6 months of treatment the average FARS scores (a measure of disease progression) improved by 9% (Sullivan *et al.*, 2016). Furthermore, a double-blind placebo-controlled trial in patients with FRDA over a 6- month period, followed by an 18-month phase was conducted and concluded that the drug was safe and well tolerated (Zesiewicz *et al.*, 2017). Even though the short term results at 6 months did not show any improvement in the patients, the extended treatment up to 18 months achieved significantly higher scores on neurological measures when compared to natural history data (Zesiewicz *et al.*, 2017). However, the efficacy of EPI-743 is still under debate and more clinical evidence would be beneficial.

Omaveloxolone is another molecule with antioxidant properties which works by slowing down the degradation of nuclear factor erythroid-derived 2-related factor 2 (Nrf2). Nrf2 is a transcription factor that targets a large network of antioxidant enzymes by binding to DNA, specifically to the antioxidant response element. Thus, it has an impact on mitochondrial function by defending against reactive oxygen species (ROS) production (Holmström, Kostov and Dinkova-Kostova, 2016). In FRDA, decrease Nrf2 expression has been linked both *in vitro* and *in vivo*, to the down-regulation of the frataxin gene and decreased production of the frataxin protein (Paupe *et al.*, 2009; Shan *et al.*, 2013). Omaveloxolone is a semi-synthetic triterpenoid that restored mitochondrial membrane potential in fibroblasts from a mouse model of FRDA (Abeti *et al.*, 2015). Furthermore, another Nrf2 activator, namely dyclonine, appears to reverse frataxin deficiency in FRDA patient lymphoblasts and multiple mouse models (Sahdeo *et al.*, 2014). In addition,

dimethyl fumarate, another Nrf2-inducer, increased frataxin mRNA levels in *FXN*-silenced motor neurons (Petrillo *et al.*, 2017). All of these results point towards Nrf2 as a promising therapeutic target. Therefore, a multisite Phase II clinical trial (double-blind, placebo-controlled trial) of omaveloxolone capsules was conducted, where it showed improvements in mitochondrial and neurological function by induction of Nrf2 (Lynch *et al.*, 2017). In June 2017, Reata Pharmaceuticals received orphan drug designation for omaveloxolone for the treatment of FRDA and announced the start of the second part of the clinical study. Other promising drugs and therapeutic strategies and their stages of clinical/preclinical testing are summarized in Figure 4.

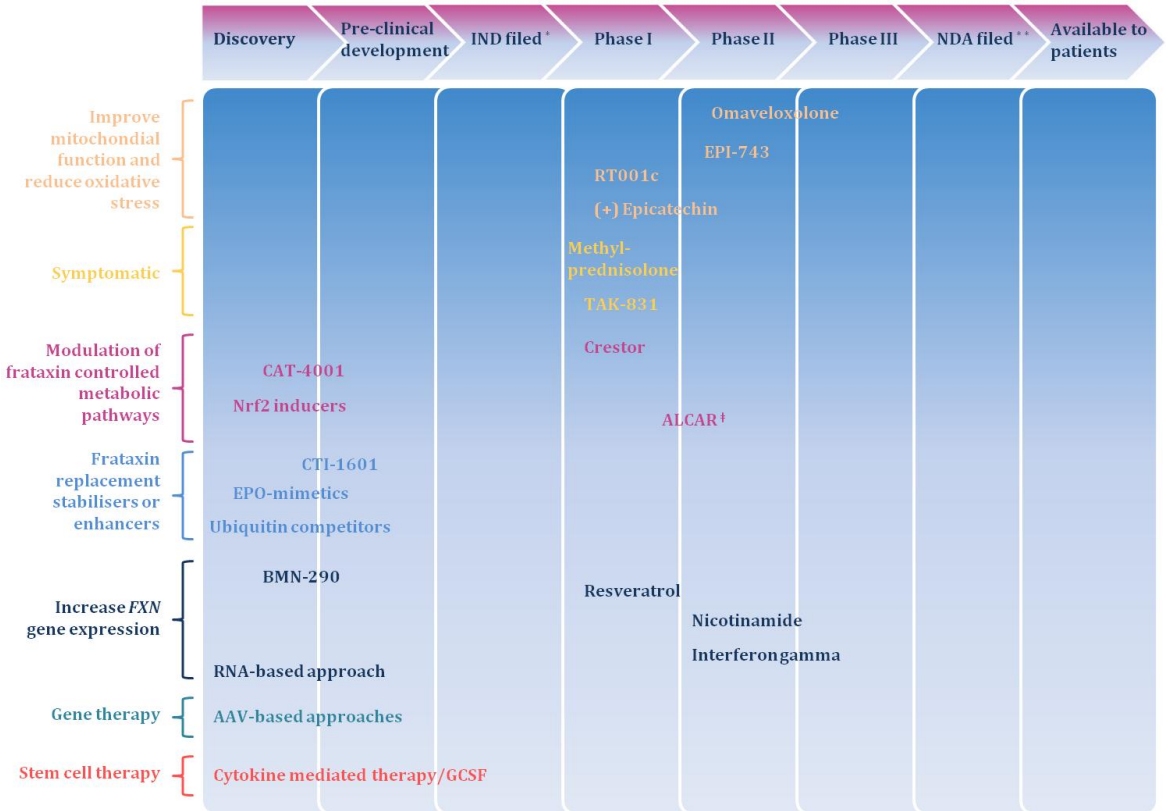


Figure 4. Friedreich's ataxia treatment pipeline

*IND filing is a regulatory stage with the United States Food and Drug Administration (FDA) **NDA filing is a new drug application filing with the FDA ǂ acetyl-l-carnitine. This figure is an adaptation of the research pipeline by the Friedreich's Ataxia Research Alliance (2018).

1.6.2. Frataxin-raising therapies

Erythropoietin (EPO), more precisely recombinant human erythropoietin (rhuEPO), has been shown to increase frataxin expression in lymphocytes, cardiomyocytes, and cardiofibroblasts *in vitro* and in primary lymphocytes of patients with renal disease (Sturm *et al.*, 2005). In light of these results, EPO was taken to a 6-month open-label trial in FRDA patients, which demonstrated therapeutic benefit, with significant improvements in frataxin levels and on scores on the Ataxia Rating Scales (Boesch *et al.*, 2008). However, half of the patients in the trial required phlebotomy at the end of the study due to excessive haemoglobin levels. Moreover, two additional open-label studies also found increases in frataxin, but without clinical improvements in disease symptoms (Nachbauer *et al.*, 2011; Saccà *et al.*, 2011). Furthermore, two double-blind placebo- controlled trials did not show differences in clinical outcomes between the drug treatment and the placebo groups (Mariotti *et al.*, 2012; Boesch *et al.*, 2014). Finally, small molecule EPO-mimetics showed benefits *in vitro* and in a mouse model of FRDA, suggesting that they might be beneficial for FRDA patients (Miller *et al.*, 2017).

Interferon gamma is another endogenous cytokine, which is involved in the immune response to viral infections. Interferon gamma-1b (Actimmune®) is a FDA-approved drug for the treatment of severe malignant osteopetrosis and chronic granulomatous disease. It has been tested in cell and mouse models of FRDA where it increased frataxin mRNA and protein levels (Tomassini *et al.*, 2012). Considering that the drug is FDA-approved and that it increased frataxin in various models, the drug was taken for clinical trial in FRDA. A 12-week open-label trial showed an average improvement in the FARS of 5 points without a significant change in

frataxin protein levels analysed in whole blood or buccal swab samples (Seyer *et al.*, 2015). In contrast, in an exploratory dose-escalation study that was carried out for 35 days, there were no changes in frataxin levels or neurologic function as measured by the SARA scale (Marcotulli *et al.*, 2016). Since none of the previously mentioned studies showed serious adverse effects and the drug was well tolerated, a phase III multicenter study was conducted. This study concluded that there was no statistically significant difference between the patients taking the drug compared to the placebo controls, as assessed by the modified FARS exam scores (Horizon Pharma, 2016). Whether or not this drug is going to be taken for further studies is unclear.

1.6.3. Gene therapy

This strategy has lately been the subject of intense research. A mouse model of FRDA with a *Fxn* conditional knockout in the heart has been used to show that the adeno-associated viral delivery of frataxin with a AAV9 based vector was efficacious in preventing cardiomyopathy *in vivo*. This effect was evident not only on presymptomatic FRDA mice, but also on mice experiencing heart failure (Perdomini *et al.*, 2014). Moreover, mice treated with the AAV9-frataxin showed increased expression of frataxin protein, reduced cardiac hypertrophy, and a prolonged lifespan versus control FRDA mouse models (Gérard *et al.*, 2014). These findings point to a potential future clinical use of AAV9-frataxin vectors.

High-capacity herpes simplex virus type 1 (HSV-1) based vectors have also been used to deliver *FXN* to FRDA fibroblasts, resulting in a reduction in their sensitivity to oxidative stress (Gomez-Sebastian *et al.*, 2007). Furthermore, the delivery of the same vector to adult mouse cerebellum cells increased the expression of *FXN* in the

brain (Gimenez-Cassina *et al.*, 2011). Finally, a mouse model in which frataxin was eliminated in neurons was injected with a HSV-1 amplicon vector expressing *FXN* into the brainstem, which effectively restored the motor coordination of the animals (Lim *et al.*, 2007). These results show that gene therapy has the potential to be used therapeutically to increase the expression of frataxin in FRDA patients, with potential clinical benefit.

1.7. Thesis hypothesis

The overall hypothesis of this thesis is that *FXN* can be up-regulated in various *in vitro* models of FRDA by directly targeting epigenetic modulators such as histone deacetylases and methyltransferases.

1.8. Thesis aims

The overall aim of this thesis is to target different histone deacetylases and methyltransferases to find therapeutic alternatives to restore frataxin protein expression and function.

This aim will be broken down according to the following results chapters:

Chapter 3. Exploring the role of histone deacetylase 3 and Euchromatic histone-lysine N-methyltransferase 2 in the expression of FXN

- To assess the effect of the down-regulation of HDAC3 and G9a on frataxin mRNA and protein levels.

Chapter 4. Identification of novel therapeutic targets for FRDA using the Structural Genomics Consortium (SGC) epigenetics probes collection

- To identify potential therapeutic targets for FRDA by screening a 36-compound epigenetic probe library set, which is part of the SGC.

Chapter 5. Validation of A-196 in FRDA patient-derived cell lines

- To assess the expression and function of FXN protein after A-196 treatment in FRDA patient-derived fibroblasts and lymphoblastoid cells.

Chapter 6. Improving the potency and stability of A-196 as a potential therapeutic molecule

- To study the effect of the combination of several epigenetic modifiers as well as several A-196 derivatives in the expression of FXN protein.

CHAPTER 2

Materials and Methods

2.1. Materials

2.1.1. Cell lines used

A list of the cell lines used in this study has been summarized in Table 6.

Table 6. List of the cell lines used in this study

Name	Type of cell	Affected	Number of GAA repeats	Supplier
FXN-Luc	HEK293	Resembling to non-affected	6	Generated in our lab (Silva *et al.*, 2015)
FXN-GAA-Luc	HEK293	Resembling to affected	~310	Generated in our lab (Silva *et al.*, 2015)
GM03816	Fibroblasts	Affected	330/380	Coriell Institute
GM04078	Fibroblasts	Affected	541/420	Coriell Institute
GM03440	Fibroblasts	Non-affected	normal/normal	Coriell Institute
GM15850	B-Lymphocyte	Affected	650/1030	Coriell Institute
GM16220	B-Lymphocyte	Affected	460/460	Coriell Institute
GM15848	B-Lymphocyte	Non-affected/carrier	830/normal	Coriell Institute
GM15851	B-Lymphocyte	Non-affected	normal/normal	Coriell Institute

The frataxin-luciferase reporter cell lines were built in a HEK293 (from embryonic kidney) background (Lufino *et al.*, 2013). These cells carry the human *FXN* locus and either 6 GAA repeats (*FXN*-Luc) resembling the wild type allele; or ~310 GAA repeats (*FXN*-GAA-Luc) resembling the pathological allele. These cell lines were

later modified with the MS2 protein-binding sites (MBS) to fluorescently label the transgenic FXN mRNA (Silva *et al.*, 2015). The cell lines containing the MBS cassette were used throughout this thesis, and for simplicity were named *FXN*-Luc and *FXN*-GAA-Luc. Figure 5 shows a schematic representation of both constructs.

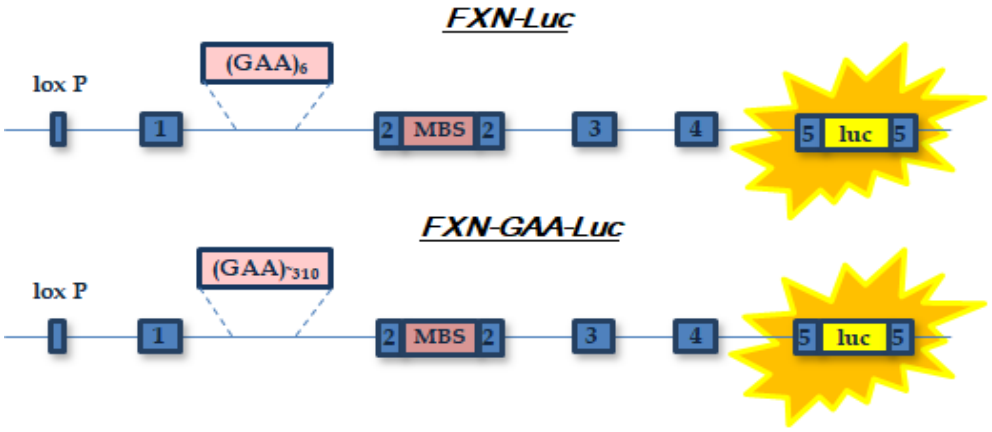


Figure 5. Schematic representation of the pBAC-FXN-MS2-Luc and pBAC-FXN-GAA-MS2-Luc vectors

Both constructs have MS2 protein-binding sites (MBS) to fluorescently label the transgenic FXN mRNA. MS2 bacteriophage coat protein was previously used to detect RNA in living cells (Silva *et al.*, 2015).

2.1.2. Media and buffers formulations

Reagents were obtained from Sigma-Aldrich unless otherwise stated

Table 7. List of the media and buffers formulations

Reporter cell line media	Dulbecco's Modified Eagle's Medium - high glucose + 10% Fetal Bovine Serum (FBS) + 1% L-Glutamine + 1% Penicillin-Streptomycin (Pen-Strep) + 100 mg/ml Hygromycin B (ThermoFisher Scientific)
Fibroblasts media	Minimum Essential Medium + 15% FBS + 1% MEM Non-essential Amino Acid Solution (100X) + 1% Pen-Strep
Lymphoblasts media	Roswell Park Memorial Institute (RPMI) 1640 Medium (ThermoFisher Scientific) + 15% FBS + 1% L-Glutamine + 1% Pen-Strep

Laemmli Buffer (6X)	12% Sodium dodecyl sulfate (SDS) + 30% β-mercaptoethanol + 60% glycerol + 0.012 % Bromophenol blue + 375 mM Tris pH 6.8
Western blot running buffer (10X)	144 g Glycine + 30.3 g Trizma® base + 10 g SDS + ultrapure water up to 1 L
Western blot Transfer buffer (10X)	144 g Glycine + 30.3 g Trizma® base + 0.375% SDS + ultrapure water up to 1 L
Western blot Transfer buffer (1X)	20% Methanol + 10% transfer buffer 10X + ultrapure water up to 1 L
TBS buffer (10X)	200 mL Tris 1 M pH 7.5 + 80 g Sodium chloride
Radioimmunoprecipitation assay (RIPA) buffer	50 mM Tris pH 8 + 150 mM Sodium chloride + 1 % IGEPAL® CA-630 + 0.5 % Sodium deoxycholate + 0.1 % SDS + 1 Protease inhibitor cocktail tablet per 10 ml
TBE buffer	45 mM Tris-borate + 1 mM EDTA
TE buffer	10 mM Tris-HCl + 1 mM EDTA - pH 8
KREBS buffer	1.26 M NaCl + 25 mM KCl + 250 mM $NaHCO_3$ + 12 mM NaH_2PO_4 + 12 mM $MgCl_2$ + 25 mM $CaCl_2$ Adjust pH to 7.2, autoclave
GET solution	20% glucose + 0.1 M EDTA + 1 M Tris pH 7 + distilled water up to 500 mL
NaOH/SDS solution	5 M NaOH + 20% SDS + distilled water up to 500 mL
3M Potassium Acetate	147.21 g of Potassium acetate + 57.7 mL of glacial acetic acid + distilled water up to 500 mL
Agarose electrophoresis 6X loading buffer	15% Ficoll in distilled water + 0.012 % Orange G + 0.012 % Bromophenol blue

2.1.3. List of primers

Table 8. List of primers and their sequences

qFXN-Luc-F*	5′-CGGAAAAGATGCTGGAAGTG-3′
qFXN-Luc-R*	5′-AACCAGGGCGTATCTCTTCA-3′
GAPDH-F	5′-GGTCTCCTCTGACTTCAACA-3′
GAPDH-R	5′-AGCCAAATTCGTTGTCATAC-3′
SUV4-20H1-F	5′-TGCGAATGTTTGCAACTGACA-3′
SUV4-20H1-R	5′- TTCGGCAATACAACCGACCA-3′
HPRT1-F	5′-GCCAGACTTTGTTGGATTTG-3′
HPRT1-R	5′-CTCTCATCTTAGGCTTTGTATTTTG-3′

* Primers anneal to exon 5a–luciferase junction (Lufino *et al.*, 2013).

2.1.4. List of antibodies

Table 9. List of antibodies used for western blotting, fluorescence cytochemistry, immunocytochemistry and 3D DNA FISH

Name	Concentration	Blocking	Species	Supplier	Catalog #
Actin	1:25000	5% w/v nonfat dry milk	Mouse	Abcam	ab49900
Frataxin	1:1000	5% w/v nonfat dry milk	Mouse	Abcam	ab110328
HDAC3	1:5000	5% w/v nonfat dry milk	Rabbit	Abcam	ab7030
G9a	1:500	5% BSA	Rabbit	Cell Signaling	3306
GLP	1:2000	3% BSA	Mouse	Abcam	ab41969
SUV4-20H2	1:500	5% w/v nonfat dry milk	Rabbit	Abcam	ab91224
EZH1	1:1000	5% BSA	Rabbit	Cell Signaling	42088
EZH2	1:2500	3% BSA	Rabbit	Cell Signaling	5246
DOT1L	1:1000	5% w/v nonfat dry milk	Rabbit	Abcam	ab72454
H4	1:2000	5% w/v nonfat dry milk	Rabbit	Abcam	ab10158
H4K20me1	1:500	5% w/v nonfat dry milk	Rabbit	Abcam	ab9051
H4K20me2	1:2000	5% w/v nonfat dry milk	Rabbit	Abcam	ab9052
H4K20me3	1:2000	5% w/v nonfat dry milk	Rabbit	Abcam	ab9053
Mouse IgG (HRP)	1:2500	5% w/v nonfat dry milk	Goat	Bio-Rad	170-6516
Rabbit IgG (HRP)	1:5000	5% w/v nonfat dry milk	Goat	Bio-Rad	170-6515
Mitotracker™ Deep Red FM*	1:10000	N/A	-	Invitrogen™	M22426
MitoSOX™ Red*	4 µM	N/A	-	Invitrogen™	M36008
Hoechst 33342*	1:5000	N/A	-	Invitrogen™	62249
Alexa Fluor™ 488 Phalloidin*	1:500	5% normal donkey serum	-	Invitrogen™	A12379

Nrf2*	1:200	5% normal donkey serum	Rabbit	Abcam	ab31163
Tom20*	1:200	5% normal donkey serum	Mouse	Santa Cruz	sc-17764
Rabbit IgG (Alexa Fluor™ 555) *	1:1000	5% normal donkey serum	Donkey	Invitrogen™	ab31572
Mouse IgG (Alexa Fluor™ 647)*	1:1000	5% normal donkey serum	Donkey	Invitrogen™	A31571
Lamin**		10% FBS in PBS	Goat	Santa Cruz	sc-6217
Cy3 Streptavidin**	1:200	3% BSA in 4X SSC	-	Jackson Immuno-Research	016-160-084
Anti-Digoxigenin-Fluorescein**	1:50	3% BSA in 4X SSC	Sheep	Roche	11207741910
Fluorescein anti-Sheep**	1:100	3% BSA in 4X SSC	Rabbit	Vector laboratories	FI-6000
Mouse IgG (Alexa Fluor™ 647) **	1:200	10% FBS in PBS	Goat	Invitrogen™	A21236

* Antibodies used for fluorescence cytochemistry and immunicytochemistry, ** antibodies used for 3D DNA FISH

2.1.5. siRNA sequences

Table 10. List of the siRNA sequences

Gene	Sequence 5′- > 3′	Supplier	Catalog #
HDAC3	GCAACCCAGCUGAACAACAtt	ThermoFisher Scientific	120349
EHMT2/G9a	GGACCUUCAUCUGCGAGUA GAACAUCGAUCGCAACAUC GGAGGUAGCCCGUUACAUG GGAGAGGUGUACUGCAUAG	Dharmacon	10919

EHMT1/GLP	UCAUGCUGGUGGACGGAAU GCUGCAGUAUCUCGGAAGA ACUUCUGCACAGCGGGUAA GGAAGGCGGUGACGAGUCU	Dharmacon	79813
KMT5B/SUV4-20H1	GUGUCAACUGGUCGAGAUA GGGUUGUAUUGCCGAACUU AUGUUUGACUUCAGGCGAA AAUGAAUACUAGCGCCUUU	Dharmacon	51111
KMT5C/SUV4-20H2	CGACAGAGUGACAGCACGA GUGCUAUCCUGGUGCUAUU GCGGUGAAGAGCUGUGACA GUGAAGGUGCUCCGGGACA	Dharmacon	84787
EZH1	GGAAAGGUCUAUGACAAAU GAAAGCGACAUGCUAUUGA GAUCCGUUCUGAUUAGUGA GCAGUCAAAGAAUCACUUA	Dharmacon	2145
EZH2	GAGGACGGCUUCCCAAUAA GCUGAAGCCUCAAUGUUUA UAACGGUGAUCACAGGAUA GCAAAUUCUCGGUGUCAAA	Dharmacon	2146
DOT1L	UGACUAUGGCGUCGAGAAA GCUAUGGAGAAUUACGUUU GCAGAAUCGUGUCCUCGAA AAGAGUGGAGGGAGCGAAU	Dharmacon	84444
Non targeting	UGGUUUACAUGUCGACUAA UGGUUUACAUGUUGUGUGA UGGUUUACAUGUUUUCUGA UGGUUUACAUGUUUUCCUA	Dharmacon	D-001810-10

Lysine methyltransferase 5B (KMT5B) also known as SUV4-20H1, Lysine methyltransferase 5C (KMT5C), also known as SUV4-20H2.

2.1.6. List of chemical probes

The epigenetic probe collection was obtained from the Structural Genomics Consortium (SGC). Prof Paul Brennan, Robert Quinlan and Roberta Mazzone from SGC, University of Oxford provided modified versions of the lead compound. Dr Suzanne Ackloo from SGC, University of Toronto provided negative probes for the lead compound.

A complete description of all of the SGC epigenetics chemical probes collection that were used in this thesis can be found in Table 17 of the appendices. All of the probes taken for validation are described in Table 11.

Table 11. List of chemical probes used for the validation of targets

Probe name	Target	Supplier	Catalog #
A-196	SUV4-20H1/H2	Sigma-Aldrich	SML1595
A-366	G9a/GLP	Sigma-Aldrich	SML1410
GSK343	EZH1/H2	Sigma-Aldrich	SML0766
GSK591	PRMT5	Sigma-Aldrich	SML1751
SGC0946	DOTL1L	Sigma-Aldrich	SML1107

2.2. Methods

2.2.1. Cell culture

All cell lines (Table 6) were cultured in the media previously described (Table 7) in a 5% CO_2 atmosphere at 37°C. Sub-culture of adherent cells was performed as follows: cells were rinsed with PBS and then incubated for five minutes with trypsin-EDTA (Sigma-Aldrich - T3924). Trypsin was then neutralised with media containing FBS, cells were spun (five minutes at 1500 rpm) and re-suspended at the

desired concentration in medium. Suspension cells were directly spun in the same conditions and seeded accordingly. Cells growing in suspension were regularly passaged by dilution in fresh medium in order to achieve a concentration of 250000 cells/mL.

2.2.2. siRNA-mediated down-regulation of targets

FXN-Luc and *FXN*-GAA-Luc cell lines were counted in an automated cell analyser NucleoCounter® NC-250™ (ChemoMetec) and seeded in a 12 well poly-L-lysine coated plate (12000 cells/well) in complete medium minus antibiotics. Cells were then allowed to grow for 24 hours. On the day of transfection, cells were rinsed in Opti-MEM (Gibco™ 31985047) prior to the liposomes delivery. siRNA and RNAiMAX transfection reagents (Gibco™ 13778075) were prepared in Opti-MEM. Final concentrations of 12 nM for HDAC3 siRNA, 12, 25 and 50 nM for G9a siRNA and 12 nM and 25 nM for the rest of the targets were used. Equal volumes of siRNA and RNAiMAX transfection reagent were mixed and allowed to form complexes for 20 minutes. The mix was then added to the cells drop-by-drop and incubated for six hours. The final concentration of RNAiMAX used for each condition was 2 µL/1200 mL/well. Subsequently, the media was supplemented with FBS and was completely changed the next day. Cells were collected for western blot, luciferase and qRT-PCR assays at different time points according to the assay.

2.2.3. Protein quantification

Protein content was quantified by Bicinchoninic acid (BCA) assay (Pierce™ BCA Protein assay kit 23227 Thermo Scientific™). Protein standards were prepared using Bovin Serum Albumin (BSA) in serial dilutions ranging from 1000 to 0 µg/mL.

The lysis reagent (RIPA buffer Table 7) used to extract protein was employed as a blank and to make the dilutions. Each sample (in triplicate) was incubated at 37°C for 30 minutes with the reagents, after which the absorbance was read at 562 nm using the Synergy HT plate reader (BioTek). Protein concentration was determined after subtracting the blank value from all samples and extrapolated from the standard curve.

For protein quantification of samples lysed in the luciferase assay lysis buffer the Pierce™ BCA Protein Assay Kit - Reducing Agent Compatible (23250 Thermo Scientific™) was used following manufacturer's instructions.

2.2.4. Western blot assay

Cells were washed in PBS and lysed directly on the plate with RIPA buffer (Table 7) on ice. The lysates were then transferred to a collection tube and sonicated for a few seconds at an amplitude of 5 (Fisher Scientific sonicator FB50). After that, samples were centrifuged at 1500 rpm for 15 min at 4°C and the supernatant collected. At this stage, protein concentration was measured. Samples were reduced in Laemmli buffer (Table 7) and incubated for 5 min at 95°C. Thirty micrograms of protein was resolved for 50 min at 200V on a 8%-15% SDS-polyacrylamide (handcast) gel electrophoresis. Following protein transfer onto a PVDF membrane (BioRad), the membrane was blocked in the corresponding blocking buffer and incubated with the primary antibodies at 4°C overnight, according to Table 9. HRP-conjugated secondary antibodies were used as previously specified in Table 9 and the GE Healthcare Amersham™ ECL™ Prime Western Blotting Detection Reagent (10308449 Fisher Scientific) was used to produce a chemiluminescent signal that was then captured on a ChemiDoc™ Imaging System (Bio-Rad). Protein relative

quantities were determined by densitometry using Image Lab software (Bio-Rad). β-actin was used as house-keeping gene to normalise protein loading (relative protein concentration).

2.2.5. Protein transfer from gel to membrane

PVDF membrane was activated for 20 seconds in methanol and then rinsed in distilled water. Membrane was equilibrated in transfer buffer 1X (see Table 7) for five minutes before the procedure. A western blot transfer sandwich was assembled as follows: gel holder cassette (cathode facing down), foam pad, three western blot filter papers, gel, membrane, three filter papers and foam pad before closing the cassette. Cassettes were fitted in the electron assembly pack and run for one hour at 350 mA, using a western blot transfer system (Bio-Rad).

2.2.6. Luciferase assay

Cells were washed in PBS and lysed directly onto the plate using the Cell Culture Lysis Reagent from the Luciferase Assay System (Promega#E1500). Lysates were transferred to microcentrifuge tubes, vortexed for 15 sec and then centrifuged at 10000 rpm for 15 sec. Twenty-five microlitres of the supernatant was transferred to a white opaque 96-well microplate (PerkinElmer). Luciferase activity was determined by measuring luminescence with a PHERAstar FSX microplate reader (BMG LABTECH) equipped with injectors pumps, using the following program: injection of 100 µl of Luciferase Assay Reagent, shaking of the plate for 3 sec at 300 rpm, followed by a 10 sec measurement read. Data was normalized to total protein concentration as determined by BCA protein assay (relative luciferase expression).

2.2.7. Adenylate kinase assay

The adenylate kinase assay (ToxiLight™ bioassay kit LT07-217 Lonza) was used to assess toxicity. This kit is based on the principle that a damaged cell loses its plasma membrane integrity, allowing the leakage of a number of factors from the cultured cells into the surrounding medium. Amongst these factors, adenylate kinase (AK), which is present in all cells, can be used to determine cytotoxicity and cytolysis, by measuring its release into the medium. The reaction is carried out by the addition of ADP (AK substrate), which is converted into ATP (Figure 6 A). Subsequently, this ATP in combination with luciferin and the enzyme luciferase, are used to produce a bioluminescent reaction (as in Figure 6 B), which is linearly related to AK concentration.

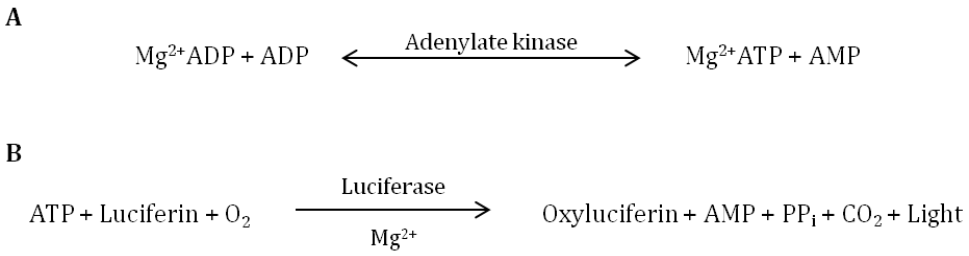


Figure 6. Adenylate kinase reaction for bioluminescent assay

(A) First step of the reaction where ADP is converted to ATP **(B)** In this final step the enzyme luciferase transforms ATP and luciferin into light in a bioluminescent reaction.

Five microliters of the media where cells were cultured was transferred to a 384 Greiner LUMITRAC™ white plate and allowed to reach room temperature. Twenty-five microliters of the adenylate kinase detection reagent was then added to each well and incubated for five minutes. After which the plate was read in the PHERAstar FSX microplate reader (BMG LABTECH).

2.2.8. RNA extraction

Total RNA was extracted using the RNeasy® Mini kit (74104 Qiagen), according to the following protocol: cells were lysed directly in the plate using 350 µL of buffer RLT. One volume of 70% ethanol was then added to the lysate and mixed by pipetting. Lysates were transferred to an RNeasy Mini spin column placed in a 2 mL collection tube and spun for 15 seconds at 10000 rpm. Columns were washed with 350 µL of buffer RW1 before centrifugation for 15 seconds at the same speed. DNA was then digested into the column with 80 µL of DNase I in buffer RDD for 15 minutes at room temperature. Samples were then washed with 350 µL of buffer RW1, then spun for 15 seconds at 1000 rpm. Then, 500 µL of buffer RPE were added to the column that was spun as above. A second wash with 500 µL of buffer RPE was performed and the columns were spun for two minutes at 1000 rpm. To dry the membrane, columns were centrifuged at full speed for one minute. Finally, the columns were placed in a clean collection tube and RNA was eluted with 30 µL of RNase-free water following centrifugation for one minute at 1000 rpm.

2.2.9. cDNA synthesis

cDNA was made using the SuperScript™ III reverse transcriptase (18080093 Invitrogen™). First-strand cDNA synthesis was obtained with 1 µL of random primers, 1 µL of 10 nM dNTP mix, 1 µg of RNA and ultra pure water up to 13 µL. This mix was then incubated for five minutes at 65°C and then placed on ice for a further minute. Next, 4 µL of 5X first-strand buffer, 1 µL of 0.1 M DTT, 1 µL of RNaseOUT (40 units/ µL) and 1 µL of SuperScript™ III reverse transcriptase (200 units/ µL) were added and mixed by pipetting. This reaction was incubated for five minutes at 25°C, then at 55°C for one hour and at 70°C for 15 minutes. Finally,

samples were treated with 1 µL (2 units) of RNase H and incubated for 20 minutes at 37°C.

2.2.10. qRT-PCR

qPCR was carried out using the primers described in Table 8. Three independent cDNA samples per condition were quantified in triplicate by qPCR using the SYBR™ Green PCR Master Mix (3409155 Applied Biosystems™). Each 20 µL of reaction contained 2 µL of DNA (1:10 diluted), 10 µL of SYBRGreen PCR Master Mix (2X) and 70 nM of each primer (1.4 µL of 1:10 diluted). The assay was performed using the StepOnePlus™ Real-Time PCR system (Applied Biosystems™). PCR cycling conditions were as follows: 10 minutes at 95°C for enzyme activation, followed by 40 cycles consisting of a first step at 95°C for 15 s for denaturation and a second step primer annealing and extension for 1 min at 60°C. Specificity of amplification was monitored by the generation of a melting curve. Data was normalized to GAPDH or HPRT1, and relative gene expression determined with by the $2^{-\Delta\Delta Ct}$ method (Livak and Schmittgen, 2001).

2.2.11. Bacterial culture

All bacterial cultures were grown in Luria-Bertani (LB) broth (ThermoFisher Scientific) or agar plates containing 25 µg/mL Chloramphenicol. DMSO stocks of fosmids or plasmids were streaked onto agar plates and incubated overnight at 37°C. Next day single colonies were taken for generating liquid culture or DMSO stocks. For bacteria growing in suspension a shaking incubator set to 225 rpm at 37°C was used.

2.2.12. DNA extraction for fosmids (manual method)

Inoculation of 5 mL of LB broth with a single colony taken from a plate was performed. After that, the culture was incubated for six hours at 37˚C in a shaker. Followed by the transfer of 200 µL of this culture to 250 mL of LB plus antibiotic and grown at 37˚C with shaking overnight. The entire volume was then transferred to a 250 mL conical bottomed bottle and centrifuged at 4°C and 4000 rpm for 20 minutes (Beckman J-6B centrifuge). Subsequently, the supernatant was discarded and the cell pellet re-suspended using 50 mL of ice-cold GET solution (Table 7). Next, 50 mL of NaOH/SDS solution (Table 7) was added and by gentle inversion, the homogenate was mixed before incubation at room temperature for five minutes. Immediately after, 50 mL of ice-cold 3 M potassium acetate solution was added and mixed by inversion, followed by 20 minutes incubation on ice. At that time, the mixture was centrifuged at 4˚C and 4500 rpm for 40 minutes and the supernatant was filtered and transferred to a new 250 mL conical bottle. Next, 90 milliliters of 70% isopropanol was added to precipitate the DNA and incubated for five minutes. A new centrifugation step was carried out with the same conditions, the supernatant was discarded and the pellet was washed with 20 mL of 70% ethanol. The entire volume was transferred to a 50 mL falcon tube and spun down at 4˚C and 4500 rpm for 30 minutes. Finally, the supernatant was discarded and the cell pellet was re-suspended in 500 mL of TE buffer (see Table 7). DNA concentration was measured using the Qubit® dsDNA Assay kit (Invitrogen™) according to the manufacturer's instructions and the DNA quality was evaluated using the ND-1000 NanoDrop spectrophotometer.

2.2.13. Maxiprep

Bacterial single colonies were cultured in 1.5 mL of LB broth with chloramphenicol at 37°C for eight hours. Subsequently, the cultures were transferred to 250 mL of LB + antibiotic and bacteria were allowed to grow shaking overnight. The cultures were then decanted to a 250 mL centrifuge bottle and spun at 6000 rpm for 15 minutes at 4°C using an Avanti J-E centrifuge (Beckman Coulter) and a JA10.5 rotor. Next, the supernatant was discarded and the pellet was re-suspended with 15 mL of buffer P1 from the QIAGEN Plasmid Maxi kit (12165). Fifteen mL of buffer P2 was then added for cell lysis and the mix was incubated for five minutes with gentle swirling every minute. To stop the reaction 15 mL of ice cold buffer P3 was added and mixed immediately by inversion. Right after, the mixture was placed on ice for 20 minutes before centrifugation at 9000 rpm for 35 minutes at 4°C. QIAGEN-tip 500/G columns were equilibrated with 15 mL of buffer QBT before loading supernatants that were precleared through paper filtering. Columns were then rinsed twice with 30 mL of buffer QC. DNA was then eluted using 15 mL of 50°C pre-heated QF solution. After, the DNA was precipitated using 10.5 mL of isopropanol and the container was mixed by inversion a couple of times. This mixture was afterwards centrifuged at 14000 rpm and 4°C for 30 minutes to pellet the DNA (using the J-17 rotor). The supernatant was discarded and 3.5 mL of 70% ethanol was added to the DNA pellet. It was once again centrifuged at 14000 rpm and 4°C for 30 minutes and after that, the supernatant was discarded and the pellet was allowed to air dry for 15 minutes. Finally, the DNA was re-suspended with 250 µL of TE buffer and left to dissolve at 4°C overnight. DNA concentration was measured using the Qubit® dsDNA Assay kit (Invitrogen™) according to the manufacturer's

instructions and the DNA quality was evaluated using the ND-1000 NanoDrop spectrophotometer.

2.2.14. Agarose gel electrophoresis

Agarose gel electrophoresis was used to check the integrity and quality of the cDNA synthesized before qPCR and was used to check the fragment length of the labelled probes before 3D DNA FISH. Agarose gels were prepared at a concentration of 1% agarose (w/v), in TBE buffer (see Table 7) containing 0.25 µg/mL of ethidium bromide. Each sample was prepared by adding the corresponding volume of 6X DNA Loading Buffer (Table 7). Electrophoresis was carried out using a Bio-Rad electrophoresis tank at 120 V in TBE buffer (Table 7) until DNA ladder was sufficiently resolved (one hour approximately). The ladders used were the HyperLadder™ 1 kb (BIO-33053 Bioline) or the HyperLadder™ 50 bp (BIO-33054 Bioline). Gels were imaged on a ChemiDoc™ Imaging System (Bio-Rad) and images were analysed using Image Lab software (Bio-Rad).

2.2.15. Pulsed-field gel electrophoresis

Pulsed-field gel (PFG) electrophoresis was used to confirm the purchased fosmids. One percent agarose gel in 0.5X TBE was prepared. The tank was filled with 2 L of 0.5X TBE, the pump was set to 60% and the cooling system was switched on to allow the buffer to reach 14°C. Once the gel was ready, the Lambda PFG ladder (New England BioLabs) was added to the first lane and the gel was placed in the tank to load the samples. The Drive Control module was set with the following conditions: 6 V/cm, 16 hours for running time, initial switch of two seconds and

final switch of 16 seconds. The gel was stained with ethidium bromide and it was imaged on a ChemiDoc™ Imaging System (Bio-Rad).

2.2.16. Labelling of the probes for 3D Fluorescence In Situ Hybridization (3D FISH)

Human *FXN* gene was detected using fosmid clones (G248P87590H8 or G248P89980G8) obtained from the BACPAC Resources Center. The transgene was detected using the small plasmid PhFRTHy. Probes were labelled using either a DIG-Nick or a Biotin-Nick translation mix (Roche). One microgram of fosmid or plasmid DNA was treated with 200 ng RNase (Sigma) for 30min at 37°C. Each probe was then mixed with 4 µl of nick translation mix [stabilized reaction buffer in 50% glycerol (v/v) and DNA Polymerase I, DNase I, 0.25 mM dATP, 0.25 mM dCTP, 0.25 mM dGTP, 0.17 mM dTTP and 0.08 mM DIG-11-dUTP/Biotin-16-dUTP]. Probes were nick translated at 15°C for different amounts of time, which will be described in chapter 3 (3D DNA FISH protocol optimization). The desired fragment length of the probes was between 200 and 500 nucleotides. Once this length was achieved, the reaction was stopped by adding 1 µL 0.5 M EDTA (pH 8.0) and heating the mixture to 65°C for 10 min. Unincorporated nucleotides were removed using the Illustra G-50 columns (GE Healthcare), following the manufacturer's instructions.

2.2.17. 3D DNA FISH

All steps were carried out at room temperature unless otherwise stated.

One hundred thousand cells were seeded onto poly-L-lysine coated coverslips and allowed to settle for 24 h following cell culture conditions previously described. Cells were fixed using 4% paraformaldehyde in 25 mM 4-(2-hydroxyethyl)-1-

piperazineethanesulfonic acid (HEPES) for 15 minutes and permeabilised in 0.5% Triton X-100 (Sigma) in PBS for 10min. Free aldehydes were quenched using ammonium chloride (267 mg/100 mL PBS) for ten minutes. Coverslips were then rinsed three times with PBS before blocking in 10% FBS-PBS for at least 30 minutes. The lamin antibody (see Table 9) was incubated for 30 minutes and three washes were done before incubating with the secondary antibody (Alexa Fluor™ 647) for a further 30 minutes. The protein and antibodies were anchored by cross-linking in 4% PFA - 0.25 M HEPES for ten minutes, after which the coverslips were rinsed three times with PBS. RNA was removed with 100 µg/mL RNAse in 2x SSC (saline-sodium citrate) from Sigma at 37°C for 1 hour. Next, the probes were prepared as follows: 5 µL of the labelled probe, 3 µL of human COT-1 DNA™ (15279011 Invitrogen™), one tenth of the total volume of 3 M sodium acetate and 2.25 volume of 100% ethanol. This mixture was incubated for one hour at -80°C. After that, the probes were spun at 13000 rpm and 4°C for 30 minutes, before washing them in 70% ethanol and once more spun for 10minutes at 4°C. Ethanol was air dried at 37°C and 12 µL of hybridisation mix/reaction was added. Probes were denatured at 90°C for ten minutes and kept on ice until they were required. The DNA on the coverslips was also denatured. This was performed for 20 minutes using 3N HCl and neutralized in ice-cold PBS. Hybridization of the probes was carried out overnight at 37°C. Cells were washed twice for 30 min in 2x SSC at 37°C and once at room temperature for an additional 30 min in 1 x SSC. They were blocked using 3% BSA in 4 x SSC for 1 h. Coverslips were incubated with anti-DIG antibody for 30 minutes and then with Cy3 and digoxigenin FITC for a further 30 minutes (see Table 9 for details). Antibodies were fixed by incubation in 4% PFA - 0.25 M HEPES for 10 minutes. Finally, coverslips were mounted in Vectashield

(Vector Laboratories) with 1 µg/ml 4′,6-diamidino-2- phenylindole (DAPI) counterstain.

2.2.18. Dot blot

This technique was used to confirm that the probes used for 3D DNA FISH were labelled. The protocol was performed according to the DIG high prime DNA labelling and detection starter kit II (Roche, 11585614910). Briefly, 1 uL of the labelled probe was spotted on a nylon membrane (Bio-Rad). Nucleic acids were fixed by backing the membrane for 30 minutes at 120°C. The membrane was then incubated for two minutes at room temperature in maleic acid buffer (0.1 M maleic acid, 0.15 M NaCl pH 7.5). Unspecific binding sites were blocked by incubating the membrane for 30 minutes with 1X blocking solution (provided in the kit), followed by anti-digoxigenin-AP (provided in the kit) incubation for additional 30 minutes. The membrane was then washed twice with washing buffer (0.1 M maleic acid, 0.15 M NaCl pH 7.5, 0.3% Tween 20) and equilibrated for five minutes in detection buffer (0.1 M Tris-HCl, 0.1 M NaCl, pH9.5) before developing on a ChemiDoc™ Imaging System (Bio-Rad).

2.2.19. Library and compound preparation

The epigenetic probes collection was received from the SGC and consisted of 36 small-like inhibitors of several epigenetic modifiers. Compounds were received as powder, they were re-suspended in DMSO, and all of them were aliquoted in DMSO resistant 96-well plates at a concentration of 10 mM. Negative probes and derivatives of the lead compound we also prepared in DMSO at the same concentration and were stored in aliquots at -80°C.

2.2.20. AlphaLISA for human frataxin detection

This assay was performed using the AlphaLISA human frataxin detection kit from PerkinElmer (catalogue # AL322HV/C/F) following the manufacture's recommendations. Briefly, a 2.5 X mix of AlphaLISA anti-hFXN Acceptor beads (25 µg/mL) and biotinylated anti-hFXN Antibody (3.75 nM) was prepared as follows: 50 µL of 5 mg/mL AlphaLISA anti-hFXN Acceptor beads were added to 9875 µL of 1X AlphaLISA immunoassay buffer, in addition to 75 µL of 500nM anti-hFXN Antibody. Then, a 2X streptavidin donor beads (40 µg/mL) solution was prepared by adding 100 µL of 5 mg/mL streptavidin donor beads to 12400 µL of 1X AlphaLISA immunoassay buffer. Following this, 5 µL of each sample were added to a white opaque 96-well microplate (PerkinElmer), with 20 µL of the 2.5 X mix of AlphaLISA anti-hFXN Acceptor beads and biotinylated anti-hFXN Antibody. This mixture was incubated for 60 minutes at 23°C. Next, 25 µL of the 2X streptavidin donor beads solution was added to the previous mix and incubated for 30 minutes at 23°C. Finally, the plate was read using a PHERAstar FSX microplate reader (BMG LABTECH) at a wavelength of 615 nm. Data were normalized for protein quantify using the BCA assay.

2.2.21. JC-10 mitochondrial membrane potential assay

Forty thousand fibroblasts treated with 5 µM and 10 µM A-196 were seeded on a clear flat bottom 96-well black plate (Greiner) and allowed to settle down for 48 hours. Cells were rinsed twice with KREBS buffer (Table 7), followed by a 1 hour incubation with 5 µM JC-10 (22204 AAT Bioquest). Next, the plate was placed in the PHERAstar FSX microplate reader (BMG LABTECH). JC-10 fluorescence was detected before and after injection of 50 µL of 20 µM carbonyl cyanide m-chloro

phenyl hydrazone (CCCP) (C2759 Sigma-Aldrich). At low $\Delta\Psi_m$, accumulation of JC-10 in mitochondria is low and most of the dye is in its monomeric form, which emits a green fluorescence. In contrast, at high $\Delta\Psi_m$, accumulation of JC-10 in mitochondria is high and most of the dye is in the aggregate form, which emits a red fluorescence. Results were obtained by measuring the potential-dependent shift in fluorescence from green (monomeric JC-10) to red (aggregated JC10).

2.2.22. Calcium imaging assay

This assay was performed to assess the intracellular calcium status of cells. Forty thousand A-196 treated fibroblasts (5 µM and 10µM) were seeded in a clear flat bottom 96-well black plate (Greiner) and allowed to settle down for 24 hours. Fura-2 calcium indicator (Fura-2 dye re-suspended in HBSS Ca-Mg $^{-/-}$ + 20 mM HEPES) from Thermo Fisher Scientific was added to the media in a one to two ratio. Then, cells were incubated for one hour at 37°C in 5% CO_2. The cells were then taken to the FlexStation® 3 Multi-Mode Microplate Reader (Molecular Devices) for injection of 20 µM of CCCP and 10 µM of ionomycin from Streptomyces conglobatus (I9657 Sigma-Aldrich). Both drugs were prepared in HBSS without calcium and magnesium and 20 mM HEPES (Thermo Fisher Scientific). Calcium release was measured as the ratio between the bound calcium, which fluoresces at 340 nm and the unbound calcium, which fluoresces at 380 nm. Measurements were taken every four seconds and response to CCCP and ionomycin was calculated considering the maximum response (peak) after the injection of the drugs.

2.2.23. Fluorescence cytochemistry and immunocytochemistry

All steps were performed at room temperature unless otherwise stated.

Five thousand A-196 treated fibroblasts (six days - 5 μM and 10 μM) were seeded in a clear flat bottom 96-well black plate (Greiner) and allowed to settle down for 48 hours. After that, cells were fixed with 4% PFA for 10 minutes and rinsed three times with PBS. Next, permeabilisation was carried out with 0.1% Triton for 15 minutes, followed by blocking with 5% normal donkey serum in PBS for 20 minutes. Then, primary antibodies/dyes (Tom20, Nrf2 and phalloidin see Table 9) were incubated overnight at 4°C. Three washes with PBS were performed before incubation of the secondary antibodies (see Table 9) for 30 minutes. Cells were rinsed three times with PBS and in the last wash DAPI was added for five minutes and washed away. Images were acquired using a 63X water objective on the Opera Phenix™ High Content Screening System (PerkinElmer).

2.2.24. Mitochondrial superoxide evaluation

Mitochondrial superoxide was measured using MitoSOX, a dye specifically targeted to mitochondria, which oxidation by superoxide produces a fluorescence. Five thousand A-196 treated fibroblasts (six days - 5 μM and 10 μM) were seeded in a clear flat bottom 96-well black plate (Greiner) and allowed to settle for 48 hours. Then, mitoSOX, mitotracker and Hoechst (see Table 9) were added to the cells at their respective concentrations and incubated for one hour. After which, the plate was imaged using the 20X water objective on the Opera Phenix™ High Content Screening System (PerkinElmer). This measurement was taken as a base line. Next, cells were treated with 10 μM CCCP and the plate was imaged in 6 minute intervals for one hour using the 20X water objective.

2.2.25. Image acquisition

3D DNA FISH images were obtained using a DV Elite system based on an Olympus IX71 motorized wide-field deconvolution inverted microscope with a 100 X objective. Cells were randomly chosen and recorded using the motorized stage. Images were captured in z-stacks at 0.2 μm intervals to encompass the entire volume of each cell.

Fluorescence cytochemistry and immunocytochemistry images were obtained using a 63 X water objective in ten different fields of view with 4 z-stacks captured for all wells. Images were max projected to analyse mitochondrial network, cell cytoskeleton organization and Nrf2 distribution using Harmony® software (Perkin Elmer).

Mitochondrial superoxide evaluation was performed using a 20 X objective to obtain images in four different fields of view in each well with two z-stacks, one in the middle of the cell and the other in the top. For cell analysis, cells were max projected and MitoSOX intensity was measured using Harmony® software (Perkin Elmer).

2.2.26. Statistical analysis

All experiments were conducted in triplicate unless otherwise stated. Statistical analysis for each experiment will be described in the results section. Differences were considered significant when the calculated P was ≤ 0.05

CHAPTER 3

Exploring the role of histone deacetylase 3 and Euchromatic histone lysine N-methyltransferase 2 in the expression of FXN

3.1. Introduction

3.1.1. Histone deacetylases

Histone deacetylases are enzymes which remove acetyl groups from the N-terminal lysine residues of histones. It has been shown that deacetylation leads to a more condensed chromatin structure, therefore making chromatin less accessible for the transcription machinery (Haberland, Montgomery and Olson, 2009). Amongst the various HDAC isoenzymes, HDAC3 has previously been shown to have a role in neurodegenerative diseases including Huntington's disease and spinocerebellar ataxia 7 (Kazantsev and Thompson, 2008).

Histone deacetylases are very likely involved in the mechanism of *FXN* repression, as it has been reported that compounds targeting class I HDACs (1, 2 and 3) are potent activators of *FXN* expression in several *in vitro* models such as primary lymphocytes and iPSC-derived FRDA neuronal cells, as well as in various *in vivo* mouse models (Herman *et al.*, 2006; Chou, Herman and Gottesfeld, 2008; Rai *et al.*, 2008, 2010; Sandi *et al.*, 2011; Soragni *et al.*, 2014). Moreover, a recent study from our group showed that chemical HDACi can increase frataxin mRNA levels in the reporter *FXN*-Luc cell lines (Silva *et al.*, 2015). In all of these studies, although the compounds used to target these enzymes are inhibitors of class I HDACs, two of

them (106 and 109) have shown a preference for HDAC3, potentially making it a key player in the restoration of frataxin levels. Therefore, HDAC3 can be considered as a potential therapeutic target.

3.1.2. Histone methyltransferases

In addition to the acetylation of histones, methylation is another covalent modification which has been the subject of intense research due to its involvement in gene regulation and expression (Bannister and Kouzarides, 2011). In most eukaryotes, the methylation of histone H3 on lysine 9 is required for the assembly of constitutive heterochromatin (Almouzni and Probst, 2011). One of the methyltransferases involved in the delivery of methyl groups to this histone residue is the euchromatic histone-lysine N-methyltransferase 2 also known as G9a. This enzyme belongs to the SET domain containing Su(var) 3–9 family of proteins and it catalyses the mono- and di-methylation of H3K9 (Shankar *et al.*, 2013).

Increased H3K9me2 in response to G9a up-regulation has been implicated in several diseases such as brain cancer, and it has also been linked to neurodegeneration (Subbanna *et al.*, 2013; Casciello *et al.*, 2015). Therefore, G9a inhibition has been considered as a therapeutic strategy for various types of cancer (Kim *et al.*, 2013; Casciello *et al.*, 2015). Given the accumulation of H3K9 me2 in the promoter of *FXN* as well as upstream and downstream of the GAA repeats (Table 5), the direct down-regulation of this target could have therapeutic benefits in FRDA.

3.1.3. Hypothesis

The down-regulation of HDAC3 and/or of G9a will restore frataxin mRNA and protein levels in the *FXN*-Luc reporter cell line.

3.1.4. Chapter aims

Down-regulation of HDAC3 and G9a and their consequences on FXN expression

- To down-regulate the expression of HDAC3 by siRNA to study if the potential increase in histone acetylation in the human reporter cell line of FRDA increases frataxin mRNA and protein levels.
- To reduce the expression of G9a by siRNA to test if frataxin mRNA and protein levels can be increased.

Optimization of 3D DNA Fluorescence In Situ Hybridization (3D FISH)

- To optimize the protocol for 3D DNA FISH in order to determine the role of selected epigenetic regulators in the localization of the *FXN* locus in the cell nucleus.

3.2. Results

3.2.1. The down-regulation of HDAC3 increases FXN-Luc mRNA expression

The reporter cell line *FXN*-GAA-Luc previously created in our laboratory and shown to present heterochromatin marks at the *FXN* locus similar to the ones observed in patients, was used in this set of experiments. These marks include decreased acetylation of H3K9 and H4K8 as well as increased di- and tri-methylation of H3K9 (Lufino *et al.*, 2013). The cell lines *FXN*-Luc and *FXN*-GAA-Luc, in addition to endogenous *FXN,* express a human pBAC-*FXN*-Luc fusion vector with either 310 GAA repeats (*FXN*-GAA-Luc, resembling the pathological condition in patients) or 6 GAA repeats (*FXN*-Luc, resembling the normal allele) (Figure 5). The resulting

modified transgene expresses a *FXN*-luciferase fusion protein within the context of the *FXN* genomic DNA locus. Thus, the expression of endogenous *FXN* as well as the *FXN*-luciferase fusion protein can be evaluated.

To assess the effect of HDAC3 down-regulation on the expression of *FXN*, efficient knock-down of HDAC3 needed to be achieved. For this purpose, the two cell lines were treated for 96 hours with concentrations of HDAC3 siRNA of 12, 25 and 50 nM to determine which was most effective at down regulating HDAC3 protein. Figure 7 demonstrates that HDAC3 knock-down (~70%) was achieved independently from the concentration used in both cell lines.

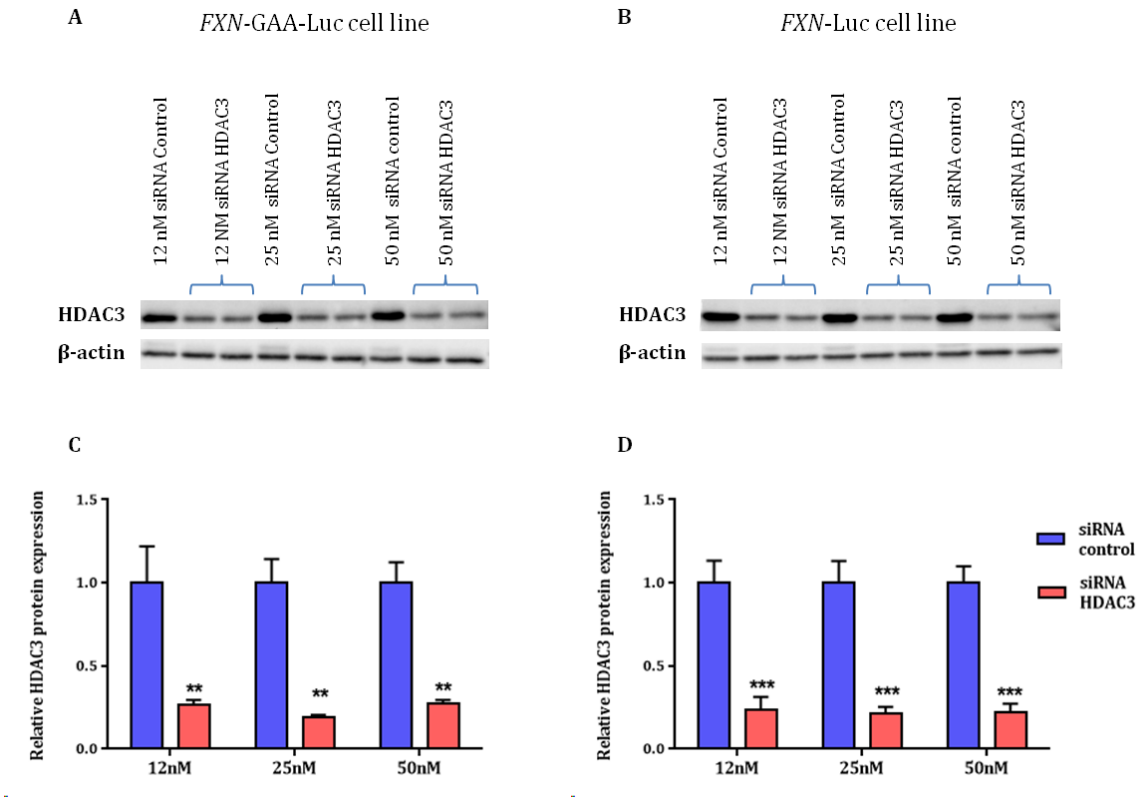


Figure 7. Different concentrations of HDAC3 siRNA down-regulate the protein to a similar extent

Western blot analysis shows effective knock-down of HDAC3 in both the GAA-expanded (**A and C**) and the non-expanded (**B and D**) cell lines. Data are presented as mean ± s.e.m. of three independent experiments completed in duplicate, two-way ANOVA Bonferroni corrected for multiple comparisons **p<0.01, ***p<0.001 with respect to control siRNA.

Based on these results and on a previous study in which HDAC3 was down-regulated with successful up-regulation of FXN mRNA (Soragni *et al.*, 2015), the 12 nM concentration of HDAC3 siRNA was chosen for the next assays.

Next, the effects of HDAC3 down-regulation on frataxin-luciferase (FXN-Luc) mRNA were assessed. Both reporter cell lines, *FXN*-GAA-Luc and *FXN*-Luc were treated with 12 nM HDAC3 siRNA and the FXN-Luc mRNA expression was assessed by qRT-PCR. HDAC3 siRNA is able to increase FXN transgene mRNA expression in both cell lines by approximately 1.5-fold (Figure 8). This result is in agreement with a previous report from our laboratory, in which a chemical compound (106) that has preference for HDAC3 inhibition amongst other HDACs, increased mRNA levels in the human reporter model (Silva *et al.*, 2015). Thus, the direct down-regulation of this target increases FXN-Luc mRNA levels.

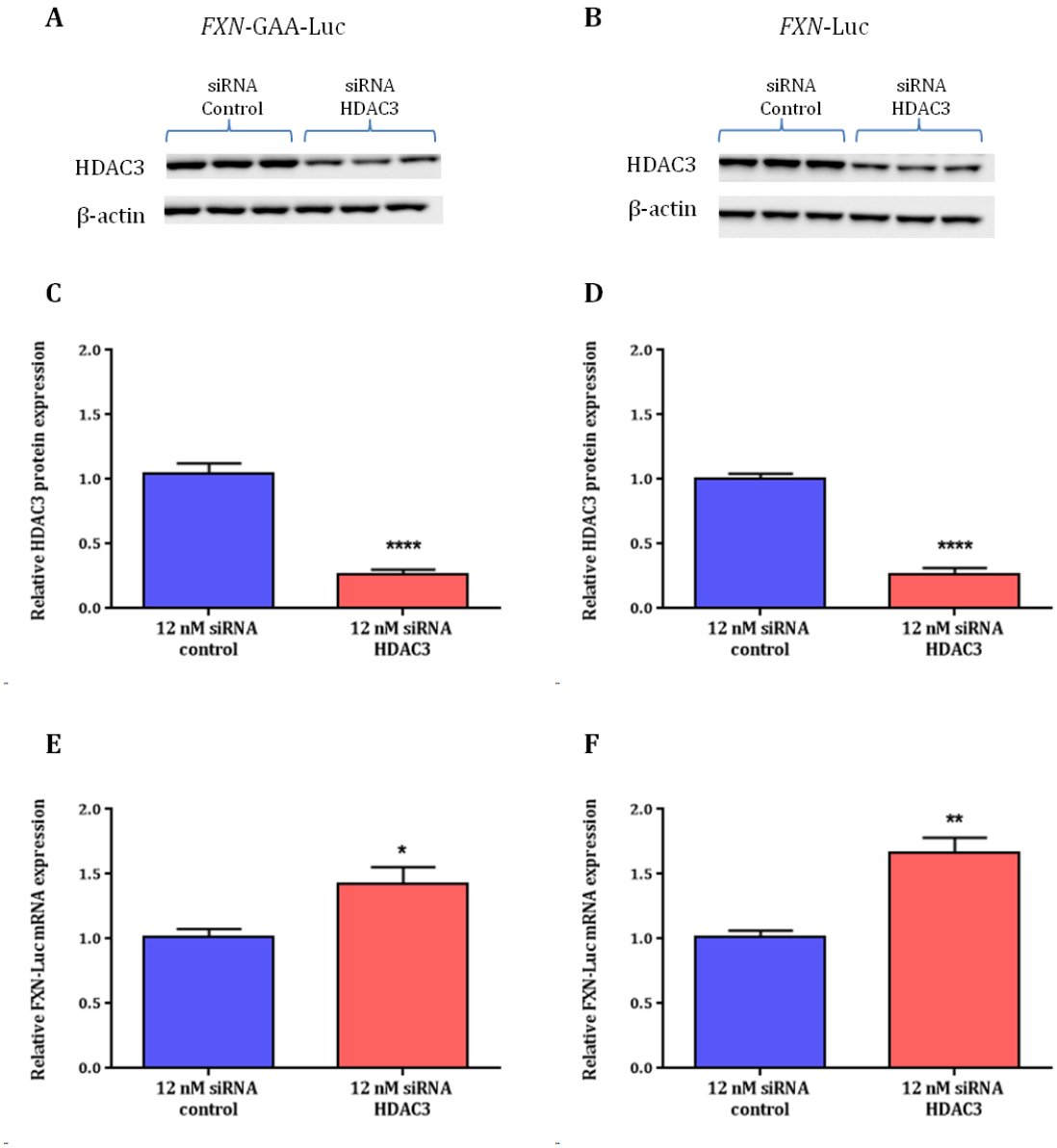


Figure 8. HDAC3 knock-down up-regulates FXN mRNA levels in both cell lines

Western blot analysis demonstrates effective knock-down of HDAC3 at a concentration of 12 nM siRNA in both the GAA-expanded (**A and C**) and the non-expanded (**B and D**) cell line. qRT-PCR experiments show that HDAC3 down-regulation increases frataxin-luciferase mRNA levels compared to siRNA negative control in both the GAA-expanded (**E**) and the non-expanded (**F**) cell line. Data are presented as mean ± s.e.m. of three independent experiments completed in triplicate, Mann-Whitney test, *p<0.05, **p<0.01

The up-regulation of FXN mRNA levels after HDAC3 siRNA treatment, posed the question of whether or not FXN protein levels are changed. Interestingly, there is no

significant difference in FXN protein expression between the negative control and HDAC3 siRNAs in any of the FXN protein forms studied in both cell lines (Figure 9).

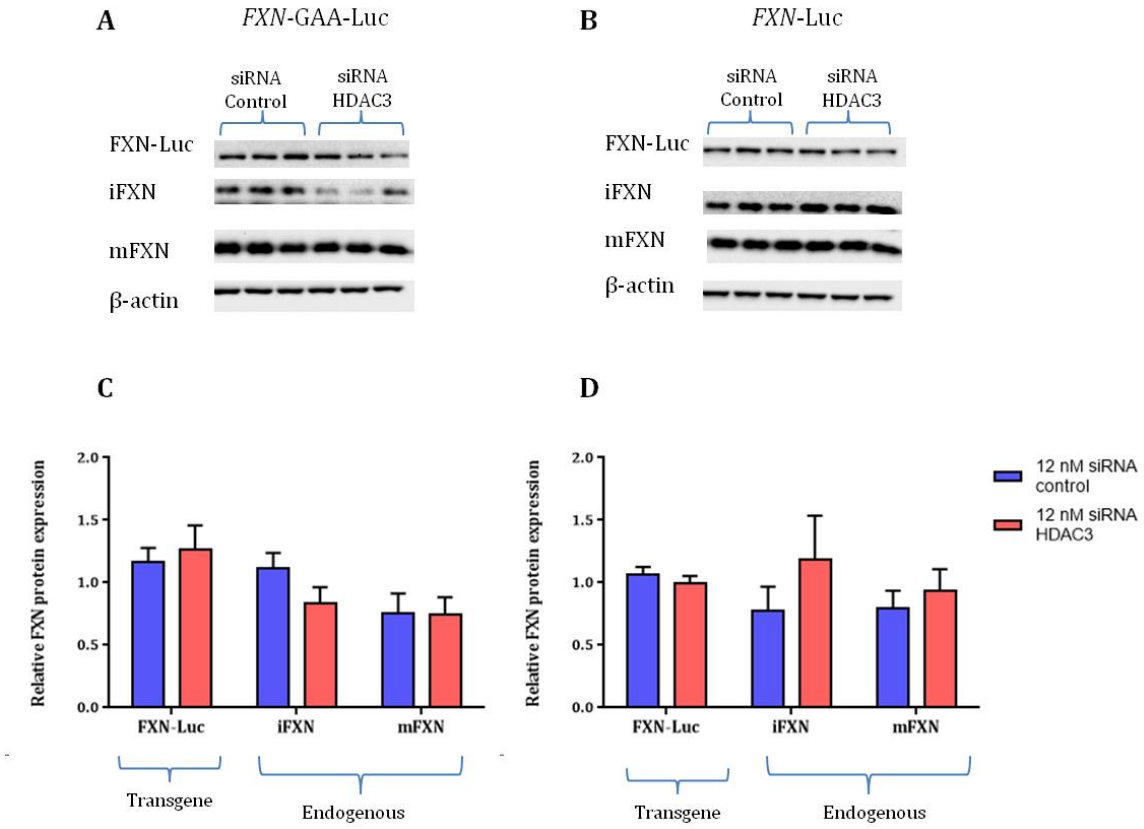


Figure 9. HDAC3 knock-down has no effect on FXN protein levels

(A) Western blot of the expanded cell line showing the endogenous frataxin proteins (immature-iFXN, mature-mFXN) and the transgene frataxin luciferase (FXN-Luc). (**B**) Non-expanded cell line. (**C**) and (**D**) analysis of the relative expression of FXN proteins. Data are presented as mean ± s.e.m. of three independent experiments completed in triplicate.

Due to the semi-quantitative evaluation of protein that western blots provide, and taking advantage that our reporter cell line expresses the FXN-Luc fusion protein, luciferase assay was used to further study FXN protein expression after HDAC3 siRNA treatment. This assay is designed to only measure *FXN*-Luc fusion protein. In accordance with the western blot assay, no statistical difference was observed in FXN protein expression in HDAC3 knocked-down cells (Figure 10).

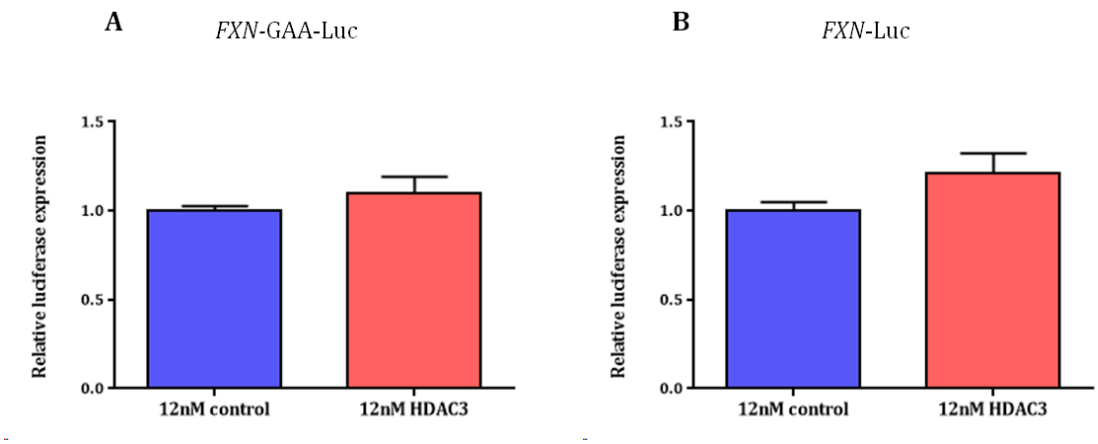


Figure 10. Luciferase assay shows no difference between the control and HDAC3 siRNA transfected cells

(A) expanded cell line **(B)** non-expanded cell line. Data are presented as mean ± s.e.m. of three independent experiments completed in triplicate.

In summary, these experiments show that down-regulation of HDAC3 was successfully achieved, leading to a statistically significant 1.5-fold up-regulation of FXN-Luc mRNA, but without an up-regulation of frataxin protein expression.

In addition to histone acetylation, histone methylation is another important epigenetic modification observed in the GAA-expanded *FXN* locus. Thus, the direct down-regulation of G9a, a histone lysine methyltransferase, was next performed to study its effects on frataxin mRNA and protein levels.

3.2.2. Down-regulation of G9a does not alter the expression of FXN-Luc mRNA or protein

First, the achievement of efficient G9a protein knock-down upon siRNA transfection was assessed by western blot analysis. Different concentrations of siRNA targeting G9a were used to treat both the reporter cell lines. The same concentrations of non-targeting control siRNA were used as comparison. Cells were harvested and subjected to western blot analysis 48 hours following transfection. Figure 11 shows

efficient G9a protein knock-down (~90%) in both *FXN*-GAA-Luc and *FXN*-Luc cell lines.

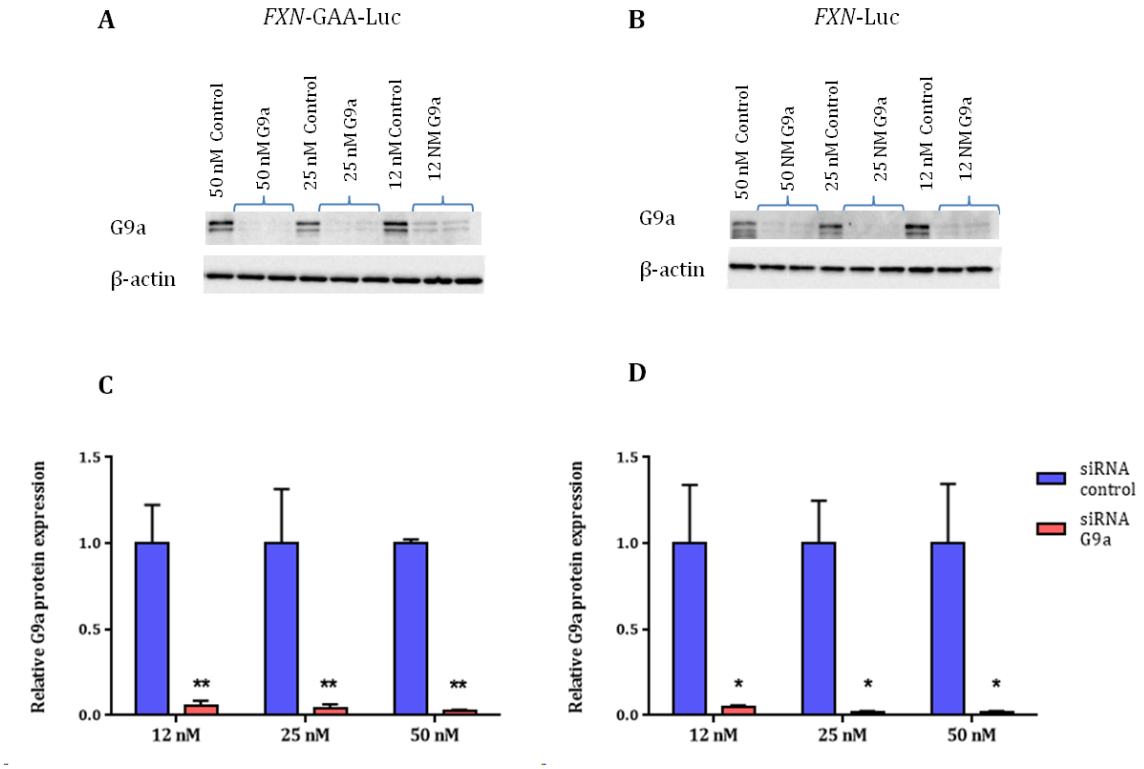


Figure 11. Different concentrations of G9a siRNA efficiently down-regulate G9a protein in Luc-reporter cell lines

Western blot of G9a shows effective knock-down in both, the GAA-expanded (**A and C**) and the non-expanded (**B and D**) cell lines. Data are presented as mean ± s.e.m. of three independent experiments completed in duplicate, two-way ANOVA Bonferroni corrected for multiple comparisons *p<0.05, **p<0.01 with respect to control siRNA.

As opposed to the siRNA-mediated knock-down of HDAC3, no report was found regarding the down-regulation of G9a and its implications in the expression of *FXN.* Hence, FXN mRNA and protein levels were assessed after all of the different siRNA treatments.

siRNA-mediated knock-down of G9a does not induce significant differences in FXN-Luc mRNA levels (Figure 12). A slight increase (~1.2-fold) is observed in the expanded line at 12 nM and 50 nM and the same minor effect is observed at all

concentrations in the non-expanded control cell line, although the differences are not statistically significant.

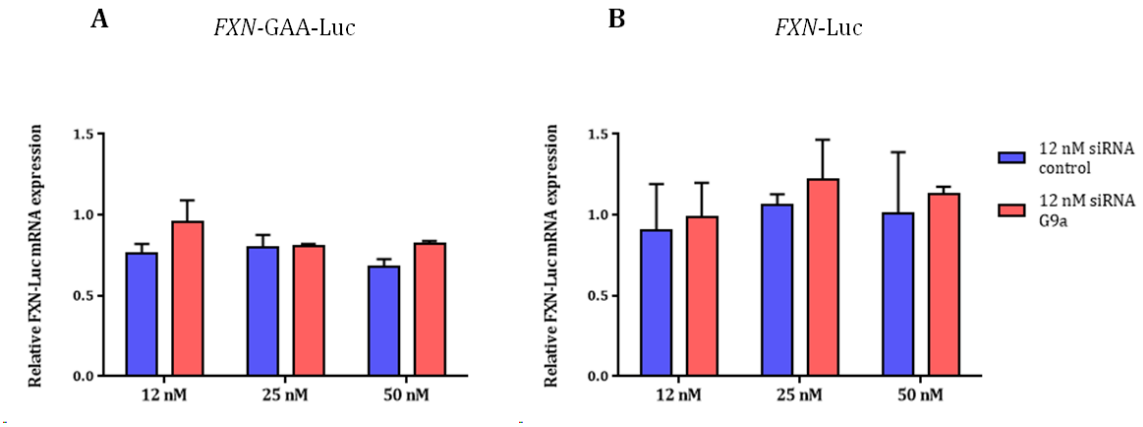


Figure 12. G9a siRNA has no effect on frataxin mRNA levels in both cell lines

qRT-PCR experiments showed that G9a down-regulation does not increase frataxin-luciferase mRNA levels compared to siRNA negative control in both the GAA-expanded (**A**) and the non-expanded (**B**) cell line. Data are presented as mean ± s.e.m. of three independent experiments completed in triplicate, two-way ANOVA Bonferroni corrected for multiple comparisons.

Following the evaluation of mRNA levels after G9a siRNA-mediated knock-down, protein levels were determined by western blot analysis and the luciferase assay. G9a siRNA knock-down do not seem to influence FXN protein expression (Figure 13 and Figure 14). Neither the *FXN*-Luc transgene, nor the endogenous *FXN* seem to be regulated by the methyltransferase G9a as evaluated by these assays. Thus, it seems unlikely that the methylation mediated by G9a has a role in the regulation of frataxin expression.

In summary, although a robust knock-down of G9A was achieved, no effects on frataxin protein or RNA were observed.

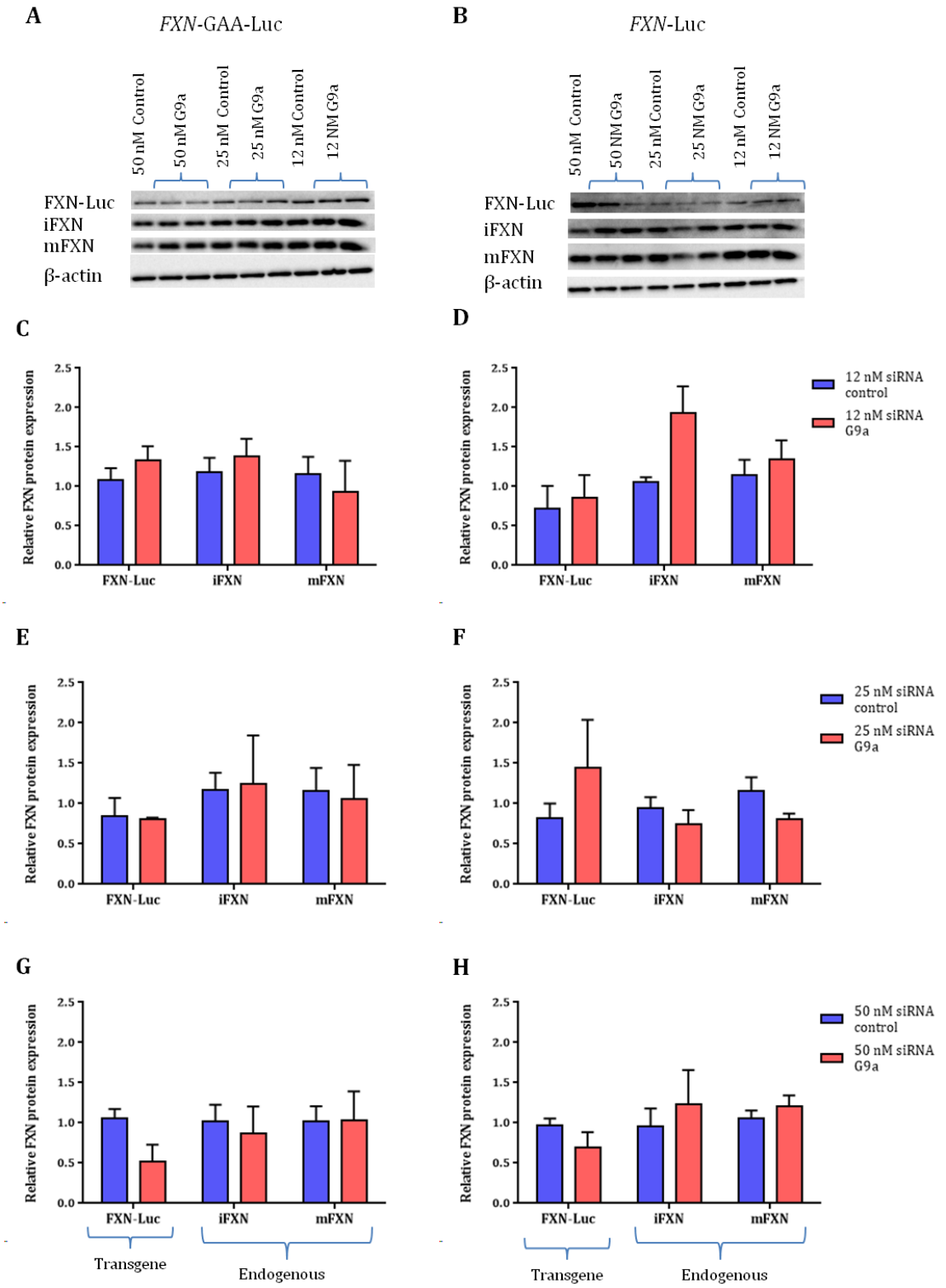


Figure 13. G9a siRNA at three different concentrations does not change FXN protein levels

(**A-B)** Representative western blots showing FXN expression following transfection of G9a siRNA or negative control siRNA in a range of concentrations. (**C-H)** densitometric analysis of FXN protein normalised to beta actin for the experiments described in (A-B). Data are presented as mean ± s.e.m. of three independent experiments completed in duplicate, two-way ANOVA Bonferroni corrected for multiple comparisons.

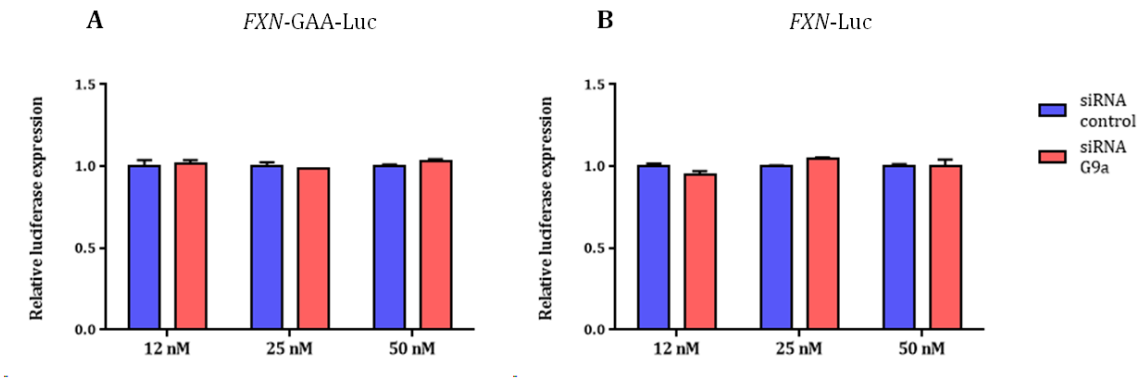


Figure 14. Luciferase expression associated with *FXN*-luciferase fusion protein is unaltered upon G9a siRNA knock-down

Luciferase assay showing unaltered FXN-Luc expression following G9a siRNA knock-down. (**A**) expanded cell line (**B**) non-expanded cell line. Data are presented as mean ± s.e.m. of three independent experiments completed in duplicate, two-way ANOVA Bonferroni corrected for multiple comparisons.

In addition to the evaluation of the expression of frataxin after the down-regulation of HDAC3 and G9a, it was important to address whether the knock-down of these epigenetics regulators could have an effect on the localization of the expended allele in the cell nucleus or not. A recent report from our laboratory showed that the GAA expanded allele is preferentially localized in the nuclear periphery, and that after chemical inhibition of histone deacetylases, it re-localizes to the centre of the nucleus (Silva *et al.*, 2015). The next section of this chapter will cover the optimization of the technique used to visualise the *FXN* locus in the nucleus.

3.2.3. Optimization of 3D DNA Fluorescence In Situ Hybridization (3D FISH)

Since pathological silencing of *FXN* develops beyond heterochromatin epigenetic marks, and has been linked to its localization at the NL, *FXN* sub-cellular localisation in cells with or without the GAA expansion was next investigated. These experiments were prompted by the evidence that the expanded allele can be re-

localized in the nucleus after HDAC chemical inhibition (Silva *et al.*, 2015). 3D DNA FISH was used for this purpose according to the protocol described in Chapter 2. This technique allows three-dimensional visualization of individual gene loci to investigate the relationship between their spatial organization and function (Chakalova *et al.*, 2005). In order to precisely localize the expanded *FXN* loci in the cell, several optimization steps of the technique were necessary.

3D FISH uses probes that correspond to genomic DNA sequences in order to localize a specific DNA region. First, fosmids (genomic DNA sequence used as probes in this assay), were confirmed to correspond to clones in the *FXN* locus. For that purpose, both fosmids were digested with the restriction enzyme XhoI in the fosmid itself and in the cloning vector, and the fragments were run in a pulsed-field gel (Figure 15).

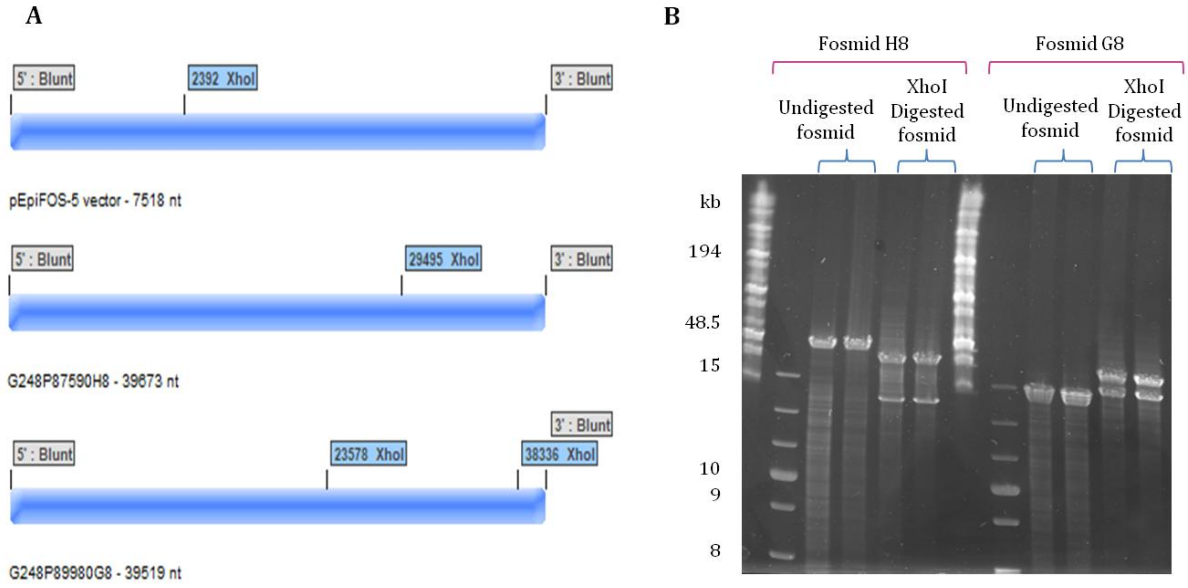


Figure 15. Pulsed-field gel confirms that both fosmids correspond to *FXN* locus sequences

(A) upper panel: pEpiFOS-5 the 7518 bp fosmid cloning vector showing the restriction site, middle panel: fosmid G248P87590H8 (H8) with the restriction enzyme site, lower panel: fosmid G248P89980G8 (G8) depicting the restriction site **(B)** pulsed-field gel of indigested and digested fosmids. Samples were run in duplicate. Cloning vector and fosmids images were made using SerialCloner.

If the probes/fosmids that were needed to identify the *FXN* locus correspond to sequences in *FXN,* they will be digested by the restriction enzyme XhoI in the pattern shown in Figure 15 A. Fosmid clone H8 (G248P87590H8) showed after XhoI digestion 34.9 kb and 12.2 kb products as expected (Figure 15 B), while fosmid clone G8 (G248P89980G8) after XhoI digestion showed 29 kb and 14.7 kb products, the smaller product of this digestion (3 kb) is not visible in this gel (Figure 15 B). Thus, both fosmid clones correspond to sequences in *FXN* and can be used to identify it.

Next, given that the quality of the fosmids clones DNA is critical for the labelling protocol, several methods of DNA extraction were tested to ensure a high quality product. The DNA extraction protocol was evaluated by determining the biological purity of DNA (absorbance ratio 260/280 using NanoDrop spectrophotometer) and the chemical purity (absorbance ratio 260/230), in addition to the visualisation of the labelled probes in an agarose gel. The best performing DNA extraction method was the Qiagen maxiprep columns kit (Figure 16).

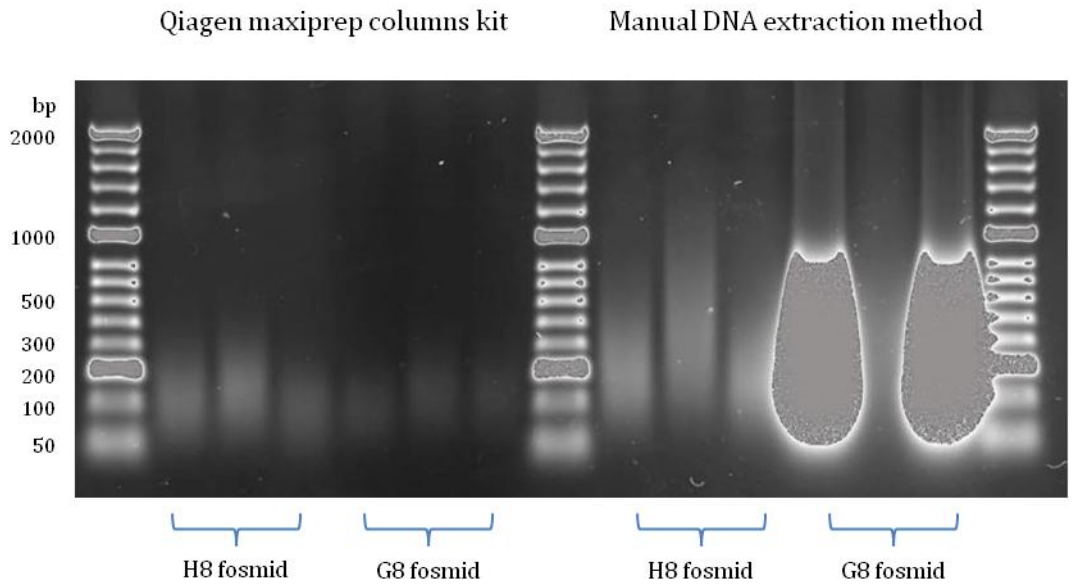


Figure 16. DNA gel electrophoresis of fosmid clones

After both fosmids clones' DNA was extracted, fosmids were labelled as previously described. Labelled probes were then loaded in an agarose gel for size determination and for the evaluation of the best DNA extraction method. Samples were loaded in triplicate.

Once the DNA extraction method was chosen, optimization of the nick translation protocol for labelling the probes was performed. Initially, probes were labelled according to the manufacturer instructions (Figure 17 A). Considering that the manufacturer's protocol resulted in bigger fragments than the ones needed for 3D FISH, different concentrations of DNAseI and incubation times were tested to obtain the desired probe sizes, which are between 200 bp and 500 bp (Figure 17 B). Additionally, confirmation of the probe labelling was carried out by visualization of each labelled probe in a dot blot (Figure 17 C).

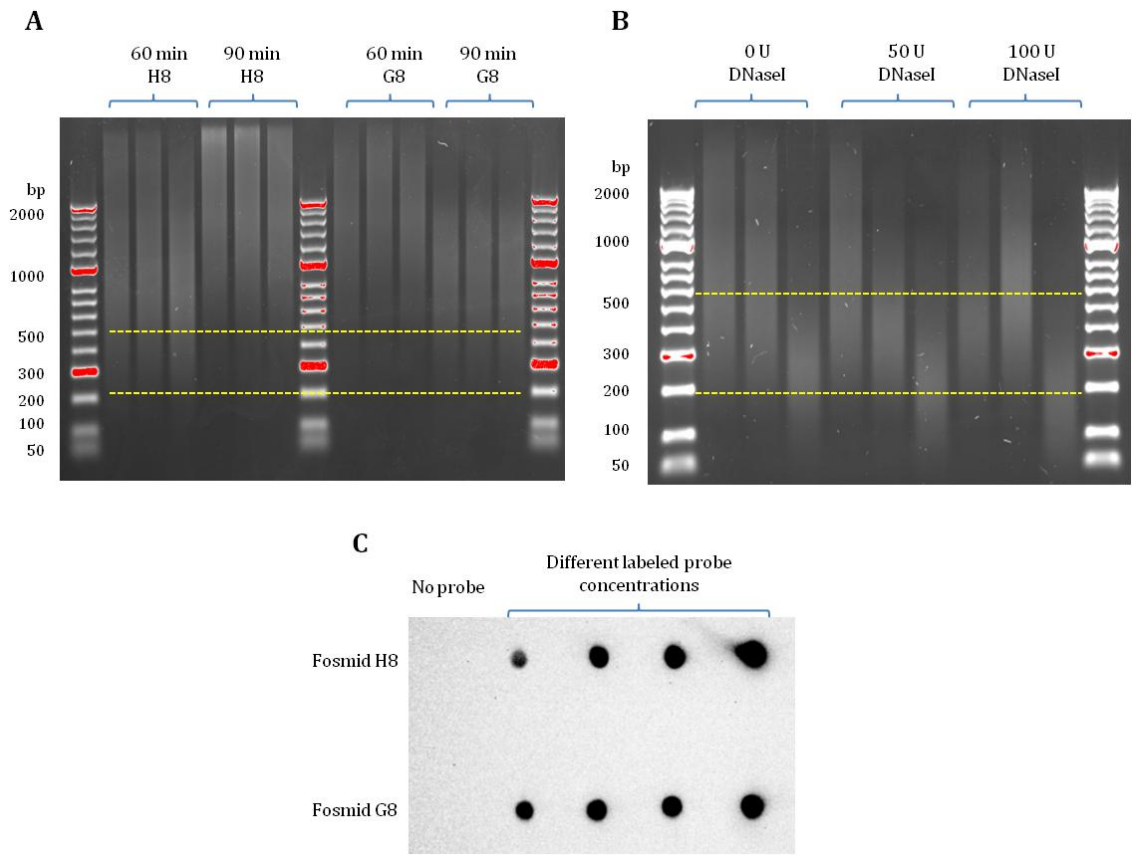


Figure 17. Optimization of the probes labelling

(A) Both probes were labelled according to the nick translation kit instructions from Roche. The obtained fragments (visible as a smear) were bigger than the ones needed, therefore incubation of the probes with additional DNaseI and different incubation times was necessary **(B)** probes were incubated for 60, 90 and 150 minutes with different concentrations of DNaseI (0-100 units) **(C)** dot blot of the labelled probes to confirm labelling in addition to confirmation of size. Dotted lines indicate the desired probes size.

Finally, different concentrations of antibodies to detect *FXN* and the NL were used to ensure a clear visualization of the expanded allele. Unfortunately, it was not possible to localize the expanded allele in the nucleus after several attempts (Figure 18). To date, the technique requires further optimization to clearly detect *FXN* in the nucleus.

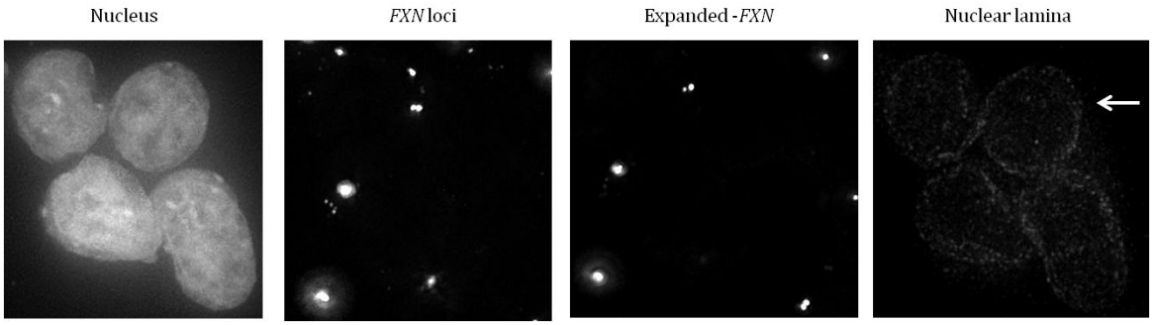


Figure 18. Optimization of 3D DNA FISH

Representative images of *FXN* localization in the nucleus of *FXN*-GAA-Luc cells. From left to right panels, images show DAPI staining, *FXN* loci, expanded-*FXN* and the nuclear lamina, respectively.

In summary, several optimization steps were completed to ensure successful visualization of the *FXN* locus in the cell nucleus. Despite all of the efforts, the technique needs further optimization.

3.3. Discussion

This chapter started with the aim of evaluating the expression of frataxin after the down-regulation of specific epigenetic modifiers, namely histone deacetylase 3 (HDAC3) and Euchromatic histone-lysine N-methyltransferase 2 (G9a). By siRNA-mediated knock-down of HDAC3, frataxin-luciferase mRNA was increased in both reporter cell lines without an effect on protein levels. Several hypotheses can explain the poor correlation between mRNA and protein after HDAC3 siRNA treatment. First, there are several complex post-transcriptional mechanisms involved in turning mRNA into protein (Greenbaum *et al.*, 2003). Although it has been shown that there is no evidence of post-transcriptional defects of FXN mRNA (Bidichandani, Ashizawa and Patel, 1998; Ohshima *et al.*, 1998), this hypothesis cannot be certainly rejected. It is generally accepted in the field, that FRDA is caused

by problems in *FXN* transcription. However, there is one report that showed that FRDA might be caused by inefficient pre-mRNA splicing rather than by aberrant transcription (Baralle *et al.*, 2008). Even though the study claims that the GAA repeats affect pre-mRNA processing, it is important to note that it was conducted in COS7 and HeLa cells transfected with a plasmid containing only part of the *FXN* gene. Thus, abnormal mRNA processing has to be demonstrated further in patient-derived cell lines or in *in vivo* models of FRDA.

Second, it is important to keep in mind that the primary transcripts of pathogenic *FXN* alleles hold long GAA-repeat RNA sequences, and the mechanism by which the down-regulation of HDAC3 is increasing FXN mRNA levels has not been elucidated yet.

Third, proteins have different half-lives as the result of varied protein synthesis and degradation processes (Greenbaum *et al.*, 2003). It is known that the degradation of cellular proteins is a highly complex, timely controlled, and tightly regulated process (Glickman and Ciechanover, 2002), which can make difficult the correlation between mRNA levels and protein expression in all of the cases. Moreover, the differential timings of frataxin mRNA and protein expression might account for this discrepancy.

Finally, the experimental error and noise inherent to both mRNA and protein experiments could lead to an inaccurate estimation of mRNA and protein expression in some cases (Greenbaum *et al.*, 2003).

In addition, the down-regulation of G9a was shown not to have an effect on *FXN* expression. These results suggest that the potential removal of methylation marks

mediated by this methyltransferase might not be sufficient to increase frataxin mRNA and protein levels in a significant manner. Similar studies from other groups using chemical compounds to target G9a, showed that even though methylation marks were removed from the GAA repeat track, mRNA levels remained unaffected. Just a small increase in FXN mRNA levels was previously observed only in the FRDA cell lines with shorter repeats (Punga and Bühler, 2010). In a similar context, a different group has proposed that inhibition of G9a could stimulate *FXN* expression, only if accompanied by targeting DNA-RNA hybrids (Groh *et al.*, 2014; Polak *et al.*, 2016).

In summary, the down-regulation of HDAC3 increased FXN mRNA levels. However, neither the down-regulation of HDAC3; nor of G9a, affected FXN protein expression.

CHAPTER 4

Identification of novel therapeutic targets for FRDA using the SGC epigenetic probes collection

4.1. Introduction

Chemical probes are selective small-molecules that modulate a protein function with a defined mode of action (MoA), thereby allowing the investigation of mechanisms and phenotypes associated with the molecular target (Arrowsmith *et al.*, 2015). The Structural Genomics Consortium (SGC) epigenetic chemical probes collection is a well-characterized library of drug-like small molecules that selectively and potently inhibit/antagonize specific target proteins *in vitro.* The SGC probes set now comprises more than 46 compounds that target specific chromatin regulatory proteins or domains such as bromodomains, demethylases, and methyltransferases (Structural Genomics Consortium, 2018). At the time that this work started, the collection had 39 compounds, but only 36 were available and tested. The list of probes used in this work can be found in appendices Table 17.

4.1.1. Bromodomains

Bromodomains are a common feature of a set of proteins that share the ability to identify and bind to acetylated lysine residues of histones, and have an important role in transcriptional co-activation (Filippakopoulos *et al.*, 2012). The bromodomain-containing family of proteins are termed “readers” of the code, given that they recognize and bind to histone modifications. For instance, bromodomain-

containing proteins can bind to acetylated histones and mediate gene regulation, mostly promoting gene transcription (Arrowsmith *et al.*, 2012).

4.1.2. Methyltransferases

Histone methyltransferases are termed "writers" of the code because they covalently attach methyl groups to lysine and arginine residues in histones. Histone methylation is carried out by a variety of histone methyltransferases (Figure 3) and it is reversed by histone demethylases (refer to section 1.4 for a detailed explanation of histones methylation). Arginine methylation on the other hand, is carried out by protein arginine methyltransferases (PRMTs), a family of proteins that has nine members (PRMT 1-9). Arginines can be mono-, symmetrically or asymmetrically di-methylated. Arginine methylation can either antagonize or promote the interaction of nuclear factors with other nearby histone marks, playing in this way an important role in transcriptional regulatory mechanisms (Di Lorenzo and Bedford, 2011).

4.1.3. Demethylases

Demethylases are enzymes that remove methyl groups from histones and are termed as "erasers". This action is mediated either by the flavin-dependent enzymes lysine-specific histone demethylase 1 and 2 (LSD1 and LDS2) or by the Jumonji family of 2-oxoglutarate-dependent demethylases (Arrowsmith *et al.*, 2012). Histone demethylases are part of large multiprotein complexes, which synergize with histone methyltransferases, histone deacetylases, and nuclear receptors, to control developmental and transcriptional programs (Cloos *et al.*, 2008).

4.1.4. Hypothesis

The screen of a well-characterized collection of chromatin regulatory protein inhibitors will lead to the identification of epigenetic targets, which can be linked to the regulation of *FXN* expression.

4.1.5. Aims

Screening of the SGC epigenetic probes collection using the FXN-GAA-Luc reporter cell line

- To screen by the luciferase assay in a 36-compound epigenetic probe library set for molecules that can increase FXN-Luc protein expression using the *FXN*-GAA-Luc cell line.
- To assess if any of those compounds are toxic for the GAA reporter cell model by the adenylate kinase assay.

Target validation using the FXN-GAA-Luc reporter cell line

- To perform concentration-response curves of the chemical probes that up-regulate the expression of FXN-Luc protein in the *FXN*-GAA-Luc cell line.
- To down-regulate each molecule's target by siRNA-mediated knock-down in the GAA reporter cell model.
- To assess the changes in histone modifications that may be relevant for the increase of FXN-Luc protein expression in the *FXN*-GAA-Luc cell line.
- To test the negative control probes in their ability to modify histone marks and FXN-Luc protein expression using the GAA reporter cell line.

4.2. Results

4.2.1. *The screen of the SGC epigenetic probes collection using the FXN-GAA-Luc reporter cell line highlights a group of methyltransferases as important for FXN expression*

Taking advantage of the available information on the chemical probes provided by the SGC, the experiment was designed based on the recommended maximum and minimum concentrations, and incubation time. The 36 compounds were divided into three groups for the screen (Table 12).

Table 12. List of probes divided by groups based on the SGC recommendations

	Name and number of the probe	Minimum concentration (µM)*	Maximum concentration (µM)	Minimum time**	Concentration to work with (µM)	Incubation time to work with
Group A	**(R)-PFI-2 (2)**	1	10	1d	4	48 h
	BAY-598 (5)	1	10	24h	4	48 h
	BAZ2-ICR (6)	1	5	1h	4	48 h
	BI-9564 (7)	1	10	1h	4	48 h
	GSK2801 (10)	1	10	1h	4	48 h
	I-BRD9 (17)	1	5	18h	4	48 h
	I-CBP112 (18)	1	5	1h	4	48 h
	LP99 (22)	1	10	1h	4	48 h
	NI-57 (25)	1	5	1h	4	48 h
	OF-1 (27)	1	5	1h	4	48 h
	OICR-9429 (28)	3	5	1d	4	48 h
	PFI-1 (30)	1	10	1h	4	48 h
	PFI-3 (31)	1	10	1h	4	48 h
	PFI-4 (32)	1	5	1h	4	48 h
	SGC707 (34)	1	10	1d	4	48 h

Group B	**A-196 (3)**	1	10	24-48h	4	6 d
	A-366 (4)	1	5	3d	4	6 d
	GSK343 (11)	3	5	3d	4	6 d
	GSK591 (13)	1	5	4d	4	6 d
	MS023 (23)	1	10	20 h (PRMT6) 2 days (PRMT1)	4	6 d
	SGC0946 (33)	1	10	4-14d	4	6 d
	UNC0638 (36)	1	5	3d	4	6 d
	UNC0642 (37)	1	5	3d	4	6 d
	UNC1215 (38)	1	5	3d	4	6 d
	UNC1999 (39)	3	5	3d	4	6 d
Group C	**(+)-JQ1 (1)**	1	1	1h	1	48 h
	Bromosporine (8)	5	5	1h	5	48 h
	GSK484 (12)	10	10	3h	10	48 h
	GSK864 (14)			48h	1	48 h
	GSK-J4 (15)	5	10	1d	5	48 h
	GSK-LSD1 (16)	1	1	1-2d	1	48 h
	LAQ824 (21)			48h	6	48 h
	MS049 (24)	5	10	20h	5	48 h
	NVS-CECR2-1 (26)	1	1	1h	1	48 h
	Olaparib (29)				1	48 h
	SGC-CBP30 (35)	1	3	1h	3	48 h

*Dose to achieve significant inhibition of in-cell biomarker activity, **Minimum time required for full reduction of in-cell biomarker activity. This information was granted by the SGC together with the chemical probes.

Considering that there might be a discrepancy in the assessment of mRNA and protein levels after epigenetic modifiers inhibition, and that the ultimate goal for a FRDA potential therapy is to increase frataxin protein expression, the following experiments were designed to measure FXN protein.

Figure 19 shows the pipeline for the SGC epigenetic probes collection screen.

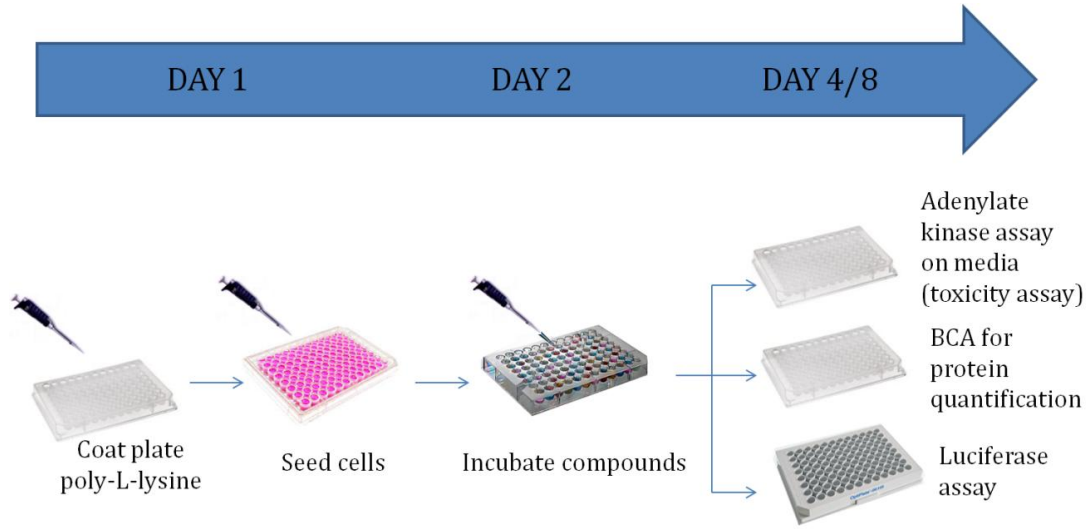
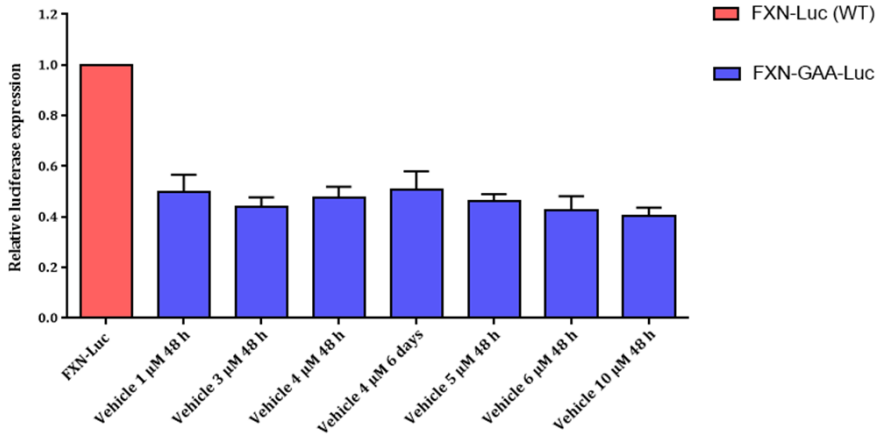


Figure 19. Pipeline used for the SGC epigenetic chemical probes screen

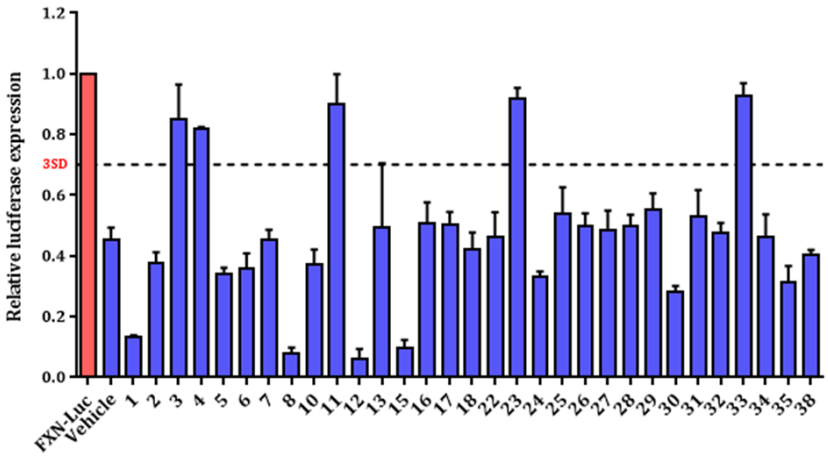
The *FXN*-GAA-Luc cell line was used to screen the epigenetic chemical probes collection. Cells were seeded in a coated 96-well plate to avoid cell detachment. After 24 hours from seeding, cells were treated with the probes. On the media change day (48 hours posttreatment), media was taken for toxicity assay and cells were collected for luciferase assay at the end of the incubation time.

The screen uncovered five candidate compounds as capable of increasing the expression of FXN-Luc protein (Figure 20). All of the identified chemical probes are inhibitors of different methyltransferases which methylate lysines in histones H3 and H4, as well as one arginine residue in histone H3. This finding suggests that the increased histone methylation found in the *FXN* gene constitute an important silencing mark, and that the inhibition of these methyltransferases can increase *FXN* expression.

A



B



C

# 1: (+)-JQ1	# 2: (R)-PFI-2	#3: A-196	#4: A-366
# 5: BAY-598	# 6: BAZ2-ICR	#7: BI-9564	#8: Bromosporine
# 10: GSK2801	# 11: GSK343	#12: GSK484	#13: GSK591
# 14: GSK864	# 15: GSK-J4	#16: GSK-LSD1	#17: I-BRD9
# 18: I-CBP112	#22: LP99	#23: MS023	# 24: MS049
# 25: NI-57	#26: NVS-CECR2-1	#27: OF-1	# 28: OICR-9429
# 29: Olaparib	#30: PFI-1	#31: PFI-3	# 32: PFI-4
# 33: SGC0946	#34: SGC707	#35: SGC-CBP30	#38: UNC1215

Figure 20. A group of chemical inhibitors of several methyltransferases increase FXN-Luc protein expression in the *FXN*-GAA-Luc cell line

(A) Luciferase assay of the *FXN*-GAA-Luc cell line treated with all the different concentrations and conditions of DMSO used in the screen. The wild type line (*FXN*-Luc) is shown as a reference. **(B)** Luciferase assay of the *FXN*-GAA-Luc cell line after treatment with the SGC epigenetic probes collection. The vehicle treated cells shown in this panel represent the average of the conditions in panel A. **(C)** Name of the probes shown in panel B. Data are presented as mean ± s.e.m. of two independent experiments completed in duplicate. The dotted line represents three standard deviations (3SD) from the cells treated with vehicle (DMSO), indicating that five probes are distinctly separated from the vehicle-treated cells.

Following the evaluation of FXN-Luc protein expression, toxicity of the probes was assessed by the adenylate kinase assay. This assay shows that the compounds that increase FXN expression are not toxic. However, some probes can cause the release of adenylate kinase from the cells, indicating cell damage (Figure 21). These probes were too toxic that it was not possible to have a luciferase reading due to the few cells that were left after treatment, hence the discrepancy between the number of probes in Figure 20 and Figure 21.

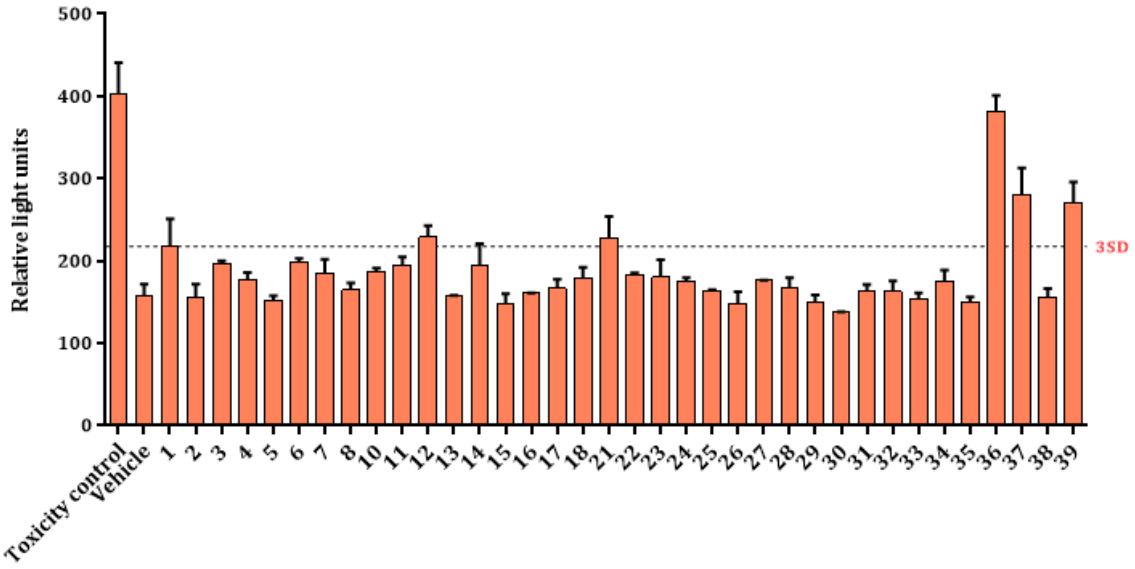


Figure 21. Hit probes show not to be toxic for the *FXN*-GAA-Luc cell line

Adenylate kinse assay of the *FXN*-GAA-Luc cell line after treatment with the SGC epigenetics probes collection. Data are presented as mean ± s.e.m. of two independent experiments completed in duplicate. The dotted line represents three standard deviations (3SD) from the cells treated with the vehicle.

In summary, the screening of the SGC epigenetic probes collection identified a group of methyltransferases as important for the regulation of *FXN*. The chemical inhibition of these specific targets, increases the expression of FXN-Luc protein without causing cell toxicity, pointing to novel therapeutic targets.

4.2.2. Target validation using the FXN-GAA-Luc reporter cell line uncovers the methyltransferases of the SUV4-20 family as novel candidate therapeutic targets in FRDA

The first step in the validation of the hit molecules was to understand the effect of each one of the chemical probes and confirm their targets.

Compound # 3: A-196

A-196 is a potent and selective inhibitor of the methyltranferases SUV4-20H1 and SUV4-20H2. It has been shown to be selective for the SUV4-20 enzymes over 29 other methyltransferases, including protein arginine methyltransferases and DNA methyltransferases, a panel of epigenetic readers and chromatin binders, and 125 non-epigenetic targets, including kinases, G-protein-coupled receptors (GPCRs), ion channels, and transporters (for more information of the selectivity profile of this chemical probe, refer to Bromberg *et al.*, 2017). Biochemical and co-crystallization analyses of the probe revealed that A-196 is a substrate-competitive inhibitor of both homologous SUV4-20 enzymes. In cells, A-196 induces a global decrease in the di- and tri-methylation of H4K20, with a concomitant increase in H4K20me1 (Bromberg *et al.*, 2017).

Compound # 4: A-366

A-366 is a selective inhibitor of the methyltransferase G9a and the G9a-related methyltransferase GLP. Selectivity was assessed in a panel of 20 protein methyltransferases and DNMT1(Sweis *et al.*, 2014). This probe is a peptide-competitive inhibitor of both enzymes, and induces a reduction of H3K9me2 in cells (Sweis *et al.*, 2014).

Compound # 11: GSK343

GSK343 is a highly potent, selective, S-adenosylmethionine-competitive (SAM-competitive) EZH1 and EZH2 inhibitor. It is selective over 21 other methyltransferases, with little to no cross-reactivity in a broad screening panel of 44 receptors and enzymes. This small molecule induces a global H3K27me3 reduction (Verma *et al.*, 2012).

Compound # 23: MS023

MS023 is a selective, potent, and cell-active inhibitor of human type I PRMTs, including PRMT1, -3, -4, -6, and -8. Selectivity was determined against a panel of 25 protein lysine methyltransferses and DNMTs and three histone lysine demethylases. MS023 binds the substrate binding site and potently decreases cellular levels of histone arginine asymmetric di-methylation. Thus, reducing global levels of arginine asymmetric di-methylation and at the same time increasing the levels of arginine mono-methylation and symmetric di-methylation in cells (Eram *et al.*, 2016).

Compound # 33: SGC0946

SGC0946 is the first –SAM competitive inhibitor of the methyltransferase DOT1L, which showed selectivity for this target amongst 12 other methyltransferases. In cells, SGC0946 decreases the levels of H3K79 methylation (Yu *et al.*, 2012).

Next, using a concentration-response assay, the change in expression of FXN-Luc protein as the result of different concentrations of the inhibitors was assessed

(Figure 22). This assay was performed with the commercially available probes that correspond to the ones provided by the SGC.

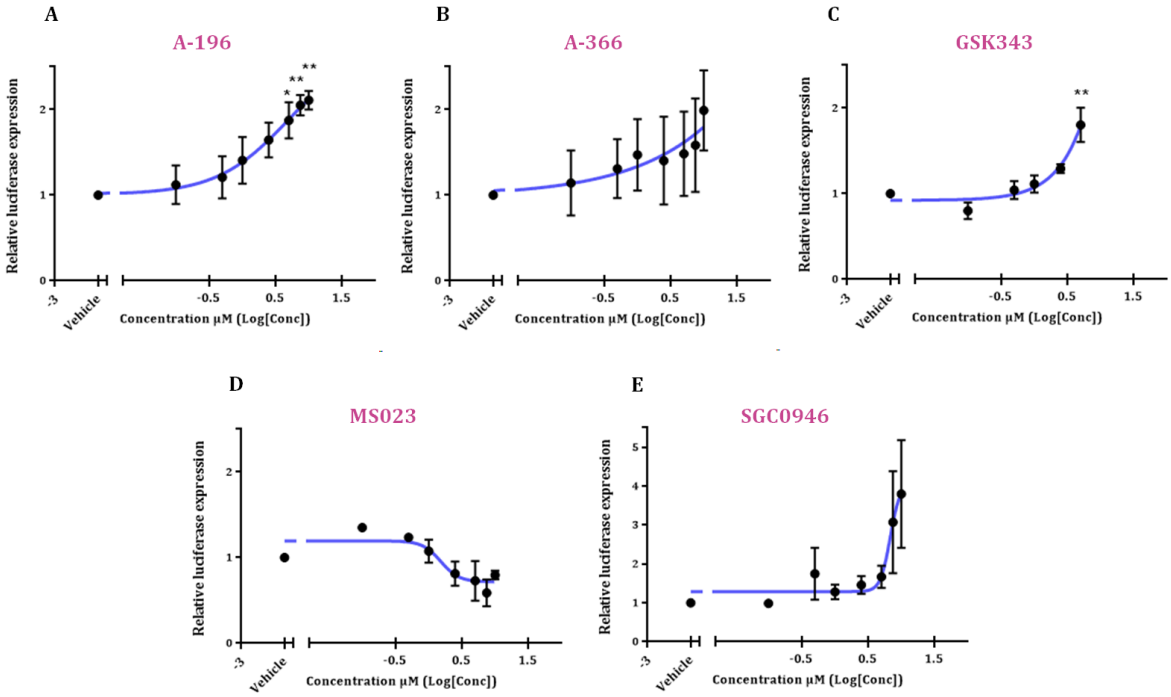


Figure 22. Concentration-response curves of the hit molecules

Luciferase assay of the *FXN*-GAA-Luc cell line treated for six days with increasing concentrations of **(A)** A-196, **(B)** A-366, **(C)** GSK343, **(D)** MS023 and **(E)** SGC0946. Concentrations are in the range between 0.1 µM to 10 µM. Data are presented as mean ± s.e.m. of three independent experiments completed in triplicate, one-way ANOVA Bonferroni corrected for multiple comparisons, *p<0.05, **p<0.01

Figure 22 shows that for most of the molecules, the expression of FXN-Luc protein increases in a dose-dependent fashion. The only exception is MS023, which decreases the expression of FXN-Luc protein while increasing its concentration. Therefore, this methyltransferase inhibitor was excluded for further assays.

Next, since the biological targets of each probe are known, siRNA-mediated knock-down was performed to down-regulate the corresponding methyltransferases in order to confirm their involvement in the regulation of FXN expression from a GAA expanded locus.

Down-regulation of SUV4-20H1 and SUV4-20H2 (A-196 probe) links these proteins to the regulation of FXN expression

Using the *FXN*-GAA-Luc cell line, the knock-down of the methyltransferases of the SUV4-20 family was carried out individually and in combination to understand their role in the regulation of FXN-Luc protein. The cell line was treated with SUV4-20H1, SUV4-20H2 and control siRNA for six days, which was the time used for the treatment with the chemical probe. As control siRNA a SMARTpool (Dharmacon) consisting of four non-targeting siRNA sequences was utilized (Table 10). Figure 23 A shows that knock-down of SUV4-20H1 (~80%) was achieved at concentrations of siRNA of 12 nM and 25 nM. Knock-down of SUV4-20H1 led to a significant 1.9-fold up-regulation of FXN-Luc protein (Figure 23 B). The knock-down of SUV4-20H2 (~20% at 12 nM and ~50% at 25 nM) was not as efficient as for SUV4-20H1 (Figure 23 C-D), and did not produce a significant increase of FXN-Luc protein (Figure 23 E). However, when both homologous proteins were knocked-down together, the increase in FXN-Luc protein was significant at 12 nM SUV4-20H1+SUV4-20H2 siRNA (2.1-fold change) (Figure 23 F-G). These results suggest that the methyltransferase SUV4-20H1 plays a role directly or indirectly in the regulation of *FXN*-Luc expression confirming this protein as a good target to study further.

It is important to clarify that SUV4-20H2 cannot be ruled out as a potential target and that optimization of the knock-down of this methyltransferase is necessary to reach clear conclusions. However, the involvement of SUV4-20H1 is sufficient to highlight H4K20 as an important histone modification in the GAA expanded *FXN* gene. This modification has not been widely studied in the FRDA field.

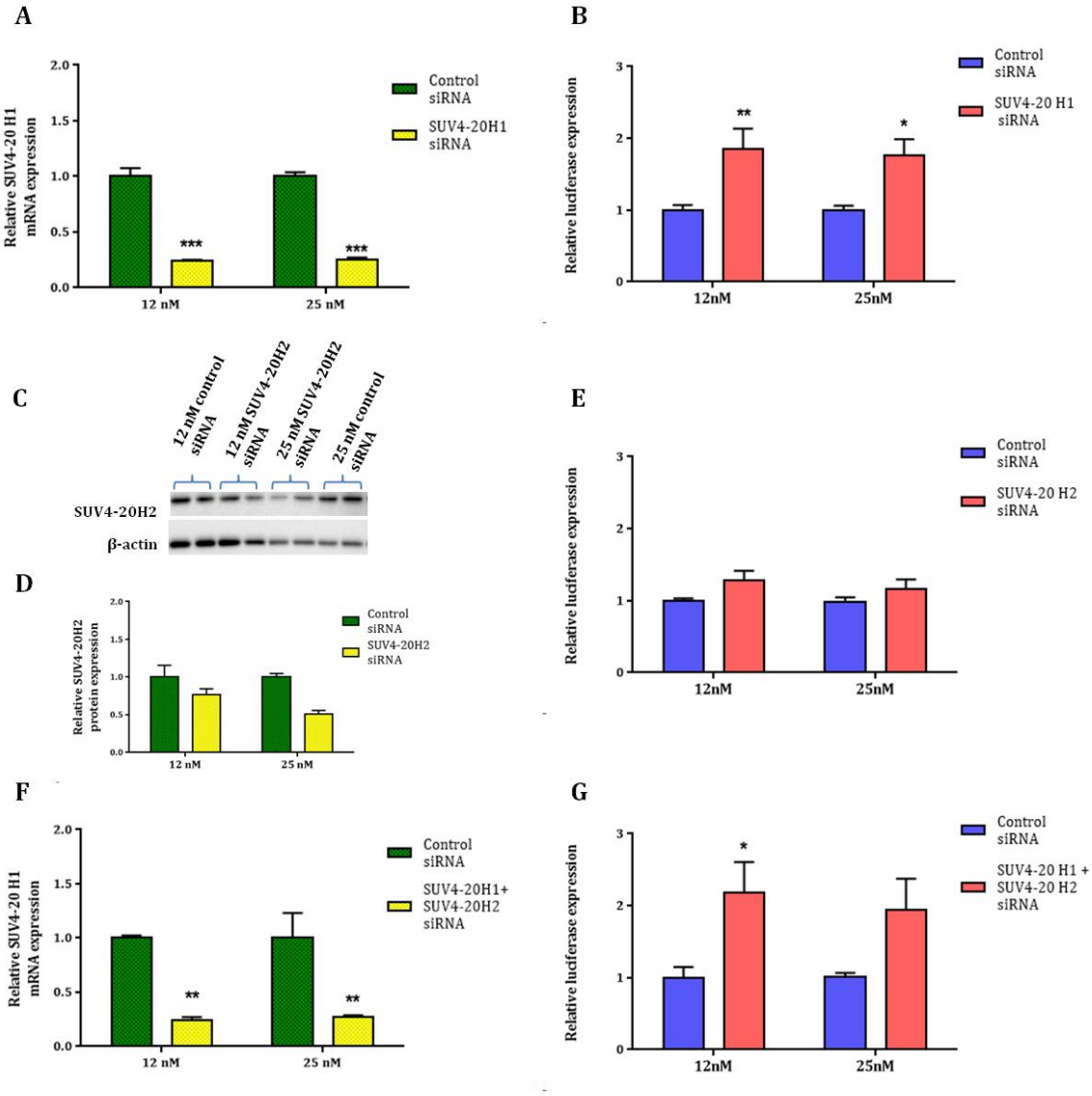


Figure 23. siRNA-mediated knock-down of SUV4-20H1 and SUV4-20H1 + SUV4-20H2 up-regulate FXN-Luc protein expression

(A) SUV4-20H1 mRNA expression assessed by qRT-PCR after siRNA treatment showing down-regulation of the target, **(B)** FXN-Luc protein expression after SUV4-20H1 down-regulation, assessed by the luciferase assay **(C)** Western blot of SUV4-20H2 treated cells, **(D)** Quantification of panel C corresponding to SUV4-20H2 protein expression after siRNA treatment , **(E)** FXN-Luc protein expression after SUV4-20H2 down-regulation assessed by the luciferase assay, **(F)** SUV4-20H1 mRNA expression assessed by qRT-PCR after double knock-down of the SUV4-20 proteins, **(G)** FXN-Luc protein expression after the down-regulation of both SUV4-20 methyltransferases assessed by the luciferase assay. Western blot antibodies for SUV4-20H1 were not good, hence the expression of SUV4-20H1 was determined by qRT-PCR. Data are presented as mean ± s.e.m. of three independent experiments completed in triplicate, except for the SUV4-20H2 down-regulation confirmation that was done two times in duplicate, two-way ANOVA Bonferroni corrected for multiple comparisons, *p<0.05, **p<0.01, ***p<0.001

siRNA targeting of G9a and GLP (A-366 probe) suggests that H3K9 methylation might be a secondary histone modification involved in the repression of FXN expression in FRDA

In Chapter 3 the down-regulation of G9a was shown not to have an effect on the expression of FXN-Luc protein. However, the probe A-366 identified in the screen targets both G9a and its homolog GLP. Therefore, the simultaneous down-regulation of both methyltransferases was performed in order to assess if FXN-Luc protein levels were changed. The *FXN*-GAA-Luc cell line was treated with the indicated siRNA concentrations for six days as described in the previous section (Figure 24).

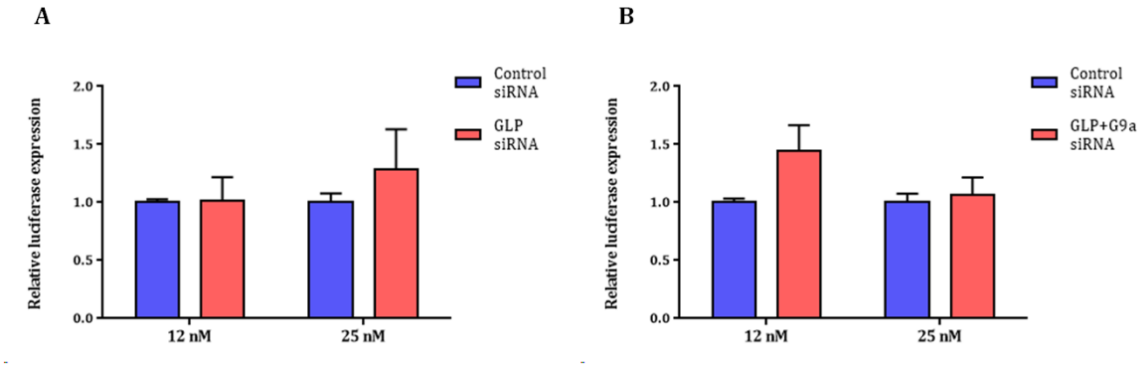


Figure 24. siRNA targeting of G9a+GLP shows a trend in increase of FXN-Luc protein expression assessed by the luciferase assay

(A) siRNA targeting of GLP shows no effect on the levels of FXN-Luc protein in the *FXN*-GAA-Luc cell line, **(B)** siRNA targeting of G9a and GLP shows a slight increase (~1.4-fold change) in the levels of FXN-Luc protein at 12 nM siRNA, without reaching any significance (p=0.06). Data are presented as mean ± s.e.m. of three independent experiments completed in triplicate, except for the G9a+GLP down-regulation that was performed four times, two-way ANOVA.

Figure 24 illustrates the effect of siRNA targeting of GLP and of G9a+GLP in the expression of FXN-Luc protein. However, due to the poor specificity of the available GLP antibodies and the formation of non-specific amplification products by the

designed primers, it was not possible to confirm the knock-down of GLP. It is therefore difficult to draw clear conclusions of the role of these methyltransferases in the regulation of *FXN*. However, considering that in Chapter 3 the down-regulation of G9a did not change FXN-Luc protein expression, it was decided that the probe A-366 and its targets are not high priority for further testing.

Down-regulation of EZH1 and EZH2 (GSK343 probe) have little effect on FXN-Luc protein levels

The effect of the down-regulation of these methyltransferases was assessed in a similar manner as the ones previously described. The *FXN*-GAA-Luc cell line was treated with EZH1, EZH2, EZH1+EZH2 and control siRNAs for six days before assessment of FXN-Luc protein expression by the luciferase assay.

Figure 25 describes the results of the down-regulation of EZH1 and EZH2 in FXN-Luc protein expression. Unfortunately, a low knock-down efficiency was achieved for all siRNA (less than 40% for EZH1 and approximately 60% for EZH2). However, an almost significant increase ($p=0.053$) of FXN-Luc protein after 25 nM EZH1 siRNA treatment was observed, pointing to this target as an interesting one to follow up in the future. A series of optimization steps of the knock-down protocol in order to achieve a good transfection efficiency are needed before reaching any conclusions. Therefore, the probe GSK343 and its targets, were excluded from further assays.

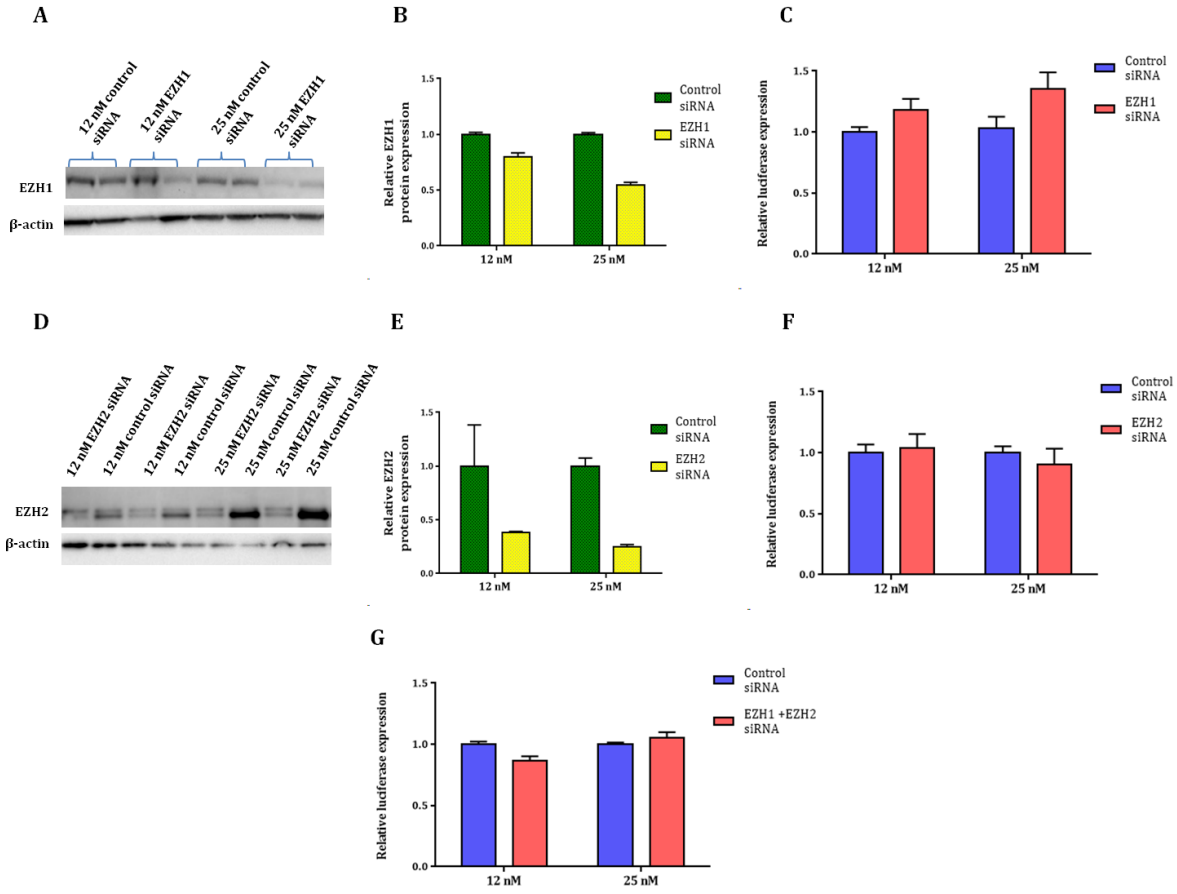


Figure 25. Down-regulation of EZH1 and EZH2 have little effect on the expression of FXN-Luc protein assessed by the luciferase assay

(A) Western blot of EZH1 after transfection, **(B)** Quantification of panel A corresponding to EZH1 protein expression after EZH1 siRNA treatment, **(C)** Luciferase assay of *FXN*-GAA-Luc cell line after EZH1 siRNA-mediated knock-down, **(D)** Western blot of EZH2 after the down-regulation of the protein, **(E)** Quantification of panel D corresponding to EZH2 protein expression after siRNA treatment, **(F)** FXN-Luc protein expression after EZH2 knock-down, assessed by the luciferase assay **(G)** FXN-Luc protein expression after EZH1 and EZH2 down-regulation assessed by the luciferase assay. Data are presented as mean ± s.e.m. of three independent experiments completed in triplicate, except for the confirmation of the knock-downs which was performed twice in duplicate, two-way ANOVA.

Down-regulation of DOT1L (probe SGC0946) does not increase FXN-Luc protein levels

The *FXN*-GAA-Luc cell line was treated with siRNA for DOT1L and control siRNA for six days before evaluation of FXN-Luc protein expression. Clear down-regulation of the target was achieved (~80% using 25 nM siRNA) (Figure 26 A-B) without any

effect on FXN-Luc protein levels (Figure 26 C). This result suggest that DOT1L may not be involved in the regulation of *FXN* expression. Thus, SGC0946 and its target are not going to be subject of further investigation in this thesis.

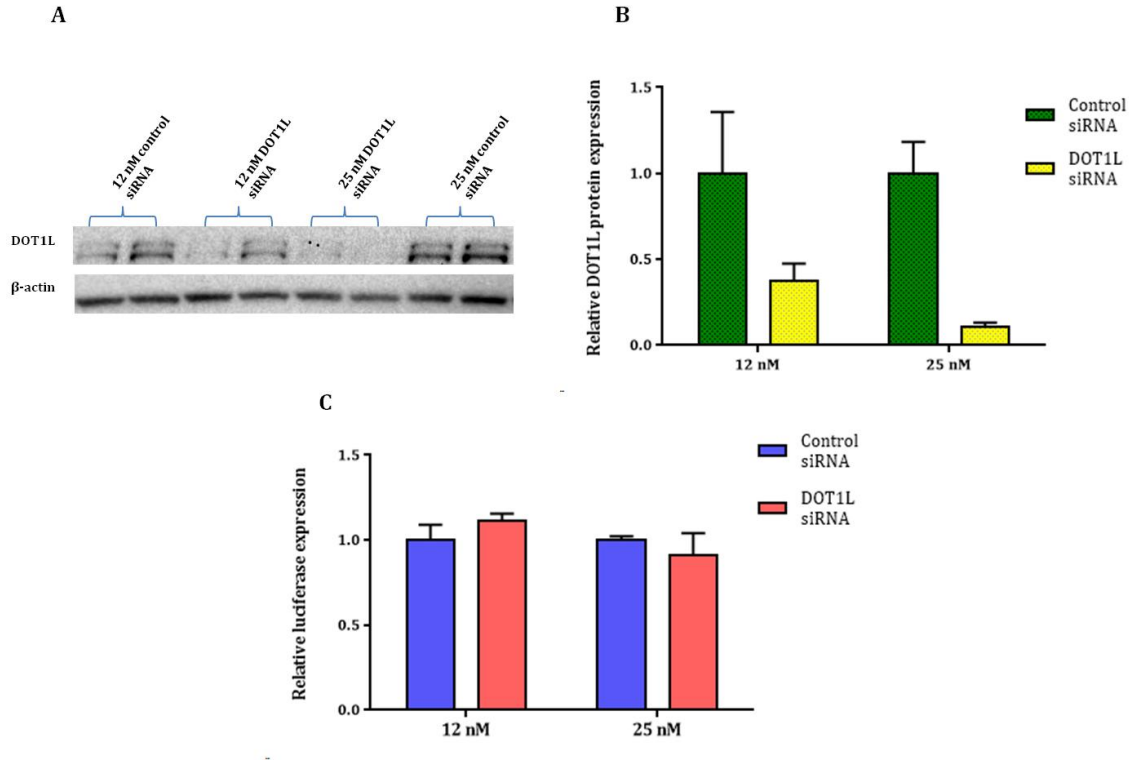


Figure 26. Knock-down of DOT1L in the *FXN*-GAA-Luc cell line

(A) Western blot of the *FXN*-GAA-Luc cell line after DOT1L and control siRNA treatment, **(B)** Quantification of panel A corresponding to DOT1L protein expression after siRNA treatment and **(C)** FXN-Luc protein expression after down-regulation of DOT1L assessed by the luciferase assay. Data are presented as mean ± s.e.m. of three independent experiments completed in triplicate, except for the knock-down evaluation which was performed twice in duplicate, two-way ANOVA.

In summary, the screening of the SGC epigenetic probes collection highlighted the SUV4-20 family of methyltransferases as important for the regulation of *FXN* expression resulting in A-196 (SUV4-20) as the lead probe that will be further validated. Additional work is needed in order to understand the role of GLP, EZH1 and EZH2 in the regulation of the expression of *FXN*-Luc protein.

A-196 treatment decreases the di- and tri-methylation of H4K20, with a concomitant increase in the mono-methylation of the same lysine residue in H4, in the FXN-GAA-Luc cell line

Most of the SGC probes have a control compound that shares a similar structure as the active one, but have little or no effect on the target. A-196 has two control probes named A-197 and SGC2043, which have shown not to have an effect on SUV4-20H1 and SUV4-20H2 (Bromberg *et al.*, 2017; Structural Genomics Consortium, 2018). The chemical structures of the lead compound and its related negative controls are illustrated in Figure 27.

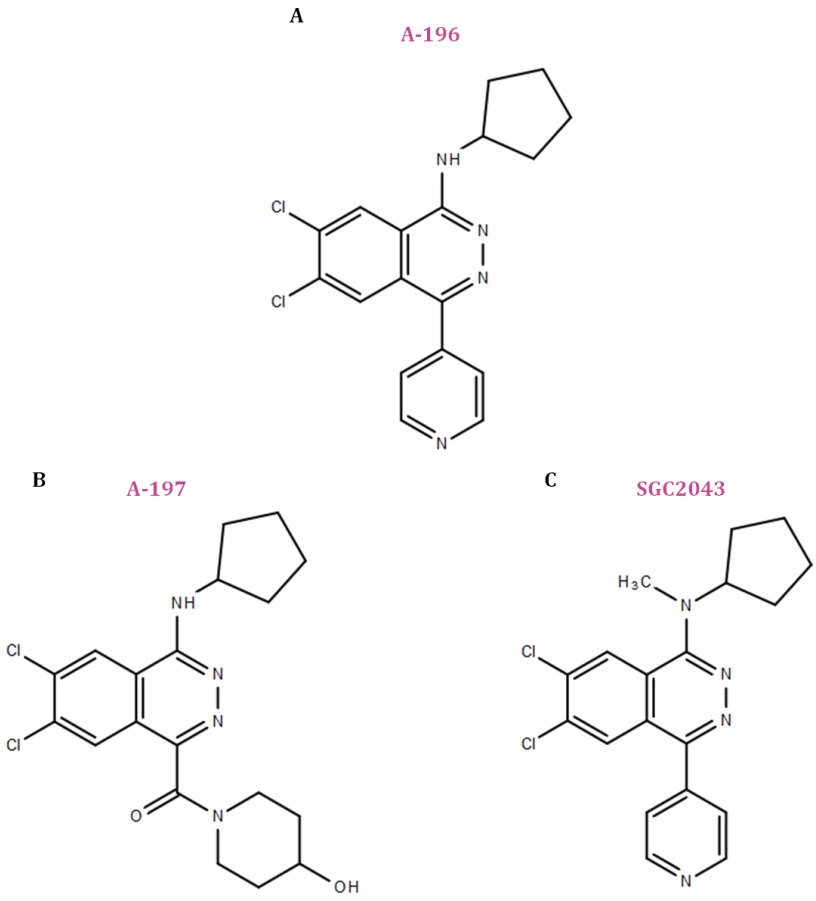


Figure 27. Chemical structures of the lead compound and its related inactive probes

(A) The lead compound A-196, **(B)** inactive control compound A-197 and **(C)** inactive control compound SGC2043.

All of these molecules share the same core, but some of their substituents are changed, turning them either into active or inactive probes against the targets. The use of inactive compounds is helpful to control for potential off-target effects of the specic probe under scrutiny.

It has been shown that A-196 decreases global levels of H4K20me2 and H4K20me3, while increasing H4K20me1 (Bromberg *et al.*, 2017). Thus, global methylation of H4K20 was next assessed in the FXN-GAA-Luc cell line.

Consistent with Bromberg and colleagues, the treatment of the *FXN*-GAA-Luc cell line for six days with 5 μM or 10 μM A-196, results in the global decrease of H4K20me2 (~60% with 10 μM A-196) and H4K20me3 (~90%) (Figure 28 A-C) with the respective accumulation of H4K20me1 (~1.7-fold) (Figure 28 D) assessed by western blot. This finding suggests that A-196 indeed inhibits the methyltransferases SUV4-20H1 and SUV4-20H2 preventing in this way the methylation of lysine 20 in histone 4. Additionally, it demonstrates that the inactive probes A-197 and SGC2043 do not alter the global methylation of H4K20 (Figure 28 A-D). These results also confirm that these inactive probes are good controls, given their poor ability to inhibit the SUV4-20 family of proteins.

Next, FXN-Luc protein expression was assessed by western blot after A-196 treatment. Figure 28 E shows that FXN-Luc protein does not change with the inactive controls, but it increases by 1.5 fold at the highest concentration (10 μM) of A-196. However, this increase does not reach significance, possibly due to insufficient power and the assay variability. Therefore, the luciferase assay was used as a second way of measurement of FXN-Luc protein expression. This

experiment was performed with the active probe and the two inactive ones similarly to the previous assay (six days of treatment with 10 µM and 5 µM of each probe).

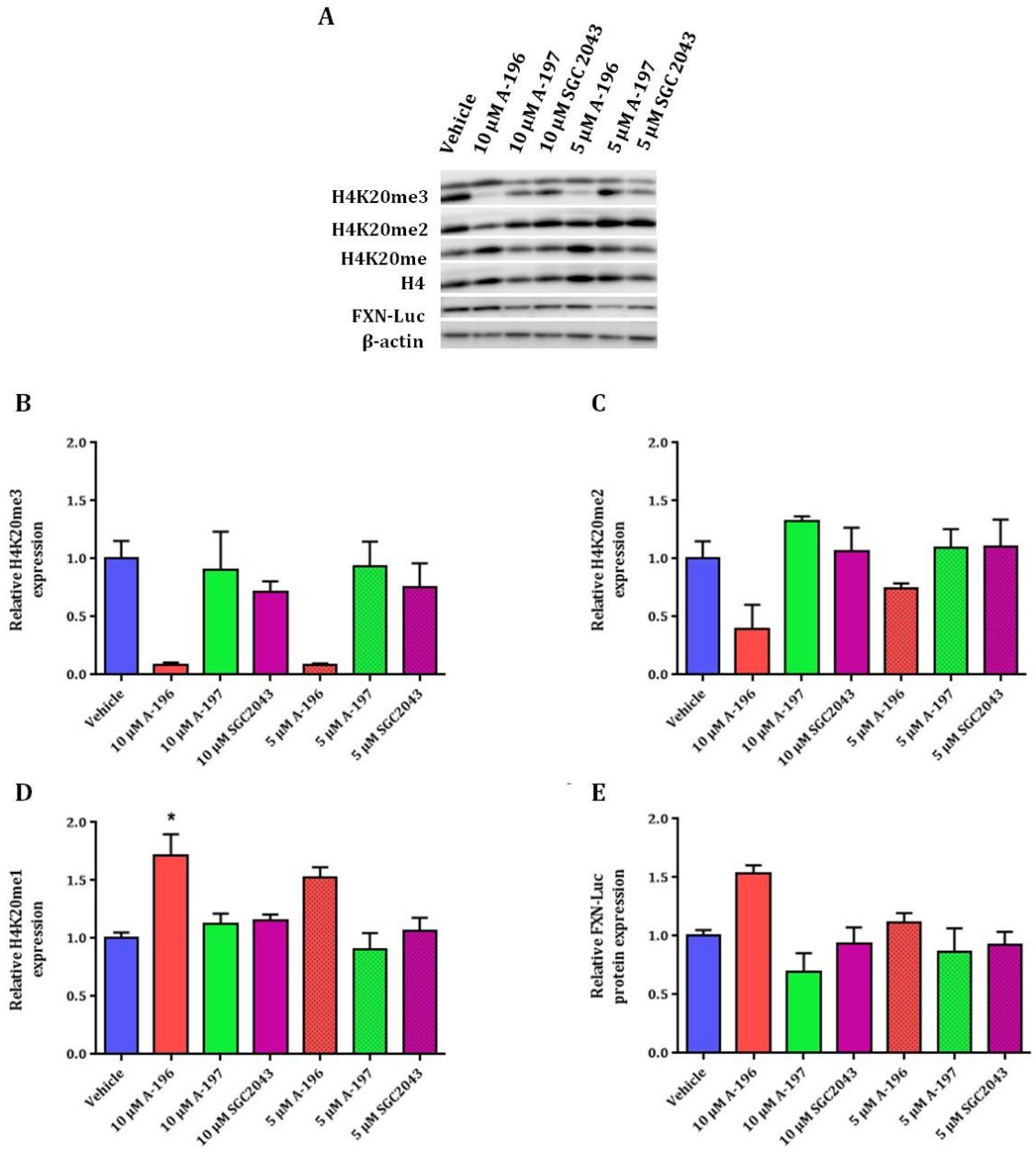


Figure 28. A-196 decreases H4K20me2 and H4K20me3 while increasing H4K20me1 by inhibiting the SUV4-20 family of proteins

(A) Western blot of the *FXN*-GAA-Luc cell line after six days treatment with 10 µM and 5 µM of A-196, **(B)** Quantification of the tri-methylation of H4K20, **(C)** Quantification of the di-methylation of H4K20, **(D)** Quantification of the mono-methylation of H4K20 and **(E)** Quantification of FXN-Luc protein expression. Data are presented as mean ± s.e.m. of three independent experiments completed in duplicate, one-way ANOVA Bonferroni corrected for multiple comparisons, *p<0.05

The evaluation of FXN-Luc protein using the luciferase assay demonstrates that A-196 has the potential to up-regulate FXN-Luc protein expression significantly at 10 μM, and that both negative probes do not have the same ability (Figure 29). These results are in accordance with the western blot data that was previously shown. Amongst the negative controls SGC2043 does not alter the expression of FXN-Luc protein as opposed to A-197 that reduces FXN-Luc protein expression. Considering that SGC2043 is more closely related to A-196 (Figure 27), SGC2043 was selected as the negative control for the next assays.

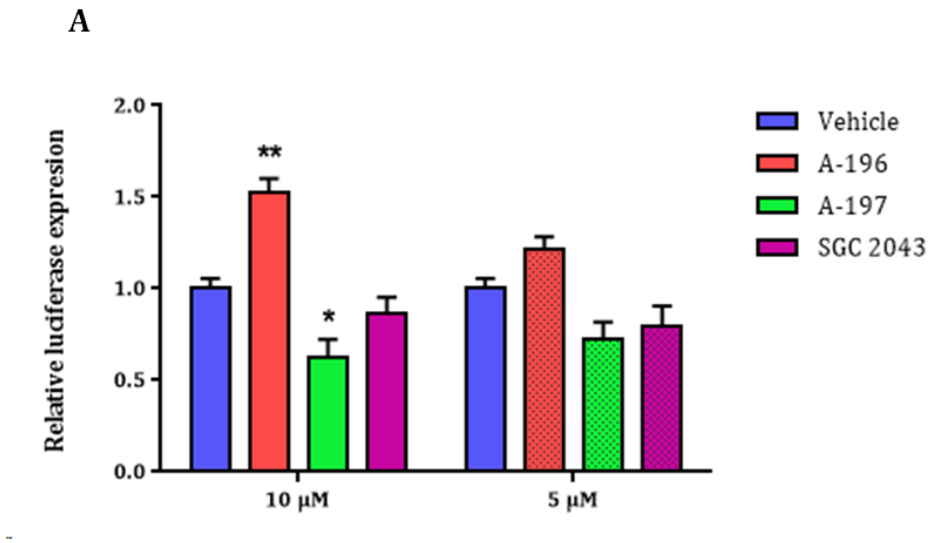


Figure 29. A-196 increases FXN-Luc protein expression in a significant manner at 10 μM

(A) Luciferase assay of the *FXN*-GAA-Luc cell line after the treatment with A-196, A-197 and SGC2043. At the highest concentration of A-196 FXN-Luc protein increases significantly, while A-197 decreases its expression at the same concentration. SGC2043 seems not to have any effect on FXN-Luc protein levels at both studied concentrations. Data are presented as mean ± s.e.m. of three independent experiments completed in triplicates, two-way ANOVA Bonferroni corrected for multiple comparisons, *p<0.05, **p<0.01

In summary, in the *FXN*-GAA-Luc cell line, A-196 inhibits SUV4-20 and decreases the global levels of H4K20me2 and H4K20me3, while increasing H4K20me1, a

change that results in the up-regulation of FXN-Luc protein. The control probes A-197 and SGC234 do not have an effect on the global levels of H4K20, nor on the expression of FXN-Luc protein, confirming that the increase in expression of *FXN* is due to the biochemical inhibition of the SUV4-20 family of proteins and not caused by potential off-target effects.

4.3. Discussion

This chapter describes the screen of the SGC epigenetic probes collection to identify potential therapeutic targets for FRDA. The hypothesis was that amongst several epigenetic modifiers, some will be relevant to modify the expression of the GAA expanded *FXN* gene. Despite the fact that the SGC epigenetic probes collection represents a small library, a number of methyltransferases were identified for their capacity of regulating the expression of *FXN*. This finding was not surprising, given that there is a significant amount of evidence linking epigenetics with the repression of *FXN* in FRDA.

After a primary screen of several inhibitors of chromatin regulatory proteins or domains (bromodomains, demethylases, and methyltransferases), a group of methyltransferases that modify H4R3, H3K9, H3K27, H3K79 and H4K20, were found to increase FXN-Luc protein expression in the *FXN*-GAA-Luc reporter cell line.

Methylation of histone H4 arginine 3 (MS023)

Examination of the literature on the *FXN* gene revealed that the hyper-methylation of the lysine residues herein identified have been described in FRDA models (Sandi *et al.*, 2014). However, to the best of my knowledge, H4R3 methylation has not been previously linked to FRDA. It has been shown that symmetric methylation of

histone H4 in arginine 3 (H4R3me2s) is required for subsequent DNA methylation. This process is carried out through direct binding of the methylated histone with the DNA methyltransferase DNMT3A. It has also been shown that loss of H4R3me2s resulted in loss of DNA methylation, with a concomitant activation of gene expression (Zhao *et al.*, 2009). Therefore, even though H4R3 has not been associated with the frataxin gene, its importance in driving DNA methylation, which has been reported to be increased in GAA expanded *FXN,* made the initial discovery an interesting one to follow up. Unfortunately, the concentration-response curve showed that FXN-Luc protein decreased with increasing concentrations of the probe that selectively targets H4R3. A possible explanation to this could be that the probe is effective in increasing FXN-Luc at lower concentrations than the ones tested (<0.1 μM see Figure 22). However, the screen was carried out at 4 μM, which initially was shown to increase FXN-Luc protein. A possible explanation for this discrepancy may be that the screen was performed with the probes provided by the SGC whereas dose-responses were performed with commercially available compounds. Theoretically, if the probe is correctly synthesized, the source of it should not matter. Nonetheless, on rare occasions, commercially available probes may be of insufficient purity, stability or quality (Arrowsmith *et al.*, 2015). It would be therefore useful to repeat this experiment using the original SGC compounds or alternative chemical manufacturers.

Methylation of histone H3 lysine 79 (SGC0946)

On a close examination of H3K79 methylation, it was surprising to find that the inhibition of DOT1L, the methyltransferase responsible for this histone modification, was beneficial for the expression of FXN-Luc protein. This is taking

into account that H3K79me2 is decreased upstream and downstream of the GAA repeats (Kim, Napierala and Dent, 2011) and that inhibition of DOT1L will only contribute to a further reduction of H3K79. However, considering that DOT1L is the enzyme driving all methylation states of H3K79, and that H3K79me1 has been associated with gene activation, H3K79me3 was linked to gene repression (Barski *et al.*, 2007), and that H3K79me2 was linked to active transcription in humans (Okada *et al.*, 2005), it is clear that a tight control of DOT1L activity is necessary for gene expression. Therefore, a study which shows the abundance of each possible H3K79 methylation state in FRDA patient-derived cells would help clarify the role of DOT1L.

Methylation of histone H3 lysine 9 (A-366)

In spite of the fact that in Chapter 3 the direct down-regulation of G9a did not show to alter the expression of FXN-Luc protein (Figure 13), it was interesting to find as hit a probe that inhibits G9a and its homologous protein GLP, suggesting that GLP or G9a and GLP together may be involved in the regulation of *FXN.* In fact, Tachibana and colleagues have shown that G9a and GLP cooperatively exert the methylation of H3K9 by forming a heterodimeric G9a–GLP complex, which was described as the only functional mono- and di-methyltransferase of H3K9 *in vivo* (Tachibana *et al.*, 2005). This cooperative role of both homologous proteins could potentially explain why the down-regulation of one of these two methyltransferases individually did not have an effect on FXN-Luc protein expression. Further support to this idea was obtained when siRNA targeting of G9a and GLP showed a slight increase in FXN-Luc protein levels (Figure 24 B). Unfortunately, this modest increase did not reach

significance, therefore additional validation of the targets is necessary to draw cleared conclusions.

Methylation of histone H3 lysine 27 (GSK343)

Considering that H3K27me3 has been found to be increased at the 5'UTR, upstream and downstream of the GAA repeats in several models of FRDA (Table 5), the inhibition of EZH1 and EZH2, which drive H3K27 methylation, could potentially reverse the disease-associated methylation pattern. In the experiments here described, it seems that EZH1 may be important for the expression of *FXN*. However, a more efficient knock-down of the targets needs to be achieved to confirm any potential role of these methyltransferases in the silencing of *FXN*, particularly in light of the fact that several groups have reported the accumulation of H3K27me3 in the frataxin gene (De Biase *et al.*, 2009; Kim, Napierala and Dent, 2011; Chan *et al.*, 2013). Gene editing by CRISPR delivering guide RNAs for EZH1 and EZH2 may be an interesting approach to effectively reduce the expression of these methyltransferases.

Methylation of histone H4 lysine 20 (A-196)

A novel interesting finding is that inhibition of the methyltransferases of the SUV4-20 family was found to increase the expression of FXN-Luc protein from the *FXN* GAA expanded locus. The GAA expanded *FXN* gene was shown to have increased H4K20me3 in the flanking regions of the GAA repeats (Kim, Napierala and Dent, 2011) and decreased H4K20me1 downstream of the repeats (Li *et al.*, 2015), both epigenetic marks regulated by the chemical probe A-196. A-196 has been shown to reduce global levels of H4K20me3 and H4K20me2, increasing at the same time

H4K20me1 (Bromberg *et al.*, 2017), which can potentially reverse the H4K20 epigenetic signature of the *FXN* gene. Despite the evidence that there is an aberrant expression of H4K20, this lysine residue has not been widely studied in the FRDA field. Thus, the contribution of this work is valuable for the scientific community, highlighting the importance of the methylation of lysine 20 in histone 4 in the silencing of *FXN*, and in addition revealing a novel potential therapeutic target for FRDA.

Some of the observations made here, need to be confirmed with additional experiments. Based on the data presented, a decision was made to take the chemical probe A-196 forward for further validation, not only in light of the results described in this chapter, but also for the novelty of the targets SUV4-20H1 and SUV4-20H2 in FRDA.

CHAPTER 5

Validation of A-196 in FRDA patient-derived cell lines

5.1. Introduction

The *FXN*-GAA-Luc cell line used for the initial screen has been shown to recapitulate the epigenetic modifications of the *FXN* locus, as well as the repression of *FXN* gene expression seen in FRDA patients (Lufino *et al.*, 2013). However, considering that this reporter cell line was built in human embryonic kidney cells 293 (HEK 293) which have endogenous normal levels of frataxin, a more appropriate model of the disease was necessary for the validation of the observations here made. Therefore, FRDA patient-derived cells, which constitute a more relevant model of the disease because they more closely mimic the features of a FRDA cell, were used for the validation of the initial findings.

5.1.1. Consequences of frataxin deficiency

The mature frataxin protein is located in the mitochondrial matrix, where it is associated with the inner mitochondrial membrane (Campuzano *et al.*, 1997). The GAA trinucleotide expansion in the first intron of *FXN,* which has been associated with epigenetic changes, reduces the amount of frataxin within the cell and mitochondria (Campuzano *et al.*, 1996; Festenstein, 2006; Sandi *et al.*, 2011). Mitochondria are important organelles in the cell with a significant number of functions in the CNS, such as neuronal development and maintenance. In these

processes mitochondria participate in a variety of mechanisms such as energy production, maintenance of membrane potential, calcium homeostasis, amongst others. Therefore, frataxin deficiency leads to a decrease of mitochondrial biogenesis and an increase of mitochondrial iron load, which is linked to an increase of the generation of reactive oxygen species (González-Cabo and Palau, 2013).

FRDA patient-derived fibroblasts and lymphoblastoid cells have been shown to have increased sensitivity to oxidative stress (Wong *et al.*, 1999; Napoli, Taroni and Cortopassi, 2006). Although the precise mechanism by which frataxin deficiency causes oxidative stress is not known, it has been suggested that is a consequence of altered cellular iron metabolism, due to deficiency in ISC biogenesis. Thus, deficient formation of ISC may increase mitochondrial free iron that in turn could increase the production of ROS and oxidative stress through Fenton reaction (Rötig *et al.*, 1997; Tamarit, Obis and Ros, 2016). In this reaction, ferrous iron can produce ROS by reducing oxygen to the superoxide radical in addition to reducing hydrogen peroxide to the very reactive hydroxyl radical (Armstrong, Khdour and Hecht, 2010).

Deficiency of the iron-sulphur components of the electron transport chain complexes, as a result of frataxin deficit, has been shown to decrease the activity of the mitochondrial electron transport chain and therefore impair oxidative phosphorylation (Rötig *et al.*, 1997; Bürk, 2017). This abnormal energy production in frataxin-deficient cells has been linked to altered mitochondrial membrane potential ($\Delta\Psi_{\mathrm{m}}$) and mitochondrial calcium homeostasis as a downstream effect

(Wong *et al.*, 1999; Brookes *et al.*, 2004; Shidara and Hollenbeck, 2010; Abeti *et al.*, 2015; Zhao *et al.*, 2017).

Frataxin deficiency has also been associated with Nrf2, the master regulator of the cellular redox homeostasis. For instance, in the DRG and the cerebella of a FRDA mouse model, frataxin depletion has been shown to reduce the expression of Nrf2 (Shan *et al.*, 2013). Moreover, Nrf2 translocation to the nucleus, where it exerts its function activating cytoprotective genes, has been reported to be impaired in fibroblasts derived from FRDA patients as well as frataxin-deficient cultured motor neurons (D'Oria *et al.*, 2013; Petrillo *et al.*, 2017).

Oxidative stress and mitochondrial dysfunction play an important role in the pathogenesis of FRDA, where neurodegeneration primarily affects the DRG with the loss of large sensory neurons and follows to the dentate nucleus of the cerebellum (Campuzano *et al.*, 1996).

5.1.2. Hypothesis

The treatment of FRDA patient-derived cell lines with A-196 will increase frataxin protein expression and will ameliorate disease phenotypes.

5.1.3. Aims

Validation of A-196 in FRDA patient-derived cell lines

- To evaluate FXN protein expression in fibroblasts and lymphoblastoid cell lines derived from FRDA patients after A-196 treatment.

Phenotypic analysis of FRDA patient-derived cell lines

- To establish cellular phenotypes derived from *FXN* deficiency in FRDA patient-derived fibroblasts, in order to be able to study how they change after a drug treatment.
- To assess mitochondrial membrane potential, mitochondrial calcium release, mitochondrial superoxide, mitochondria intrinsic properties such as area and length and Nrf2 cellular localization in FRDA patient-derived fibroblasts.

Phenotypic analysis of FRDA patient-derived cell lines after A-196 treatment

- To assess the effect of A-196 treatment in the described phenotypes.

The experiments of this chapter were performed with the help of Dr Irene del Molino del Barrio (AlphaLISA), Dr Saba Saqlain (Mitochondrial membrane potential), Dr Gabriele Corda and Dr Dayne Beccano-Kelly (calcium release) and Dr Marta Cherubini (image analysis).

5.2. Results

5.2.1. A-196 increases mature frataxin protein in FRDA patient-derived fibroblasts

The inhibition of the SUV4-20 methyltransferases up-regulated FXN-Luc protein in the *FXN*-GAA-Luc cell line. Therefore the evaluation of the expression of FXN protein in a more relevant model of the disease, such as FRDA patient-derived cells, was next studied. FXN protein is found in cells as an intermediate 19 kDa form and as a mature 14 kDa form (see Figure 2). The mature form has been shown to be the

fully functional form for cell survival and hence the most beneficial species to up-regulate and investigate in functional studies (Pastore and Puccio, 2013).

First, confirmation of the different levels of expression of the mature form of FXN protein was performed by western blot. Consistent with the literature, the two FRDA patient-derived fibroblast lines (GM03816 and GM04078) express less FXN protein compared to the control line (GM03440) (Figure 30 A-B).

Next, the two FRDA patient-derived cells, GM04078 and GM03816 (details of the cell lines can be found in Table 6) were treated for six days with 5 μM and 10 μM A-196 before processing them for protein analysis as previously described in section 2.2.5. Cells treated with vehicle (0.1% DMSO) where used as control since the control probes A-197 and SGC2043 were not yet available when this set of experiments was performed.

A-196 treatment was able to up-regulate mature FXN protein in the patient cell line GM04078 by approximately 1.5-fold (Figure 30 C-D). Even though the same trend was seen in the patient line GM03816 (Figure 30 E), the increase in expression was not significant. These results suggest that A-196 is able to up-regulate mature FXN protein in FRDA patient-derived cells, an effect that may be dependent on the genetic variability of each cell line.

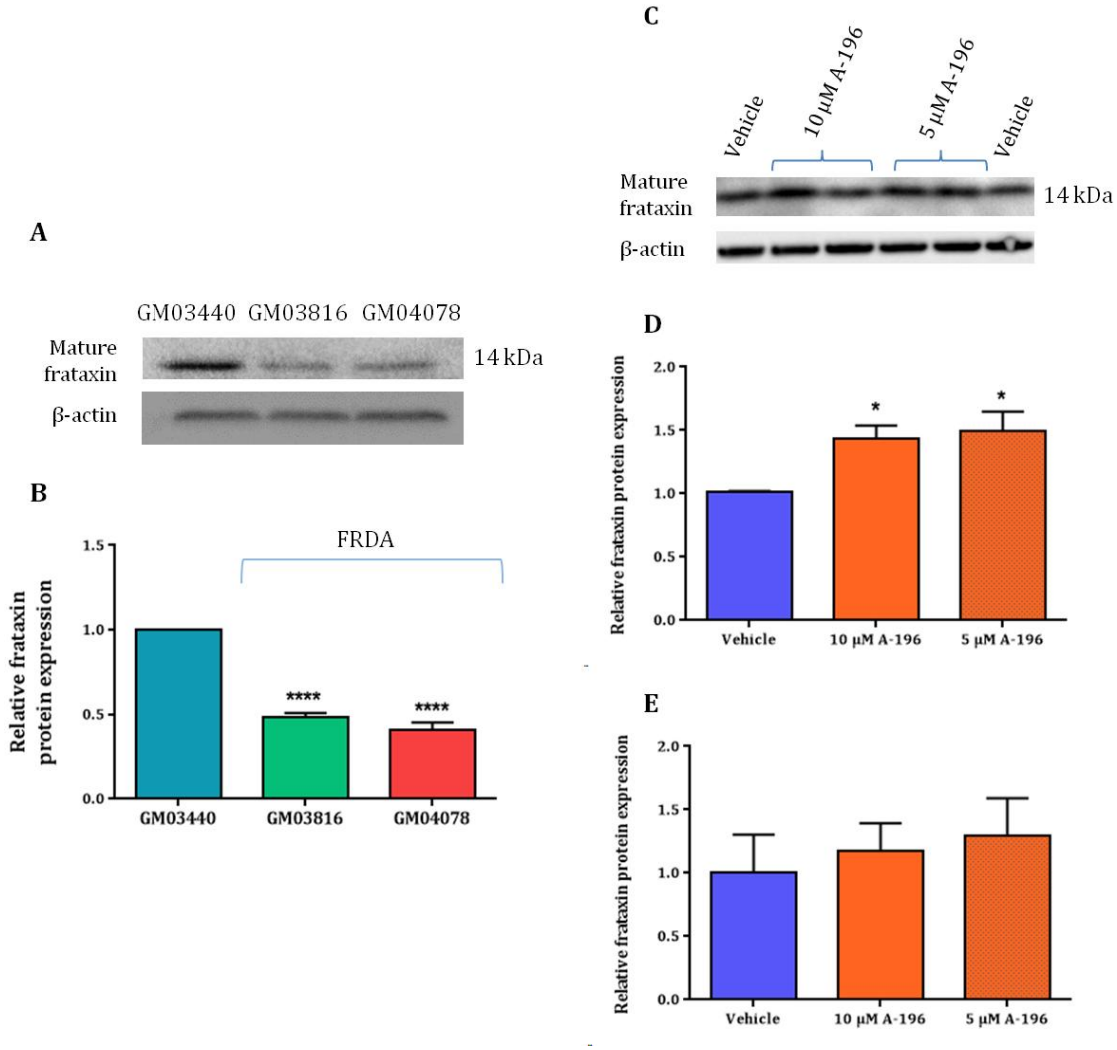


Figure 30. A-196 increases mature frataxin protein expression in the GM04078 cell line

(A) Western blot analysis of the cell lines GM03440 (control), GM03816 and GM04078 (patients) showing different expression of FXN protein, image provided by Dr Gabriele Corda **(B)** Quantification of mature FXN expression in the primary fibroblast lines, **(C)** Expression of FXN protein in the GM04078 cell line after six days treatment with A-196, **(D)** Quantification of mature frataxin protein expression in the GM04078, **(E)** Quantification of mature frataxin protein expression in the GM03816 cell line. Data are presented as mean ± s.e.m. of three independent experiments completed in duplicates, one-way ANOVA Bonferroni corrected for multiple comparisons, *p<0.05, **** p<0.0001

In order to confirm the pharmacological activity of A-196 in multiple cell lines, Epstein–Barr virus-transformed lymphoblastoid cell lines (GM15851, GM15848 GM16220 and GM15850) were also used (details of the cell lines can be found in Table 6). Frataxin protein was measured by AlphaLISA. The AlphaLISA assay uses a

Biotinylated anti-FXN antibody which binds to the Streptavidin-coated donor bead, while the anti-FXN is conjugated to the acceptor bead. In the presence of FXN the beads come into close proximity. The excitation of the donor bead stimulates the release of singlet oxygen which triggers energy transfer in the acceptor bead, resulting in a peak of light emission at 615 nm (Figure 31 A).

First, the levels of FXN protein were assessed in all of the cell lines by AlphaLISA (Figure 31 B). Then, both patient-derived cells (GM16220 and GM15850) were treated for six days with 5 μM and 10 μM of either A-196 or SGC2043 and FXN protein levels were determined by AlphaLISA (Figure 31 C-D).

The evaluation of frataxin protein levels by AlphaLISA in lymphoblastoid cell lines of FRDA patients, shows that the expression of FXN protein is dependent on the length of the GAA expansion (Figure 31 B). This result confirms that this technique is useful for the assessment of FXN protein levels in Epstein–Barr virus-transformed lymphoblastoid cell lines.

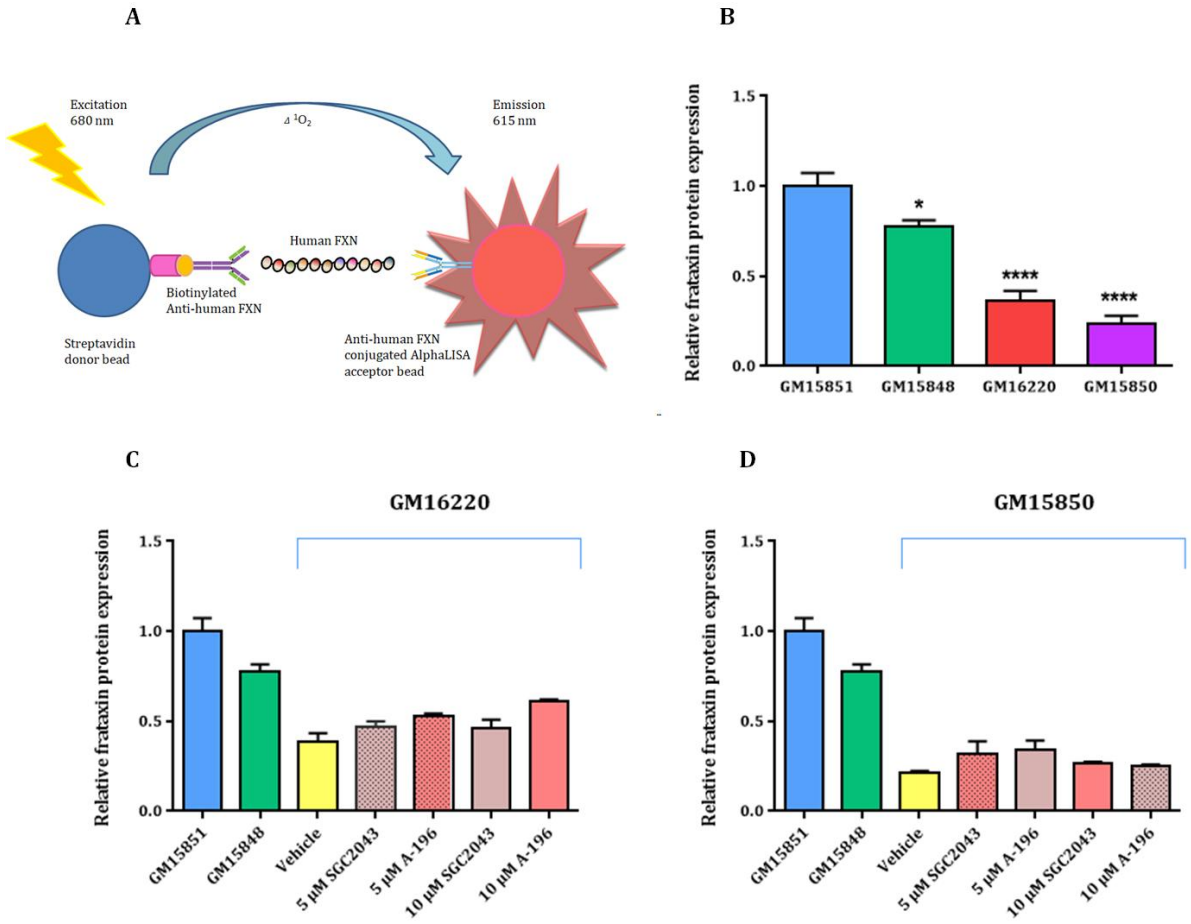


Figure 31. The lymphoblastoid cell line GM16220 has a modest increase in FXN protein after A-196 treatment

(A) Schematic representation of the AlphaLISA principle **(B)** FXN protein expression in lymphoblastoid cell lines GM15851 (control), GM15848 (carrier), GM16220 and GM15850 (patients) assessed by AlphaLISA, **(C)** FXN expression as determined by AlphaLISA in GM16220 cells treated with vehicle (0.1% DMSO), SGC2043 and A-196, **(D)** FXN expression as determined by AlphaLISA in GM15850 cells treated with vehicle (0.1 DMSO), SGC2043 and A-196. Untreated GM15851 and GM15848 cells are presented as reference. Data are presented as mean ± s.e.m., of three independent experiments completed in triplicate, except for the treatment of the patient lines (panels C-D) that was performed twice in triplicate, one-way ANOVA Bonferroni corrected for multiple comparisons, *p<0.05, ****p<0.0001

The treatment of the cell line GM16220 with 10 µM A-196 up-regulates FXN protein expression by approximately 1.6-fold with respect to the vehicle treated cells. However, this increase is not statistically significant by ANOVA in the context of the whole experiment. The cell line GM15850, which has a severe depletion of FXN

protein (~80% assessed by AlphaLISA), also shows an approximate 1.6-fold increase in FXN protein expression after 5 μM A-196 treatment. Interestingly, 5 μM SGC2043 also increases FXN protein expression by approximately 1.4-fold compared to the vehicle treated cells, suggesting that FXN protein up-regulation, in this genetic background, may be due to off target effects. It would be interesting to correlate these findings with the assessment of H4K20 methylation states in the cell line GM15850 to reach clear conclusions.

In summary, A-196 increases by approximately 1.5-fold the levels of mature FXN protein in the FRDA patient-derived fibroblast cell line GM04078. In lymphoblastoid cell lines A-196 also seems to up-regulate FXN protein expression (~1.6-fold); however it is unclear if this effect is mediated by the inhibition of SUV4-20, as the negative probe SGC2043 (5 μM) also seems to have an effect on the GM15850 cell line.

5.2.2. Phenotypic analysis of FRDA patient-derived fibroblasts

Patient-derived cells such as primary cells or immortalized cell lines are important laboratory tools for the *in vitro* study of cellular responses. Amongst these two types of cells, primary cells better resemble patient phenotypes, not only because they are more representative of the tissues that they were isolated from, but also because they have not accumulated mutations that usually arise during immortalization or continual passage in tissue culture (Hare *et al.*, 2016). Therefore, primary fibroblasts derived from FRDA patients were used for the description of phenotypes in frataxin depleted cells, with the aim of studying them later after A-196 treatment.

Mitochondrial morphology assessment

FRDA has been described as an inherited mitochondrial disease due to the strong evidence that supports an oxidative stress pathomechanism caused by an imbalance in mitochondrial function (Hayashi and Cortopassi, 2015). Considering the importance of mitochondria in a variety of cellular functions (as described in section 5.1.1), and that oxidative stress will have a direct impact on mitochondria, first, mitochondrial morphology was analysed in control and FRDA patient-derived fibroblasts.

Figure 32 illustrates the four mitochondrial parameters assessed, mitochondrial number per cell (mitochondrial mass), mitochondrial area, length and length-to-width ratio. Amongst all analysed parameters, only mitochondrial mass seems to be reduced as a result of FXN protein depletion (Figure 32 A-B). Even though the other analysed parameters are not statistically different, there appears to be a trend for a general mitochondrial network alteration in FRDA patient-derived cells (Figure 32 A-B). These results are perhaps expected considering the importance of FXN protein for cellular functions such as mitochondrial biogenesis (Jasoliya *et al.*, 2017).

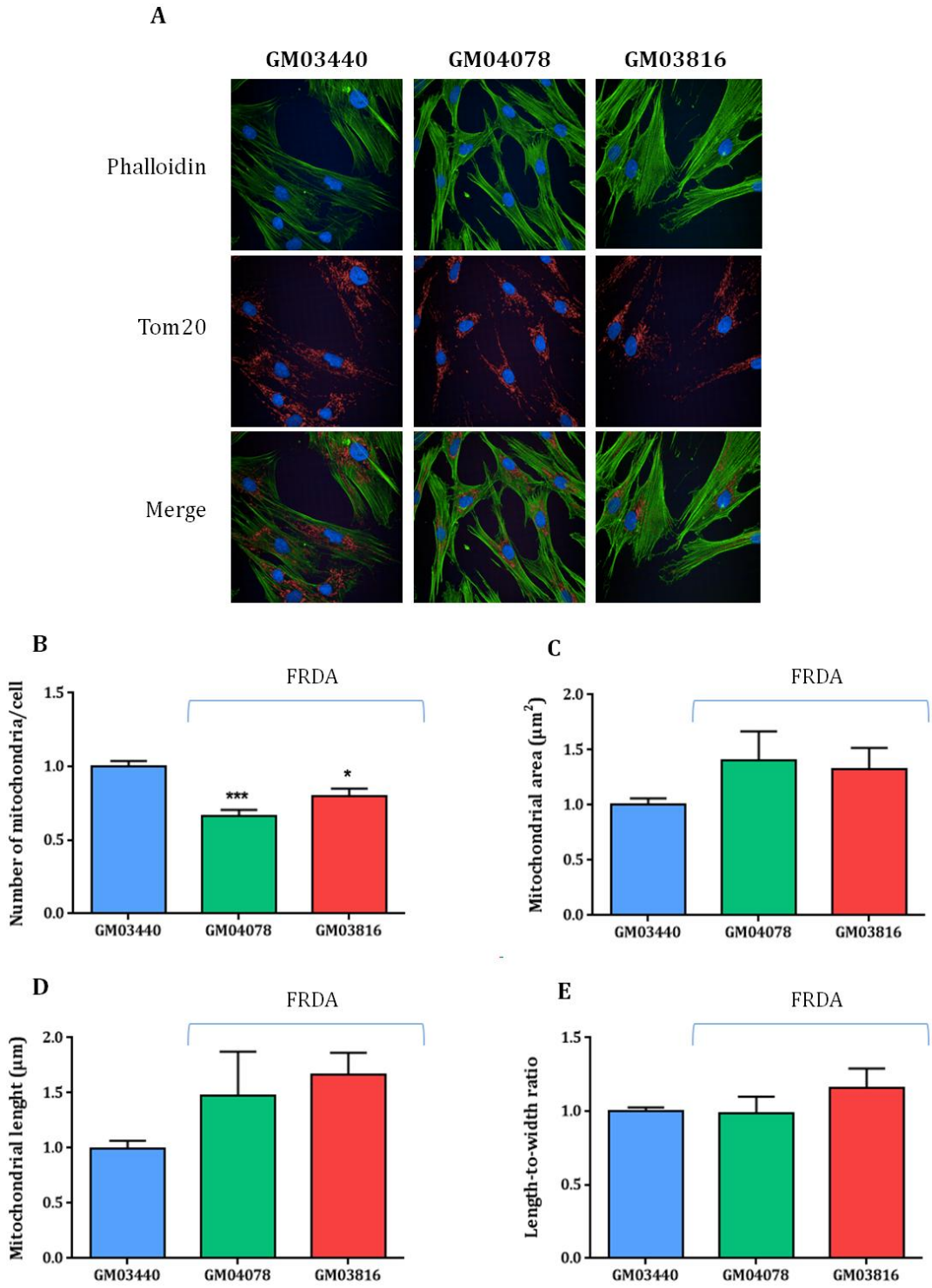


Figure 32. Mitochondrial mass is decreased in patient-derived fibroblasts

(A) Representative images of the mitochondrial network in control fibroblasts (GM03440) and FRDA patient-derived fibroblasts (GM04078 and GM03816), **(B)** Quantification of mitochondrial mass, **(C)** Mitochondrial area, **(D)** Mitochondrial length and **(E)** Mitochondrial length-to-width ratio (Aspect ratio). Phalloidin: actin network marker used to define each cell, Tom20: mitochondrial marker. Data are presented as mean ± s.e.m. of three independent experiments completed in triplicate, one-way ANOVA Bonferroni corrected for multiple comparisons, *p<0.05, ***p<0.001

Mitochondrial membrane potential evaluation

Mitochondrial membrane potential, which is considered as an indicator of mitochondrial integrity and function, was assessed with the lipophilic cationic dye JC-10. At low $\Delta\Psi_m$, accumulation of JC-10 in mitochondria is low and most of the dye is in its monomeric form, which emits a green fluorescence. In contrast, at high $\Delta\Psi_m$, accumulation of JC-10 in mitochondria is high and most of the dye is in the aggregate form, which emits a red fluorescence. By measuring a shift in fluorescence from green to red, as a result of the ability of JC-10 to form aggregates as a function of mitochondrial membrane polarization, $\Delta\Psi_m$ can be calculated (Nicholls, 2004; Perry *et al.*, 2011).

FRDA patient-derived fibroblasts show a reduced $\Delta\Psi_m$ compared to control fibroblasts (Figure 33). The line GM04078 has approximately a 50% reduction, while the line GM03816 has approximately a 30% reduction. This result suggest that FXN has an important role in the maintenance of $\Delta\Psi_m$, as it was previously shown by other groups (Shidara and Hollenbeck, 2010; Abeti *et al.*, 2015; Zhao *et al.*, 2017).

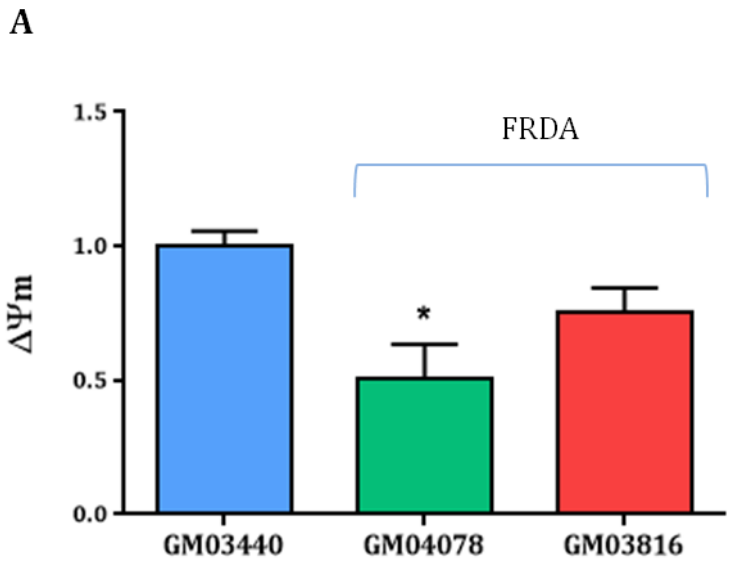


Figure 33. Mitochondrial membrane potential is reduced in FRDA patient-derived fibroblasts

(A) Mitochondrial membrane potential in control (GM03440) and FRDA patient-derived fibroblasts (GM04078 and GM03816) assessed by JC-10 as the a shift in fluorescence from green to red as a result of CCCP depolarization. Data are presented as mean ± s.e.m. of four independent experiments completed in triplicate, one-way ANOVA Bonferroni corrected for multiple comparisons, *p<0.05

Mitochondrial ROS generation assessment

Mitochondrial membrane potential is the key bioenergetic parameter that controls ROS generation amongst other essential features of mitochondrial activity (Nicholls, 2004). Considering that $\Delta\Psi_m$ is altered as a result of the lack of FXN, ROS generation was next assessed in live fibroblasts of control and FRDA patients utilizing the mitochondrial superoxide-sensitive anion MitoSOX. First, the base line of ROS production was measured by MitoSOX staining as the intensity of MitoSOX over the number of mitochondria stained with Mitotracker (Figure 34 A). Next, the effect on ROS generation of the protonophore CCCP, which depolarizes mitochondria by increasing their permeability to protons hence generating mitochondrial ROS

(Perry *et al.*, 2011), was assessed. CCCP (10 µM) was added to all primary fibroblast lines and MitoSOX intensity was measured (Figure 34 B).

FRDA patient-derived fibroblasts show at base line (without any additional oxidative stress) approximately 1.2-fold increase in ROS generation compared to the control fibroblast line (Figure 34 A). The addition of CCCP (additional oxidative stress that depolarizes the $\Delta\Psi_m$ inducing ROS generation) to the primary cultures, shows that all fibroblasts generate more ROS over time (Figure 34 B). This result suggest that mitochondria in the primary fibroblasts lines are able to generate ROS in response to CCCP.

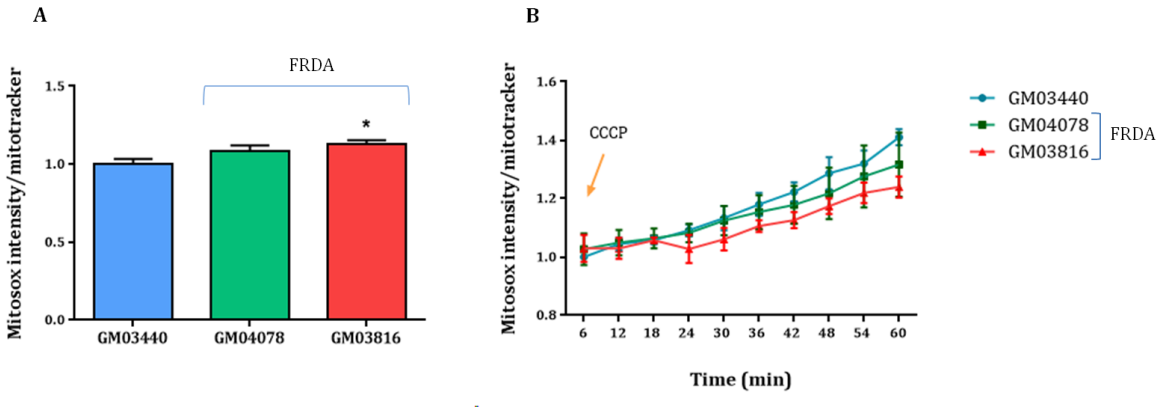


Figure 34. FRDA patient-derived fibroblasts have more mitochondrial ROS than control fibroblasts

(A) MitoSOX intensity over mitotracker in control (GM03440) and FRDA patient-derived fibroblasts (GM04078 and GM03816) assessed by microscopy, **(B)** MitoSOX intensity over mitotracker after a single injection of CCCP (10 µM) evaluated every six minutes for one hour. Data are presented as mean ± s.e.m. of three independent experiments completed in triplicate, one-way ANOVA Bonferroni corrected for multiple comparisons, *p<0.05

Nrf2 cellular localization

Considering that ROS generation is increased in the FRDA patient-derived fibroblasts GM03816, and that Nrf2, the master regulator of the cellular redox

homeostasis, counterbalances the mitochondrial ROS production and is critical as regulator of cytoprotective gene expression (Hayes and Dinkova-Kostova, 2014; Holmström, Kostov and Dinkova-Kostova, 2016), Nrf2 cellular localization was next assessed. Under normal conditions, Nrf2 is restrained to the cytoplasm, binds Keap1 which promotes Nrf2 ubiquitination and subsequent proteasome degradation. During oxidative stress, Nrf2 is unbound from Keap1, translocates to the nucleus, and it activates transcription of cytoprotective genes, maintaining in this way, the redox balance in the cell (Suzuki, Motohashi and Yamamoto, 2013). To study if Nrf2 is accumulated in the nuclei of FRDA patient-derived fibroblasts as a result of increased ROS generation, all of the primary lines were stained with Nrf2 and phallodin to determine Nrf2 cellular localization.

Even though mitochondrial ROS are increased in the FRDA patient-derived fibroblasts GM03816, Nrf2 seems to be reduced in their nuclei by approximately 60% (Figure 35 A-B) and preferentially localized to the cytoplasm (Figure 35 A, C). This result suggest that under basal conditions, without any additional exposure of the cells to oxidants, Nrf2 is not localized in the nucleus, despite the increased ROS generation seen in the FRDA patient-derived fibroblasts GM03816.

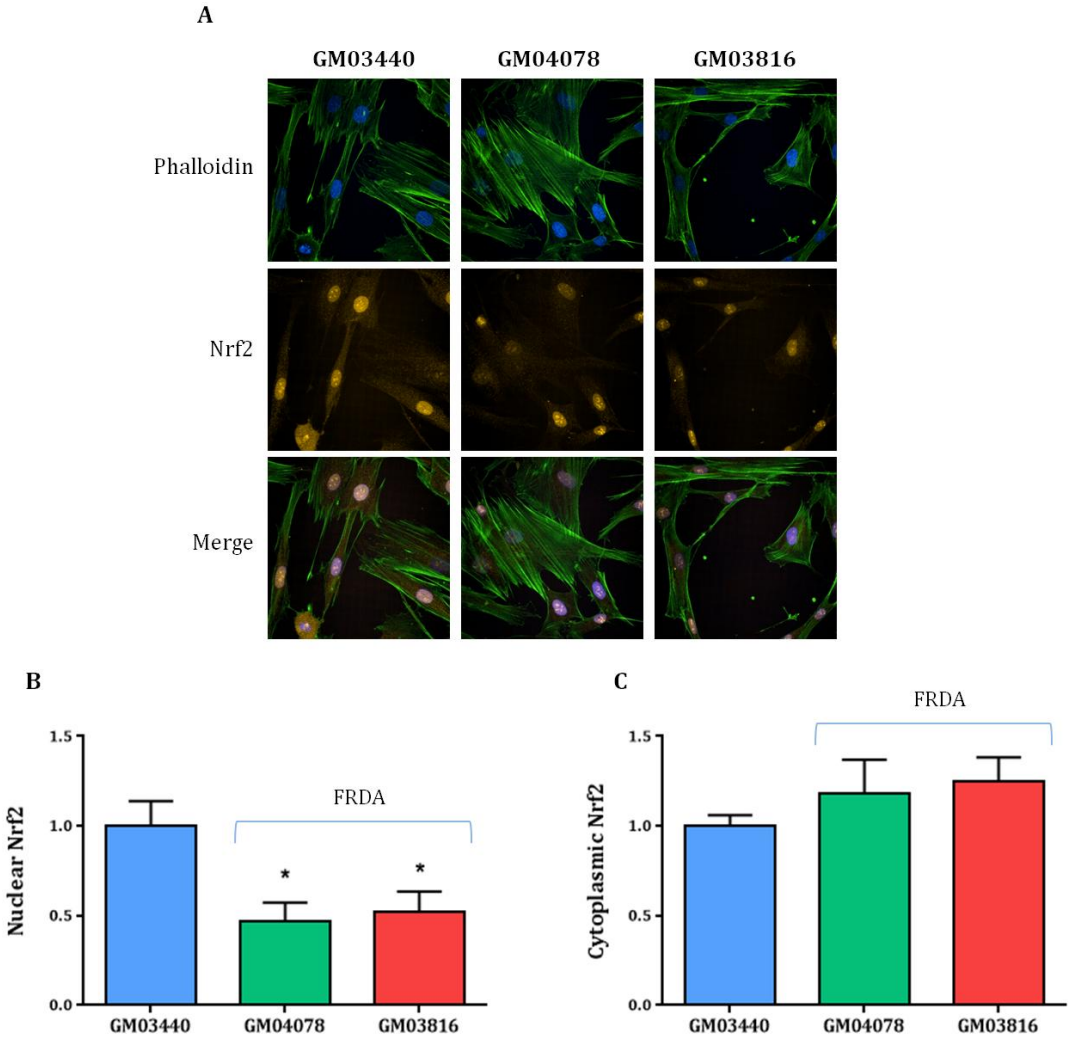


Figure 35. Nrf2 is reduced in the nucleus of FRDA patient-derived fibroblasts

(A) Representative images of cellular Nrf2 localization in control (GM03440) and FRDA patient-derived fibroblasts (GM04078 and GM03816), **(B)** Quantification of nuclear Nrf2, **(C)** Quantification of cytoplasmic Nrf2. Data are presented as mean ± s.e.m. of three independent experiments completed in triplicates, one-way ANOVA Bonferroni corrected for multiple comparisons, *p<0.05

Calcium release evaluation

Another downstream effect of altered $\Delta\Psi_m$ is mitochondrial membrane potential-dependent calcium homeostasis. Calcium is a key regulator of mitochondrial function and its dysregulation affects numerous cell signaling pathways such as ATP synthesis, ROS generation and apoptosis. Calcium homeostasis relies on

mitochondrial calcium uptake and release, both processes highly dependent on $\Delta\Psi_m$ (Brookes *et al.*, 2004). Given the altered $\Delta\Psi_m$ in FRDA patient-derived fibroblasts, calcium release from mitochondria and from all internal cellular stores was next assessed by calcium imaging as described in section 2.2.22 of the methods chapter.

Mitochondrial calcium release is reduced in the FRDA patient-derived fibroblast line GM03816 by approximately 30% (Figure 36 B), while calcium release from all internal cellular stores is reduced by approximately 40% (Figure 36 C). This result suggests that frataxin deficiency leads to several downstream effects, with calcium dyshomeostasis being one of them. Interestingly, the FRDA primary line GM04078, which also showed a decreased $\Delta\Psi_m$, shows a similar calcium release as the control primary line GM03440 (Figure 36 B-C). This result was unexpected, but could be explained considering the genetic variability of each cell line and the fine balance of calcium homeostasis needed under stress conditions in different genetic backgrounds.

In summary, several phenotypes which could be associated with *FXN* deficiency have been described in this section. These phenotypes include reduced mitochondrial mass, reduced $\Delta\Psi_m$, increased ROS generation, decreased calcium release and decreased nuclear Nrf2 localization.

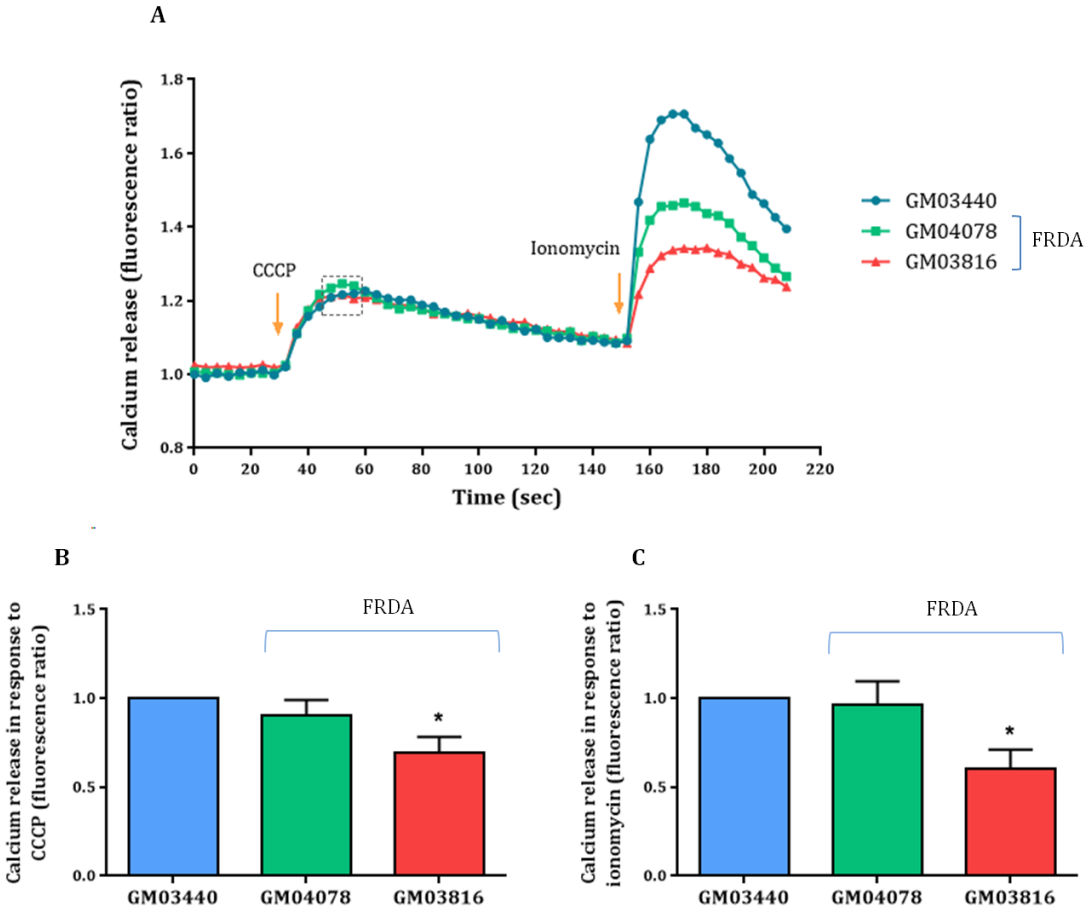


Figure 36. Calcium release is altered in the FRDA patient-derived cell line GM03816

(A) Representative traces of calcium release after CCCP and ionomycin treatment of control (GM03440) and FRDA patient-derived fibroblasts (GM04078 and GM03816). Dotted box shows the time points that were considered to measure calcium release after CCCP in order to estimate the immediate mitochondrial calcium release. The same consideration was made to measure calcium release after ionomycin (calcium release from all cellular stores). Calcium release in response to CCCP and ionomycin were measured separately **(B)** calcium release after CCCP addition, **(C)** calcium release after ionomycin addition. Fluorescence ratio corresponds to the ratio between bound and unbound calcium (340 nm/380 nm). Data are presented as mean ± s.e.m. of three independent experiments completed in quadruplicate, one-way ANOVA Bonferroni corrected for multiple comparisons, *p<0.05

5.2.3. Assessment of the cellular phenotypes after A-196 treatment of FRDA patient-derived fibroblasts

The treatment of the FRDA patient-derived fibroblasts GM04078 with the inhibitor of the methyltransferases SUV4-20, A-196, up-regulates FXN protein expression by

approximately 1.5-fold (Section 5.2.1 Figure 30 C-E). To determine if this increase in FXN protein has an effect on the described phenotypes, the FRDA patient-derived fibroblast lines GM04078 and GM03816 were treated for six days with 5 μM and 10 μM A-196 and the negative control SGC2043, after which mitochondrial mass, $\Delta\Psi_m$, ROS generation, calcium release and Nrf2 localization were analysed.

Mitochondrial mass evaluation after A-196 treatment

Mitochondrial mass is reduced by approximately 40% as a result of frataxin deficiency. Considering that A-196 increases FXN protein, mitochondrial mass was assessed in FRDA patient-derived fibroblasts after A-196 treatment.

A-196 treatment seems to slightly increase (~ 15%) the number of mitochondria in both primary lines (Figure 37), with 10 μM A-196 being the best concentration with almost a 20% increase in the line GM03816 (Figure 37 B). Despite the modest increase, there is no statistically significant difference between the cells treated with the vehicle or with the negative probe SGC2043 and both patient-derived lines treated with A-196.

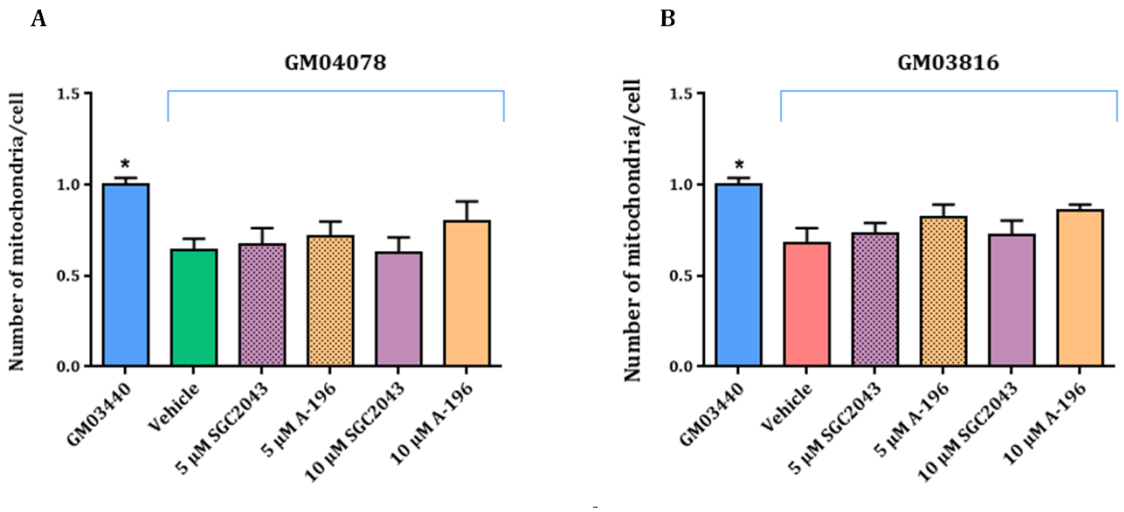


Figure 37. A-196 increases slightly the number of mitochondria in FRDA patient-derived fibroblasts

Number of mitochondria per cell assessed by immunofluorescence in **(A)** GM04078 and in **(B)** GM03816. The control line GM03440 is presented as a reference. Comparisons were made against the vehicle treated cells. Data are presented as mean ± s.e.m. of three independent experiments completed in triplicate, one-way ANOVA Bonferroni corrected for multiple comparisons, *p<0.05

Mitochondrial membrane potential evaluation after A-196 treatment

The reduced frataxin in FRDA patient-derived fibroblasts results in a decreased $\Delta\Psi_m$ as assessed by the fluorescent dye JC-10. A reduction of approximately 70% in the line GM04078 and 60% in the line GM03816 is described in Figure 38.

The treatment of both cell lines with 5 µM A-196 increases the $\Delta\Psi_m$ by approximately 10% in the line GM04078 (Figure 38 A) and by 20% in the line GM03816 (Figure 38 B). This slight increase in both primary lines is not statistically different when compared with the vehicle treated cells or with the cells treated with the negative probe SGC2043. Interestingly, in this set of experiments the $\Delta\Psi_m$ of the line GM03816 reached significance as opposed to Figure 33, confirming that

$\Delta\Psi_m$ is altered in both primary lines, but suggesting that the measurement of $\Delta\Psi_m$ by JC-10 can be variable.

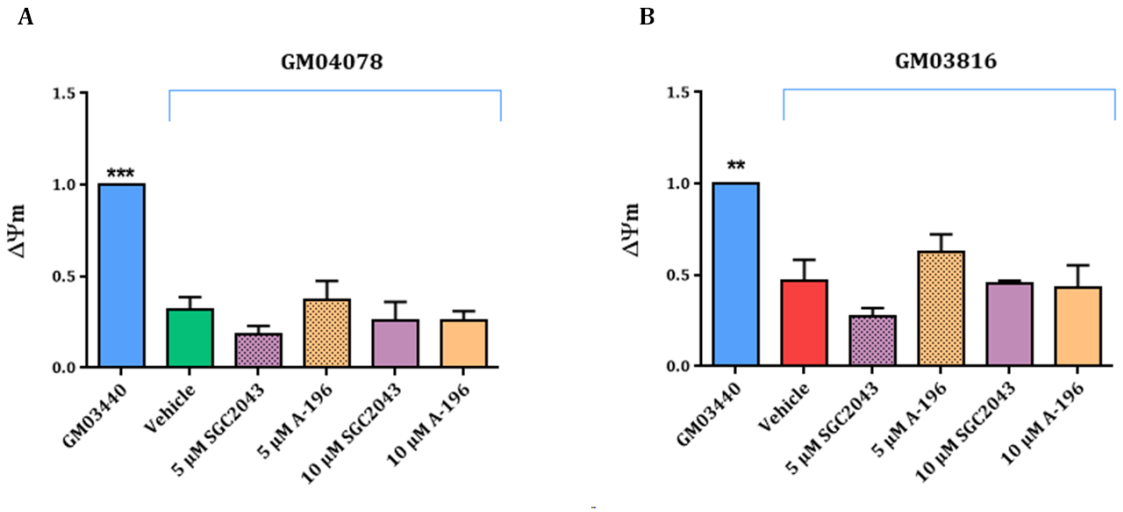


Figure 38. Mitochondrial membrane potential is slightly increased in FRDA patient-derived fibroblasts after A-196 treatment

Mitochondrial membrane potential assessed by the fluorescent dye JC-10 in **(A)** GM04078 and in **(B)** GM03816. The control line GM03440 is presented as a reference. Comparisons were made against the vehicle treated cells. Data are presented as mean ± s.e.m. of three independent experiments completed in triplicates, one-way ANOVA Bonferroni corrected for multiple comparisons, **p<0.01, ***p<0.001

Mitochondrial ROS generation after A-196 treatment

The FRDA patient-derived fibroblast line GM03816 presents a 20% increase in the generation of mitochondrial ROS (Figure 39 B) compared to the control primary line, while the line GM04078 seems no to have a difference when compared to the healthy control (Figure 39 A). A-196 treatment seems to slightly decrease ROS generation in the FRDA line GM03816, with 10 μM A-196 being the best concentration reaching almost 15% reduction (Figure 39 B).

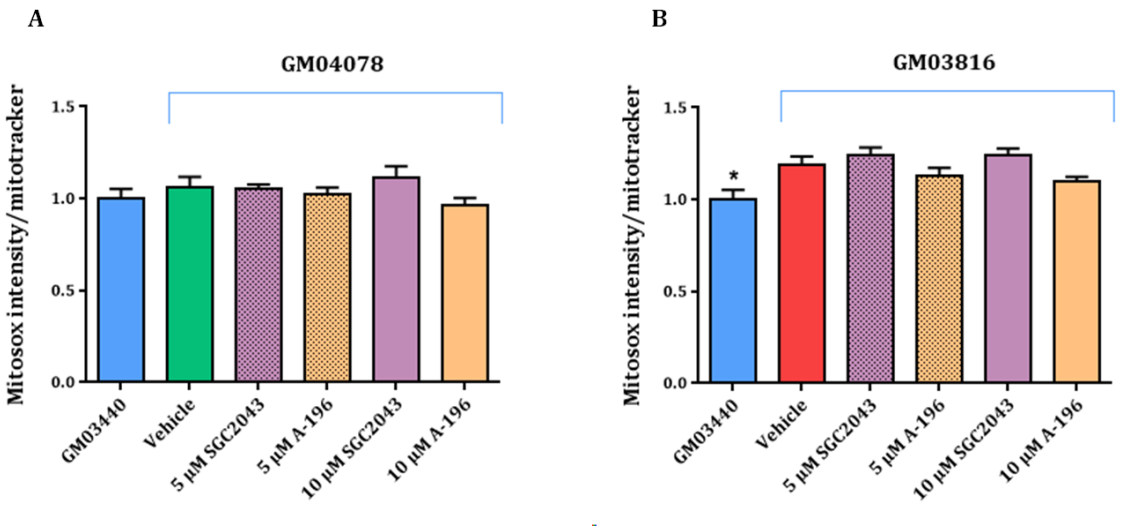


Figure 39. FRDA patient-derived fibroblasts show a modest decrease in mitochondrial ROS production after A-196 treatment

Mitochondrial ROS assessed by immunofluorescence with dye MitoSOX in **(A)** GM04078 and in **(B)** GM03816. The control line GM03440 is presented as a reference. Comparisons were made against the vehicle treated cells. Data are presented as mean ± s.e.m. of three independent experiments completed in triplicates, one-way ANOVA Bonferroni corrected for multiple comparisons, *p<0.05

Nrf2 cellular localization after A-196 treatment

FRDA patient-derived fibroblasts show a decreased nuclear Nrf2 localization (~70%) compared to control fibroblasts (Figure 40). A-196 treatment (5 µM) seems to slightly increase the localization of Nrf2 in the nucleus of the line GM04078 (Figure 40 A). However, this effect is not statistically significant.

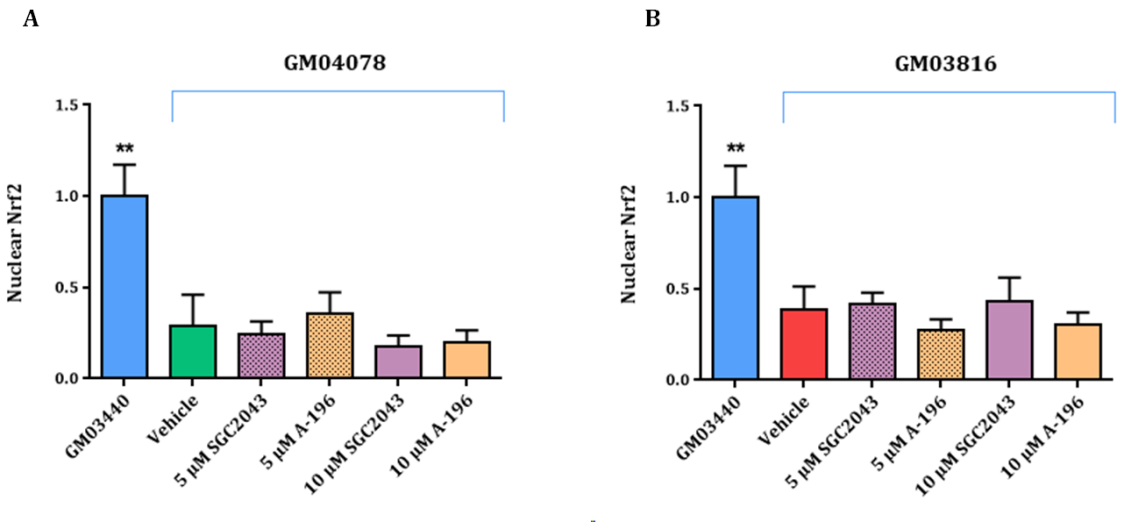


Figure 40. A-196 treatment of FRDA patient-derived lines has no effect on the cellular localization of Nrf2

Nrf2 nuclear localization assessed by immunofluorescence in **(A)** GM04078 and in **(B)** GM03816. The control line GM03440 is presented as a reference. Comparisons were made against the vehicle treated cells. Data are presented as mean ± s.e.m. of three independent experiments completed in triplicate, one-way ANOVA Bonferroni corrected for multiple comparisons, **p<0.01, ***p<0.001

Calcium release assessment after A-196 treatment

Calcium release from mitochondria and from all cellular stores is reduced in the FRDA patient-derived fibroblast line GM03816 (~30% and 40% respectively), while the line GM04078 shows a variable calcium release response (Figure 41). Interestingly, in this set of experiments, the difference seen in the line GM03816 is not statistically significant, as the one seen in Figure 36. This discrepancy may be due to the number of treatments (comparisons) that were carried out in this experiment, the ones that can account for the lost in significance.

The treatment of the lines GM04078 and GM03816 with A-196 increases the calcium release from mitochondria and from all internal stores by approximately 20% (Figure 41). However, the negative control probe SGC2043 seems to further

increase calcium release (~2-fold) in response to CCCP and ionomycin in the line GM03816 (Figure 41 B, D), while the response of the line GM04078 is once more variable. More experiments that can clarify the effect of A-196 and the control probe SGC043, such as calcium uptake are necessary.

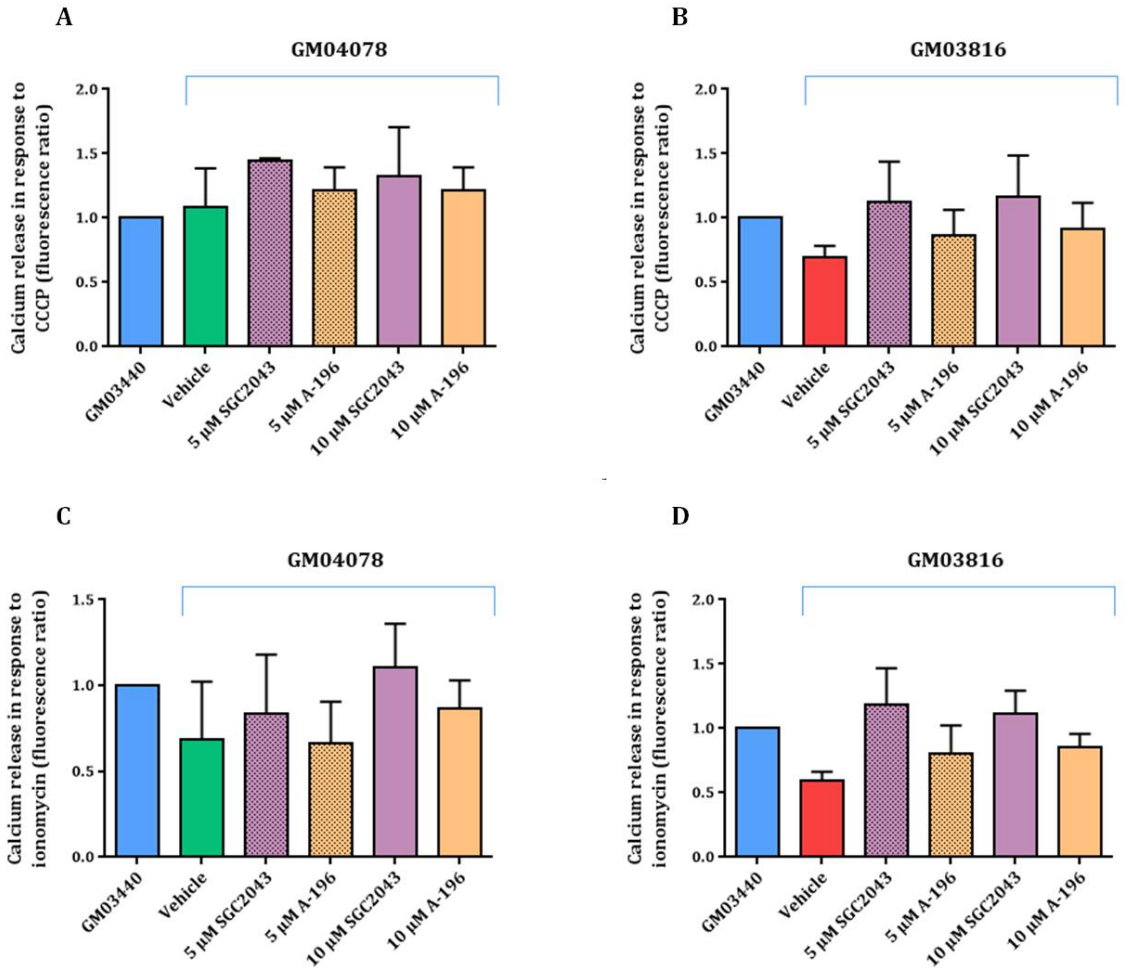


Figure 41. Calcium release shows a differential response to A-196 treatment in FRDA patient-derived fibroblasts

Calcium release assessed by calcium imaging in response to CCCP in **(A)** GM04078 and in **(B)** GM03816, and in response to ionomycin in **(C)** GM04078 and in **(D)** GM03816. The control line GM03440 is presented as a reference. Comparisons were made against the vehicle treated cells. Fluorescence ratio corresponds to the ratio between bound and unbound calcium (340 nm/380 nm). Data are presented as mean ± s.e.m. of three independent experiments completed in quadruplicate, one-way ANOVA Bonferroni corrected for multiple comparisons.

5.3. Discussion

Validation of A-196 in FRDA patient-derived cell lines

In this chapter A-196 was tested in FRDA patient-derived cells to confirm effective elevation of FXN protein expression. A-196 was found to up-regulate mature FXN protein in the primary FRDA patient-derived cell line GM04078. This cell line has approximately 43% of residual frataxin compared to the healthy control GM03440 (Figure 30 A-B), a difference that is in line with previous reports from several groups (Gomez-Sebastian *et al.*, 2007; De Biase *et al.*, 2009; Li *et al.*, 2015). Even though the increase of mature FXN protein was modest, it was significant when compared to the cells treated with vehicle. As important as it is to up-regulate FXN protein in patients, it is necessary to bear in mind that this up-regulation does not have to reach control FXN protein levels. Asymptomatic carriers of the GAA expansion, have approximately 50% of normal frataxin expression (Campuzano *et al.*, 1997), suggesting that a modest increase that can reach this percentage can be beneficial for some FRDA patients. However, not every single cell line/patient will react in the same way to a drug. Genetic variability added to the culture conditions, especially in cells lines, make a universal response to a drug far from ideal. Primary cells derived from patients will account for interindividual differences in disease susceptibility and responsiveness to any therapeutic treatment (Fry *et al.*, 2008). Therefore, the differences in response from the tested cell lines is not surprising. On the contrary, it reflects the differential response that patients may have if they were given this epigenetic modulator, as well as what it is expected in subsequent experiments, or in a potential translational approach.

In the patient line GM03816, although an increase in FXN protein was observed (5 μM and 10 μM A-196), the difference does not reach statistical significance. The semi-quantitative nature of the western blot technique may account for the variability of mature FXN protein assessment, suggesting that elevation of FXN protein needs to be further confirmed with an additional technique.

A modest increase in FXN protein after A-196 treatment was also observed in the FRDA lymphoblastoid cell line GM16220. However, more statistical power is needed to reach clear conclusions and therefore more experiments need to be performed. Considering the results described in Chapters 4 and 5, it is possible to think that FXN protein up-regulation is not cell dependent and it can be accomplished not only in the *FXN*-GAA-Luc reporter cell line (Figure 29), but also in the FRDA patient-derived fibroblast line GM04078 (Figure 30 C-D). These results highlight the role of the methyltransferases SUV4-20 in the repression of *FXN* expression in particular in the regulation of protein expression.

Phenotypic analysis of FRDA patient-derived fibroblasts after A-196 treatment

Additionally in this chapter, several phenotypes derived from decreased FXN protein expression were described. FRDA patient-derived fibroblasts present a reduced mitochondrial mass (Figure 32) when compared to control fibroblasts, suggesting that the lack of frataxin results in a decreased number of mitochondria per cell. This result is in accordance with the study by Jasoliya and colleagues where they showed a 68% residual mitochondrial mass in the line GM04078 and a 51% in the line GM03816 (Jasoliya *et al.*, 2017). The authors of this study conclude that FXN expression correlates with mitochondrial biogenesis, therefore when FXN is reduced, mitochondrial biogenesis is impaired resulting in less mitochondria per

cell. However, more analysis such as the relationship of FXN levels with mitochondrial biogenesis replication factors involved in mitochondrial DNA transcription and replication (e.g. mitochondrial transcription factor A, and nuclear respiratory factory 1) are needed for this work to conclude that mitochondrial biogenesis is impaired. Further supporting the reduced mitochondrial number as a result of FXN depletion, a reduction in the number of mitochondria has also been reported in a SH-SY5Y FXN-silenced cell model (Bolinches-Amorós *et al.*, 2014). Thus, reduced mitochondrial number represents a clear phenotype derived from FXN decreased levels. When mitochondrial mass was assessed after A-196 treatment, there was a modest increase in the number of mitochondria per cell, suggesting that A-196 is able to increase the number of mitochondria, but it is limited by the increase in FXN protein, which was shown to be of only ~1.5-fold (Figure 30). More experiment in this direction would help elucidating if inhibition of SUV4-20 has an effect in mitochondria biogenesis in FRDA models.

Another described phenotype was the reduced $\Delta\Psi_m$ in FRDA patient-derived fibroblasts. A reduction in $\Delta\Psi_m$ has been shown by several groups in different models such as *Drosophila* (Shidara and Hollenbeck, 2010), SH-SY5Y FXN-silenced cells (Bolinches-Amorós *et al.*, 2014), cerebellar granule cells derived from a FRDA mouse model (Abeti *et al.*, 2016), rat primary DRG sensory neurons transduced with lentiviral vectors encoding short-hairpin RNAs targeting FXN (Mincheva-Tasheva *et al.*, 2014), FRDA lymphoblastoid cell lines (Zhao *et al.*, 2017) and primary human fibroblasts (Abeti *et al.*, 2018). Taking into consideration the results reported in human fibroblasts by Abeti and collegues, the results herein described, show a similar differential $\Delta\Psi_m$ reduction which is dependent on each line,

supporting the observations here made. The treatment of both FRDA patient-derived fibroblasts with 5 μM A-196 slightly increased $\Delta\Psi_m$. However, a more pronounced effect was seen on the line GM03816, where 5 μM A-196 increased $\Delta\Psi_m$ by 1.5-fold similarly to the increased observed by Abeti and colleagues (~1.3-fold) after the treatment of human primary fibroblasts with the Nrf2 inducer omaveloxolone (Abeti *et al.*, 2018). Considering that omaveloxolone is a drug in clinical trials, the modest increase of $\Delta\Psi_m$ here reported is encouraging. However, more statistical power is needed to reach clear conclusion and statistical significance.

An additional well-reported consequence of FXN deficiency is the increased generation of mitochondrial ROS (Wong *et al.*, 1999; Bolinches-Amorós *et al.*, 2014; Abeti *et al.*, 2016, 2018; Zhao *et al.*, 2017). In the present work, FRDA patient-derived fibroblasts assessed for ROS generation at base line (without any additional oxidative stress) showed an increased (~1.2-fold) ROS production in the FRDA primary line GM03816 (Figure 34 A). However, the observed increase in ROS generation was small compared to another report in human primary fibroblasts, where ROS generation was 1.7-fold increased in FRDA (Abeti *et al.*, 2018). This discrepancy can be explained by the difference in genetic variability of the primary fibroblasts, considering that the lines used in this study are different from the ones used by Abeti and colleagues. Furthermore, when the FRDA primary lines GM04078 and GM03816 were challenged for one hour with a mitochondrial depolarizaring agent, CCCP, they respond by generating more mitochondrial ROS, suggesting that the mitochondria of these cells are responsive. Therefore, the altered $\Delta\Psi_m$ here

reported correlates with the mitochondrial ROS generation phenotype already described by others.

Increased ROS production has been associated with the transcription factor Nrf2 (Paupe *et al.*, 2009; Shan *et al.*, 2013; Abeti *et al.*, 2015, 2016, 2018). For instance, a report from Shan and colleagues showed a decreased Nrf2 expression in the nucleus of the DRG and cerebella of a FRDA mouse model (Shan *et al.*, 2013). Furthermore, nuclear Nrf2 translocation has been shown to be important in the oxidative stress response in human primary fibroblasts (Paupe *et al.*, 2009). In this regard, nuclear localization of Nrf2 has been shown to be crucial for the activation of cytoprotective genes in response to oxidative stress (Holmström, Kostov and Dinkova-Kostova, 2016). Therefore, appropriate compartmentalization of Nrf2 is important in FRDA. In this work, a decrease in nuclear Nrf2 (~60%) was found in all FRDA patient-derived fibroblasts (Figure 35 A-B). Despite the fact that in this work nuclear Nrf2 was assessed by immunofluorescence and not by immunoblot of nuclear extracts as the report from Shan and colleagues, the levels of Nrf2 in the nucleus in both works are around 40% residual Nrf2. Interestingly, A-196 seems not to have an effect on the Nrf2 localization in the cell. A possible explanation is that the up-regulation of FXN protein observed upon treatment with A-196 is not sufficient to increase Nrf2 localization in the nucleus. The observation that A-196 treatment of the FRDA patient-derived fibroblast line GM03816 modestly decreases ROS generation (~15%) without increasing the localization of Nrf2 in the nucleus of the cell, suggests that alternative antioxidant pathways such as the activation of the STAT family of transcription factors (Simon *et al.*, 1998; Madamanchi *et al.*, 2001) may be playing a role as the antioxidant defence after A-196 treatment. Additional

experiments have to be performed to better understand the mechanisms by which A-196 contributes to the amelioration of certain phenotypes such as ROS generation.

Finally, calcium homeostasis has been shown to be affected as a result of FXN deficiency (Wong *et al.*, 1999; Shidara and Hollenbeck, 2010; Bolinches-Amorós *et al.*, 2014; Mincheva-Tasheva *et al.*, 2014; Lee *et al.*, 2016). One of the downstream effects of reduced $\Delta\Psi_{\mathrm{m}}$ is the alteration of calcium homeostasis, since uptake and release of calcium depend on $\Delta\Psi_{\mathrm{m}}$ (Brookes *et al.*, 2004). Therefore, the decreased calcium release described here is consistent with an altered $\Delta\Psi_{\mathrm{m}}$. In order to dissect the mechanism by which calcium release is impaired, additional experiments such as the study of voltage-gated calcium channels in the mitochondrial membrane are necessary. To the best of my knowledge, no study has reported deficits in mitochondrial calcium release from a model of FRDA. Nevertheless, the work by Bolinches-Amorós and colleagues reported calcium release from the endoplasmic reticulum (ER) and showed, in a SH-SY5Y FXN-silenced cell model, that there was no effect on calcium release from the ER in the absence of FXN (Bolinches-Amorós *et al.*, 2014). In contrast to that work, here a reduced calcium release from all cellular stores in the FRDA primary line GM03816 was described (Figure 36 C). Despite the fact that ionomycin induces calcium release from the ER, it also releases calcium from all internal stores and this can account for the different observations made in this two studies. The treatment of FRDA patient-derived fibroblasts with A-196 did not show any beneficial effect on calcium release, whereas the treatment of the fibroblasts with the negative control probe SGC2043, although not statistically significant, showed to increase calcium release. The effects seen on calcium release

upon treatment of FRDA patient-derived fibroblasts with either A-196 or with SGC2043, are largely variable making it difficult to reach clear conclusions on the role of the inhibition of the methyltransferases SUV4-20 in calcium homeostasis. More experiments that for instance use different cell lines or that look at calcium uptake, may help to clarify the differential responses of the cells to the chemical probes.

CHAPTER 6

Improving the potency and stability of A-196 as a potential therapeutic molecule

6.1. Introduction

The effect that A-196 has on FXN protein levels demonstrates that methylation of H4K20 represents an important epigenetic silencing mark in the GAA expanded *FXN* gene, and that the methyltransferases SUV4-20 are important modulators of *FXN* expression. However, the described increase in the cell models is modest, and moreover, not sufficient to rescue the studied phenotypes. Therefore, in this chapter ways of increasing the potency of A-196, as well as its metabolic stability, will be explored.

6.1.1. Drug combination studies

Drug combination studies have been use for decades to hit multiple targets, multiple subpopulations, or multiple diseases simultaneously. The use of a combination of drugs with different mechanisms or modes of action against the same target or different targets, may treat a disease more effectively. Some of the possible positive outcomes for synergism include increasing the efficacy of the therapeutic effect, and decreasing the dosage of the drug, while increasing or maintaining the same efficacy to avoid toxicity (Chou, 2006).

6.1.2. Hit-to-lead phase in drug discovery

Drug discovery initiates because there is a disease without suitable medical products available, as in FRDA. Drug discovery commonly starts from pre-clinical academic research which generates data to develop a hypothesis that, either the inhibition or the activation of a protein/pathway, may result in a therapeutic effect that modifies a disease state. After this initial step, drug discovery has to follow several consequential phases, and the hit-to-lead phase is one of them. The aim of the hit-to-lead phase is to refine the hit molecule to try to produce more potent and selective compounds to examine their efficacy in any available *in vivo* models (Hughes *et al.*, 2011).

Drug combination studies and the initial steps of the hit-to-lead phase in drug discovery will be addressed in this chapter.

6.1.3. Hypotheses of this chapter

First, the combination of A-196 with other drugs that act as epigenetic modifiers may help potentiate its effect on the expression of *FXN.* Second, the modification of the original molecule may produce a more potent and metabolically stable compound that can be taken for *in vivo* assays.

6.1.4. Aims of this chapter

Drug combination studies using the SGC chemical probes to increase FXN protein expression

- To combine several compounds identified as hits in the SGC chemical probes library screen and test the combination in the *FXN*-GAA-Luc cell line to find possible synergistic effects between them.

Hit-to-lead development of A-196

- To test A-196 for metabolic stability using the liver microsomes assay.
- To test A-196 derivatives using the *FXN*-GAA-Luc cell line to find analogues that may be more potent than A-196.

6.2. Results

6.2.1. Combination of A-196 and GSK343 and of A-366 and GSK343 show potential synergistic effects in increasing FXN levels in the FXN-GAA-Luc reporter cell line

The combinatorial nature of histone lysine modifications requires an organized interplay between different histone lysine methylation systems. Loss of a given HMT may also affect methylation on lysine residues where the enzyme has no intrinsic activity. For instance, loss of Suv39H (tri-methylates H3K9) results in the conversion of pericentric H3K27me1 to H3K27me3 by a mechanism not fully understood (Peters *et al.*, 2003). This effect may be due to the interplay between distinct methylation marks such as H3K9, H3K27 and H4K20, all of which have been shown to be marks of repressive chromatin states (Schotta *et al.*, 2004), and to be accumulated in the *FXN* locus (Sandi *et al.*, 2014).

To test the possible effects of drug combinations, the *FXN*-GAA-Luc cell line was treated for six days with a combination of probes that were shown to increase FXN-

Luc protein levels in the initial SGC epigenetic probes collection screen. The probes chosen for combination studies were the lead compound A-196 and the probes A-366 and GSK343. A-366 inhibits the methyltransferases G9a and GLP which when knocked-down simultaneously induce a 1.4-fold increase of FXN-Luc protein (Figure 24). Finally, the probe GSK343 which inhibits EZH1 and EZH2 (EZH1 knock-down lead to a ~ 1.4-fold up-regulation of FXN-Luc protein levels, Figure 25). The reporter cell line was treated with a constant concentration of one of the probes while the other was increasing in concentration. The concentrations varied from 0.1 μM to 10 μM.

A-196 and GSK343 potentiate their effects when used together

The treatment of the *FXN*-GAA-Luc cell line with different concentrations and combinations of A-196 (SUV4-20 inhibitor) and GSK343 (EZH1 and EZH2 inhibitor), shows that both drugs potentiate each other (Figure 42).

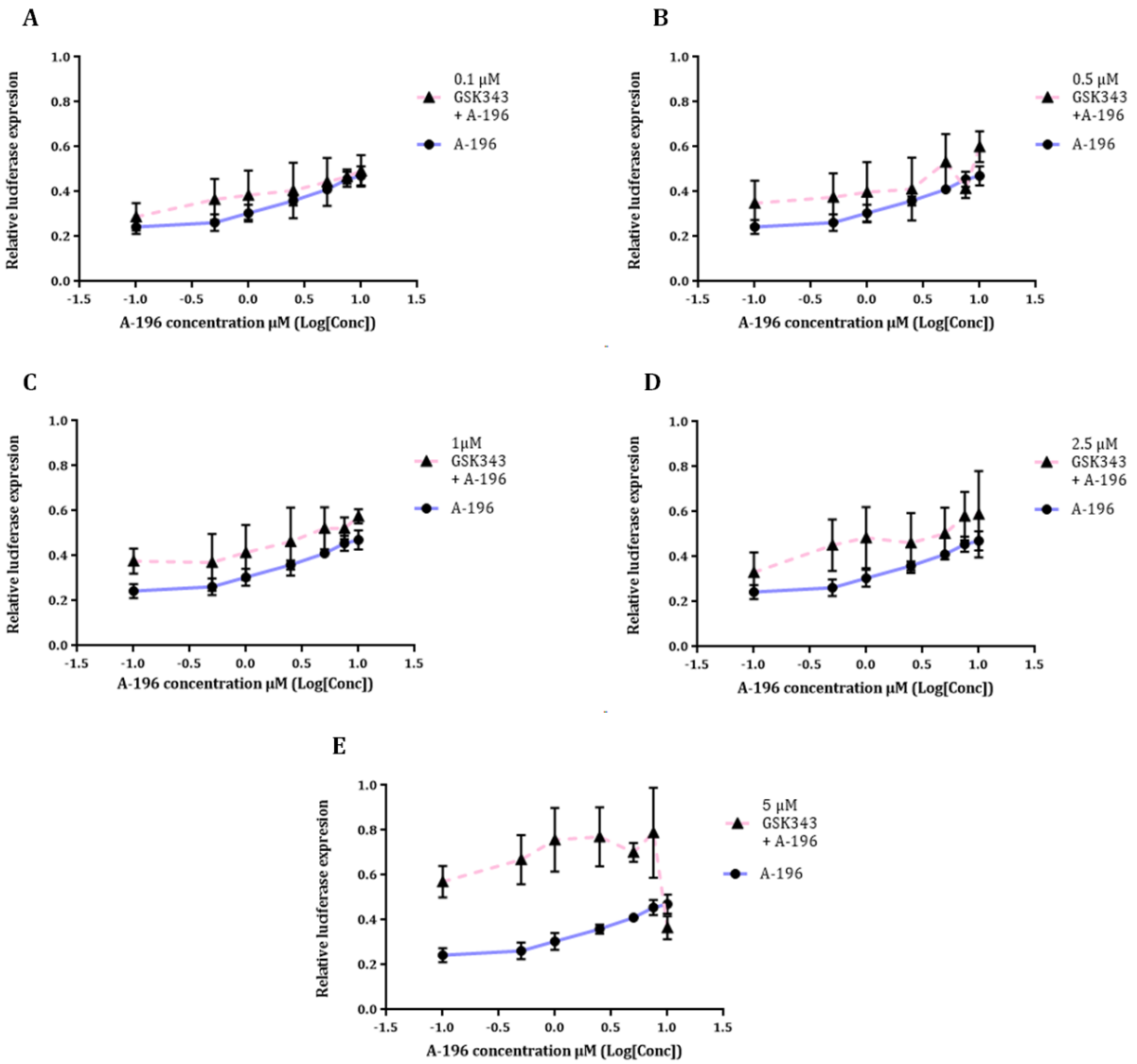


Figure 42. A-196 and GSK343 show synergistic effects at several concentrations of both drugs

(A) Luciferase assay on the *FXN*-GAA-Luc cell line where concentrations from 0.1 µM to 10 µM of A-196 were combined with 0.1 µM of GSK343, **(B)** Luciferase assay using concentrations from 0.1 µM to 10 µM of A-196, combined with 0.5 µM of GSK343, **(C)** Luciferase assay using concentrations from 0.1 µM to 10 µM of A-196, combined with 1 µM of GSK343, **(D)** Luciferase assay combining A-196 with 2.5 µM of GSK343, **(E)** Luciferase assay combining A-196 with 5 µM of GSK343. Data are presented as mean ± s.e.m. of three independent experiments completed in triplicates, synergy quantification using the Chou-Talalay method.

The analysis of drug combination experiments has been debated in the last years. Countless attempts have been made to quantitatively measure the dose-effect relationships of single drugs and their combinations in order to determine whether

or not a particular combination could gain a synergistic effect (Chou, 2006). In 2015 Ashton commented on a *Nature methods* paper (Krzywinski and Altman, 2014) regarding the use of ANOVA to analyse drug combination experiments arguing a misleading interpretation of the results (Ashton, 2015). In that article, Ashton supported alternative methods such as the combination index (CI) which was proposed by Chou-Talalay (Chou, 2010) as a more accurate way of measuring synergism. The CI method has been reported as being a rigorous drug-combination analysis methods to assess drugs interactions (Jia *et al.*, 2009). In the present work, analysis of the possible synergism between drugs was performed using the CI method. This method is based on the median-effect equation, derived from the mass-action law principle and takes into account the Michaelis-Menten, Hill, Henderson-Hasselbalch, and Scatchard equations (Chou, 2010). The resulting CI indicates synergism (CI < 1), additive effect (CI = 1), and antagonism (CI > 1) in drug combinations.

The results of the CI for all of the combinations are summarized in Table 13. A-196 has a synergistic effect at all concentrations when combined with 0.1 μM of GSK343, suggesting that the addition of a low concentration of GSK343 is enough to potentiate the effects of A-196 in FXN-Luc protein expression. The stronger synergistic effect of this combination is at 0.5 μM A-196 and 0.1 μM GSK343 (CI 0.45). Even a stronger synergism is observed when 5 μM of GSK343 is combined with A-196 except for the lowest concentrations that show a nearly additive effect (CI 1.18) and the highest showing a very strong antagonism (CI 16.62). The greatest synergism for the combination of these two probes was found combining 7.5 μM A-196 with 5 μM GSK343 (CI 0.05, ~ 2-fold compared to the single dose).

Table 13. Combination index corresponding to the combination of A-196 and GSK343

	A-196 concentration (µM)	GSK343 concentration (µM)	CI
Figure 42 A	0.1	0.1	0.89704
	0.5	0.1	0.45875
	1.0	0.1	0.57260
	2.5	0.1	0.67980
	5.0	0.1	0.74393
	7.5	0.1	0.65684
	10.0	0.1	0.61779
Figure 42 B	0.1	0.5	1.65724
	0.5	0.5	1.27472
	1.0	0.5	1.11111
	2.5	0.5	1.29080
	5.0	0.5	0.33289
	7.5	0.5	2.34491
	10.0	0.5	0.17218
Figure 42 C	0.1	1	2.23178
	0.5	1	2.69524
	1.0	1	1.73832
	2.5	1	1.07617
	5.0	1	0.59337
	7.5	1	0.67860
	10.0	1	0.33549
Figure 42 D	0.1	2.5	10.4215
	0.5	2.5	2.43515
	1.0	2.5	1.74562
	2.5	2.5	2.34760
	5.0	2.5	1.56943
	7.5	2.5	0.61838
	10.0	2.5	0.57143
Figure 42 E	0.1	5	1.18104
	0.5	5	0.34500
	1.0	5	0.09544
	2.5	5	0.08173
	5.0	5	0.23716
	7.5	5	0.05929
	10.0	5	16.6299

A-366 used at concentrations from 0.5 μM to 10 μM in combination with 0.5 μM of GSK343 show synergism

In addition to testing the lead compound in combination with another epigenetic modifier, it was important to address whether or not the inhibition of silencing epigenetic marks located on the same histone could have an effect on the expression of FXN-Luc protein. It has been shown that cross-talk between histone modifications in a single histone tail occur in order to direct the local and global function of chromatin (Fischle, Wang and Allis, 2003). For instance, H3K27me3 in conjunction with H3K9me2 are considered epigenetic imprints of the inactive X chromosome (Peters *et al.*, 2003; Plath *et al.*, 2003; Silva *et al.*, 2003). In FRDA patient-derived fibroblasts and lymphoblastoid cells, high levels of H3K27me3 and H3K9me2 have been reported at the *FXN* locus (Greene *et al.*, 2007; De Biase *et al.*, 2009). Therefore, chemical inhibitors of the methyltransferases that modify H3K9 and H3K27 were combined at different concentrations in a six days incubation period (Figure 43).

Results of the combination of A-366 (G9a and GLP inhibitor) and GSK343 (EZH1 and EZH2 inhibitor) are summarized in Table 14. GSK343 at concentrations of 1 μM and 2.5 μM result to be synergistic with almost all concentrations of A-366. Exceptions are the combination of 0.1 μM A-366 with either 1 μM (CI 1.28) or 2.5 μM (CI 1.06) GSK343, which are nearly additive, while 7.5 μM A-366 combined with 2.5 μM (CI 3.64) GSK 343 are antagonistic. The strongest synergistic effect was found when 2.5 μM A-366 and 1 μM GSK343 were combined (CI 0.18). This result suggests that the combination of 2.5 μM A-366 with 1 μM GSK343 increases FXN-Luc protein more efficiently that the single treatment (~1.5-fold).

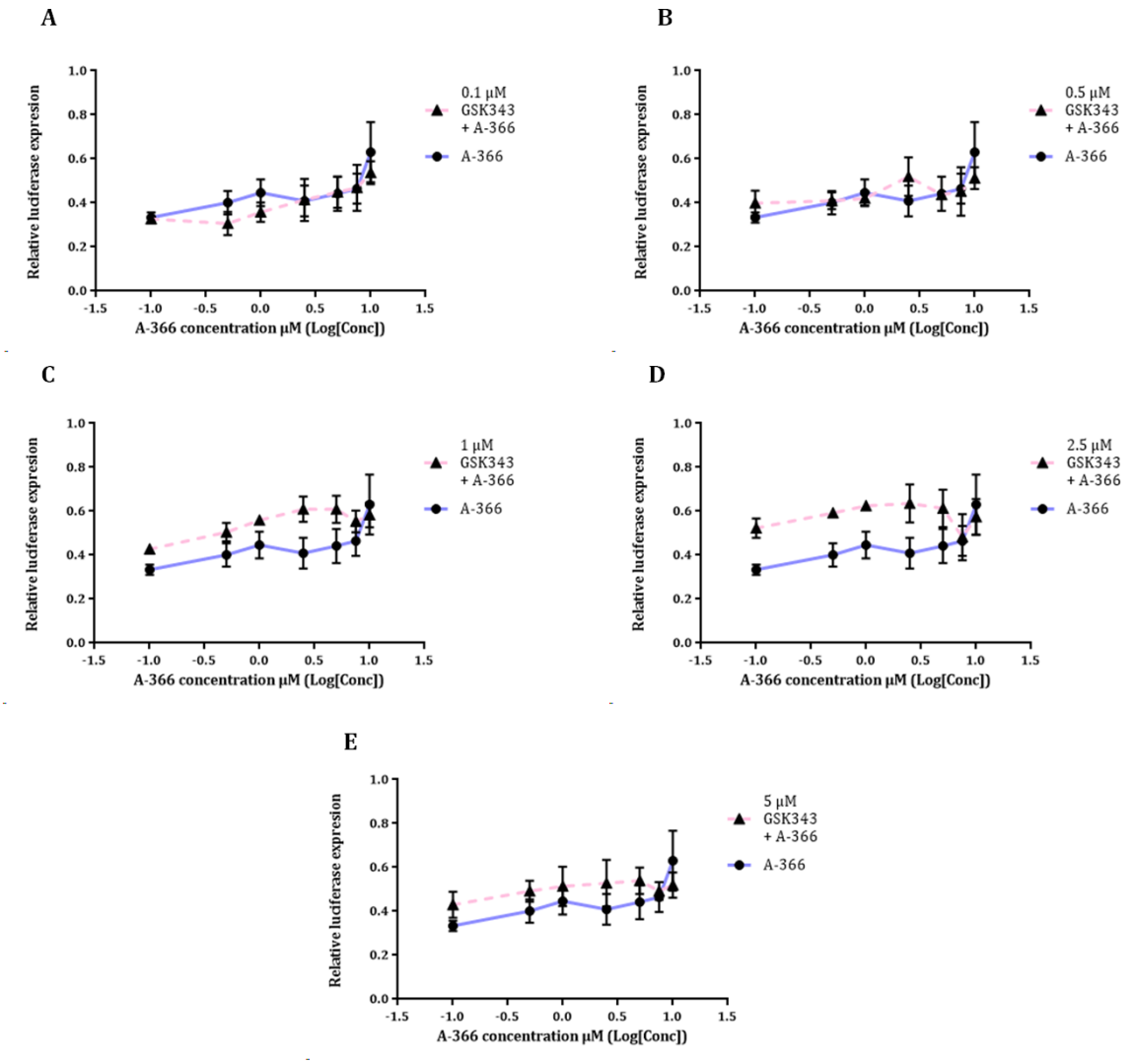


Figure 43. Chemical inhibition of the methyltransferases of H3K9 and H3K27 in conjunction, show to increase FXN-Luc protein expression more efficiently that the inhibition of each lysine residue alone

(A) Luciferase assay on the *FXN*-GAA-Luc cell line where concentrations from 0.1 µM to 10 µM of A-366 were combined with 0.1 µM of GSK343, **(B)** Luciferase assay using concentrations from 0.1 µM to 10 µM of A-366, combined with 0.5 µM of GSK343, **(C)** Luciferase assay using concentrations from 0.1 µM to 10 µM of A-366, combined with 1 µM of GSK343, **(D)** Luciferase assay combining A-366 with 2.5 µM of GSK343, **(E)** Luciferase assay combining A-366 with 5 µM of GSK343. Data are presented as mean ± s.e.m. of three independent experiments completed in triplicate, synergy quantification using the Chou-Talalay method.

Table 14. Combination index corresponding to the combination of A-366 and GSK343

	A-366 concentration (μM)	GSK343 concentration (μM)	CI
Figure 43 A	0.1	0.1	1.29317
	0.5	0.1	7.89513
	1.0	0.1	4.46729
	2.5	0.1	3.36101
	5.0	0.1	2.66973
	7.5	0.1	2.53695
	10.0	0.1	0.71726
Figure 43 B	0.1	0.5	1.02300
	0.5	0.5	1.40540
	1.0	0.5	1.69722
	2.5	0.5	0.47929
	5.0	0.5	3.76417
	7.5	0.5	4.33796
	10.0	0.5	1.57760
Figure 43 C	0.1	1	1.28565
	0.5	1	0.61689
	1.0	1	0.30888
	2.5	1	0.18053
	5.0	1	0.21487
	7.5	1	0.70761
	10.0	1	0.48524
Figure 43 D	0.1	2.5	1.06798
	0.5	2.5	0.47604
	1.0	2.5	0.33428
	2.5	2.5	0.26913
	5.0	2.5	0.43415
	7.5	2.5	3.64684
	10.0	2.5	0.93633
Figure 43 E	0.1	5	6.10394
	0.5	5	3.09717
	1.0	5	2.50816
	2.5	5	2.09699
	5.0	5	2.01815
	7.5	5	4.56472
	10.0	5	3.18586

In summary, the combination of A-196 with 0.1 μM GSK343 show synergism, in a similar way as the combination of A-366 with 1 μM of GSK343. Results that suggest that it may be possible to further increase *FXN* expression targeting at the same time several methyltransferases.

6.2.2. A-196 derivatives increase FXN-Luc protein in the FXN-GAA-Luc reporter cell line

The finding of the methyltransferases SUV4-20 as key players in the regulation of FXN protein expression was interesting. Considering that H4K20 methylation is not one of the most studied histone modifications, understanding if epigenetic modulation of H4K20 can be achieved *in vivo* to increase *FXN* expression is important. The A-196 selective chemical inhibitor of SUV4-20 was only identified last year and *in vivo* data using this novel probe has not been reported yet (Bromberg *et al.*, 2017). Here, A-196 was tested for metabolic stability using the microsomal stability assay, with the idea of assessing whether this chemical probe is suitable for testing *in vivo* or not.

Almost 60% of marketed drugs are cleared metabolically by the liver cytochrome P450 enzymes (McGinnity *et al.*, 2004). Correlation between *in vivo* clearance values and *in vitro* calculated clearance values from liver microsomal metabolism has been reported (Rane, Wilkinson and Shand, 1977; Obach, 1999). The microsomal stability assay uses these principles to study the stability of a given drug in a determined species *in vitro*. This assay was outsourced to Cyprotex, a company that is renowned for their expertise in absorption, distribution, metabolism and excretion (ADME) studies.

The measured half-life of A-196 using human liver microsomes is approximately 7 minutes (Table 15), while the half-life of A-196 using mouse liver microsomes is almost 6 minutes (Table 16). These values suggest that A-196 is rapidly metabolised in the liver, and therefore would be probably unsuitable for *in vivo* administration.

Table 15. Metabolic stability of A-196 in human liver microsomes

Metabolic Stability (Species=Human)						
Compound Remaining (% of 0 min)						**t1/2 (min)**
0 min	5 min	15 min	30 min	45 min	Control	
100	63.6	29.6	6.49	1.36	83.0	**7.28**

Table 16. Metabolic stability of A-196 in mouse liver microsomes

Metabolic Stability (Species=Mouse)						
Compound Remaining (% of 0 min)						**t1/2 (min)**
0 min	5 min	15 min	30 min	45 min	Control	
100	60.6	19.5	2.70	0.498	89.9	**5.79**

To address the question of the *in vivo* effect of the inhibition of the methyltransferases SUV4-20 on FXN protein expression, new variants of A-196 were synthesized by Robert Quinlan, Roberta Mazzone and Professor Paul Brennan (SGC Oxford), with the aim of achieving higher stability and potency (Figure 44).

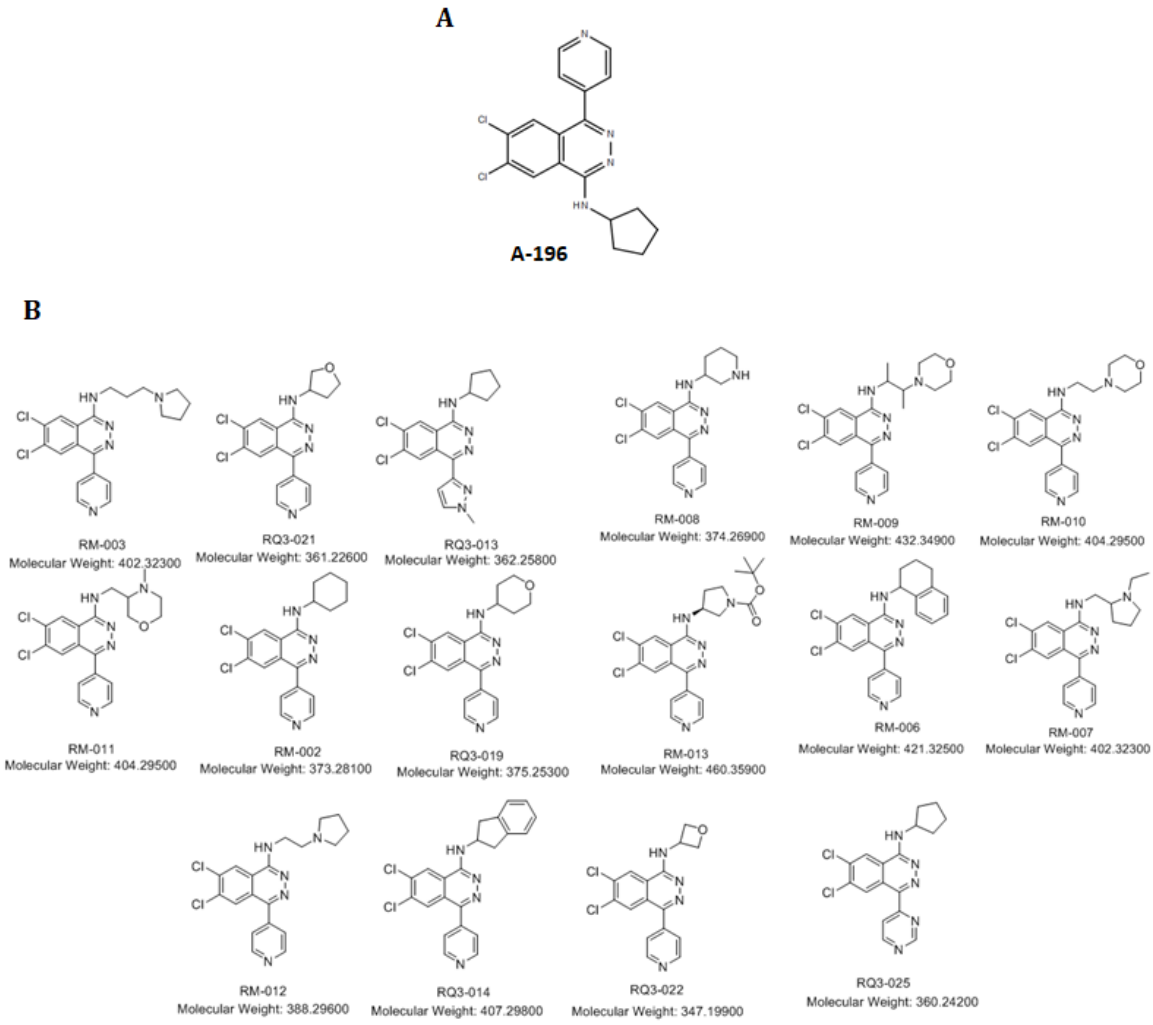


Figure 44. Synthesized A-196 analogues

(A) Chemical structure of the lead compound A-196, **(B)** Chemical structures of A-196 analogues synthesized by Robert Quinlan and Paul Brennan from Oxford SGC.

Sixteen different analogues of A-196 were screened using the *FXN*-GAA-Luc reporter cell line. Two compounds RQ3-014 and RM-002 were able to increase FXN-Luc protein expression significantly when compared either with the vehicle treated cells or with the negative probe SGC2043 (Figure 45 A). None of the analogues was found to be toxic as assessed by the adenylate kinase assay (Figure 45 B). These results suggest that the modification of A-196 could lead to the

generation of new molecules capable of further increasing *FXN* expression with the potential of being metabolically stable.

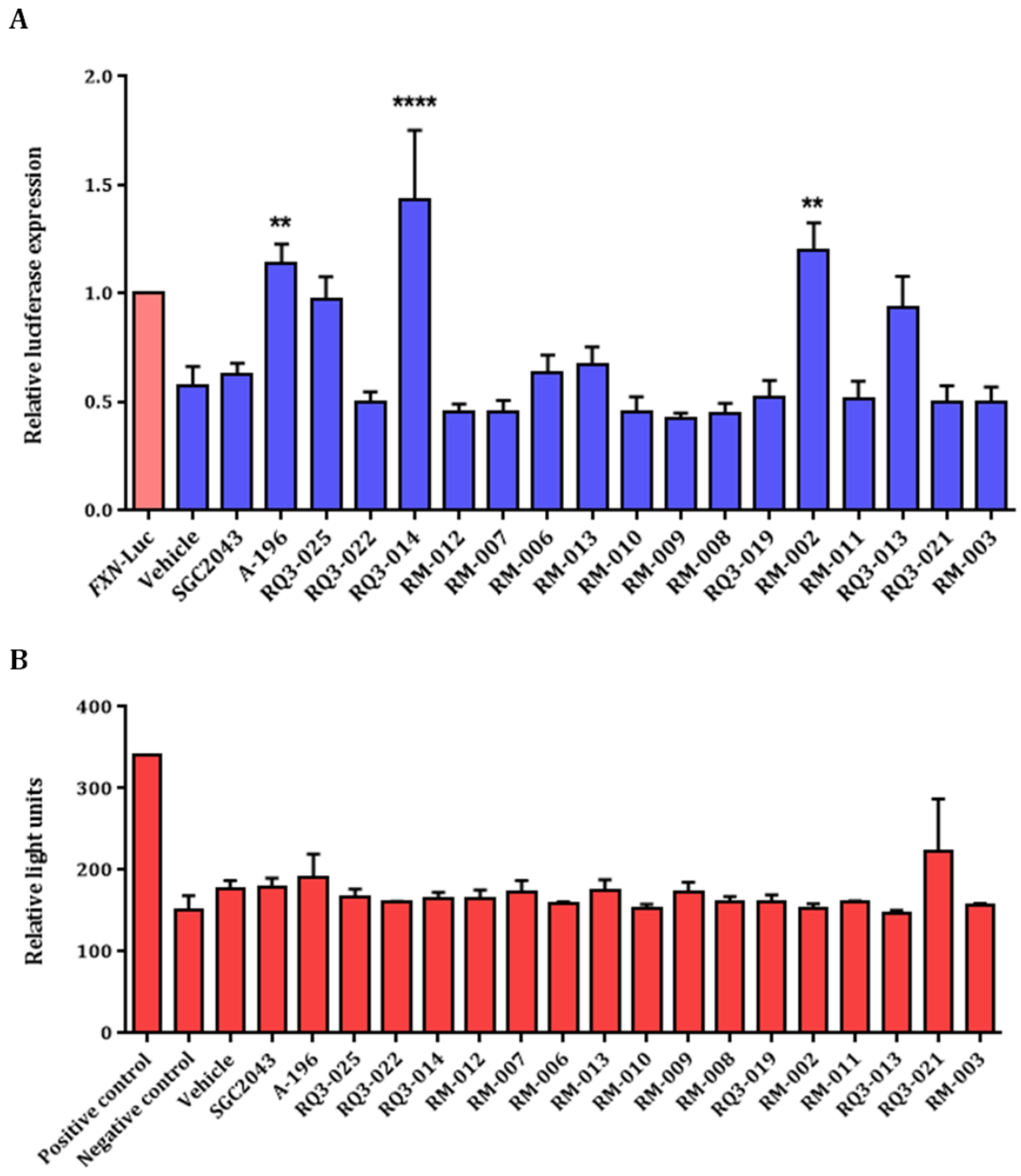


Figure 45. Screen of A-196 derivatives using the *FXN*-GAA-Luc cell line finds new compounds capable of increasing FXN-Luc protein

(A) Luciferase assay of the *FXN*-GAA-Luc cell line after treatment with 5 µM of each A-196 analogue, **(B)** Adenylate kinase assay of the analogues to evaluate toxicity. Two negative controls were used, DMSO (0.1%) and SGC2043. Data are presented as mean ± s.e.m. of three independent experiments completed in triplicate, one-way ANOVA Bonferroni corrected for multiple comparisons, **p<0.01, ****p<0.0001

To evaluate the concentration-response of the *FXN*-GAA-Luc cell line to increasing concentrations of the analogue RQ3-014, the cell line was treated for six days with 0.1 µM to 10 µM of the probe. The concentration-response curve shows that FXN-Luc protein levels are increasing in a dose dependent manner (Figure 46 A). Concentrations between 0.5 µM to 5 µM RQ3-014 up-regulate FXN-Luc protein significantly when compared to the vehicle treated cells. However, concentrations of 7.5 µM and 10 µM seem to be toxic (Figure 46 B), therefore no luciferase measurement was obtained, as only few cells survived the treatment.

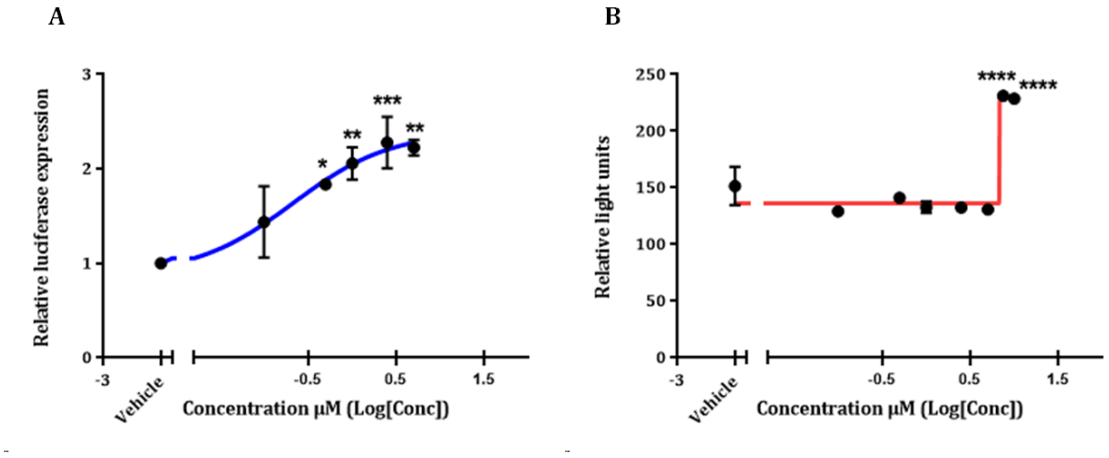


Figure 46. RQ3-014 increases FXN-Luc protein in a concentration-dependent manner

(A) Relative FXN-Luc protein expression assessed by luciferase assay of the *FXN*-GAA-Luc cell line treated with increasing concentrations of RQ3-014, **(B)** Adenylate kinase assay to evaluate toxicity of the treatment with increasing concentrations of RQ3-014. Data are presented as mean ± s.e.m. of three independent experiments completed in duplicates, one-way ANOVA Bonferroni corrected for multiple comparisons, *p<0.05, **p<0.01, ***p<0.001, ****p<0.0001

The analogue RM-002 was also tested in a concentration-response assay following the same protocol as for RQ3-014. RM-002 increases significantly the expression of FXN-Luc protein at all assessed concentrations (Figure 47 A) and seems not to be toxic (Figure 47 B). Interestingly, the lowest concentration of RM-002 tested, is

enough to increase FXN-Luc protein more than 2-fold, suggesting that this analogue may be a more potent variant of A-196.

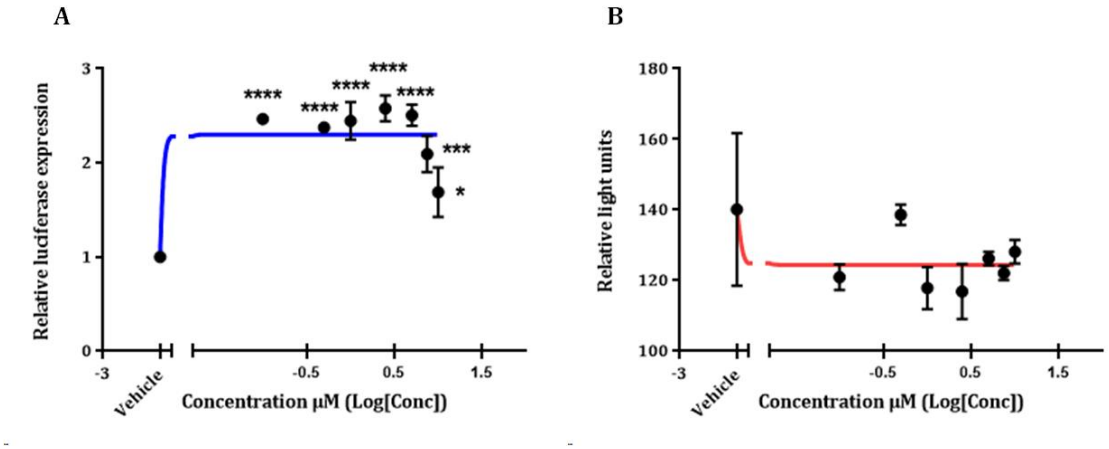


Figure 47. RM-002 increases FXN-Luc protein expression significantly at concentrations between 0.1 µM to 10 µM

(A) Relative FXN-Luc protein expression assessed by luciferase assay of the *FXN*-GAA-Luc cell line treated with increasing concentrations of RM-002, **(B)** Adenylate kinase assay to evaluate toxicity of the treatment with increasing concentrations of RM-002. Data are presented as mean ± s.e.m. of three independent experiments completed in duplicates, one-way ANOVA Bonferroni corrected for multiple comparisons, *p<0.05, ***p<0.001, ****p<0.0001

In summary, A-196 is quickly metabolised in the microsomal stability assay, suggesting that is not a good candidate for *in vivo* testing. Its calculated half-life in humans is 7 minutes and 6 minutes in mice. Two new variants of A-196, RQ3-014 and RM-002 were able to up-regulate FXN-Luc protein expression, with some concentrations being more effective than the original probe (RM-002 ~2.5-fold, RQ3-014 ~2-fold, A-196 ~1.5-fold at 2.5 µM).

6.3. Discussion

In this chapter, a number of approaches to further increase FXN-Luc protein expression and metabolic stability were studied, including combination of several

chemical probes and generation of improved analogues of the lead compound A-196.

The combination of A-196 with either GSK343 or A-366 was able to reach a synergistic effect and further enhance FXN expression in the FXN-GAA-Luc cell line. A single 10 μM dose of A-196 increased 1.5-fold FXN-Luc protein, while the combination of 10 μM A-196 with 0.1 μM GSK343, showed to be synergistic (CI 0.61 Table 13). Confirmation of the observations here reported in the *FXN*-GAA-Luc cell line need to carried out in FRDA patient-derived cell lines.

Similarly, the combination of A-366 and GSK343, was also found to be synergistic when concentrations of 1 μM and 2.5 μM GSK343 were used. A-366 at 10 μM up-regulates FXN-Luc protein almost 2-fold. Therefore, the synergy of A-366 and GSK343 may increase FXN-Luc protein further.

Interestingly, not only synergistic effects were found when the probes were combined. Several additive effects and antagonisms were also found. The strongest antagonism found for the first combination was at the highest tested concentrations of the chemical probes (10 μM A-196 and 5 μM GSK343) in which the combination index was 16.62. This result suggests that higher concentrations of the drugs could be deleterious for the expression of frataxin, possibly due to a toxic effect of the probes, although this hypothesis needs to be tested with a toxicity assay as the adenylate kinase.

A correct modulation of the enzymes driving chromatin remodelling is essential for *FXN* expression. This is further supported by the differential effects found when the chemical probes were combined at certain concentrations. For instance, 1 μM

GSK343 combined with either 0.1 μM, 0.5 μM or 1 μM A-196 were found to be antagonistic, whereas 1 μM GSK343 combined with higher concentrations (5 μM, 7.5 μM and 10 μM) of A-196 showed to be synergistic. This means that low concentrations of A-196 combined with 1 μM GSK343 instead of potentiating the effect of A-196 are worse than the single treatment. Thus, higher concentrations of GSK343 are needed to increase FXN-Luc protein levels above the levels already reached by the single treatment.

Considering that *in vivo* data is essential to translate the finding reported here to a potential therapeutic compound, A-196 was tested for metabolic stability. Microsomes derived from mouse, which will be the first *in vivo* model to use, showed a rapid clearance of the probe in a similar way as microsomes derived from human. The importance of evaluating the effect of the chemical inhibition of the methyltransferases SUV4-20 in an *in vivo* model of FRDA prompted our laboratory to establish a collaboration with Oxford SGC to modify the original A-196 molecule with the intention of finding new analogues, which maintain the inhibition of SUV4-20 and the efficacy of up-regulating FXN protein expression and would be more metabolically stable.

Sixteen variants of A-196 were synthesized by our collaborators, which were tested for their ability to up-regulate FXN-Luc protein levels using the *FXN*-GAA-Luc cell line. Two analogues, RQ3-014 and RM-002, tested at 5 μM, were found to increase FXN-Luc protein expression by approximately 2-fold. None of the other molecules increased FXN-Luc protein levels in a significant manner. However, the probes RQ3-025 and RQ3-013 increased FXN-Luc protein expression by 1.5-fold, although this increase was not statistically significant.

Although the other molecules may be more stable, they do not to change *FXN* expression in the reporter cell line. Therefore, it is unlikely that these variants will be considered for additional analysis.

The RQ3-014 concentration-response curve showed that effective concentrations to achieve FXN-Luc protein up-regulation are between 0.5 μM and 5 μM, with the maximal effect reached at 2.5 μM of RQ3-014 (> 2-fold). The comparison between concentration-response curves of A-196 and RQ3-014 demonstrates that RQ3-014 may be more potent than A-196, given that it increases FXN-Luc protein more than 2-fold at 2.5 μM compared to almost 1.5-fold of A-196 at the same concentration. However, additional experiments in FRDA patient-derived cell lines are needed to confirm this first observation in regards to potency. Moreover, microsomal stability assays will be needed to evaluate the metabolic stability of A-196 analogues.

RM-002 seems to be a even more potent variant of A-196 considering that 0.1 μM RM-022 is enough to up-regulate FXN-Luc protein expression approximately by 2.5-fold. The concentration-response curve of this analogue showed that FXN-Luc protein expression does not increase with increasing concentrations of RM-002. This observation may be due to using a too high range of concentrations used for the assay and the increased potency of this compound. Evaluating FXN-Luc protein using nM concentrations of RM-002 will help to clarify if this probe increases expression in a concentration-response fashion. Additional evaluation of the concentration-dependent up-regulation of FXN-Luc protein may be carried out using concentrations of RM-002 ranging from 1 nM to 100 nM. This probe also needs be taken for the microsomal stability assay and tested in FRDA patient-derived cell lines.

In summary, it is possible to increase the up-regulation of FXN-Luc protein using chemical probes that target epigenetic remodelling proteins, by either combining some of the probes, as shown in the combination studies, or by modifying the original molecules to make them more potent. One of the advantages of using a combination therapy is to reduce the concentration/dose of the drugs to achieve the same or better results. However, if one single molecule can be used at low concentrations because of its potency, the potential side effects and the undesired genome-wide changes may be minor. As a proof of principle, it might be interesting assessing *FXN* expression using RQ3-014 and RM-002 in combination with GSK343 to find a combination that can further increase the levels of FXN protein.

CHAPTER 7

Final discussion and future directions

Despite intense research carried out in the last few years, the mechanisms by which the frataxin gene gets silenced leading to pathology in FRDA are still unclear. Epigenetic silencing of *FXN* has been shown to be driven by several mechanisms, including post-translational modifications of histones. The alleviation of the repression caused by the accumulation of several repressive histone modifications in the flanking regions of the GAA repeats, may therefore be a potential therapeutic strategy. The present work is aimed to study the potential modification of the expression of frataxin following down-regulation or chemical inhibition of several proteins involved in histone acetylation and methylation. The results obtained in this thesis and their implications will be further discussed in this chapter.

7.1. Exploring the role of HDAC3 and G9a in the expression of FXN

The increase in the literature regarding the effect of HDACi on the regulation of the expression of *FXN* prompted this work to start by looking to the potential epigenetic modulation of the *FXN* gene. Even though most of the studies involving HDACi used compounds that target several histone deacetylases, the compounds that present a preferential specificity for HDAC3 seemed to have a stronger capacity of up-regulating the expression of *FXN*. For instance, the inhibitor 106 has a calculated inhibition constant (K_i) of 14 nM for HDAC3, which is approximately 15 times lower than the K_i for HDAC1 (Chou, Herman and Gottesfeld, 2008). Another

inhibitor, compound 109 has a K_i of 5 nM for HDAC3 compared to the K_i of 32 nM for HDAC1, almost seven fold lower (Rai *et al.*, 2010), suggesting that the compounds used as epigenetic modulators inhibit preferentially HDAC3 and through this inhibition they regulate the expression of *FXN.* This thesis therefore focused on HDAC3 as a potential target. Considering that those compounds were already shown to increase the expression of frataxin, this thesis first used RNA interference to directly target HDAC3. Even though an increase in FXN mRNA levels after the down-regulation of HDAC3 was achieved, no effect was observed in protein expression. These results were not entirely surprising in light of the previous reports in which HDACi were used to increase the expression of *FXN*. In fact, most studies failed to convincingly prove that there is indeed an up-regulation of frataxin *protein*, showing only experiments were FXN *mRNA* was quantified and a single western blot for the protein. Some studies report that protein assessment was done in two different experiments and fold changes were described, but most focus on FXN mRNA (Herman *et al.*, 2006; Chou, Herman and Gottesfeld, 2008; Rai *et al.*, 2008, 2010; Chan *et al.*, 2013).

This observation can possibly be explained in several ways. For instance, one explanation could be that there is no correlation between the up-regulation of FXN mRNA and protein, similar as reported in this thesis. A second explanation can be that both methods vary in technical complexity. Western blots are less quantifiable than qRT-PCR, hence the preferential use of mRNA quantification to shown increased FXN expression. A further explanation can be that after HDAC inhibition either chemically or mediated by siRNA, even though there is an increase in FXN mRNA, it fails to be translated to protein. Finally, a prolonged treatment with

chemical inhibitors or siRNA may be necessary in order to increase FXN protein expression. In fact, Sandi and colleagues suggested that prolonged treatment with chemical HDAC inhibitors is essential for the up-regulation of FXN protein in a mouse model of FRDA (Sandi *et al.*, 2011). It is therefore likely that any epigenetic intervention on the gene requires a prolonged treatment to allow epigenetic modification to take place.

Taking into account all of the aforementioned, and more importantly that any therapeutic intervention for FRDA patients needs to restore protein levels, it would be interesting to study the long term effects of the exposure of FRDA patient-derived cells to HDAC3 siRNA, and evaluate at the same time the global acetylation changes as well as changes in the acetylation pattern at the *FXN* gene.

At the *FXN* locus, in addition to the reduced acetylation of histones, an increase in histone methylation has also been reported. Even though there is enough evidence that shows that the methylation of histones is an important factor contributing to the silencing of *FXN*, the regulation of proteins involved in methylation has not been extensively explored as a potential therapeutic strategy in FRDA. Amongst the histones lysine residues that seem to contribute to the pathology, H3K9 methylation has been shown to negatively regulate *FXN* expression (Herman *et al.*, 2006; Greene *et al.*, 2007; Al-Mahdawi *et al.*, 2008; Rai *et al.*, 2008). One of the predominant marks present in the *FXN* gene is H3K9me2, which is driven by the methyltransferase G9a (Tachibana *et al.*, 2005; Shinkai and Tachibana, 2011). In 2010, Punga and Bühler showed that a compound which specifically inhibits G9a, BIX-01249, was able to remove efficiently the H3K9me2 mark from the GAA repeat tract without changing FXN mRNA levels. The authors of that work concluded that H3K9 methylation is

dispensable for *FXN* silencing (Punga and Bühler, 2010). To some extent, the results obtained by Punga and Bühler are similar to the data presented in this thesis, where down-regulation of G9a did not lead to the up-regulation of *FXN* expression. Considering that the epigenetic modification of the *FXN* gene seems to be a process that requires several days, it is possible that the time window used in both experiments to treat the cells (72 hours – Punga and Bühler; 48 hours this work) and assess FXN expression was not ideal. Therefore, before dismissing the role of H3K9 methylation in *FXN* silencing, it might be worth to perform longer term treatment experiments. Moreover, another study in which BIX-01249 was used, showed that H3K9me2 was not the primary cause for the transcriptional repression of *FXN,* and that the presence of this epigenetic mark was likely to be caused by R-loop formation or as a consequence of the reduced transcription (Groh *et al.*, 2014). Groh and colleagues treated cells for 72 hours, so again it is not possible to exclude that BIX-01249 may elicit a positive effect on *FXN* expression with longer treatments.

Therefore, in light of the existing evidence, a longer treatment of FRDA models with G9a inhibitors may be necessary to confirm or refute the possible role of this methyltransferase in *FXN* silencing. Additionally, it might be interesting to study the interplay that histone acetylation and methylation could have, and if any, explore it as a possible therapeutic strategy. Finally, a combination of inhibitors targeting more than one epigenetic mechanism such as histones methylation and R-loop formation, as proposed by Polak and colleagues (Polak *et al.*, 2016) could be a possible way to go forward with the epigenetic modification of *FXN*.

7.2. Identification of novel therapeutic targets for FRDA using the SGC epigenetic probes collection

The SGC epigenetic probe set, a well-characterized chemical probe library, enables researchers to link selective inhibition of a specific target with a biological response with high confidence. The SGC collection of epigenetic modifiers was used in the present work to identify potential therapeutic targets for the treatment of FRDA. The screen of this collection of probes highlighted the role of histone methylation in *FXN* repression, suggesting that there is the possibility of modulating the activity of some methyltransferases to increase the expression of *FXN.*

As opposed to acetyltransferases, lysine methyltransferases have enormous specificity, and usually modify one single lysine on a single histone. These modifications can either lead to activation or repression of transcription (Bannister and Kouzarides, 2005). This specificity is of great importance from a pharmacological point of view, as selective inhibitors for specific methyltransferases, if found to modify a disease phenotype, could have therapeutic potential with possibly less side effects. Herein, a significant up-regulation of FXN-Luc protein was achieved by inhibiting the PKMT SUV4-20 with the selective inhibitor A-196.

The main concern regarding epigenetic therapies is the potentially broad biological effects caused by the multiple genes that can be transcriptionally controlled by post-translational modifications in histone and non-histone proteins (Kim and Bae, 2011). A-196 (1 μM or 10 μM) was proven to selectively inhibit SUV4-20, with no inhibition of other PKMTs, including the other methyltransferase modifying H4K20,

SET8, or those that use H3K4, H3K9, H3K27, and H3K79 as substrates (Bromberg *et al.*, 2017). Additionally, it is inactive against several DNA methyltransferases, protein arginine methyltransferases, epigenetic readers and chromatin binders such as the tandem Tudor domain containing protein 53BP1, which recognizes p53K382me2 and facilitates an interaction between p53 and 53BP1 in the DNA damage response pathway. In addition to all of the aforementioned proteins, A-196 is also selective against 125 non-epigenetic targets including kinases, ion channels, and transporters, as well as G-protein-coupled receptors (Kachirskaia *et al.*, 2008; Bromberg *et al.*, 2017). The fine selectivity of A-196 brings the opportunity of modifying SUV4-20, not only to up-regulate *FXN*, but also to study in more detail the role of H4K20 methylation in the pathology of FRDA.

To date, epigenetic modification of the *FXN* gene has focussed on achieving chromatin remodelling using non-specific HDACi (Herman *et al.*, 2006; Chou, Herman and Gottesfeld, 2008; Rai *et al.*, 2008, 2010; Sandi *et al.*, 2011; Chan *et al.*, 2013; Chutake *et al.*, 2016). At least 50 non-histone proteins have been reported to be HDAC substrates, including several transcription factors (RUNX3, p53, c-Myc, nuclear factor kappa-light-chain-enhancer of activated B cells), chaperones (HSP90), signalling mediators (Stat3 and Smad7) and DNA repair proteins (Ku70) (Kim and Bae, 2011). The potential genome-wide effects that HDACi may have in patients, invite to great caution.

On the contrary, lysine methyltransferases have been shown to modify only a few non-histone substrates (Zhang, Wen and Shi, 2012; Ümit Kaniskan, Martini and Jin, 2018). Amongst them, p53 is the most common modified protein, since it can be methylated by the methyltransferases Set7/9 (K372), SMYD2 (K370), G9a (K373),

GLP (K373) and SET8 (K382) (Bissinger *et al.*, 2010; Zhang, Wen and Shi, 2012). To the best of my knowledge, amongst the methyltransferases responsible for the methylation of H4K20, only SET8 (H4K20me1) is able to methylate non-histone proteins such as p53 and proliferating cell nuclear antigen (PCNA) (Ümit Kaniskan, Martini and Jin, 2018). To date, no studies have reported that the methyltransferases SUV4-20 are able to methylate non-histone proteins, suggesting their selectivity for histones. Moreover, it has been shown that this family of proteins preferentially methylate histone H4K20 on nucleosomes rather than free histones (Schotta *et al.*, 2004); limiting in this way even more the epigenetic modification of SUV4-20 genome-wide.

Although A-196 is highly selective, it has the potential to modify all of the nucleosomal histones throughout the genome, a consequence that is likely to happen with all epigenetic modulators. A point of caution of the inhibition of SUV4-20 may be the potential genome-wide transition to an H4K20me1 state. Schotta and collegues have shown in mice that a chromatin-wide transition to H4K20me1 impairs genome integrity and programmed DNA rearrangements (Schotta *et al.*, 2008). They also showed that the complete loss of both SUV4-20 enzymes in SUV4-20h1$^{-/-}$ SUV4-20h2$^{-/-}$ double-null mice resulted in an ablation of nearly all H4K20me3 and H4K20me2, a change that is incompatible with life. In addition, a genome-wide transition to a mono-methylated H4K20 state led to increased sensitivity to damaging stress, with a mechanism that is dependent on inefficient DNA double-strand break repair and consequent chromosomal aberrations. Furthermore, B cells lacking SUV4-20 were shown to be defective in immunoglobulin class-switch recombination, a process required for antibody

isotype diversification. Moreover, SUV4-20 deficiency impaired the stem cell pool of lymphoid progenitors (Schotta *et al.*, 2008). Nonetheless, chemical inhibition of SUV4-20 can be modulated to bypass complete inhibition of these methyltransferases, avoiding in this way an aberrant transition of H4K20 methylated states.

7.3. Validation of A-196 in FRDA patient-derived cell lines

A-196 activity has been tested in several cell models including prostate cancer cells (PC-3 cells and LNCaP), human osteosarcoma cells (U-2 0S), cervical cancer cells (HeLa) and in mouse embryonic fibroblasts (Bromberg *et al.*, 2017). Additionally, in this thesis, the HEK *FXN*-GAA-Luc reporter cell line was used to describe the inhibition of the methyltransferases SUV4-20 an its effects on the expression of FXN protein. This work shows for the first time, that A-196 exerts its inhibitory role in a cell line with expanded GAA repeats (see Figure 5 and Figure 28). However, confirmation of effective elevation of FXN protein in FRDA patient-derived cells after A-196 treatment was necessary, taking into account that cells derived from patients will better recapitulate the genomic context and epigenetic landscape of the *FXN* locus. As expected, A-196 treatment of the FRDA patient-derived primary fibroblasts GM04078 showed to up-regulate FXN protein expression (Figure 30). These results show once more that inhibition of the family of proteins SUV4-20 may be a potential therapeutic strategy for FRDA.

Currently, there is no treatment that can prevent the progression of FRDA, or any effective symptomatic treatment that can improve the patient's condition (for instance as levodopa does for Parkinson’s disease) or slow the progression of the

neurodegenerative process (Pandolfo, 2009). Medical intervention in patients aims only to improve their life quality. The main therapeutic approaches have been described by Corben and colleagues (Corben *et al.*, 2014):

- Physical therapy: to maintain motor and muscle control for as long as possible.
- Occupational therapy: helps to manage patient's everyday lives, for example helping them be familiar with the use of walking canes, wheelchairs and other devices to feel as independent as possible.
- Surgery: to help straighten and support the spine, given that many patients develop scoliosis and foot abnormalities.
- Medications: even though exisiting medication cannot reverse or slow down the ataxia, they can help manage complications such as arrhythmias, heart disease or diabetes.
- Diet: because of the high risk to develop heart disease and diabetes, patients are advised to eat a diet that helps control their blood sugar levels.

Even thought this standard of care is important for FRDA patients to manage their condition, the need for treatments that truly modify the disease are essential. Currently, clinical trials primarily explore strategies directed at improving mitochondrial function and iron modulation, as well as treatment of FRDA symptoms rather than disease modification (Cook and Giunti, 2017; Strawser *et al.*, 2017). As these interventions pass through different clinical trial phases, it is possible that some of the mitochondrial-targeted approaches may prove to be efficacious. However, it is unlikely that they could provide a definitive cure for FRDA given that the primary deficit in frataxin expression will remain. Therefore,

therapies aiming to restore frataxin expression such as epigenetic modulation of *FXN,* are urgently needed.

Previous attempts to modify the *FXN* epigenetic landscape have relied on the inhibition of multiple class I HDACs (HDAC 1, 2 and 3), given that they are all required to activate FXN mRNA synthesis (Chou, Herman and Gottesfeld, 2008; Rai *et al.*, 2010). However, HDAC inhibition is likely to increase the potential for harmful off-target effects. Despite the poor selectivity of HDACi, compared to the one offered by methyltransferase inhibitors, HDACi have rapidly advance from their *in vitro* identification in 2006 to being used in clinical trials in 2014 (Herman *et al.*, 2006; Soragni *et al.*, 2014). Unfortunately, the HDACi (RG2833) that progressed to clinical trials showed poor central nervous system (CNS) penetrance, conversion of the active drug into poorly excreted, toxic metabolites, and a high-risk for inducing QT interval prolongation (that is a significant risk factor for ventricular arrhythmias and sudden cardiac death). Given the cardiac complications of FRDA, important heart side effects make unlikely the use of this drug in the clinic (Soragni *et al.*, 2014; Niemeijer *et al.*, 2015). However, an epigenetic therapy for FRDA still holds hope since this approach was shown to alleviate the transcription repression of the *FXN* locus. Therefore, taking into account that this work shows that modification of one single histone lysine residue is sufficient to up-regulate FXN protein levels, and that this is achieved through the selective inhibition of the SUV420 methyltransferase, therapies that aim to inhibit histone methylation can be considered as worthy of development and further exploitation.

Gene therapy is also a promising therapeutic approach that aims at frataxin restoration. It has been shown that intravenous injection of adeno-associated virus

rh10 vector expressing human *FXN* in mice, prevented the onset of cardiac disease. Moreover, administration of the *FXN*- expressing vector after the onset of heart failure, was able to reverse the cardiomyopathy of these animals at the functional, cellular and molecular levels only in a few days (Perdomini *et al.*, 2014). A recently published report from the same research group showed that post-symptomatic delivery of *FXN*-expressing AAV allowed rapid and complete rescue of the sensory neuropathy in parvalbumin- positive cells (e.g. proprioceptive afferent sensory neurons in the DRG) of a conditional mouse model with complete *FXN* deletion (Piguet *et al.*, 2018). In the same line of research, another study exploited the lentivirus-meditated *FXN* gene delivery to induce a long-term over-expression of FXN mRNA in fibroblasts derived from both FRDA mice and patients. (Khonsari *et al.*, 2016). Even though these studies show that gene therapy could potentially increase frataxin expression, there are several major issues that need to be addressed before beginning human trials. These problems include immunological response to viral vectors, their delivery to the brain and sustained transgene expression. Moreover, the effects of *FXN* over-expression are still not clear. A study in a FRDA *Drosophila* model reported that frataxin over-expression was deleterious to life span, impaired locomotor ability and caused brain damage (Llorens *et al.*, 2007). However, over-expression of *FXN* in mice has been shown to have no deleterious effects (Miranda *et al.*, 2004; Perdomini *et al.*, 2014). Despite the fact that *FXN* over-expression studies show discrepancies, any gene therapy approach for FRDA patients should demand a strict control of frataxin gene expression.

Although there will always be concerns about any novel therapy, the approach of targeting histone methylation exploits a new pharmacological opportunity to

reactivate the expression of *FXN* using the endogenous cellular machinery, and brings significant advantages of target specificity and CNS penetrance over existing HDACi, and confers the ease of small molecule systemic delivery over potentially immunogenic viral vectors.

7.4. Improving the potency and stability of A-196 as a potential therapeutic molecule

Drug combinations have been used since the earliest days of recorded history to treat diseases and reduce suffering. Traditional herbal Chinese medicine is a good example of this ancient practice (Chou, 2006). For instance, a legendary formula that utilizes four herbs (*Coptis chinensis*, *Scutellaria baicalensis*, *Phellodendron amurense*, and *Gardenia florida*) is used to treat the common cold (Gu and Pei, 2017). Nowadays, combination therapy has been mostly used to treat cancer patients. The combination of cancer drugs has been shown to have enhanced efficacy compared to the mono-therapy, where several drugs target several key pathways in a characteristically synergistic fashion (Bayat Mokhtari *et al.*, 2017).

Combination therapy aimed to modify epigenetic DNA features has also been reported. Combination of drugs targeting DNA methylation and histone acetylation has been studied in the treatment of cancer and neurodegenerative diseases (Chiurazzi *et al.*, 1999; Luszczek *et al.*, 2010). In FRDA, several groups have proposed the use of epigenetic combination therapy to relief the repression of *FXN* (Punga and Bühler, 2010; Chapdelaine *et al.*, 2013; Groh *et al.*, 2014; Polak *et al.*, 2016). The main proposed strategies comprehend the use of DNA demethylating

agents in combination with HDACi, without considering the role of histone methylation as a critical epigenetic silencing mark.

In the present work, epigenetic combination therapy using several inhibitors of PKMTs was tested as an approach to reduce the possible genome-wide adverse effects that global changes in histone methylation patterns may have. This is taking into consideration the undesired effects that the inhibition of SUV4-20 may have such as the genome-wide transition to a H4K20me1 state (the effects of the ablation of SUV4-20 were revised in section 7.2). The strategy here proposed to avoid an excessive modification of H4K20 is to use a low concentration of A-196 (H4K20) combined with GSK343 (H3K27) as a proof of principle that a further up-regulation of FXN protein can be obtained if synergy of several methyltransferase inhibitors can be achieved. In fact, 100 nM of A-196 combined with 100 nM of GSK343 are enough for both drugs to potentiate each other (Table 13), demonstrating that epigenetic combination therapy may be an interesting approach in FRDA.

Combination therapy has also been proposed for another triplet repeat disease, fragile X syndrome. In this disease, the *FMR1* gene is epigenetically repressed and the treatment of lymphoblastoid cell lines of fragile X patients with a DNA demethylating agent 5-aza-CdR in combination with HDACi (4-phenylbutyrate, sodium butyrate and trichostatinA), showed to increase *FMR1* mRNA levels in a 2- to 5-fold increase compared to the mRNA levels obtained with 5-aza-CdR alone (Chiurazzi *et al.*, 1999). Thus, considering that repeat diseases share common features of gene repression, combination therapy opens a new avenue for potential therapeutic opportunities in FRDA.

A different strategy here proposed to improve the potency of the lead compound A-196, was the modification of the original molecule by medicinal chemistry. This approach aims to improve not only the potency of A-196, but also its stability, in order to accomplish physicochemical properties that are adequate for *in vivo* testing. Despite the fact that cultured cells treated with A-196 do not show any apparent toxicity, the *in vivo* evaluation of SUV4-20 inhibition may provide more information about any potential consequences of epigenetic modification in a complex organism, and moreover, will allow to further develop this novel *FXN* raising therapeutic strategy.

7.5. Future directions

The possibility of advancing knowledge regarding the mechanisms of epigenetic repression of the *FXN* gene has been further suggested by the finding that H4K20 methylation plays an important role in the silencing of the *FXN* gene. Moreover, dissecting the mechanism by which H4K20me2 and H4K20me3 are accumulated in the *FXN* locus may provide insights on the epigenetic repression of other genes, for example those silenced in repeat expansion diseases.

Combination therapies aimed to target multiple genes involved in the epigenetic repression of *FXN* may prove to be important therapeutic approaches just as combination therapy is in cancer. H3K9 methylation has been shown to be accompanied by increased methylation of H3K27 and H4K20 at the *FXN* locus harbouring the hyperexpanded GAA repeats, hence targeting at the same time the methyltransferases responsible for these marks may be necessary (Kim, Napierala and Dent, 2011). Additionally, combinatorial patterns of histone acetylation and

methylation have been reported in the human genome (Wang *et al.*, 2008). Thus, combination of HDACi with inhibitors of SUV4-20 may be beneficial for restoring the expression of *FXN.* Another possible drug combination that may be interesting to investigate could be DNA demethylating agents with histone methyltransferases inhibitors. Combination therapy for neurodegenerative diseases offers a new opportunity for novel findings.

To advance further with the potential therapeutic use of SUV4-20 inhibition in FRDA, new A-196 analogues have to be tested for potency and stability in several cell models such as FRDA patient-derived lines and in specific cell types affected by frataxin repression and relevant to FRDA such as cardiomyocytes or sensory neurons that can be derived from iPSCs. Once a metabolically stable analogue has been synthesized, safety and efficacy will have to be tested in FRDA mice models. Global gene expression analysis at the RNA and protein levels (RNA-Seq, mass spectrometry and proteomics) have to be performed following chemical inhibition of the methyltransferases SUV4-20. These data would help to understand the possible effect of SUV4-20 inhibition on key cellular pathways, and will be crucial for determining the functional selectivity and safety of methyltransferases inhibitors. Finally, the established collaboration with SGC Oxford and Toronto will provide with the opportunity to perform in depth pharmacokinetic measurements of all A-196 analogues as well as to evaluate their selectivity against a panel of chromatin remodeling proteins and non-epigenetic targets.

REFERENCES

Abeti, R. *et al.* (2015) 'Targeting lipid peroxidation and mitochondrial imbalance in Friedreich's ataxia.', *Pharmacological research*. Elsevier Ltd, 99, pp. 344–50. doi: 10.1016/j.phrs.2015.05.015.

Abeti, R. *et al.* (2016) '"Mitochondrial energy imbalance and lipid peroxidation cause cell death in Friedreich's ataxia".', *Cell death & disease*. Nature Publishing Group, 7(5), p. e2237. doi: 10.1038/cddis.2016.111.

Abeti, R. *et al.* (2018) 'Novel Nrf2-Inducer Prevents Mitochondrial Defects and Oxidative Stress in Friedreich's Ataxia Models', *Frontiers in Cellular Neuroscience*. Frontiers, 12, p. 188. doi: 10.3389/fncel.2018.00188.

Adamec, J. *et al.* (2000) 'Iron-dependent self-assembly of recombinant yeast frataxin: implications for Friedreich ataxia.', *American journal of human genetics*. Elsevier, 67(3), pp. 549–62. doi: 10.1086/303056.

Adinolfi, S. *et al.* (2002) 'A structural approach to understanding the iron-binding properties of phylogenetically different frataxins', *Human Molecular Genetics*. Oxford University Press, 11(16), pp. 1865–1877. doi: 10.1093/hmg/11.16.1865.

Akhtar, A. and Gasser, S. M. (2007) 'The nuclear envelope and transcriptional control', *Nature Reviews Genetics*. doi: 10.1038/nrg2122.

Al-Mahdawi, S. *et al.* (2008) 'The Friedreich ataxia GAA repeat expansion mutation induces comparable epigenetic changes in human and transgenic mouse brain and heart tissues', *Human Molecular Genetics*, 17(5), pp. 735–746. doi: 10.1093/hmg/ddm346.

Al-Mahdawi, S. *et al.* (2013) 'Friedreich Ataxia Patient Tissues Exhibit Increased 5-Hydroxymethylcytosine Modification and Decreased CTCF Binding at the FXN Locus', *PLoS ONE*. Edited by A. Pastore. Public Library of Science, 8(9), p. e74956. doi: 10.1371/journal.pone.0074956.

Al-Mahdawi, S., Pook, M. and Chamberlain, S. (2000) 'A novel missense mutation (L198R) in the Friedreich's ataxia gene', *Human Mutation*, 16(1), pp. 95–95. doi: 10.1002/1098-1004(200007)16:1<95::AID-HUMU29>3.0.CO;2-E.

Allis, C. D., Jenuwein, T. and Reinberg, D. (2007) *Epigenetics*. Cold Spring Harbor, N.Y. : Cold Spring Harbor Laboratory Press. Available at: https://www.worldcat.org/title/epigenetics/oclc/855727437?referer=di&ht=edition (Accessed: 7 July 2018).

Almouzni, G. and Probst, A. V. (2011) 'Heterochromatin maintenance and establishment: Lessons from the mouse pericentromere', *Nucleus*, 2(5). doi: 10.4161/nucl.2.5.17707.

Armstrong, J. S., Khdour, O. and Hecht, S. M. (2010) 'Does oxidative stress contribute to the pathology of Friedreich's ataxia? A radical question', *The FASEB Journal*. Federation of American Societies for Experimental Biology, 24(7), pp. 2152–2163. doi: 10.1096/fj.09-143222.

Arrowsmith, C. H. *et al.* (2012) 'Epigenetic protein families: a new frontier for drug discovery', *Nature Reviews Drug Discovery*. Nature Publishing Group, 11(5), pp. 384–400. doi: 10.1038/nrd3674.

Arrowsmith, C. H. *et al.* (2015) 'The promise and peril of chemical probes.', *Nature chemical biology*. NIH Public Access, 11(8), pp. 536–41. doi: 10.1038/nchembio.1867.

Ashton, J. C. (2015) 'ANOVA and the analysis of drug combination experiments', *Nature Methods*, 12(12), p. 1108. doi: 10.1038/nmeth.3663.

Bannister, A. J. *et al.* (2001) 'Selective recognition of methylated lysine 9 on histone H3

by the HP1 chromo domain', *Nature*, 410(6824), pp. 120–124. Available at: http://eds.a.ebscohost.com/ehost/pdfviewer/pdfviewer?sid=275ef212-d2eb-490d-93cb-f9d7652580c3%40sessionmgr4005&vid=1&hid=4208.
Bannister, A. J. and Kouzarides, T. (2005) 'Reversing histone methylation', *Nature*. Nature Publishing Group, 436(7054), pp. 1103–1106. doi: 10.1038/nature04048.
Bannister, A. J. and Kouzarides, T. (2011) 'Regulation of chromatin by histone modifications', *Cell Research*. Nature Publishing Group, 21(3), pp. 381–395. doi: 10.1038/cr.2011.22.
Baralle, M. *et al.* (2008) 'Influence of Friedreich ataxia GAA noncoding repeat expansions on pre-mRNA processing', *American journal of human genetics*. Elsevier, 83(1), pp. 77–88. doi: 10.1016/j.ajhg.2008.06.018.
Barski, A. *et al.* (2007) 'High-Resolution Profiling of Histone Methylations in the Human Genome', *Cell*. Cell Press, 129(4), pp. 823–837. doi: 10.1016/J.CELL.2007.05.009.
Bartolo, C., Mendell, J. R. and Prior, T. W. (1998) 'Identification of a missense mutation in a Friedreich's ataxia patient: implications for diagnosis and carrier studies.', *American journal of medical genetics*, 79(5), pp. 396–9. Available at: http://www.ncbi.nlm.nih.gov/pubmed/9779809 (Accessed: 8 May 2018).
Bashkirov, V. N. (2002) '[The origin of heterochromatin in eukaryotes].', *Genetika*, 38(6), pp. 789–92. Available at: http://www.ncbi.nlm.nih.gov/pubmed/12138777 (Accessed: 8 July 2018).
Bayat Mokhtari, R. *et al.* (2017) 'Combination therapy in combating cancer.', *Oncotarget*. Impact Journals, LLC, 8(23), pp. 38022–38043. doi: 10.18632/oncotarget.16723.
Berger, S. L. *et al.* (2009) 'An operational definition of epigenetics.', *Genes & development*. Cold Spring Harbor Laboratory Press, 23(7), pp. 781–3. doi: 10.1101/gad.1787609.
De Biase, I. *et al.* (2009) 'Epigenetic silencing in Friedreich ataxia is associated with depletion of CTCF (CCCTC-binding factor) and antisense transcription', *PLoS ONE*, 4(11). doi: 10.1371/journal.pone.0007914.
Bickmore, W. A. and Van Steensel, B. (2013) 'Genome Architecture: Domain Organization of Interphase Chromosomes', *Cell*, 152, pp. 1270–1284. doi: 10.1016/j.cell.2013.02.001.
Bidichandani, S. I., Ashizawa, T. and Patel, P. I. (1997) 'Atypical Friedreich ataxia caused by compound heterozygosity for a novel missense mutation and the GAA triplet-repeat expansion.', *American Journal of Human Genetics*, 60(5), pp. 1251–1256. Available at: https://www.ncbi.nlm.nih.gov/pmc/articles/PMC1712428/pdf/ajhg00005-0244.pdf (Accessed: 7 May 2018).
Bidichandani, S. I., Ashizawa, T. and Patel, P. I. (1998) 'The GAA triplet-repeat expansion in Friedreich ataxia interferes with transcription and may be associated with an unusual DNA structure.', *American journal of human genetics*, 62(1), pp. 111–21. doi: 10.1086/301680.
Bidichandani, S. I. and Delatycki, M. B. (1993) *Friedreich Ataxia*, *GeneReviews®*. University of Washington, Seattle. Available at: http://www.ncbi.nlm.nih.gov/pubmed/20301458 (Accessed: 28 April 2018).
Bird, A. *et al.* (1985) 'A fraction of the mouse genome that is derived from islands of nonmethylated, CpG-rich DNA', *Cell*, 40(1), pp. 91–99. doi: 10.1016/0092-8674(85)90312-5.
Bird, A. P. and Wolffe, A. P. (1999) 'Methylation-Induced Repression— Belts, Braces, and Chromatin', *Cell*, 99(5), pp. 451–454. doi: 10.1016/S0092-8674(00)81532-9.

Bissinger, E.-M. *et al.* (2010) 'Targeting epigenetic modifiers: Inhibitors of histone methyltransferases', *MedChemComm*, 1(2), pp. 114–124. doi: 10.1039/C0MD00062K.
Boehm, T. *et al.* (2011) 'Variations of frataxin protein levels in normal individuals', *Neurological Sciences*. Springer Milan, 32(2), pp. 327–330. doi: 10.1007/s10072-010-0326-1.
Boesch, S. *et al.* (2008) 'Neurological effects of recombinant human erythropoietin in Friedreich's ataxia: A clinical pilot trial', *Movement Disorders*. Wiley-Blackwell, 23(13), pp. 1940–1944. doi: 10.1002/mds.22294.
Boesch, S. *et al.* (2014) 'Safety and tolerability of carbamylated erythropoietin in Friedreich's ataxia', *Movement Disorders*. Wiley-Blackwell, 29(7), pp. 935–939. doi: 10.1002/mds.25836.
Bolinches-Amorós, A. *et al.* (2014) 'Mitochondrial dysfunction induced by frataxin deficiency is associated with cellular senescence and abnormal calcium metabolism', *Frontiers in Cellular Neuroscience*. Frontiers, 8, p. 124. doi: 10.3389/fncel.2014.00124.
Bromberg, K. D. *et al.* (2017) 'The SUV4-20 inhibitor A-196 verifies a role for epigenetics in genomic integrity', *Nature Chemical Biology*. Nature Publishing Group, 13(3), pp. 317–324. doi: 10.1038/nchembio.2282.
Brookes, P. S. *et al.* (2004) 'Calcium, ATP, and ROS: a mitochondrial love-hate triangle', *American Journal of Physiology-Cell Physiology*. American Physiological Society, 287(4), pp. C817–C833. doi: 10.1152/ajpcell.00139.2004.
Bürk, K. (2017) 'Friedreich Ataxia: current status and future prospects.', *Cerebellum & ataxias*. BioMed Central, 4, p. 4. doi: 10.1186/s40673-017-0062-x.
De Bustos, C. *et al.* (2009) 'Tissue-specific variation in DNA methylation levels along human chromosome 1', *Epigenetics & Chromatin*. BioMed Central, 2(1), p. 7. doi: 10.1186/1756-8935-2-7.
Butler, R. and Bates, G. P. (2006) 'Histone deacetylase inhibitors as therapeutics for polyglutamine disorders', *Nature Reviews Neuroscience*. Nature Publishing Group, 7(10), pp. 784–796. doi: 10.1038/nrn1989.
Campuzano, V. *et al.* (1996) 'Friedreich's Ataxia : Autosomal Recessive Disease Caused by an Intronic GAA Triplet Repeat Expansion Published by : American Association for the Advancement of Science Stable URL : http://www.jstor.org/stable/2890274 Accessed : 04-04-2016 23 : 20 UTC Yo', *Science*, 271(March), pp. 1423–1427.
Campuzano, V. *et al.* (1997) 'Frataxin is reduced in Friedreich ataxia patients and is associated with mitochondrial membranes.', *Human molecular genetics*. Oxford University Press, 6(11), pp. 1771–80. doi: 10.1093/HMG/6.11.1771.
Casazza, F. and Morpurgo, M. (1996) 'The varying evolution of friedreich's ataxia cardiomyopathy', *The American Journal of Cardiology*. Excerpta Medica, 77(10), pp. 895–898. doi: 10.1016/S0002-9149(97)89194-1.
Casciello, F. *et al.* (2015) 'Functional Role of G9a Histone Methyltransferase in Cancer', *Frontiers in Immunology*. Frontiers, 6, p. 487. doi: 10.3389/fimmu.2015.00487.
Castaldo, I. *et al.* (2008) 'DNA methylation in intron 1 of the frataxin gene is related to GAA repeat length and age of onset in Friedreich ataxia patients.', *Journal of medical genetics*, 45(12), pp. 808–12. doi: 10.1136/jmg.2008.058594.
De Castro, M. *et al.* (2000) 'Genotype and phenotype analysis of Friedreich's ataxia compound heterozygous patients.', *Human genetics*, 106(1), pp. 86–92. Available at: http://www.ncbi.nlm.nih.gov/pubmed/10982187 (Accessed: 8 May 2018).
Cavadini, P. *et al.* (2002) 'Assembly and iron-binding properties of human frataxin, the protein deficient in Friedreich ataxia', *Human Molecular Genetics*. Oxford University Press, 11(3), pp. 217–227. doi: 10.1093/hmg/11.3.217.
Cermak, T. *et al.* (2011) 'Efficient design and assembly of custom TALEN and other

TAL effector-based constructs for DNA targeting.', *Nucleic acids research*. Oxford University Press, 39(12), p. e82. doi: 10.1093/nar/gkr218.
Chakalova, L. *et al.* (2005) 'Replication and transcription: shaping the landscape of the genome.', *Nature reviews. Genetics*, 6(9), pp. 669–677. doi: 10.1038/nrg1673.
Chamberlain, S. *et al.* (1988) 'Mapping of mutation causing Friedreich's ataxia to human chromosome 9', *Nature*, 334, pp. 248–250. doi: 10.1038/334248a0.
Chan, P. K. *et al.* (2013) 'Heterochromatinization induced by GAA-repeat hyperexpansion in Friedreich's ataxia can be reduced upon HDAC inhibition by vitamin B3', *Human Molecular Genetics*. Oxford University Press, 22(13), pp. 2662–2675. doi: 10.1093/hmg/ddt115.
Chapdelaine, P. *et al.* (2013) 'A Potential New Therapeutic Approach for Friedreich Ataxia: Induction of Frataxin Expression With TALE Proteins', *Molecular Therapy - Nucleic Acids*. Cell Press, 2. doi: 10.1038/MTNA.2013.41.
Chauhan, C. *et al.* (2002) 'Origin and Instability of GAA Repeats: Insights from Alu Elements', *Journal of Biomolecular Structure and Dynamics*, 20(2), pp. 253–263. doi: 10.1080/07391102.2002.10506841.
Chiurazzi, P. *et al.* (1999) 'Synergistic Effect of Histone Hyperacetylation and DNA Demethylation in the Reactivation of the FMR1 Gene', *Human Molecular Genetics*. Oxford University Press, 8(12), pp. 2317–2323. doi: 10.1093/hmg/8.12.2317.
Chou, C. J., Herman, D. and Gottesfeld, J. M. (2008) 'Pimelic diphenylamide 106 is a slow, tight-binding inhibitor of class I histone deacetylases.', *The Journal of biological chemistry*. American Society for Biochemistry and Molecular Biology, 283(51), pp. 35402–9. doi: 10.1074/jbc.M807045200.
Chou, T.-C. (2006) 'Theoretical basis, experimental design, and computerized simulation of synergism and antagonism in drug combination studies.', *Pharmacological reviews*. American Society for Pharmacology and Experimental Therapeutics, 58(3), pp. 621–81. doi: 10.1124/pr.58.3.10.
Chou, T.-C. (2010) 'Drug combination studies and their synergy quantification using the Chou-Talalay method', *Cancer research*. American Association for Cancer Research, 70(2), pp. 440–446. doi: 10.1158/0008-5472.can-09-1947.
Chutake, Y. K. *et al.* (2016) 'Reversal of epigenetic promoter silencing in Friedreich ataxia by a class I histone deacetylase inhibitor.', *Nucleic acids research*, p. gkw107-. doi: 10.1093/nar/gkw107.
Cloos, P. A. C. *et al.* (2008) 'Erasing the methyl mark: histone demethylases at the center of cellular differentiation and disease.', *Genes & development*. Cold Spring Harbor Laboratory Press, 22(9), pp. 1115–40. doi: 10.1101/gad.1652908.
Cnop, M. *et al.* (2012) 'Central role and mechanisms of β-cell dysfunction and death in friedreich ataxia-associated diabetes', *Annals of Neurology*. Wiley-Blackwell, 72(6), pp. 971–982. doi: 10.1002/ana.23698.
Cnop, M., Mulder, H. and Igoillo-Esteve, M. (2013) 'Diabetes in Friedreich Ataxia', *Journal of Neurochemistry*. Wiley/Blackwell (10.1111), 126, pp. 94–102. doi: 10.1111/jnc.12216.
Compere, S. J. and Palmiter, R. D. (1981) 'DNA methylation controls the inducibility of the mouse metallothionein-I gene lymphoid cells', *Cell*, 25(1), pp. 233–240.
Condò, I. *et al.* (2007) 'In vivo maturation of human frataxin.', *Human molecular genetics*. Oxford University Press, 16(13), pp. 1534–40. doi: 10.1093/hmg/ddm102.
Cook, A. and Giunti, P. (2017) 'Friedreich's ataxia: clinical features, pathogenesis and management', *British Medical Bulletin*. Oxford University Press, 124(1), pp. 19–30. doi: 10.1093/bmb/ldx034.
Corben, L. A. *et al.* (2006) 'Towards an understanding of cognitive function in

Friedreich ataxia', *Brain Research Bulletin*, 70(3), pp. 197–202. doi: 10.1016/j.brainresbull.2006.06.001.
Corben, L. A. *et al.* (2010) 'Impairment in motor reprogramming in Friedreich ataxia reflecting possible cerebellar dysfunction', *Journal of Neurology*, 257(5), pp. 782–791. doi: 10.1007/s00415-009-5410-1.
Corben, L. A. *et al.* (2011) 'Impaired inhibition of prepotent motor tendencies in Friedreich ataxia demonstrated by the Simon interference task', *Brain and Cognition*, 76(1), pp. 140–145. doi: 10.1016/j.bandc.2011.02.002.
Corben, L. A. *et al.* (2014) 'Consensus clinical management guidelines for Friedreich ataxia.', *Orphanet journal of rare diseases*. BioMed Central, 9, p. 184. doi: 10.1186/s13023-014-0184-7.
Corben, L. A. *et al.* (2017) 'Measuring Inhibition and Cognitive Flexibility in Friedreich Ataxia', *The Cerebellum*, 16(4), pp. 757–763. doi: 10.1007/s12311-017-0848-7.
Cossée, M. *et al.* (1997) 'Evolution of the Friedreich's ataxia trinucleotide repeat expansion: Founder effect and premutations', *Proceedings of the National Academy of Sciences of the United States of America*, 94(14), pp. 7452–7457. doi: 10.1073/pnas.94.14.7452.
Cossée, M. *et al.* (1999) 'Friedreich's ataxia: point mutations and clinical presentation of compound heterozygotes.', *Annals of neurology*, 45(2), pp. 200–6. Available at: http://www.ncbi.nlm.nih.gov/pubmed/9989622 (Accessed: 5 November 2016).
Cossée, M. *et al.* (2000) 'Inactivation of the Friedreich ataxia mouse gene leads to early embryonic lethality without iron accumulation', *Human Molecular Genetics*. Oxford University Press, 9(8), pp. 1219–1226. doi: 10.1093/hmg/9.8.1219.
D'Oria, V. *et al.* (2013) 'Frataxin Deficiency Leads to Reduced Expression and Impaired Translocation of NF-E2-Related Factor (Nrf2) in Cultured Motor Neurons', *International Journal of Molecular Sciences*. Multidisciplinary Digital Publishing Institute, 14(4), pp. 7853–7865. doi: 10.3390/ijms14047853.
Delatycki, M. B., Paris, D., *et al.* (1999) 'Clinical and genetic study of Friedreich ataxia in an Australian population', *American Journal of Medical Genetics*. Wiley-Blackwell, 87(2), pp. 168–174. doi: 10.1002/(SICI)1096-8628(19991119)87:2<168::AID-AJMG8>3.0.CO;2-2.
Delatycki, M. B., Knight, M., *et al.* (1999) 'G130V, a common FRDA point mutation, appears to have arisen from a common founder', *Human genetics*, 105(4), pp. 343–6. Available at: http://www.ncbi.nlm.nih.gov/pubmed/10543403 (Accessed: 3 June 2018).
Delatycki, M. B. and Corben, L. A. (2012) 'Clinical features of Friedreich ataxia.', *Journal of child neurology*. NIH Public Access, 27(9), pp. 1133–7. doi: 10.1177/0883073812448230.
Dhasarathy, A. and Wade, P. A. (2008) 'The MBD protein family-Reading an epigenetic mark?', *Mutation Research - Fundamental and Molecular Mechanisms of Mutagenesis*, 647(1–2), pp. 39–43. doi: 10.1016/j.mrfmmm.2008.07.007.
Doudney, K. *et al.* (1998) 'A novel splice site mutation (384+ 1G-A) in the Friedreich's ataxia gene', *Human Mutation*, 11(5), p. 415.
Van Driest, S. L. *et al.* (2005) 'Molecular and functional characterization of a human frataxin mutation found in hypertrophic cardiomyopathy.', *Molecular genetics and metabolism*, 85(4), pp. 280–5. doi: 10.1016/j.ymgme.2005.04.010.
Dürr, A. *et al.* (1996) 'Clinical and Genetic Abnormalities in Patients with Friedreich's Ataxia', *New England Journal of Medicine*. Massachusetts Medical Society , 335(16), pp. 1169–1175. doi: 10.1056/NEJM199610173351601.
Ehrlich, M. *et al.* (1982) 'Amount and distribution of 5-methylcytosine in human DNA from different types of tissues or cells', *Nucleic Acids Research*, 10(8), pp. 2709–2721.

doi: 10.1093/nar/10.8.2709.
Elgin, S. C. R. *et al.* (2003) 'Heterochromatin: silence is golden.', *Current biology : CB*. Elsevier, 13(23), pp. R895-8. doi: 10.1016/J.CUB.2003.11.006.
Eram, M. S. *et al.* (2016) 'A Potent, Selective, and Cell-Active Inhibitor of Human Type I Protein Arginine Methyltransferases', *ACS Chemical Biology*. American Chemical Society, 11(3), pp. 772–781. doi: 10.1021/acschembio.5b00839.
Evans-Galea, M. V. *et al.* (2012) 'FXN methylation predicts expression and clinical outcome in Friedreich ataxia', *Annals of Neurology*, 71(4), pp. 487–497. doi: 10.1002/ana.22671.
Fahey, M. C. *et al.* (2008) 'Vestibular, saccadic and fixation abnormalities in genetically confirmed Friedreich ataxia', *Brain*. Oxford University Press, 131(4), pp. 1035–1045. doi: 10.1093/brain/awm323.
Fang, J. *et al.* (2002) 'Purification and Functional Characterization of SET8, a Nucleosomal Histone H4-Lysine 20-Specific Methyltransferase', *Current Biology*. Cell Press, 12(13), pp. 1086–1099. doi: 10.1016/S0960-9822(02)00924-7.
Feng, Q. *et al.* (2002) 'Methylation of H3-lysine 79 is mediated by a new family of HMTases without a SET domain.', *Current biology : CB*. Elsevier, 12(12), pp. 1052–8. doi: 10.1016/S0960-9822(02)00901-6.
Festenstein, R. *et al.* (1996) 'Locus Control Region Function and Heterochromatin-Induced Position Effect Variegation Published by : American Association for the Advancement of Science Stable URL : http://www.jstor.org/stable/2889848 digitize , preserve and extend access to Science Locu', *Science*, 271(5252), pp. 1123–1125.
Festenstein, R. (2006) 'Breaking the silence in Friedreich's ataxia', *Nature Chemical Biology*. Nature Publishing Group, 2(10), pp. 512–513. doi: 10.1038/nchembio1006-512.
Filippakopoulos, P. *et al.* (2012) 'Histone recognition and large-scale structural analysis of the human bromodomain family.', *Cell*. Elsevier, 149(1), pp. 214–31. doi: 10.1016/j.cell.2012.02.013.
Filla, A. *et al.* (1990) 'Genetic data and natural history of Friedreich's disease: a study of 80 Italian patients', *Journal of Neurology*. Springer-Verlag, 237(6), pp. 345–351. doi: 10.1007/BF00315657.
Filla, A. *et al.* (1996) 'The relationship between trinucleotide (GAA) repeat length and clinical features in Friedreich ataxia.', *American journal of human genetics*, 59(3), pp. 554–60. Available at: http://www.ncbi.nlm.nih.gov/pubmed/8751856 (Accessed: 8 May 2018).
Fischle, W., Wang, Y. and Allis, C. D. (2003) 'Histone and chromatin cross-talk', *Current Opinion in Cell Biology*. Elsevier Current Trends, 15(2), pp. 172–183. doi: 10.1016/S0955-0674(03)00013-9.
Fisher, A. G. and Merkenschlager, M. (2002) 'Gene silencing, cell fate and nuclear organisation', *Current Opinion in Genetics and Development*, 12(2), pp. 193–197. doi: 10.1016/S0959-437X(02)00286-1.
Folker, J. *et al.* (2010) 'Dysarthria in Friedreich's ataxia: a perceptual analysis.', *Folia phoniatrica et logopaedica : official organ of the International Association of Logopedics and Phoniatrics (IALP)*. Karger Publishers, 62(3), pp. 97–103. doi: 10.1159/000287207.
Forrest, S. M. *et al.* (1998) 'The correlation of clinical phenotype in Friedreich ataxia with the site of point mutations in the FRDA gene.', *Neurogenetics*, 1(4), pp. 253–7. Available at: http://www.ncbi.nlm.nih.gov/pubmed/10732799 (Accessed: 8 May 2018).
Fortuna, F. *et al.* (2009) 'Visual system involvement in patients with Friedreich's ataxia', *Brain*. Oxford University Press, 132(1), pp. 116–123. doi: 10.1093/brain/awn269.
Friedreich, N. (1863a) 'Ueber degenerative Atrophie der spinalen Hinterstränge', *Archiv*

f. pathol. Anat., 27(1–2), pp. 1–26.
Friedreich, N. (1863b) 'Ueber degenerative Atrophie der spinalen Hinterstränge', *N. Archiv f. pathol. Anat.*, 26(3–4), pp. 391–419.
Friedreich, N. (1863c) 'Ueber degenerative Atrophie der spinalen Hinterstränge', *Archiv f. pathol. Anat*, 26(5–6), pp. 433–459.
Friedreich, N. (1876) 'Ueber Ataxie mit besonderer Berücksichtigung der hereditären Formen', *Archiv f. pathol. Anat.*, 68(2), pp. 145–245.
Friedreich, N. (1877) 'Ueber Ataxie mit besonderer Berücksichtigung der hereditären Formen', *N. Archiv f. pathol. Anat.*, 70(1), pp. 140–152.
Fry, R. C. *et al.* (2008) 'Genomic predictors of interindividual differences in response to DNA damaging agents.', *Genes & development*. Cold Spring Harbor Laboratory Press, 22(19), pp. 2621–6. doi: 10.1101/gad.1688508.
Gellera, C. *et al.* (2007) 'Frataxin gene point mutations in Italian Friedreich ataxia patients', *Neurogenetics*. Springer-Verlag, 8(4), pp. 289–299. doi: 10.1007/s10048-007-0101-5.
Gérard, C. *et al.* (2014) 'An AAV9 coding for frataxin clearly improved the symptoms and prolonged the life of Friedreich ataxia mouse models', *Molecular Therapy - Methods & Clinical Development*. Cell Press, 1. doi: 10.1038/MTM.2014.44.
Gimenez-Cassina, A. *et al.* (2011) 'Infectious delivery and long-term persistence of transgene expression in the brain by a 135-kb iBAC-FXN genomic DNA expression vector', *Gene Therapy*. Nature Publishing Group, 18(10), pp. 1015–1019. doi: 10.1038/gt.2011.45.
Glickman, M. H. and Ciechanover, A. (2002) 'The Ubiquitin-Proteasome Proteolytic Pathway: Destruction for the Sake of Construction', *Physiological Reviews*, 82(2), pp. 373–428. doi: 10.1152/physrev.00027.2001.
Gomez-Sebastian, S. *et al.* (2007) 'Infectious Delivery and Expression of a 135 kb Human FRDA Genomic DNA Locus Complements Friedreich's Ataxia Deficiency in Human Cells', *Molecular Therapy*. Cell Press, 15(2), pp. 248–254. doi: 10.1038/SJ.MT.6300021.
González-Cabo, P. and Palau, F. (2013) 'Mitochondrial pathophysiology in Friedreich's ataxia', *Journal of Neurochemistry*, 126(SUPPL.1), pp. 53–64. doi: 10.1111/jnc.12303.
Grabczyk, E., Mancuso, M. and Sammarco, M. C. (2007) 'A persistent RNA·DNA hybrid formed by transcription of the Friedreich ataxia triplet repeat in live bacteria, and by T7 RNAP in vitro', *Nucleic Acids Research*, 35(16), pp. 5351–5359. doi: 10.1093/nar/gkm589.
Grabczyk, E. and Usdin, K. (2000) 'The GAA*TTC triplet repeat expanded in Friedreich's ataxia impedes transcription elongation by T7 RNA polymerase in a length and supercoil dependent manner.', *Nucleic acids research*, 28(14), pp. 2815–2822. doi: 10.1093/nar/28.14.2815.
Greenbaum, D. *et al.* (2003) 'Comparing protein abundance and mRNA expression levels on a genomic scale.', *Genome biology*. BioMed Central, 4(9), p. 117. doi: 10.1186/gb-2003-4-9-117.
Greene, E. *et al.* (2007) 'Repeat-induced epigenetic changes in intron 1 of the frataxin gene and its consequences in Friedreich ataxia', *Nucleic Acids Research*, 35(10), pp. 3383–3390. doi: 10.1093/nar/gkm271.
Groh, M. *et al.* (2014) 'R-loops Associated with Triplet Repeat Expansions Promote Gene Silencing in Friedreich Ataxia and Fragile X Syndrome', *PLoS Genetics*, 10(5). doi: 10.1371/journal.pgen.1004318.
Gu, S. and Pei, J. (2017) 'Innovating Chinese Herbal Medicine: From Traditional Health Practice to Scientific Drug Discovery.', *Frontiers in pharmacology*. Frontiers Media SA,

8, p. 381. doi: 10.3389/fphar.2017.00381.
Haberland, M., Montgomery, R. L. and Olson, E. N. (2009) 'The many roles of histone deacetylases in development and physiology: implications for disease and therapy', *Nature Reviews Genetics*. Nature Publishing Group, 10(1), pp. 32–42. doi: 10.1038/nrg2485.
Harding, A. E. (1981) 'FRIEDREICH'S ATAXIA: A CLINICAL AND GENETIC STUDY OF 90 FAMILIES WITH AN ANALYSIS OF EARLY DIAGNOSTIC CRITERIA AND INTRAFAMILIAL CLUSTERING OF CLINICAL FEATURES', *Brain*. Oxford University Press, 104(3), pp. 589–620. doi: 10.1093/brain/104.3.589.
Hare, D. *et al.* (2016) 'The Importance of Physiologically Relevant Cell Lines for Studying Virus-Host Interactions.', *Viruses*. Multidisciplinary Digital Publishing Institute (MDPI), 8(11), p. 297. doi: 10.3390/v8110297.
Hayashi, G. and Cortopassi, G. (2015) 'Oxidative stress in inherited mitochondrial diseases', *Free Radical Biology and Medicine*. Elsevier, 88, pp. 10–17. doi: 10.1016/j.freeradbiomed.2015.05.039.
Hayes, J. D. and Dinkova-Kostova, A. T. (2014) 'The Nrf2 regulatory network provides an interface between redox and intermediary metabolism', *Trends in Biochemical Sciences*. Elsevier Current Trends, 39(4), pp. 199–218. doi: 10.1016/J.TIBS.2014.02.002.
Herman, D. *et al.* (2006) 'Histone deacetylase inhibitors reverse gene silencing in Friedreich's ataxia.', *Nature chemical biology*, 2(10), pp. 551–558. doi: 10.1038/nchembio815.
Holliday, A. R. and Pugh, J. E. (1975) 'DNA Modification Mechanisms and Gene Activity during Development', *Science*, 187(4173), pp. 226–232.
Holmström, K. M., Kostov, R. V. and Dinkova-Kostova, A. T. (2016) 'The multifaceted role of Nrf2 in mitochondrial function', *Current Opinion in Toxicology*. Elsevier, 1, pp. 80–91. doi: 10.1016/J.COTOX.2016.10.002.
Horizon Pharma (2016) *Horizon Pharma plc Announces Topline Results from Phase 3 Study of ACTIMMUNE® (interferon gamma-1b) in Friedreich's Ataxia*. Available at: http://ir.horizon-pharma.com/news-releases/news-release-details/horizon-pharma-plc-announces-topline-results-phase-3-study.
Huang, J. and Berger, S. L. (2008) 'The emerging field of dynamic lysine methylation of non-histone proteins', *Current Opinion in Genetics & Development*. Elsevier Current Trends, 18(2), pp. 152–158. doi: 10.1016/J.GDE.2008.01.012.
Hughes, J. P. *et al.* (2011) 'Principles of early drug discovery.', *British journal of pharmacology*. Wiley-Blackwell, 162(6), pp. 1239–49. doi: 10.1111/j.1476-5381.2010.01127.x.
Huynen, M. A. *et al.* (2001) 'The phylogenetic distribution of frataxin indicates a role in iron-sulfur cluster protein assembly', *Human Molecular Genetics*. Oxford University Press, 10(21), pp. 2463–2468. doi: 10.1093/hmg/10.21.2463.
Jasoliya, M. J. *et al.* (2017) 'Frataxin deficiency impairs mitochondrial biogenesis in cells, mice and humans', *Human Molecular Genetics*. Oxford University Press, 26(14), pp. 2627–2633. doi: 10.1093/hmg/ddx141.
Jia, J. *et al.* (2009) 'Mechanisms of drug combinations: interaction and network perspectives', *Nature Reviews Drug Discovery*. Nature Publishing Group, 8(2), pp. 111–128. doi: 10.1038/nrd2683.
Johnson, D. C. *et al.* (2005) 'Structure, Function, and Formation of Biological Iron-Sulfur Clusters', *Annual Review of Biochemistry*, 74(1), pp. 247–281. doi: 10.1146/annurev.biochem.74.082803.133518.
Justice, C. M. *et al.* (2001) 'Phylogenetic Analysis of the Friedreich Ataxia GAA

Trinucleotide Repeat', *Journal of Molecular Evolution*. Springer-Verlag, 52(3), pp. 232–238. doi: 10.1007/s002390010151.
Kachirskaia, I. *et al.* (2008) 'Role for 53BP1 Tudor domain recognition of p53 dimethylated at lysine 382 in DNA damage signaling.', *The Journal of biological chemistry*. American Society for Biochemistry and Molecular Biology, 283(50), pp. 34660–6. doi: 10.1074/jbc.M806020200.
Karmodiya, K. *et al.* (2012) 'H3K9 and H3K14 acetylation co-occur at many gene regulatory elements, while H3K14ac marks a subset of inactive inducible promoters in mouse embryonic stem cells', *BMC Genomics*. BMC Genomics, 13(1), p. 1. doi: 10.1186/1471-2164-13-424.
Kazantsev, A. G. and Thompson, L. M. (2008) 'Therapeutic application of histone deacetylase inhibitors for central nervous system disorders', *Nature Reviews Drug Discovery*. Nature Publishing Group, 7(10), pp. 854–868. doi: 10.1038/nrd2681.
Keshet, I. *et al.* (2006) 'Evidence for an instructive mechanism of de novo methylation in cancer cells', *Nature Genetics*. Nature Publishing Group, 38(2), pp. 149–153. doi: 10.1038/ng1719.
Khonsari, H. *et al.* (2016) 'Lentivirus-meditated frataxin gene delivery reverses genome instability in Friedreich ataxia patient and mouse model fibroblasts', *Gene Therapy*, 23, pp. 846–856. doi: 10.1038/gt.2016.61.
Kim, E., Napierala, M. and Dent, S. Y. R. (2011) 'Hyperexpansion of GAA repeats affects post-initiation steps of FXN transcription in Friedreich's ataxia', *Nucleic Acids Research*, 39(19), pp. 8366–8377. doi: 10.1093/nar/gkr542.
Kim, H.-J. and Bae, S.-C. (2011) 'Histone deacetylase inhibitors: molecular mechanisms of action and clinical trials as anti-cancer drugs.', *American journal of translational research*. e-Century Publishing Corporation, 3(2), pp. 166–79. Available at: http://www.ncbi.nlm.nih.gov/pubmed/21416059 (Accessed: 22 August 2018).
Kim, Y. *et al.* (2013) 'BIX-01294 induces autophagy-associated cell death via EHMT2/G9a dysfunction and intracellular reactive oxygen species production', *Autophagy*, 9(12), pp. 2126–2139. doi: 10.4161/auto.26308.
Kind, J. and van Steensel, B. (2010) 'Genome–nuclear lamina interactions and gene regulation', *Current Opinion in Cell Biology*, 22(3), pp. 320–325. doi: 10.1016/j.ceb.2010.04.002.
Klopper, F. *et al.* (2011) 'The Test of Everyday Attention Reveals Significant Sustained Volitional Attention and Working Memory Deficits in Friedreich Ataxia', *Journal of the International Neuropsychological Society*, 17(01), pp. 196–200. doi: 10.1017/S1355617710001347.
Koeppen, A. H. (2013) 'Nikolaus Friedreich and degenerative atrophy of the dorsal columns of the spinal cord.', *Journal of neurochemistry*. NIH Public Access, 126 Suppl 1(0 1), pp. 4–10. doi: 10.1111/jnc.12218.
de Koning, A. P. J. *et al.* (2011) 'Repetitive Elements May Comprise Over Two-Thirds of the Human Genome', *PLoS Genetics*. Edited by G. P. Copenhaver. Public Library of Science, 7(12), p. e1002384. doi: 10.1371/journal.pgen.1002384.
Kourmouli, N. *et al.* (2004) 'Heterochromatin and tri-methylated lysine 20 of histone H4 in animals', *Journal of Cell Science*, 117(12), pp. 2491–2501. doi: 10.1242/jcs.01238.
Koutnikova, H. *et al.* (1997) 'Studies of human, mouse and yeast homologues indicate a mitochondrial function for frataxin', *Nature Genetics*. Nature Publishing Group, 16(4), pp. 345–351. doi: 10.1038/ng0897-345.
Koutnikova, H., Campuzano, V. and Koenig, M. (1998) 'Maturation of wild-type and mutated frataxin by the mitochondrial processing peptidase.', *Human molecular genetics*. Oxford University Press, 7(9), pp. 1485–9. doi: 10.1093/HMG/7.9.1485.

Kouzarides, T. (2007) ‘Chromatin Modifications and Their Function’, *Cell*. Cell Press, 128(4), pp. 693–705. doi: 10.1016/J.CELL.2007.02.005.
Kriaucionis, S. and Heintz, N. (2009) ‘The Nuclear DNA Base 5-Hydroxymethylcytosine Is Present in Purki je Neurons and the Brain’, *Science*, 324(5929), pp. 929–930.
Krzywinski, M. and Altman, N. (2014) ‘Two-factor designs’, *Nature Methods*, 11(12), pp. 1187–1188. doi: 10.1038/nmeth.3180.
Kumari, D., Biacsi, R. E. and Usdin, K. (2011) ‘Repeat expansion affects both transcription initiation and elongation in Friedreich ataxia cells’, *Journal of Biological Chemistry*, 286(6), pp. 4209–4215. doi: 10.1074/jbc.M110.194035.
Labelle, H. *et al.* (1986) ‘Natural history of scoliosis in Friedreich’s ataxia.’, *The Journal of bone and joint surgery. American volume*, 68(4), pp. 564–72. Available at: http://www.ncbi.nlm.nih.gov/pubmed/3957980 (Accessed: 27 May 2018).
Labuda, M., Poirier, J. and Pandolfo, M. (1999) ‘A missense mutation (W155R) in an American patient with Friedreich Ataxia’, *Human Mutation*. Wiley-Blackwell, 13(6), pp. 506–506. doi: 10.1002/(SICI)1098-1004(1999)13:6<506::AID-HUMU20>3.0.CO;2-E.
Lachner, M., O’Sullivan, R. J. and Jenuwein, T. (2003) ‘An epigenetic road map for histone lysine methylation’, *Journal of Cell Science*, 116(11), pp. 2117–2124. doi: 10.1242/jcs.00493.
Lee, D. Y. *et al.* (2005) ‘Role of Protein Methylation in Regulation of Transcription’, *Endocrine Reviews*. Oxford University Press, 26(2), pp. 147–170. doi: 10.1210/er.2004-0008.
Lee, Y. K. *et al.* (2016) ‘Efficient attenuation of Friedreich’s ataxia (FRDA) cardiomyopathy by modulation of iron homeostasis-human induced pluripotent stem cell (hiPSC) as a drug screening platform for FRDA’, *International Journal of Cardiology*. The Authors, 203, pp. 964–971. doi: 10.1016/j.ijcard.2015.11.101.
van Leeuwen, F., Gafken, P. R. and Gottschling, D. E. (2002) ‘Dot1p Modulates Silencing in Yeast by Methylation of the Nucleosome Core’, *Cell*. Cell Press, 109(6), pp. 745–756. doi: 10.1016/S0092-8674(02)00759-6.
Lemaître, C. and Bickmore, W. a (2015) ‘Chromatin at the nuclear periphery and the regulation of genome functions.’, *Histochemistry and cell biology*. Springer Berlin Heidelberg, 144(2), pp. 111–122. doi: 10.1007/s00418-015-1346-y.
Li, K. *et al.* (2008) ‘Iron-dependent regulation of frataxin expression: implications for treatment of Friedreich ataxia’, *Human molecular genetics*. Oxford University Press, 17(15), pp. 2265–73. doi: 10.1093/hmg/ddn127.
Li, Y. *et al.* (2015) ‘Expanded GAA repeats impede transcription elongation through the FXN gene and induce transcriptional silencing that is restricted to the FXN locus’, *Human Molecular Genetics*, 24(24), pp. 6932–6943. doi: 10.1093/hmg/ddv397.
Libri, V. *et al.* (2014) ‘Epigenetic and neurological effects and safety of high-dose nicotinamide in patients with Friedreich’s ataxia: an exploratory, open-label, dose-escalation study’, *The Lancet*. Elsevier, 384(9942), pp. 504–513. doi: 10.1016/S0140-6736(14)60382-2.
Lim, F. *et al.* (2007) ‘Functional Recovery in a Friedreich’s Ataxia Mouse Model by Frataxin Gene Transfer Using an HSV-1 Amplicon Vector’, *Molecular Therapy*. Cell Press, 15(6), pp. 1072–1078. doi: 10.1038/SJ.MT.6300143.
Livak, K. J. and Schmittgen, T. D. (2001) ‘Analysis of Relative Gene Expression Data Using Real-Time Quantitative PCR and the 2−ΔΔCT Method’, *Methods*, 25(4), pp. 402–408. doi: 10.1006/meth.2001.1262.
Llorens, J. V *et al.* (2007) ‘Causative role of oxidative stress in a Drosophila model of Friedreich ataxia.’, *FASEB journal : official publication of the Federation of American*

Societies for Experimental Biology, 21(2), pp. 333–44. doi: 10.1096/fj.05-5709com.
Di Lorenzo, A. and Bedford, M. T. (2011) 'Histone arginine methylation', *FEBS Letters*. No longer published by Elsevier, 585(13), pp. 2024–2031. doi: 10.1016/J.FEBSLET.2010.11.010.
Low, S.-C. *et al.* (2013) 'Excessive motor overflow reveals abnormal inter-hemispheric connectivity in Friedreich ataxia', *Journal of Neurology*, 260(7), pp. 1757–1764. doi: 10.1007/s00415-013-6869-3.
Lufino, M. M. P. *et al.* (2013) 'A GAA repeat expansion reporter model of friedreich's ataxia recapitulates the genomic context and allows rapid screening of therapeutic compounds', *Human Molecular Genetics*, 22(25), pp. 5173–5187. doi: 10.1093/hmg/ddt370.
Luszczek, W. *et al.* (2010) 'Combinations of DNA methyltransferase and histone deacetylase inhibitors induce DNA damage in small cell lung cancer cells: correlation of resistance with IFN-stimulated gene expression.', *Molecular cancer therapeutics*, 9(8), pp. 2309–21. doi: 10.1158/1535-7163.MCT-10-0309.
Lynch, D. *et al.* (2017) *Safety, Efficacy, and Pharmacodynamics of Omav (Omaveloxolone) in Friedreich's Ataxia Patients (MOXIe Trial): Part 1 Results*. Available at: https://reatapharma.gcs-web.com/static-files/227d92ef-d6f2-484a-98ab-69854ed7cd9e.
Madamanchi, N. R. *et al.* (2001) 'Reactive oxygen species regulate heat-shock protein 70 via the JAK/STAT pathway.', *Arteriosclerosis, thrombosis, and vascular biology*, 21(3), pp. 321–6. Available at: http://www.ncbi.nlm.nih.gov/pubmed/11231909 (Accessed: 21 August 2018).
Mantovan, M. C. *et al.* (2006) 'Exploring mental status in Friedreich's ataxia: a combined neuropsychological, behavioral and neuroimaging study', *European Journal of Neurology*, 13(8), pp. 827–835. doi: 10.1111/j.1468-1331.2006.01363.x.
Marcotulli, C. *et al.* (2016) 'GIFT-1, a phase IIa clinical trial to test the safety and efficacy of IFNγ administration in FRDA patients', *Neurological Sciences*. Springer Milan, 37(3), pp. 361–364. doi: 10.1007/s10072-015-2427-3.
Mariotti, C. *et al.* (2012) 'Erythropoietin in Friedreich ataxia: No effect on frataxin in a randomized controlled trial', *Movement Disorders*. Wiley-Blackwell, 27(3), pp. 446–449. doi: 10.1002/mds.24066.
Martelli, A., Napierala, M. and Puccio, H. (2012) 'Understanding the genetic and molecular pathogenesis of Friedreich's ataxia through animal and cellular models', *Disease Models & Mechanisms*, 5(2), pp. 165–176. doi: 10.1242/dmm.008706.
McCabe, D. J. H. *et al.* (2002) 'Intrafamilial phenotypic variability in Friedreich ataxia associated with a G130V mutation in the FRDA gene.', *Archives of neurology*, 59(2), pp. 296–300. Available at: http://www.ncbi.nlm.nih.gov/pubmed/11843702 (Accessed: 8 May 2018).
McCormack, M. L. *et al.* (2000) 'Frataxin point mutations in two patients with Friedreich's ataxia and unusual clinical features.', *Journal of neurology, neurosurgery, and psychiatry*, 68(5), pp. 661–4. Available at: http://www.ncbi.nlm.nih.gov/pubmed/10766903 (Accessed: 8 May 2018).
McGinnity, D. F. *et al.* (2004) 'Evaluation of fresh and cryopreserved hepatocytes as in vitro drug metabolism tools for the prediction of metabolic clearance.', *Drug Metabolism and Disposition*. American Society for Pharmacology and Experimental Therapeutics, 32(11), pp. 1247–53. doi: 10.1124/dmd.104.000026.
De Michele, G. *et al.* (2000) 'Atypical Friedreich ataxia phenotype associated with a novel missense mutation in the X25 gene.', *Neurology*, 54(2), pp. 496–9. Available at: http://www.ncbi.nlm.nih.gov/pubmed/10668723 (Accessed: 8 May 2018).

Mikkelsen, T. S. *et al.* (2007) 'Genome-wide maps of chromatin state in pluripotent and lineage-committed cells', *Nature*. Nature Publishing Group, 448(7153), pp. 553–560. doi: 10.1038/nature06008.
Milbrandt, T. A., Kunes, J. R. and Karol, L. A. (2008) 'Friedreich's ataxia and scoliosis: the experience at two institutions.', *Journal of pediatric orthopedics*, 28(2), pp. 234–8. doi: 10.1097/BPO.0b013e318164fa79.
Miller, J. L. *et al.* (2017) 'Erythropoietin and small molecule agonists of the tissue-protective erythropoietin receptor increase FXN expression in neuronal cells in vitro and in Fxn-deficient KIKO mice in vivo', *Neuropharmacology*. Pergamon, 123, pp. 34–45. doi: 10.1016/J.NEUROPHARM.2017.05.011.
Mincheva-Tasheva, S. *et al.* (2014) 'Apoptotic cell death and altered calcium homeostasis caused by frataxin depletion in dorsal root ganglia neurons can be prevented by BH4 domain of Bcl-xL protein', *Human Molecular Genetics*. Oxford University Press, 23(7), pp. 1829–1841. doi: 10.1093/hmg/ddt576.
Miranda, C. J. *et al.* (2004) 'Frataxin overexpressing mice', *FEBS Letters*, 572(1–3), pp. 281–288. doi: 10.1016/j.febslet.2004.07.022.
Mohn, F. *et al.* (2008) 'Lineage-Specific Polycomb Targets and De Novo DNA Methylation Define Restriction and Potential of Neuronal Progenitors', *Molecular Cell*. Cell Press, 30(6), pp. 755–766. doi: 10.1016/J.MOLCEL.2008.05.007.
Montermini, L. *et al.* (1997) 'The Friedreich ataxia GAA triplet repeat: premutation and normal alleles.', *Human molecular genetics*. Oxford University Press, 6(8), pp. 1261–6. doi: 10.1093/HMG/6.8.1261.
Moore, L. D., Le, T. and Fan, G. (2012) 'DNA Methylation and Its Basic Function', *Neuropsychopharmacology*. Nature Publishing Group, 38(1), pp. 23–38. doi: 10.1038/npp.2012.112.
Muller, H. J. (1930) 'Types of visible variations induced by X-rays in Drosophila', *Journal of Genetics*, 22(3), pp. 299–334.
Nachbauer, W. *et al.* (2011) 'Effects of Erythropoietin on Frataxin Levels and Mitochondrial Function in Friedreich Ataxia – a Dose–Response Trial', *The Cerebellum*. Springer-Verlag, 10(4), pp. 763–769. doi: 10.1007/s12311-011-0287-9.
Nachbauer, W. *et al.* (2014) 'Friedreich Ataxia: Executive Control Is Related to Disease Onset and GAA Repeat Length', *The Cerebellum*, 13(1), pp. 9–16. doi: 10.1007/s12311-013-0513-8.
Napoli, E., Taroni, F. and Cortopassi, G. A. (2006) 'Frataxin, Iron–Sulfur Clusters, Heme, ROS, and Aging', *Antioxidants & Redox Signaling*. Mary Ann Liebert, Inc. 2 Madison Avenue Larchmont, NY 10538 USA , 8(3–4), pp. 506–516. doi: 10.1089/ars.2006.8.506.
Nardulli, R. *et al.* (1992) 'Urodynamic evaluation of 12 ataxic subjects: neurophysiopathologic considerations.', *Functional neurology*, 7(3), pp. 223–5. Available at: http://www.ncbi.nlm.nih.gov/pubmed/1500012 (Accessed: 28 May 2018).
Ng, S. S. *et al.* (2009) 'Dynamic protein methylation in chromatin biology', *Cellular and Molecular Life Sciences*. Birkhäuser-Verlag, 66(3), pp. 407–422. doi: 10.1007/s00018-008-8303-z.
Nicholls, D. G. (2004) 'Mitochondrial membrane potential and aging', *Aging Cell*. Wiley/Blackwell (10.1111), 3(1), pp. 35–40. doi: 10.1111/j.1474-9728.2003.00079.x.
Niemeijer, M. N. *et al.* (2015) 'Pharmacogenetics of Drug-Induced QT Interval Prolongation: An Update.', *Drug safety*. Springer, 38(10), pp. 855–67. doi: 10.1007/s40264-015-0316-6.
Nishioka, K. *et al.* (2002) 'PR-Set7 Is a Nucleosome-Specific Methyltransferase that Modifies Lysine 20 of Histone H4 and Is Associated with Silent Chromatin', *Molecular*

Cell. Cell Press, 9(6), pp. 1201–1213. doi: 10.1016/S1097-2765(02)00548-8.
Obach, R. S. (1999) 'Prediction of human clearance of twenty-nine drugs from hepatic microsomal intrinsic clearance data: An examination of in vitro half-life approach and nonspecific binding to microsomes', *Drug Metabolism and Disposition*, 27(11), pp. 1350–1359. doi: 10.1124/dmd.30.7.831.
Ohshima, K. *et al.* (1998) 'Inhibitory Effects of Expanded GAA.TTC Triplet Repeats from Intron I of the Friedreich Ataxia Gene on Transcription and Replicationin Vivo', *J. Biol. Chem.*, 273(23), pp. 14588–14595. doi: 10.1074/jbc.273.23.14588.
Okada, Y. *et al.* (2005) 'hDOT1L Links Histone Methylation to Leukemogenesis', *Cell*. Cell Press, 121(2), pp. 167–178. doi: 10.1016/J.CELL.2005.02.020.
Pan, M.-R. *et al.* (2018) 'Orchestration of H3K27 methylation: mechanisms and therapeutic implication.', *Cellular and molecular life sciences : CMLS*. Springer, 75(2), pp. 209–223. doi: 10.1007/s00018-017-2596-8.
Pandolfo, M. (2009) 'Friedreich ataxia: The clinical picture', *Journal of Neurology*, 256(SUPPL. 1), pp. 3–8. doi: 10.1007/s00415-009-1002-3.
Park, S. *et al.* (2003) 'Yeast frataxin sequentially chaperones and stores iron by coupling protein assembly with iron oxidation.', *The Journal of biological chemistry*. American Society for Biochemistry and Molecular Biology, 278(33), pp. 31340–51. doi: 10.1074/jbc.M303158200.
Parkinson, M. H. *et al.* (2013) 'Clinical features of Friedreich's ataxia: classical and atypical phenotypes', *Journal of Neurochemistry*. Wiley/Blackwell (10.1111), 126, pp. 103–117. doi: 10.1111/jnc.12317.
Pastore, A. and Puccio, H. (2013) 'Frataxin: A protein in search for a function', *Journal of Neurochemistry*, 126(SUPPL.1), pp. 43–52. doi: 10.1111/jnc.12220.
Patel, P. I. and Isaya, G. (2001) 'Friedreich Ataxia: From GAA Triplet–Repeat Expansion to Frataxin Deficiency', *Am. J. Hum. Genet*, 69, pp. 15–24.
Paupe, V. *et al.* (2009) 'Impaired Nuclear Nrf2 Translocation Undermines the Oxidative Stress Response in Friedreich Ataxia', *PLoS ONE*. Edited by A. L. Andreu. Public Library of Science, 4(1), p. e4253. doi: 10.1371/journal.pone.0004253.
Perdomini, M. *et al.* (2014) 'Prevention and reversal of severe mitochondrial cardiomyopathy by gene therapy in a mouse model of Friedreich's ataxia', *Nature Medicine*. Nature Research, 20(5), pp. 542–547. doi: 10.1038/nm.3510.
Perry, S. W. *et al.* (2011) 'Mitochondrial membrane potential probes and the proton gradient: a practical usage guide.', *BioTechniques*. NIH Public Access, 50(2), pp. 98–115. doi: 10.2144/000113610.
Peters, A. H. F. M. *et al.* (2001) 'Loss of the Suv39h Histone Methyltransferases Impairs Mammalian Heterochromatin and Genome Stability', *Cell*. Cell Press, 107(3), pp. 323–337. doi: 10.1016/S0092-8674(01)00542-6.
Peters, A. H. F. M. *et al.* (2003) 'Partitioning and Plasticity of Repressive Histone Methylation States in Mammalian Chromatin', *Molecular Cell*. Cell Press, 12(6), pp. 1577–1589. doi: 10.1016/S1097-2765(03)00477-5.
Petrillo, S. *et al.* (2017) 'Nrf2-Inducers Counteract Neurodegeneration in Frataxin-Silenced Motor Neurons: Disclosing New Therapeutic Targets for Friedreich's Ataxia', *International Journal of Molecular Sciences*. Multidisciplinary Digital Publishing Institute, 18(10), p. 2173. doi: 10.3390/ijms18102173.
Piguet, F. *et al.* (2018) 'Rapid and Complete Reversal of Sensory Ataxia by Gene Therapy in a Novel Model of Friedreich Ataxia', *Molecular Therapy*. Elsevier Ltd., 26(8), pp. 1–13. doi: 10.1016/j.ymthe.2018.05.006.
Plath, K. *et al.* (2003) 'Role of histone H3 lysine 27 methylation in X inactivation.', *Science*. American Association for the Advancement of Science, 300(5616), pp. 131–5.

doi: 10.1126/science.1084274.
Polak, U. *et al.* (2016) 'Alleviating GAA Repeat Induced Transcriptional Silencing of the Friedreich's Ataxia Gene During Somatic Cell Reprogramming', *Stem Cells and Development*, 25(23), pp. 1788–1800. doi: 10.1089/scd.2016.0147.
Pombo, A. and Dillon, N. (2015) 'Three-dimensional genome architecture: players and mechanisms.', *Nature reviews. Molecular cell biology*, 16(4), pp. 245–257. doi: 10.1038/nrm3965.
Pook, M. A. *et al.* (2000) 'Identification of three novel frameshift mutations in patients with Friedreich's ataxia.', *Journal of medical genetics*, 37(11), p. E38. Available at: http://www.ncbi.nlm.nih.gov/pubmed/11073547 (Accessed: 8 May 2018).
Potter, N. T., Miller, C. A. and Anderson, I. J. (2000) 'Mutation detection in an equivocal case of Friedreich's ataxia.', *Pediatric neurology*, 22(5), pp. 413–5. Available at: http://www.ncbi.nlm.nih.gov/pubmed/10913738 (Accessed: 8 May 2018).
Punga, T. and Bühler, M. (2010) 'Long intronic GAA repeats causing Friedreich ataxia impede transcription elongation', *EMBO Molecular Medicine*, 2(4), pp. 120–129. doi: 10.1002/emmm.201000064.
Puspasari, N. *et al.* (2011) 'Long range regulation of human FXN gene expression', *PLoS ONE*, 6(7), pp. 12–15. doi: 10.1371/journal.pone.0022001.
Quesada, M. P. *et al.* (2015) 'Novel aberrant genetic and epigenetic events in Friedreich's ataxia.', *Experimental cell research*. Elsevier, 335(1), pp. 51–61. doi: 10.1016/j.yexcr.2015.04.013.
Rai, M. *et al.* (2008) 'HDAC inhibitors correct frataxin deficiency in a Friedreich ataxia mouse model.', *PloS one*. Public Library of Science, 3(4), p. e1958. doi: 10.1371/journal.pone.0001958.
Rai, M. *et al.* (2010) 'Two new pimelic diphenylamide HDAC inhibitors induce sustained frataxin upregulation in cells from Friedreich's ataxia patients and in a mouse model.', *PloS one*. Public Library of Science, 5(1), p. e8825. doi: 10.1371/journal.pone.0008825.
Rance, G. *et al.* (2010) 'Auditory perception in individuals with Friedreich's ataxia.', *Audiology & neuro-otology*. Karger Publishers, 15(4), pp. 229–40. doi: 10.1159/000255341.
Rane, A., Wilkinson, G. R. and Shand, D. G. (1977) 'Prediction of hepatic extraction ratio from in vitro measurement of intrinsic clearance.', *Journal of Pharmacology and Experimental Therapeutics*, 200(2).
Reddy, K. *et al.* (2011) 'Determinants of R-loop formation at convergent bidirectionally transcribed trinucleotide repeats', *Nucleic Acids Research*, 39(5), pp. 1749–1762. doi: 10.1093/nar/gkq935.
Rötig, A. *et al.* (1997) 'Aconitase and mitochondrial iron–sulphur protein deficiency in Friedreich ataxia', *Nature Genetics*. Nature Publishing Group, 17(2), pp. 215–217. doi: 10.1038/ng1097-215.
Saccà, F. *et al.* (2011) 'Epoetin alfa increases frataxin production in Friedreich's ataxia without affecting hematocrit', *Movement Disorders*. Wiley-Blackwell, 26(4), pp. 739–742. doi: 10.1002/mds.23435.
Sahdeo, S. *et al.* (2014) 'Dyclonine rescues frataxin deficiency in animal models and buccal cells of patients with Friedreich's ataxia', *Human Molecular Genetics*. Oxford University Press, 23(25), pp. 6848–6862. doi: 10.1093/hmg/ddu408.
Sakamoto, N. *et al.* (1999) 'Sticky DNA: Self-Association Properties of Long GAA·TTC Repeats in R·R·Y Triplex Structures from Friedreich's Ataxia', *Molecular Cell*, 3(4), pp. 465–475. doi: 10.1016/S1097-2765(00)80474-8.
Sakamoto, N. *et al.* (2001) 'Sticky DNA, a Self-associated Complex Formed at Long

GAA·TTC Repeats in Intron 1 of the Frataxin Gene, Inhibits Transcription', *Journal of Biological Chemistry*, 276(29), pp. 27171–27177. doi: 10.1074/jbc.M101879200.
Sandi, C. *et al.* (2011) 'Prolonged treatment with pimelic o-aminobenzamide HDAC inhibitors ameliorates the disease phenotype of a Friedreich ataxia mouse model', *Neurobiology of Disease*. Elsevier Inc., 42(3), pp. 496–505. doi: 10.1016/j.nbd.2011.02.016.
Sandi, C. *et al.* (2014) 'Epigenetic-based therapies for Friedreich ataxia', *Frontiers in Genetics*, 5, p. 165. doi: 10.3389/fgene.2014.00165.
Sandi, C., Al-Mahdawi, S. and Pook, M. A. (2013) 'Epigenetics in Friedreich's Ataxia: Challenges and Opportunities for Therapy', *Genetics research international*. Hindawi Limited, 2013, p. 852080. doi: 10.1155/2013/852080.
Sarsero, J. P. *et al.* (2003) 'Upregulation of expression from the FRDA genomic locus for the therapy of Friedreich ataxia', *The Journal of Gene Medicine*. Wiley-Blackwell, 5(1), pp. 72–81. doi: 10.1002/jgm.320.
Saveliev, A. *et al.* (2003) 'DNA triplet repeats mediate heterochromatin-protein-1-sensitive variegated gene silencing', *Nature*, 422(6934), pp. 909–913. doi: 10.1038/nature01596.
Saxonov, S., Berg, P. and Brutlag, D. L. (2006) 'A genome-wide analysis of CpG dinucleotides in the human genome distinguishes two distinct classes of promoters.', *Proceedings of the National Academy of Sciences of the United States of America*. National Academy of Sciences, 103(5), pp. 1412–7. doi: 10.1073/pnas.0510310103.
Schmucker, S. *et al.* (2008) 'The in vivo mitochondrial two-step maturation of human frataxin.', *Human molecular genetics*. Oxford University Press, 17(22), pp. 3521–31. doi: 10.1093/hmg/ddn244.
Schmucker, S. *et al.* (2011) 'Mammalian frataxin: an essential function for cellular viability through an interaction with a preformed ISCU/NFS1/ISD11 iron-sulfur assembly complex.', *PloS one*. Public Library of Science, 6(1), p. e16199. doi: 10.1371/journal.pone.0016199.
Schmucker, S. and Puccio, H. (2010) 'Understanding the molecular mechanisms of friedreich's ataxia to develop therapeutic approaches', *Human Molecular Genetics*, 19(R1), pp. 103–110. doi: 10.1093/hmg/ddq165.
Schotta, G. *et al.* (2004) 'A silencing pathway to induce H3-K9 and H4-K20 trimethylation at constitutive heterochromatin.', *Genes & development*. Cold Spring Harbor Laboratory Press, 18(11), pp. 1251–62. doi: 10.1101/gad.300704.
Schotta, G. *et al.* (2008) 'A chromatin-wide transition to H4K20 monomethylation impairs genome integrity and programmed DNA rearrangements in the mouse.', *Genes & development*. Cold Spring Harbor Laboratory Press, 22(15), pp. 2048–61. doi: 10.1101/gad.476008.
Seyer, L. *et al.* (2015) 'Open-label pilot study of interferon gamma-1b in Friedreich ataxia', *Acta Neurologica Scandinavica*. Wiley/Blackwell (10.1111), 132(1), pp. 7–15. doi: 10.1111/ane.12337.
Shan, Y. *et al.* (2013) 'Frataxin Deficiency Leads to Defects in Expression of Antioxidants and Nrf2 Expression in Dorsal Root Ganglia of the Friedreich's Ataxia YG8R Mouse Model', *Antioxidants & Redox Signaling*. Mary Ann Liebert, Inc. 140 Huguenot Street, 3rd Floor New Rochelle, NY 10801 USA, 19(13), pp. 1481–1493. doi: 10.1089/ars.2012.4537.
Shankar, S. R. *et al.* (2013) 'G9a, a multipotent regulator of gene expression', *Epigenetics*, 8(1), pp. 16–22. doi: 10.4161/epi.23331.
Shapiro, F. and Specht, L. (1993) 'The diagnosis and orthopaedic treatment of childhood spinal muscular atrophy, peripheral neuropathy, Friedreich ataxia, and arthrogryposis.',

The Journal of bone and joint surgery. American volume, 75(11), pp. 1699–714. Available at: http://www.ncbi.nlm.nih.gov/pubmed/8245065 (Accessed: 27 May 2018).
Shidara, Y. and Hollenbeck, P. J. (2010) 'Defects in Mitochondrial Axonal Transport and Membrane Potential without Increased Reactive Oxygen Species Production in a Drosophila Model of Friedreich Ataxia', *Journal of Neuroscience*, 30(34), pp. 11369–11378. doi: 10.1523/JNEUROSCI.0529-10.2010.
Shinkai, Y. and Tachibana, M. (2011) 'H3K9 methyltransferase G9a and the related molecule GLP.', *Genes & development*. Cold Spring Harbor Laboratory Press, 25(8), pp. 781–8. doi: 10.1101/gad.2027411.
Shogren-Knaak, M. *et al.* (2006) 'Histone H4-K16 acetylation controls chromatin structure and protein interactions.', *Science (New York, N.Y.)*, 311(5762), pp. 844–7. doi: 10.1126/science.1124000.
Silva, A. M. *et al.* (2015) 'Expanded GAA repeats impair FXN gene expression and reposition the FXN locus to the nuclear lamina in single cells', *Human Molecular Genetics*, 24(12), pp. 3457–3471. doi: 10.1093/hmg/ddv096.
Silva, J. *et al.* (2003) 'Establishment of Histone H3 Methylation on the Inactive X Chromosome Requires Transient Recruitment of Eed-Enx1 Polycomb Group Complexes', *Developmental Cell*. Cell Press, 4(4), pp. 481–495. doi: 10.1016/S1534-5807(03)00068-6.
Simon, A. R. *et al.* (1998) 'Activation of the JAK-STAT pathway by reactive oxygen species.', *The American journal of physiology*, 275(6 Pt 1), pp. C1640-52. Available at: http://www.ncbi.nlm.nih.gov/pubmed/9843726 (Accessed: 21 August 2018).
Somech, R. *et al.* (2005) 'The nuclear-envelope protein and transcriptional repressor LAP2β interacts with HDAC3 at the nuclear periphery, and induces histone H4 deacetylation', *Journal of Cell Science*, 118(17), pp. 403–410. doi: 10.1242/jcs.02521.
Van Soom, A. *et al.* (2014) 'An Introduction to Epigenetics as the Link Between Genotype and Environment: A Personal View', *Reproduction in Domestic Animals*. Wiley/Blackwell (10.1111), 49, pp. 2–10. doi: 10.1111/rda.12341.
Soragni, E. *et al.* (2008) 'Long intronic GAA·TTC repeats induce epigenetic changes and reporter gene silencing in a molecular model of Friedreich ataxia', *Nucleic Acids Research*, 36(19), pp. 6056–6065. doi: 10.1093/nar/gkn604.
Soragni, E. *et al.* (2012) 'Rationale for the development of 2-aminobenzamide histone deacetylase inhibitors as therapeutics for Friedreich ataxia.', *Journal of child neurology*. NIH Public Access, 27(9), pp. 1164–73. doi: 10.1177/0883073812448533.
Soragni, E. *et al.* (2014) 'Epigenetic Therapy for Friedreich ataxia', *Annals of Neurology*, 76(4), pp. 489–508. doi: 10.1002/ana.24260.
Soragni, E. *et al.* (2015) 'Mechanism of action of 2-aminobenzamide HDAC inhibitors in reversing gene silencing in Friedreich's ataxia', *Frontiers in Neurology*, 6, pp. 1–11. doi: 10.3389/fneur.2015.00044.
Spacey, S. D. *et al.* (2004) 'Malaysian siblings with friedreich ataxia and chorea: a novel deletion in the frataxin gene.', *The Canadian journal of neurological sciences. Le journal canadien des sciences neurologiques*, 31(3), pp. 383–6. Available at: http://www.ncbi.nlm.nih.gov/pubmed/15376485 (Accessed: 8 May 2018).
Stephens, K. E. *et al.* (2013) 'Epigenetic Regulation and Measurement of Epigenetic Changes', *Biological Research for Nursing*, 15(4), pp. 373–381. doi: 10.1177/1099800412444785.
Strahl, B. D. *et al.* (2002) 'Set2 is a nucleosomal histone H3-selective methyltransferase that mediates transcriptional repression.', *Molecular and cellular biology*. American Society for Microbiology, 22(5), pp. 1298–306. doi: 10.1128/MCB.22.5.1298-1306.2002.

Strawser, C. *et al.* (2017) 'Pharmacological therapeutics in Friedreich ataxia: the present state', *Expert Review of Neurotherapeutics*, 17(9), pp. 895–907. doi: 10.1080/14737175.2017.1356721.
Structural Genomics Consortium (2018) *Epigenetics Probes Collection | SGC*. Available at: https://www.thesgc.org/chemical-probes/epigenetics (Accessed: 25 July 2018).
Sturm, B. *et al.* (2005) 'Recombinant human erythropoietin: effects on frataxin expression in vitro', *European Journal of Clinical Investigation*. Wiley/Blackwell (10.1111), 35(11), pp. 711–717. doi: 10.1111/j.1365-2362.2005.01568.x.
Subbanna, S. *et al.* (2013) 'G9a-mediated histone methylation regulates ethanol-induced neurodegeneration in the neonatal mouse brain', *Neurobiology of Disease*. Academic Press, 54, pp. 475–485. doi: 10.1016/J.NBD.2013.01.022.
Sullivan, K. *et al.* (2016) *Neurology.*, *Neurology*. Advanstar Communications. Available at: http://n.neurology.org/content/86/16_Supplement/P5.388 (Accessed: 18 July 2018).
Suzuki, T., Motohashi, H. and Yamamoto, M. (2013) 'Toward clinical application of the Keap1–Nrf2 pathway', *Trends in Pharmacological Sciences*. Elsevier Current Trends, 34(6), pp. 340–346. doi: 10.1016/J.TIPS.2013.04.005.
Sweis, R. F. *et al.* (2014) 'Discovery and development of potent and selective inhibitors of histone methyltransferase G9a', *ACS Medicinal Chemistry Letters*, 5(2), pp. 205–209. doi: 10.1021/ml400496h.
Szulwach, K. E. *et al.* (2011) '5-hmC-mediated epigenetic dynamics during postnatal neurodevelopment and aging', *Nature Neuroscience*. Nature Publishing Group, 14(12), pp. 1607–1616. doi: 10.1038/nn.2959.
Tachibana, M. *et al.* (2005) 'Histone methyltransferases G9a and GLP form heteromeric complexes and are both crucial for methylation of euchromatin at H3-K9.', *Genes & development*. Cold Spring Harbor Laboratory Press, 19(7), pp. 815–26. doi: 10.1101/gad.1284005.
Tahiliani, M. *et al.* (2009) 'Conversion of 5-Methylcytosine to 5-Hydroxymethylcytosine in Mammalian DNA by MLL Partner TET1', *Science*, 324(5929), pp. 930–935.
Tamarit, J., Obis, È. and Ros, J. (2016) 'Oxidative stress and altered lipid metabolism in Friedreich ataxia', *Free Radical Biology and Medicine*. Elsevier, pp. 1–9. doi: 10.1016/j.freeradbiomed.2016.06.007.
Therizols, P. *et al.* (2014) 'Chromatin decondensation is sufficient to alter nuclear organization in embryonic stem cells.', *Science (New York, N.Y.)*, 346(6214), pp. 1238–42. doi: 10.1126/science.1259587.
Tomassini, B. *et al.* (2012) 'Interferon gamma upregulates frataxin and corrects the functional deficits in a Friedreich ataxia model', *Human Molecular Genetics*. Oxford University Press, 21(13), pp. 2855–2861. doi: 10.1093/hmg/dds110.
Tsou, A. Y. *et al.* (2011) 'Mortality in Friedreich ataxia.', *Journal of the neurological sciences*. Elsevier, 307(1–2), pp. 46–9. doi: 10.1016/j.jns.2011.05.023.
Ümit Kaniskan, H., Martini, M. L. and Jin, J. (2018) 'Inhibitors of Protein Methyltransferases and Demethylases', *Chemical Reviews*, 118(3), pp. 989–1068. doi: 10.1021/acs.chemrev.6b00801.
Vankan, P. (2013) 'Prevalence gradients of Friedreich's Ataxia and R1b haplotype in Europe co-localize, suggesting a common Palaeolithic origin in the Franco-Cantabrian ice age refuge', *Journal of Neurochemistry*. Wiley/Blackwell (10.1111), 126, pp. 11–20. doi: 10.1111/jnc.12215.
Vaubel, R. A. and Isaya, G. (2013) 'Iron–sulfur cluster synthesis, iron homeostasis and oxidative stress in Friedreich ataxia', *Molecular and Cellular Neuroscience*, 55, pp. 50–61. doi: 10.1016/j.mcn.2012.08.003.
Verma, S. K. *et al.* (2012) 'Identification of Potent, Selective, Cell-Active Inhibitors of

the Histone Lysine Methyltransferase EZH2.', *ACS medicinal chemistry letters*. American Chemical Society, 3(12), pp. 1091–6. doi: 10.1021/ml3003346.
Vezina, J. G., Bouchard, J. P. and Bouchard, R. (1982) 'Urodynamic evaluation of patients with hereditary ataxias.', *The Canadian journal of neurological sciences. Le journal canadien des sciences neurologiques*, 9(2), pp. 127–9. Available at: http://www.ncbi.nlm.nih.gov/pubmed/7104878 (Accessed: 28 May 2018).
Vogel, A. P. *et al.* (2014) 'Dysphagia and swallowing-related quality of life in Friedreich ataxia', *Journal of Neurology*. Springer Berlin Heidelberg, 261(2), pp. 392–399. doi: 10.1007/s00415-013-7208-4.
Wang, Z. *et al.* (2008) 'Combinatorial patterns of histone acetylations and methylations in the human genome.', *Nature genetics*. NIH Public Access, 40(7), pp. 897–903. doi: 10.1038/ng.154.
Weidemann, F. *et al.* (2012) 'The heart in Friedreich ataxia: Definition of cardiomyopathy, disease severity, and correlation with neurological symptoms', *Circulation*, 125(13), pp. 1626–1634. doi: 10.1161/CIRCULATIONAHA.111.059477.
Wollmann, T. *et al.* (2002) 'Neuropsychological Test Performance of Patients With Friedreich's Ataxia', *Journal of Clinical and Experimental Neuropsychology (Neuropsychology, Development and Cognition: Section A)*, 24(5), pp. 677–686. doi: 10.1076/jcen.24.5.677.1014.
Wong, A. *et al.* (1999) 'The Friedreich's ataxia mutation confers cellular sensitivity to oxidant stress which is rescued by chelators of iron and calcium and inhibitors of apoptosis', *Human Molecular Genetics*. Oxford University Press, 8(3), pp. 425–430. doi: 10.1093/hmg/8.3.425.
Workman, J. L. and Kingston, R. E. (1998) 'ALTERATION OF NUCLEOSOME STRUCTURE AS A MECHANISM OF TRANSCRIPTIONAL REGULATION', *Annual Review of Biochemistry*. Annual Reviews 4139 El Camino Way, P.O. Box 10139, Palo Alto, CA 94303-0139, USA , 67(1), pp. 545–579. doi: 10.1146/annurev.biochem.67.1.545.
Yandim, C., Natisvili, T. and Festenstein, R. (2013) 'Gene regulation and epigenetics in Friedreich's ataxia', *Journal of Neurochemistry*, 126(SUPPL.1), pp. 21–42. doi: 10.1111/jnc.12254.
Yoon, T. and Cowan, J. A. (2004) 'Frataxin-mediated iron delivery to ferrochelatase in the final step of heme biosynthesis.', *The Journal of biological chemistry*. American Society for Biochemistry and Molecular Biology, 279(25), pp. 25943–6. doi: 10.1074/jbc.C400107200.
Yu, W. *et al.* (2012) 'Catalytic site remodelling of the DOT1L methyltransferase by selective inhibitors', *Nature Communications*. Nature Publishing Group, 3(1), p. 1288. doi: 10.1038/ncomms2304.
Zesiewicz, T. *et al.* (2017) *Neurology., Neurology*. Advanstar Communications. Available at: http://n.neurology.org/content/88/16_Supplement/S17.005 (Accessed: 18 July 2018).
Zhang, X., Wen, H. and Shi, X. (2012) 'Lysine methylation: beyond histones', *Acta Biochimica et Biophysica Sinica*. Oxford University Press, 44(1), pp. 14–27. doi: 10.1093/abbs/gmr100.
Zhao, H. *et al.* (2017) 'Peptide SS-31 upregulates frataxin expression and improves the quality of mitochondria: implications in the treatment of Friedreich ataxia', *Scientific Reports*. Nature Publishing Group, 7(1), p. 9840. doi: 10.1038/s41598-017-10320-2.
Zhao, Q. *et al.* (2009) 'PRMT5-mediated methylation of histone H4R3 recruits DNMT3A, coupling histone and DNA methylation in gene silencing', *Nature Structural & Molecular Biology*. Nature Publishing Group, 16(3), pp. 304–311. doi:

10.1038/nsmb.1568.
Zhu, D. *et al.* (2002) 'Friedreich's ataxia with chorea and myoclonus caused by a compound heterozygosity for a novel deletion and the trinucleotide GAA expansion', *Movement Disorders*. Wiley-Blackwell, 17(3), pp. 585–589. doi: 10.1002/mds.10175.
Zühlke, C. *et al.* (1998) 'Mutation of the start codon in the FRDA1 gene: linkage analysis of three pedigrees with the ATG to ATT transversion points to a unique common ancestor.', *Human genetics*, 103(1), pp. 102–5. Available at: http://www.ncbi.nlm.nih.gov/pubmed/9737785 (Accessed: 8 May 2018).
Zühlke, C. H. *et al.* (2004) 'Extension of the mutation spectrum in Friedreich's ataxia: detection of an exon deletion and novel missense mutations.', *European journal of human genetics : EJHG*, 12(11), pp. 979–82. doi: 10.1038/sj.ejhg.5201257.

APPENDICES

SGC epigenetics probes collection

Table 17. SGC chemical probes used in the screen. Information taken from SGC and uniprot.

Name	Protein family	Specific targets	Targets overview
GSK864	Dehydrogenase	Mutant isocitrate dehydrogenase 1	Magnesiun ion, NAD, NADP binding. Implicated in glutathione metabolic process
A-196	Methyltransferase	SUV420H1/H2	Di- and tri-methylate 'Lys-20' of histone H4
GSK591	Methyltransferase	PRMT5	Methylates histone H3 'Arg-8', which may repress transcription
MS023	Methyltransferase	Type I PRMTs	Catalyze mono- and asymmetric dimethylation of arginine residues
MS049	Methyltransferase	PRMT4,6	Methylates the guanidino nitrogens of arginyl residues in several proteins involved in DNA packaging, transcription regulation, pre-mRNA splicing, and mRNA stability
BAY-598	Methyltransferase	SMYD2	Methylates histone H3 'Lys-4' (H3K4me) and dimethylates histone H3 'Lys-36' (H3K36me2)
LLY-507	Methyltransferase	SMYD2	As above described
SGC707	Methyltransferase	PRMT3	Negative regulation of protein ubiquitination, regulation of transcription
A-366	Methyltransferase	G9a, GLP	Mono- and dimethylates 'Lys-9' of histone H3 (H3K9me1 and H3K9me2, respectively) in euchromatin

UNC0642	Methyltransferase	G9a, GLP	As above described
UNC0638	Methyltransferase	G9a, GLP	As above described
UNC1999	Methyltransferase	EZH2	Plays a critical role in regulating gene expression
GSK343	Methyltransferase	EZH2	As above described
PFI-2	Methyltransferase	SETD7	Monomethylates 'Lys-4' of histone H3
SGC0946	Methyltransferase	DOT1L	Methylates 'Lys-79' of histone H3
NVS-CECR2-1	Bromodomains	CECR2	Part of the CERF complex, which facilitates the perturbation of chromatin structure in an ATP-dependent manner
I-BRD9	Bromodomains	BRD9	May play a role in chromatin remodeling and regulation of transcription
BI-9564	Bromodomains	BRD9, BRD7	Transcriptional corepressor that down-regulates the expression of target genes
LP99	Bromodomains	BRD9, BRD7	As above described
GSK2801	Bromodomains	BAZ2A, BAZ2B	Essential component of the NoRC (nucleolar remodeling complex) complex that leads to heterochromatin formation and transcriptional silencing
BAZ2-ICR	Bromodomains	BAZ2A, BAZ2B	As above described
NI-57	Bromodomains	BRPF1, BRPF2, BRPF3	Scaffolding proteins assembling HAT complexes of the MOZ/MORF family
OF-1	Bromodomains	BRPF1, BRPF2, BRPF3	As above described
PFI-4	Bromodomains	BRPF1B	One of the two isoforms of BRPF1
PFI-3	Bromodomains	SMARCA,PB1	Central components of the large ATP-dependent SNF/SWI chromatin remodeling complex, which plays a key role in chromatin remodelling and transcription control

SGC-CBP30	Bromodomains	CREBBP, EP300	Transcriptional co-activators involved in biological processes like maintenance of genomic stability by affecting DNA replication and DNA repair
I-CBP112	Bromodomains	CREBBP, EP300	As above described
Bromosporine	Bromodomains	pan-Bromodomain	Protein interaction modules that read epigenetic marks recognizing ε-N-lysine acetylation motifs
PFI-1	Bromodomains	BRD2, BRD3, BRD4, BRDT (BET)	Binds hyperacetylated chromatin and plays a role in the regulation of transcription
JQ1	Bromodomains	BRD2, BRD3, BRD4, BRDT (BET)	As above described
OICR-9429	Methyl Lysine Binder	WDR5	As part of the MLL1/MLL complex it is involved in methylation and dimethylation at 'Lys-4' of histone H3
UNC1215	Methyl Lysine Binder	L3MBTL3	Maintain the transcriptionally repressive state of genes, probably via a modification of chromatin
GSK-LSD1	Lysine demethylase	LSD1	Demethylates both 'Lys-4' (H3K4me) and 'Lys-9' (H3K9me) of histone H3, thereby acting as a coactivator or a corepressor
GSK-J1	Lysine demethylase	JMJD3, UTX, JARID1B	Demethylation of histone 3 lysine 27
GSK484	Arginine deiminases	PAD-4	Catalyzes the citrullination/deimination of arginine residues of proteins such as histones
Oliparib	Poly ADP ribose polymerase	PARP1, PARP2	Regulate the repair of DNA single-strand breaks generated directly, or during base excision repair